Hydrogen supply chain design

Lei Li

THÈSE DE DOCTORAT

DE L'ÉTABLISSEMENT UNIVERSITÉ BOURGOGNE FRANCHE-COMTÉ

PRÉPARÉE À L'UNIVERSITÉ DE TECHNOLOGIE DE BELFORT-MONTBÉLIARD

École doctorale n°37

Sciences Pour l'Ingénieur et Microtechniques

Doctorat d'Automatique

par

LEI LI

Hydrogen supply chain design

Thèse présentée et soutenue à Belfort, le 18 mai 2020

Composition du Jury :

HISSEL DANIEL	Professeur, Université de Bourgogne Franche-Comté	Président
HISSEL DANIEL	Professeur, Université de Bourgogne Franche-Comté	Examinateur
MANIER MARIE-ANGE	Maître de Conférences HDR, Université de Technologie de Belfort-Montbéliard	Directrice de thèse
MANIER HERVÉ	Maître de Conférences, Université de Technologie de Belfort-Montbéliard	Co-encadrant de thèse
PRODHON CAROLINE	Maître de Conférences HDR, Université de Technologie de Troyes	Examinatrice
QUILLIOT ALAIN	Professeur, Université Clermont Auvergne	Rapporteur
SAUER NATHALIE	Professeur, Université de Lorraine	Rapporteur

N° 2020UBFCA005

ACKNOWLEDGEMENTS

Mes plus sincères remerciements à Marie-Ange MANIER et Hervé MANIER pour m'avoir accepté dans leur équipe, je leur suis très reconnaissant pour m'avoir fait partager leurs compétences scientifiques et humaines et pour leur confiance en mon travail.

Je tiens à remercier les membres du jury d'avoir accepté de juger ce travail et de me donner des remarques constructives qui vont me permettre d'améliorer le manuscrit.

À mes amis et collègues Zaher AL CHAMI et Alexis GODART, merci de leur aide et leur bonne humeur. Ce fut un plaisir de travailler avec vous. Notre amitié est un cadeau.

Cette thèse n'aurait pas été possible sans le soutien financier du CSC (China Scholarship Council).

J'ai à cœur de remercier toute ma famille. Merci à ma femme, mes parents et beaux-parents, mon fils et ma fille. Sans leur support, je n'aurais pas pu mener cette thèse à son terme.

CONTENTS

I

CONTEXT ET PROBLEMS

1

GENERAL INTRODUCTION

1.1/ CONTEXT

With the implementation of the Paris Agreement on November 4, 2016, expectations are growing for hydrogen energy as a dynamic vector. Because the 2°C warming scenario has been established to attain a carbon emission trajectory that limits the concentration of greenhouse gases in the atmosphere, the ability to reduce emissions without jeopardizing economic growth has been the objective pursued by governments and climate change campaigners alike, especially in emerging markets. It is assumed that the utilization of hydrogen not only can enhance the sustainability and reliability of the energy system, but also perform a significant function in the system's flexibility. The International Energy Agency (IEA) (International Energy Agency, 2015) noted that the use of hydrogen could link different energy sectors and energy transportation and distribution (T&D) networks; thus, it could increase the operational flexibility of future low-carbon energy systems. Today's energy system is heavily dependent on fossil fuels; moreover, apart from co-generation (simultaneous production of at least two different forms of energy in the same plant, like electricity and heat), few connections exist among the different T&D systems. In a future system, hydrogen could perform a pivotal function by linking various layers of infrastructures in a low-carbon energy system.

Hydrogen technologies and products have significantly progressed over the years and are currently being established in the market. Generally, the insufficiency of the present infrastructure is considered as one of the barriers to boost the hydrogen economy. Accordingly, large-scale infrastructure investment schemes based on the development of new strategies should be conducted. Moreover, the industry has endeavored to promote the growth of hydrogen consumption. In January 2017, 13 leading companies in energy, transport, and industry launched a global initiative—the "Hydrogen Council"—to express a unified vision and long-term goal for the used of hydrogen to foster energy transition (Brugier et al., 2017). In its new roadmap published in November 2017 (McKinsey & Company, 2017), the Hydrogen Council indicated that by 2050, hydrogen could satisfy

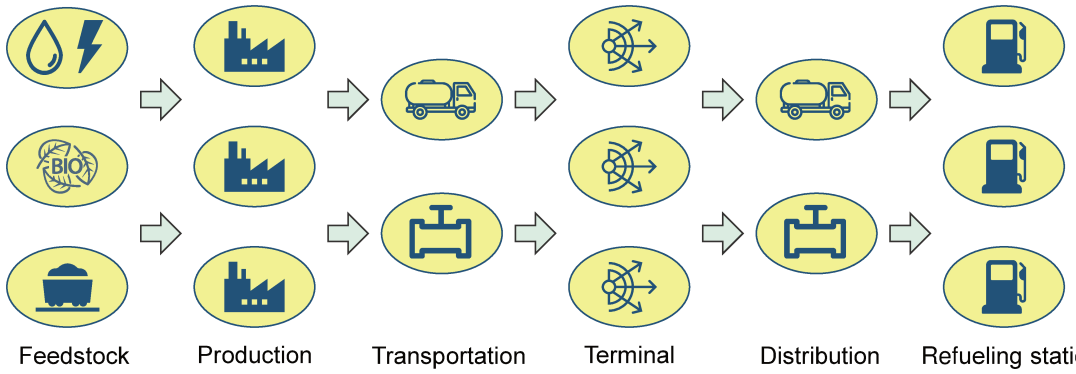

Figure 1.1: Hydrogen supply chain network (HSCN) in the transportation sector

18% of the world's total energy demands and reduce CO_2 emissions in various sectors, such as residential one, transport, and industry, by 40-60%. Moreover, policymakers and researchers continue to investigate the applicability and problems of shifting from an unsustainable carbon-based economy to a sustainable hydrogen-based economy. In general, one of the foremost concerns is the formulation of a strategy that could realize the aforementioned vision; the answers to the following "4W questions" summarizes this strategy. That is, the temporal and spatial decisions to build hydrogen infrastructures—When, Where, at What sizes and with Which technologies (Lin et al., 2008a).

The supply chain network design (SCND), also referred to as the strategic supply chain planning, is one of the most crucial planning problems in the supply chain management (SCM) (Govindan et al., 2017). The concept of the hydrogen supply chain network design (HSCND) is adopted for investigating the deployment of hydrogen infrastructures. The hydrogen supply chain network (HSCN) in the transportation sector is depicted in Fig. 1.1. It begins at the feedstock and ends at the selling of hydrogen at refueling stations. There are multiple choices available at each step of the chain. For instance, water (with electricity), biomass, and coal could be utilized as feedstock for the production process of electrolysis, biomass gasification (BG), and coal gasification (CG), respectively. Thereafter, the hydrogen produced can be transported to terminals via trucks, trains, or pipelines. Various storage solutions can be selected in terminals based on the physical form of hydrogen. There are two primary types of refueling stations: standard and on-site. Because of the inherent characteristics of a supply chain, each part is interconnected rather than isolated. In all types of renewable and sustainable energy, the development of a competitive market requires complex design, planning, and optimization methods. Several optimization methods have already been applied to address this complex design, in particular in the field of renewable and sustainable energy (Banos et al., 2011; De Meyer et al., 2014). The complexity of the problem in the HSCND depends on the modeling of the interactions that exist between the different components of the HSCN. Specifically, the production technologies are dependent on the regionally

specific characteristics of feedstocks; note that storage and transportation modes have strong relationships with the physical form of hydrogen. Moreover, the locations and technologies of refueling stations are significantly impacted by the structure of the hydrogen supply network. The optimization-based approach has been particularly influential in contributing insights into these technological and spatial interactions. After a two-decade development, an increasing number of research studies on the HSCND are now available to provide an understanding of a future HSCN in the transportation sector.

1.2/ OBJECTIVES OF THE THESIS

The main objective of the thesis is to promote the hydrogen infrastructure deployment by providing new strategies based on optimization approaches. Specifically, the classical HSCND model is extended by intercomponent and intertemporal integration planning, respectively:

- *Intercomponent integration planning.* Develop a mixed-integer linear programming (MILP) model that covers the entire hydrogen supply network (from feedstock supply to refueling stations). Through this modeling work, the interactions that exist between different components of a hydrogen supply network are investigated, thus more comprehensive construction plans (strategies) for the HSCN are guaranteed.
- *Intertemporal integration planning.* Propose a location routing model that incorporates activities over strategic and tactical planning horizons. Based on the model, the major trade-off in HSCND which lies between the transportation cost and facility capital cost is analyzed, therefore further insights on the HSCND is gained.

1.3/ OUTLINE OF THE THESIS

Following this brief introduction, the manuscript is composed of four main additional sections. Chapter 2 presents an overview of the research development regarding the use of optimization methods for the hydrogen supply chain network design. Separate sections are dedicated to analyze and classify the selected papers according to system analysis, decision variables, performance measures, uncertainties, and solution approaches. Chapter 3 addresses the intercomponent integration planning of HSCND. The classical HSCND model is integrated with the hydrogen refueling station planning (HRSP) model to generate a new formulation. The advantages of considering various components within a single framework are demonstrated through a case study in Franche-Comté, France. Chapter 4 introduces the intertemporal integration planning of HSCND. A location routing model is presented to determine simultaneously siting of hydrogen refueling stations

(HRSs) and routing decisions for hydrogen delivery trucks. Two metaheuristic algorithms are proposed to solve the model more efficiently, including adaptive large neighborhood search (ALNS) and genetic algorithm (GA). The developed model and algorithms are applied to Bourgogne-Franche-Comté, France. Chapter 5 provides the general conclusions and outlines some plans for future development. Finally, several appendices provide supplementary materials to support the previous sections.

Beforehand, we provide the list of abbreviations that we used in this manuscript:

ABBREVIATIONS

ALNS	adaptive large neighborhood search
BG	biomass gasification
CCS	carbon capture and storage
CG	coal gasification
DP	dynamic programming
FCEV	fuel cell electric vehicle
FCLM	flow-capturing location model
GH_2	gaseous hydrogen
GIS	geographic information system
HRS	hydrogen refueling station
HRSP	hydrogen refueling station planning
HSCN	hydrogen supply chain network
HSCND	hydrogen supply chain network design
IEA	International Energy Agency
LB	lower bound
LCA	life cycle assessment
LCOH	least cost of hydrogen
LH_2	liquid hydrogen
LNOS	list of non-dominated solutions
LP	linear programming
MARKAL	MARKet and ALlocation
MILP	mixed-integer linear programming
OD	origin-destination
SC	supply chain
SCM	supply chain management
SCND	supply chain network design
SMR	steam methane reforming
T&D	transportation and distribution
TIMES	The Integrated MARKAL-EFOM System
UB	upper bound

2

State of Art

This chapter reviews the papers that pertain to the hydrogen supply chain network design (HSCND) models published in scientific journals. Key components of the hydrogen supply chain are first presented; thereafter, the existing models are analyzed and classified based on their decisions, performance measures, uncertainties, solution methodologies, and other model features. As a result, the drawbacks and missing aspects identified in the literature motivate our proposal of a new comprehensive HSCND methodology. Moreover, this chapter ends with the presentation of our critical pre-optimization preparation works.

Contents

PUBLICATIONS

JOURNAL ARTICLES

- Li, L., Manier, H., and Manier, M.-A., (2019). Hydrogen supply chain network design: An optimization-oriented review. *Renewable & Sustainable Energy Reviews (RSER)* 103, 342-360, DOI:10.1016/j.rser.2018.12.060.

COMMUNICATIONS

- Li, L., Manier, H., and Manier, M.-A., Conception de la chaîne d'approvisionnement de l'hydrogène. *Symposium FUTURMOB-17: Préparer la transition vers la mobilité autonome.* Montbéliard, Bourgogne Franche-Comté, France, September 5-7, 2017.

2.1/ INTRODUCTION

The chapter is organized as follows. Three previous review papers on the hydrogen supply chain network design (HSCND) are discussed in Section 2.2. Section 2.3 describes the methodology adopted for the collection of research papers. A classification of the optimization-based studies of HSCND is performed; thereafter, papers are selected for further analysis. In Section 2.4, a detailed system analysis is presented. Modeling approaches and solution methods are explained in Section 2.5. Section 2.6 is a special section that reports on the key pre-optimization preparation works. Particular emphasis is given to data collection and hydrogen demand estimation.

2.2/ PREVIOUS REVIEWS

Limited reviews are available on the HSCND in the literature and have not covered all aspects of the problem it involves. This present review aims at reporting on them and completing this insufficiency. In this section, three previous review papers are analyzed.

Dagdougui (2012) firstly conducted a system analysis of the HSCN, which includes feedstock and production, transportation, and end users. Afterwards, Dagdougui (2012) discussed several hydrogen economy roadmaps that are deployed by different countries as well as conceptualized scenarios, which can be considered as systematic tools to support the HSCND. Dagdougui (2012) classified the approaches for the HSCND into three categories: optimization methods, geographical information system (GIS), and assessment plans toward the transition to a hydrogen infrastructure. The HSCND models in literature are studied, but detailed classification and analysis are not performed from the aspect of decisions, performance measures, and uncertainty problems. Agnolucci et al. (2013b) examined the HSCND studies across spatial scales: national scale studies using energy system models, regional-scale studies that optimize spatially disaggregated hydrogen infrastructure, and local-scale studies that optimize the locating of refueling stations. For the two latter types of studies, Agnolucci et al. (2013b) critically assessed the assumptions made regarding hydrogen demand, which they supposed to be a critical exogenous input into these studies. The unusual perspective (across different spatial scales) enables the authors to conduct a deeper analysis and therefore to provide reasonable research directions. Similarly to the review performed by Dagdougui (2012), detailed classification and analysis through decisions, performance measures, and uncertainty problems are neglected. Moreover, in this review, system analysis is not included. Maryam (2017) reviewed the modeling approaches used in the HSCND for the United Kingdom, and proposed a classification based on optimization approaches, geographical information system (GIS), transition models, and system dynamic approaches. Although the system analysis is provided, it is not comprehensive. Performance measures, such as the minimization of costs and the reduction of environmental impacts, are analyzed. However, decision levels, decision variables, and uncertainty problems are not discussed.

Until now, no comprehensive review of the optimization models for the HSCND problem has yet been performed. Therefore, this chapter aims to analyze and classify the entities and technologies (hydrogen production, transportation, etc.) studied in each model to identify which combinations have been covered or not. A detailed classification is also provided based on factors such as decisions, performance measures, and uncertainty problems to specify the contributions as well as research gaps. Moreover, some critical factors that have been neglected in previous reviews, such as solution methods and key pre-optimization preparation works are also considered in this research.

2.3/ CLASSIFICATION OF REVIEW PAPERS

2.3.1/ SEARCH FOR LITERATURE

A thorough search for related researches over the last decade is implemented to produce a synthesis of the peer-reviewed literature. Papers published in international peer-reviewed journals from the main electronic bibliographical sources (Scopus, Web of Science) are searched by entering keywords, such as hydrogen, supply chain, infrastructure, optimization, and network design in the titles or the topics covered. In all, 71 papers are collected. Figure 2.1 displays the yearly distribution of these papers, which can be found in 16 distinct journals. Most of them have been published in the *International Journal of Hydrogen Energy*; a few could be found in journals of operations research. The latter is certainly surprising because the papers propose optimization models based on operations research methods. These papers are classified according to the following parameters: model type, research object, spatial scale, and whether a full description of the mathematical formulations is included. The individual characteristics of each paper are listed in Tables 2.1 and 2.2. We have observed that linear programming and mixed-integer linear programming (LP/MILP) models are mostly used (totally 68 papers), and only three studies adopted dynamic programming (DP) models. Among the 68 LP/MILP models, 53 are geographical models (GEM), 13 are energy system models (ESM), and 2 involve both. A large portion of the studies (58 papers) tackled the multi-echelon problem (which means including multiple model components: production, transport and refueling stations). This is because one of the significant advantages of the LP/MILP model is accounting for the complex interactions among different echelons. In terms of the spatial scale, the national and regional planning problems received more attention than international and urban problems. It is worth noting that one third studies (24 out of 71) are national scale, geographically explicit, and multi-echelon models with full description. Finally two thirds of the papers provide a full description of the mathematical formulations (46 out of 71).

According to Agnolucci et al. (2013b), these optimization-based HSCND models could further be grouped into three main categories (Table 2.3).

Energy system optimization models. These models use the LP/MILP to identify the energy system that meets energy service demands at minimal cost. They can be implemented at different spatial scales, i.e., international, national, or regional ones. Energy system models typically include a detailed HSCND with the representation of various feedstocks, hydrogen production technologies, and transportation modes. Hydrogen end-use technologies compete with others (such as battery electric vehicles) to meet energy service demands (such as demands for car transport); thus, hydrogen demand and supply are both endogenously optimized (Agnolucci et al., 2013b). The MARKAL/TIMES

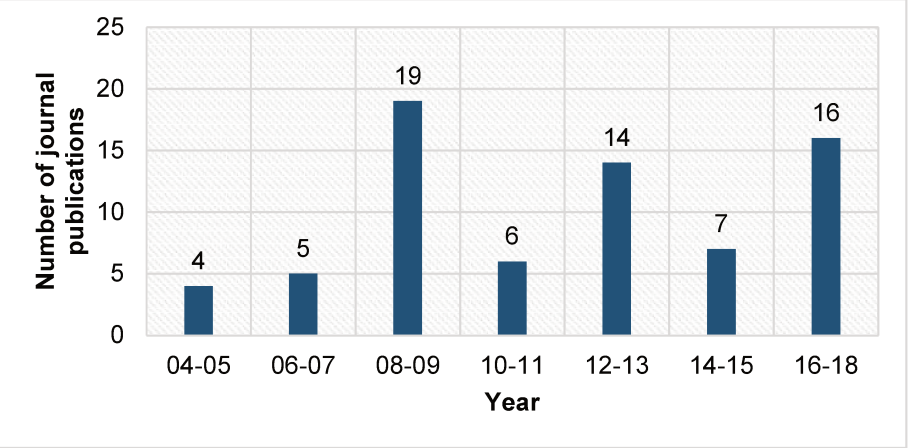

Figure 2.1: Distribution of papers (up to June 2018)

family is the most represented among the energy system models. MARKAL is a demand-driven multi-period LP model of energy supply and demand (Rath-Nagel et al., 1982) (TIMES is a successor of MARKAL). It was developed by the IEA's Energy Technology Systems Analysis Program in the 1980s. The MARKAL/TIMES model has been adopted to evaluate the role of hydrogen within an energy system in China (Rits et al., 2004), the United States (Tseng et al., 2005; Yeh et al., 2008), the United Kingdom (Strachan et al., 2009; Winskel et al., 2009), Italy (Contaldi et al., 2008), Spain (Contreras et al., 2009), Norway (Rosenberg et al., 2010), Japan (Endo, 2007), and at international scales (Gül et al., 2009).

Geographically explicit optimization models. These models consider the entire HSCN and run at a national or a regional scale. Unlike energy system models, geographically explicit models focus on the deployment of hydrogen infrastructures. Binary and integer decision variables are employed to cope with the location of facilities, sizing decisions, selection of suitable production technologies, and selection of transportation modes among facilities. Because product flows along the supply chain are modeled by continuous constraints, these models are often mixed-integer formulations (Eskandarpour et al., 2015). For instance, Almansoori et al. (2006) established a steady-state "snapshot" model that integrates multiple components, such as production, storage, and transportation within a single framework; Great Britain was selected as case study. Subsequently, Almansoori et al. (2009) extended their study by considering the availability of feedstocks and their logistics, as well as the variation of hydrogen demand over a long-term planning horizon leading to a phased infrastructure development. Samsatli et al. (2016) developed a general spatio-temporal model that determines the optimal HSCN structure and its operation; the long-term planning horizon and short-term dynamics are simultaneously considered. The spatial distribution and temporal variability of hydrogen demands and wind availability are considered in detail in the model. The objective is the minimization of the total network cost, subject to satisfying all the demands of the domestic transport sector in

Table 2.1: Individual characteristics of optimization-based models for HSCND (Part 1)

	Model type			Research object				Spatial scale				Full description	
	DP	LP / MILP		Multi-E	Mono-E			I	N	R	U	Yes	No
		ESM	GEM		P	T	RS						
Rits et al. (2004)		•		•					•				•
Hugo et al. (2005)			•	•									•
Johnson et al. (2005)			•	•						•			•
Tseng et al. (2005)		•		•					•				•
Almansoori et al. (2006)			•	•					•			•	
Brey et al. (2006)			•	•					•			•	
Lin et al. (2006)	•			•							•	•	
Ball et al. (2007)			•	•					•				•
Endo (2007)		•		•					•				•
Contaldi et al. (2008)		•		•					•				•
Ingason et al. (2008)			•		•				•			•	
Kim et al. (2008a)			•	•					•			•	
Kim et al. (2008b)			•	•					•			•	
Krzyzanowski et al. (2008)		•		•				•					•
Li et al. (2008)			•	•					•				•
Lin et al. (2008b)			•				•			•		•	
Lin et al. (2008a)	•			•						•		•	
Qadrdan et al. (2008)	•			•					•			•	
Yeh et al. (2008)		•		•					•				•
Almansoori et al. (2009)			•	•					•			•	
Bersani et al. (2009)			•				•			•		•	
Contreras et al. (2009)		•		•						•			•
Gül et al. (2009)		•		•				•					•
Hajimiragha et al. (2009)			•		•					•		•	
Kamarudin et al. (2009)			•	•					•			•	
Kuby et al. (2009)			•				•			•		•	
Strachan et al. (2009)		•		•					•				•
Winskel et al. (2009)		•		•					•				•
Guillén-Gosálbez et al. (2010)			•	•					•			•	
Parker et al. (2010)			•	•						•		•	
Rosenberg et al. (2010)		•	•	•					•				•
Sabio et al. (2010)			•	•					•			•	
Stephens-Romero et al. (2010)			•				•				•		•
Konda et al. (2011)			•	•					•			•	
Almansoori et al. (2012)			•	•					•			•	
Brey et al. (2012)			•				•			•			•

ESM, energy system model; GEM, geographically explicit model; Multi-E, multi-echelon; Mono-E, mono-echelon; P, production; T, transportation; RS, refueling station; I, international; N, national; R, regional; U, urban.

Great Britain.

Hydrogen refueling station planning (HRSP) models. The construction of refueling infrastructures is one of the most formidable barriers to the transition to a hydrogen-based road transportation system (National Research Council, U.S., 2004). Given the high cost of building new refueling stations, it is essential to coordinate the locations of initial stations in a network to facilitate a maximal consumer utilization (Kuby et al., 2009). Based on the classical facility location models, a number of new models have been developed to optimize a network of hydrogen refueling stations in a relatively small geographical space, generally a big city, or sometimes, a state (region). For example, Lin et al. (2008b) developed a locating method where station siting is treated as a “fuel-travel-back” problem, and

Table 2.2: Individual characteristics of optimization-based models for HSCND (Part 2)

	Model type			Research object				Spatial scale				Full description	
	DP	LP / MILP		Multi-E	Mono-E			I	N	R	U	Yes	No
		ESM	GEM		P	T	RS						
Dagdougui et al. (2012)			•	•						•		•	
Gim et al. (2012)			•			•			•			•	
Han et al. (2012)			•	•					•			•	
Johnson et al. (2012)			•	•						•		•	
Konda et al. (2012)			•	•					•				•
Sabio et al. (2012)			•	•					•			•	
Agnolucci et al. (2013a)			•	•					•			•	
Almaraz et al. (2013)			•	•					•			•	
André et al. (2013)			•			•			•			•	
Balta-Ozkan et al. (2013)		•	•	•					•				•
Han et al. (2013)			•	•					•			•	
Yang et al. (2013)		•		•						•			•
Almaraz et al. (2014)			•	•						•		•	
Amoo et al. (2014)		•		•					•				•
André et al. (2014)			•			•			•				•
Dayhim et al. (2014)			•	•						•		•	
Krishnan et al. (2014)			•	•					•				•
Almaraz et al. (2015)			•	•					•			•	
Nunes et al. (2015)			•	•					•			•	
Almansoori et al. (2016)			•	•					•			•	
Cho et al. (2016)			•	•					•			•	
Kim et al. (2016)			•	•					•			•	
Samsatli et al. (2016)			•	•					•			•	
Sgobbi et al. (2016)		•		•				•					•
Woo et al. (2016)			•	•						•		•	
He et al. (2017)			•				•			•		•	
Hwangbo et al. (2017)			•	•					•			•	
Kim et al. (2017)			•	•						•		•	
Moreno-Benito et al. (2017)			•	•					•			•	
Sun et al. (2017)			•				•			•		•	
Won et al. (2017)			•	•						•		•	
Biqué et al. (2018a)			•	•					•				•
Biqué et al. (2018c)			•	•					•			•	
Lahnaoui et al. (2018)			•			•				•		•	
Ogumerem et al. (2018)			•	•						•		•	

ESM, energy system model; GEM, geographically explicit model; Multi-E, multi-echelon; Mono-E, mono-echelon; P, production; T, transportation; RS, refueling station; I, international; N, national; R, regional; U, urban.

Table 2.3: Three main types of HSCND models

	Research object	Spatial scale
Energy system optimization models	Entire HSCN	International/National/Regional
Geographically explicit optimization models	Entire HSCN	National/Regional
Refueling station locating models	Part of HSCN	Urban

the only required input is the distribution of vehicle miles traveled. The model was applied to derive an optimal station roll-out scheme for Southern California. Kuby et al. (2005)

introduced the “Flow-Refueling Location Model” that locates alternative fuel stations to refuel a maximum volume of vehicle flows. The model was used to investigate strategies for initial hydrogen refueling infrastructure deployment in Florida (Kuby et al., 2009). Bersani et al. (2009) presented a model for planning a refueling station network of a given company within a competitive framework; the model was tested in a specific territory in northern Italy. He et al. (2017) created a hydrogen refueling station-siting optimization model for hydrogen energy expressway construction based on the energy life cycle cost analysis of hydrogen. Sun et al. (2017) determined optimal station construction locations on condition of multi-source hydrogen supply. A particle swarm optimization algorithm was created for the station location problem along the Shanghai-Nanjing Expressway in eastern China.

2.3.2/ SELECTION OF PAPERS FOR FURTHER ANALYSIS

After this first study of the literature, the papers are filtered for a detailed investigation as described in the following sections. Based on the purpose of this chapter, the following criteria are established: (i) the models in the papers must consider the entire HSCN as the research object; (ii) they must include definitions of objective functions, decision variables, and constraints; (iii) explicit description of mathematical formulation must be offered. Based on the first criterion, some articles that only partially consider the HSCN are excluded. This is the case for studies that only deal with refueling station-location problems and for those that focus on the problem of hydrogen production and transportation (André et al., 2013; Lahnaoui et al., 2018). The second and third criteria enable us to filter the studies that adopt the energy system model and several other papers that provide limited information on the model used in the analysis; examples of these are the works of Ball et al. (2007), Biqué et al. (2018a), Hugo et al. (2005) and Li et al. (2008). Finally, 32 papers remain identified and denoted as *reference papers*. The tool HistCite (Garfield et al., 2004) is used to examine the citational relationships among the reference papers. It is found that the work of Almansoori et al. (2006) is the seminal paper in this branch of the literature. This paper has been a source of inspiration for other reference papers, which have attempted to improve it through multiple modifications (Agnolucci et al., 2013b). As summarized in Table 2.4, these modifications have been classified into four categories. More detailed model characteristics are discussed in following sections. In this table, the modifications conducted in each reference paper in each year are briefly described to reveal the strong connections among the reference papers. This confirmed the paper selection and motivated us to investigate the role of the optimization-based approach in the HSCND by examining the characteristics of this *model group*.

All the mathematical models built in the studies reported in the reference papers are MILP-based and focus on the deployment of hydrogen in the transportation sector. The

Table 2.4: Four types of modifications of Ref. (Almansoori et al., 2006) performed in reference papers

Year	Multi-objective optimization	Multi-period optimization	Introducing uncertainty	Integration with other supply chains*
2008	(1)			
2009			(2)	
2010	(3)	(4)	(5)	
2011		(6)		
2012	(7)		(8)	
2013	(9), (10)			(11)
2014	(12)	(12)	(13)	
2015	(14)	(14)	(15)	
2016		(16)		(17), (18), (19), (20)
2017	(21)	(21)		(22), (23)

(1), (Kim et al., 2008b); (2), (Kim et al., 2008a); (3), (Guillén-Gosálbez et al., 2010); (4), (Almansoori et al., 2009); (5), (Sabio et al., 2010); (6), (Konda et al., 2011); (7), (Sabio et al., 2012); (8), (Almansoori et al., 2012); (9), (Han et al., 2013); (10), (Almaraz et al., 2013); (11), (Agnolucci et al., 2013a); (12), (Almaraz et al., 2014); (13), (Dayhim et al., 2014); (14), (Almaraz et al., 2015); (15), (Nunes et al., 2015); (16), (Moreno-Benito et al., 2017); (17), (Ball et al., 2007); (18), (Kim et al., 2016); (19), (Woo et al., 2016); (20), (Cho et al., 2016); (21), (Ogumerem et al., 2018); (22), (Won et al., 2017); (23), (Hwangbo et al., 2017).
* the term “other supply chains” refers to, for example, biomass supply chain, utility supply network, and wind power generation system.

key modeling features (i.e., system analysis, modeling approaches, and solution methods) are analyzed in the following two sections.

2.4/ SYSTEM ANALYSIS

Diwekar (2008) assesses that optimization involves several steps; the first step is to understand the system. The robustness of an HSCND model is based on the degree of understanding the real system. The descriptive superstructure of an HSCN in the transportation sector is illustrated in Fig. 2.2. In this section, we examined each key component of the system to identify the entities and technologies that have been considered in the HSCND models. The aspects that require more attention are also identified.

2.4.1/ FEEDSTOCK

Hydrogen is not an energy source; it is an energy carrier, which is produced by various feedstocks (Ren et al., 2013). Natural gas, coal, biomass, and water (with electricity from the local power grid) are the feedstocks found in most of the research projects (Agnolucci et al., 2013a; Almansoori et al., 2012; Kim et al., 2008a,b; Nunes et al., 2015). Because some concepts, such as low-carbon electrolytic hydrogen and CO_2-free HSCN

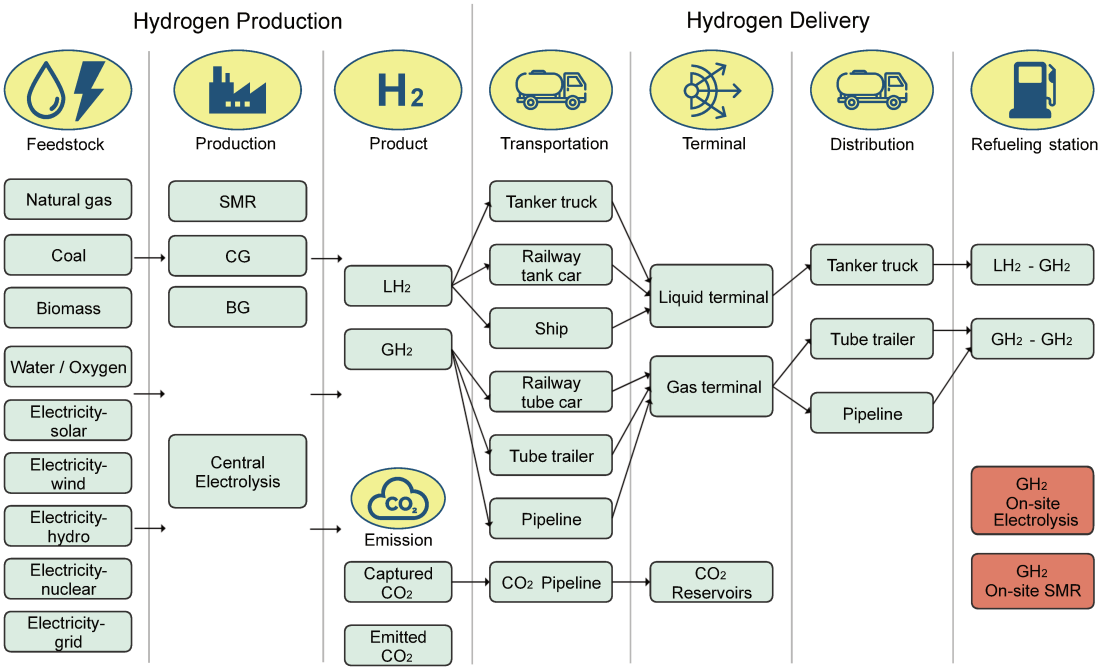

Figure 2.2: Superstructure of HSCN in the transportation sector (adapted from Moreno-Benito et al. (2017))

has gained increasing attention in the post-Paris Agreement era, renewable sources have become more popular (Abbasi et al., 2011; Chattanathan et al., 2012). Figure 2.3 shows that in addition to the traditional source (power grid), some other sources of electricity have also been considered; several models include renewable energy-based electricity. For instance, Kim et al. (2017) designed a wind-based hydrogen system. Won et al. (2017), and Kim et al. (2016) focused on the renewable energy source-based hydrogen supply system, in which the biomass, solar electricity, and wind power were selected. Almaraz et al. (2014) included four sources of electricity: solar, wind, hydro-power, and nuclear. Regarding the nuclear source, a more recent paper (Cany et al., 2017) discussed the possibility of adopting the French nuclear fleet to achieve a massive production of low-carbon hydrogen.

The feedstock, which is the first echelon of a HSCN, has not received due attention. Indeed, in several studies (e.g., Almansoori et al., 2006; Kim et al., 2008a,b; Sabio et al., 2010), the feedstock problem is excluded in the model. Only the feedstock purchasing cost is considered as part of the unit production cost; the origin (or availability), storage, and transport of feedstock have been significantly simplified or even completely ignored. In fact, the initial availability of feedstock has a significant function in the HSCND because of the dependence of hydrogen supply on the regionally specific resource characteristics (International Energy Agency, 2015). FMoreover, for some types of feedstocks (for example, coal and biomass), storage and transport become non-negligible factors. Never-

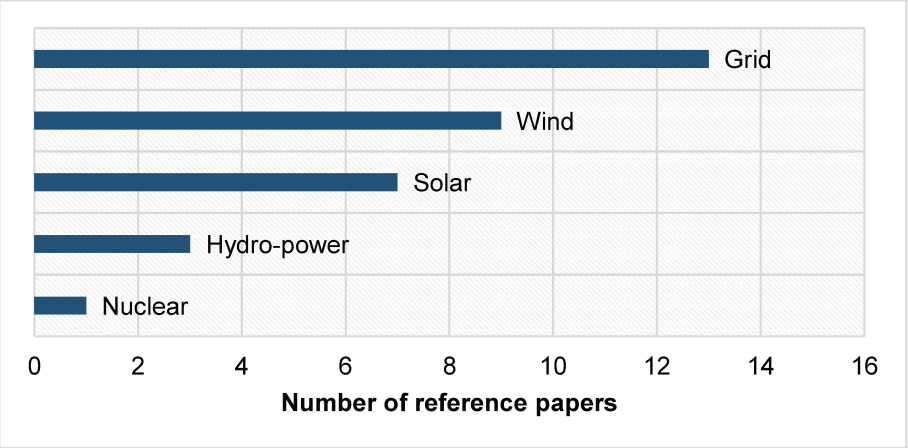

Figure 2.3: Sources of electricity

theless, considerably few studies consider these two factors. One of these studies is the work of Cho et al. (2016), in which a biomass warehouse, including handling and drying processes, is used to store biomass and maintain its properties (e.g., humidity and size). It should also be noted that water, as the main feedstock of the electrolysis process, has not been explicitly represented in several models, which integrate the feedstock echelon. Only the works of Ogumerem et al. (2018) and Won et al. (2017) involved water availability and cost in their models. To be more comprehensive, oxygen could also be included because it is a key feedstock of the gasification process (CG or BG).

2.4.2/ HYDROGEN PRODUCTION

Steam methane reforming (SMR), biomass gasification (BG), coal gasification (CG), and central electrolysis are the four primary production technologies adopted by the studies reported in the reference papers. The selected production approaches for each model are listed in Table 2.5. Nowadays, a considerable portion of hydrogen is produced by means of the SMR, which is currently the most inexpensive production method (Dominković et al., 2017). Hydrogen from biomass is the only direct way to produce hydrogen from renewable energy without the use of complex technology. However, because its primary feedstock availability is limited, biomass production will not benefit from large-scale economies (International Energy Agency, 2007). Coal gasification is regarded to have a significant potential because coal is less expensive than natural gas and biomass in many countries and regions. Moreover, CG plants include the second lowest capital and operating costs among the available production options (Almansoori et al., 2016). As for electrolysis, although the processes are more expensive, it could be a pivotal technology to achieve a more extensive deployment of low-carbon footprint hydrogen in the energy system. For recent reviews on hydrogen production processes, interested readers should refer to (Nikolaidis et al., 2017; Hosseini et al., 2016; Dincer et al., 2015). Two tendencies asso-

ciated with production technology are identified, as discussed below: CCS and on-site production.

Table 2.5: Production technologies simultaneously considered in the literature

4 technologies	**13 papers:**
SMR+CG+BG+Electrolysis	(6), (11), (15), (16), (17), (19), (20), (23), (24), (25), (26), (29), (30)
3 technologies	**6 papers:**
SMR+CG+BG	(1), (2), (3), (10)
SMR+CG+Electrolysis	(21)
SMR+BG+Electrolysis	(5)
2 technologies	**6 papers:**
SMR+Electrolysis	(4), (9), (12)
BG+Electrolysis	(7), (18), (32)
1 technology	**7 papers:**
SMR	(13)
CG	(14)
BG	(8), (22), (31)
Electrolysis	(27), (28)

(1), (Almansoori et al., 2016); (2), (Almansoori et al., 2006); (3), (Almaraz et al., 2013); (4), (Almaraz et al., 2014); (5), (Almaraz et al., 2015); (6), (Biqué et al., 2018c); (7), (Brey et al., 2006); (8), (Cho et al., 2016); (9), (Dayhim et al., 2014); (10), (Guillén-Gosálbez et al., 2010); (11), (Han et al., 2012); (12), (Han et al., 2013); (13), (Hwangbo et al., 2017); (14), (Johnson et al., 2012); (15), (Kamarudin et al., 2009); (16), (Kim et al., 2008b); (17), (Kim et al., 2008a); (18), (Kim et al., 2016); (19), (Ogumerem et al., 2018); (20), (Sabio et al., 2010); (21), (Sabio et al., 2012); (22), (Woo et al., 2016); (23), (Agnolucci et al., 2013a); (24), (Almansoori et al., 2009); (25), (Moreno-Benito et al., 2017); (26), (Konda et al., 2011); (27), (Kim et al., 2017); (28), (Samsatli et al., 2016); (29), (Almansoori et al., 2012); (30), (Nunes et al., 2015); (31), (Parker et al., 2010); (32), (Won et al., 2017).

- *Combining carbon capture and storage (CCS) with production plants.*

Hydrogen production plants, especially the large SMR and CG plants, are the primary sources of carbon emissions within the global supply chain. As noted by the International Energy Agency (2016), the CCS is the only technology capable of delivering significant emission reductions from the use of fossil fuels in power generation and industrial applications. Therefore, the combination of the CCS and hydrogen production plant serves as the solution to achieve specific carbon emission targets or avoid carbon tax penalties (Almansoori et al., 2016). Some studies introduced the CCS into their models, as listed in Table 2.6. Almansoori et al. (2016) evaluated the potential storage options for Germany; these storage options are considered as decision variables of the HSCND under emission constraints. Moreno-Benito et al. (2017) discussed the transportation problem related to

the captured carbon emissions. They noted that hydrogen production from natural gas through the SMR with the CCS is supposed to be the most cost-effective alternative that maintains a low level of carbon emissions. The International Energy Agency (2015) found that for countries such as China or India, the development of hydrogen technologies in combination with the CCS cou ld be attractive in the conversion of the abundant domestic fossil resources into low-carbon transport fuels. Additionally, Baufumé et al. (2011) indicated that the possible spatial separation of electricity generation and centralized fossil hydrogen production with the CCS allow an additional degree of freedom in the energy system in enabling the transport of hydrogen instead of electricity transmission.

- *On-site production.*

The on-site (also known as forecourt) SMR and electrolysis are considered in several studies (Table 2.6). One of the huge barriers to the deployment of hydrogen infrastructures in urban areas is the scarcity of land. Installing on-site hydrogen production equipment in existing gasoline stations is expected to facilitate the deployment of an HSCN (Katikaneni et al., 2014).

It is to remark in Table 2.6 that only two papers consider both CCS system and on-site production. They are written in bold in this table.

Table 2.6: CCS (carbon capture and storage) and on-site production

CCS (SMR+CG+BG)	(Agnolucci et al., 2013a), **(Konda et al., 2011)**, (Moreno-Benito et al., 2017)
CCS (SMR+CG)	(Almansoori et al., 2016), (Sabio et al., 2010)
CCS (SMR)	**(Han et al., 2013)**
CCS (CG)	(Johnson et al., 2012)
On-site (SMR+Electrolysis)	(Almansoori et al., 2012), **(Konda et al., 2011)**
On-site (Electrolysis)	**(Han et al., 2013)**, (Kim et al., 2017)

2.4.3/ HYDROGEN TERMINAL AND STORAGE

The terminal for hydrogen is envisioned to be similar to current gasoline terminals, where the gasoline is stored, loaded onto trailers, and delivered to stations. In the case of hydrogen, a liquid terminal includes liquid hydrogen storage, high-pressure cryogenic pumps, and equipment for loading liquid hydrogen onto trucks. A gaseous terminal is composed of compressed gas storage, compressors, and equipment for loading the hydrogen onto tube trailers (Ringer, 2006). A hydrogen terminal, which links transportation and distribution (T&D), performs a vital function in the hydrogen delivery pathway (Elgowainy et al., 2015). As reported by the reference papers, however, the terminal has not been incorporated into the HSCN because several studies do not consider hydrogen distribution; this

is discussed in a later section. In models that do not include the T&D, the storage facility is utilized as the terminal. However, storage is merely one of the functions of the terminal. Accordingly, it is suggested that the hydrogen terminal should be explicitly included in the HSCN models; consequently, a comprehensive HSCN could be built.

Hydrogen storage is used to accommodate production plant outages and demand fluctuations. Three different levels of storage in the HSCN are summarized in Table 2.7. Most studies reported by the reference papers only consider the terminal level storage, whereas the stations and network levels of storage have received limited attention. However, the inclusion of all the three levels of storage into the model is of utmost importance when renewable electricity serves as the feedstock. Specifically, the HSCN models that are based on hydrogen, which is produced by electrolysis, require additional seasonal hydrogen storage capacities to close the gap between fluctuations in renewable generation from surplus electricity and refueling station demand (Reuß et al., 2017). Moreover, as large quantities of fluctuating renewable electricity are introduced in the energy mix, the use of underground hydrogen storage as an approach to store energy and solve the problem of grid balancing has received increasing interest in recent years (The HyUnder project, 2015). Several technico-economic studies have been implemented to investigate the network level storage of the HSCN (Ringer, 2006; Elgowainy et al., 2015; Le Duigou et al., 2017; Reuß et al., 2017). The spatio-temporal optimization model developed by Samsatli et al. (2016) covered all the three levels of storage and demonstrated their function through a case study. The model showed that storage is the key enabling technology to use intermittent energy and to satisfy the temporally and spatially distributed demands.

Table 2.7: Three levels of storage in HSCN

Storage level	Main purpose	Equipment or facility	Installation place
Station level	Accommodate daily demand fluctuation	Cascade filling system	Refueling station
Terminal level	Provide extra capacity in the course of a facility shut-down	Compressed gas hydrogen storage tubes/bulk liquid hydrogen storage	Terminal or production plant
Network level	Accommodate seasonal demand fluctuation	Gaseous hydrogen geologic storage	Along with a pipeline

2.4.4/ HYDROGEN TRANSPORTATION

Hydrogen can be transported as liquid or compressed gas. Liquefied hydrogen can be transported in tankers via railways, roads, or ships, whereas gaseous hydrogen may be conveyed via high-pressure pipelines, tube trailers, or railway tube cars. As shown

in Fig. 2.4, tanker trucks, tube trailers, and pipelines are the top three most selected transportation modes. The primary factors that impact the choice of hydrogen transport modes are the hydrogen demand profile (i.e., when and where will the hydrogen demand arise and the amount of demand) and the distance from the production site to delivery points (Lahnaoui et al., 2018). When the hydrogen demand is relatively low, in most cases, compressed-gas trucks are chosen as the optimal delivery mode (Parker et al., 2010). However, an increase of the fuel delivery traffic within urban areas due to the delivery of hydrogen cannot be ignored. Parker et al. (2010) noted that, although it is not probable that hydrogen deliveries by liquid trucks would increase the number of truck trips, the figure would increase more than tenfold if compressed-gas trucks are selected.

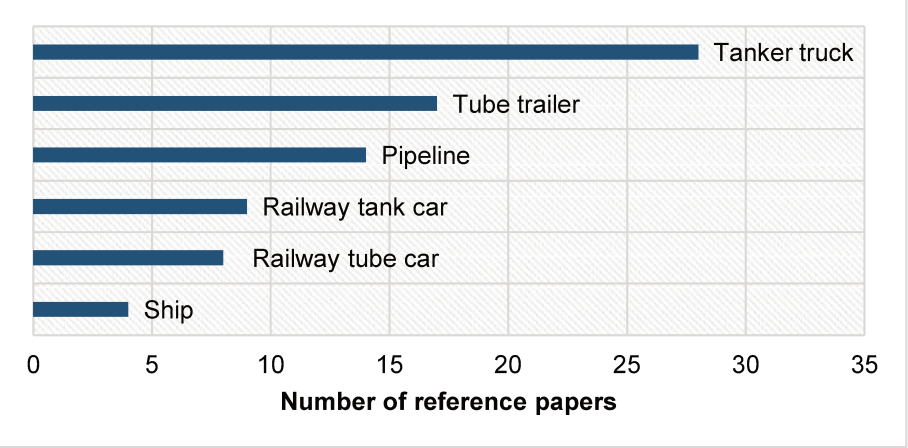

Figure 2.4: Transportation modes

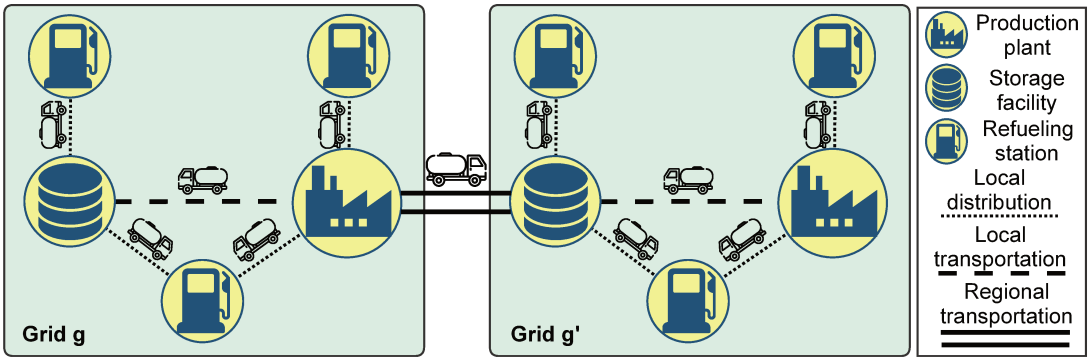

Figure 2.5: Scope definition of hydrogen transportation system

Three particular levels could be identified in hydrogen transportation systems (Almansoori et al., 2006, 2009, 2012): regional transportation, local transportation, and local distribution. The scope definition is schematized in Fig. 2.5. Regional transportation is managed among different regions (grids); local transportation and local distribution are within the region (grid). The former is conducted between production sites and terminals, whereas the latter is performed between refueling stations and terminals. Because the inclusion

of more levels would increase the model's complexity, most of the studies reported by the reference papers only considered one level (regional transportation); a few contained two levels, and only three included all the three levels, as listed in Table 2.8.

Table 2.8: Transportation system

Regional transportation	(1), (2), (3), (4),(5), (6), (7), (8), (9), (10), (11), (12) (13), (14), (15), (16), (17), (18), (19), (20), (21), (22)
Regional transportation /Local transportation	(23), (24), (25)
Regional transportation /Local distribution	(26), (27), (28)
Regional transportation /Local transportation /Local distribution	(29), (30), (31)

(1), (Almansoori et al., 2016); (2), (Almansoori et al., 2006); (3), (Almaraz et al., 2013); (4), (Almaraz et al., 2014); (5), (Almaraz et al., 2015); (6), (Biqué et al., 2018c); (7), (Brey et al., 2006); (8), (Cho et al., 2016); (9), (Dayhim et al., 2014); (10), (Guillén-Gosálbez et al., 2010); (11), (Han et al., 2012); (12), (Han et al., 2013); (13), (Hwangbo et al., 2017); (14), (Johnson et al., 2012); (15), (Kamarudin et al., 2009); (16), (Kim et al., 2008b); (17), (Kim et al., 2008a); (18), (Kim et al., 2016); (19), (Ogumerem et al., 2018); (20), (Sabio et al., 2010); (21), (Sabio et al., 2012); (22), (Woo et al., 2016); (23), (Agnolucci et al., 2013a); (24), (Almansoori et al., 2009); (25), (Moreno-Benito et al., 2017); (26), (Konda et al., 2011); (27), (Kim et al., 2017); (28), (Samsatli et al., 2016); (29), (Almansoori et al., 2012); (30), (Nunes et al., 2015); (31), (Parker et al., 2010).

2.4.5/ HYDROGEN REFUELING STATION

According to Netinform (2018), 328 hydrogen refueling stations are currently in operation—139 in Europe, 119 in Asia, 68 in North America, 1 in South America, and 1 in Australia. There are two basic types of hydrogen refueling stations: stations in which the hydrogen is produced elsewhere and delivered to the station for local storage and dispensing to fuel-cell electric vehicles (FCEVs), and stations in which hydrogen is produced, and stored on site, ready for transfer to in-vehicle hydrogen storage (Alazemi et al., 2015). As depicted in Fig. 2.6, stations that rely on delivery can be supplied with liquid or gaseous hydrogen through appropriate distribution techniques. For on-site stations, the most popular production technologies are on-site electrolysis and on-site SMR. On-site electrolysis with grid power is the most widely used technology in North America, followed by the hydrogen delivery technique. In Europe, hydrogen delivery techniques are the most common, followed by stations that produce hydrogen on-site using renewable energy (Alazemi et al., 2015). Less than one-third of the studies in the reference papers considered refueling station problems in their models.

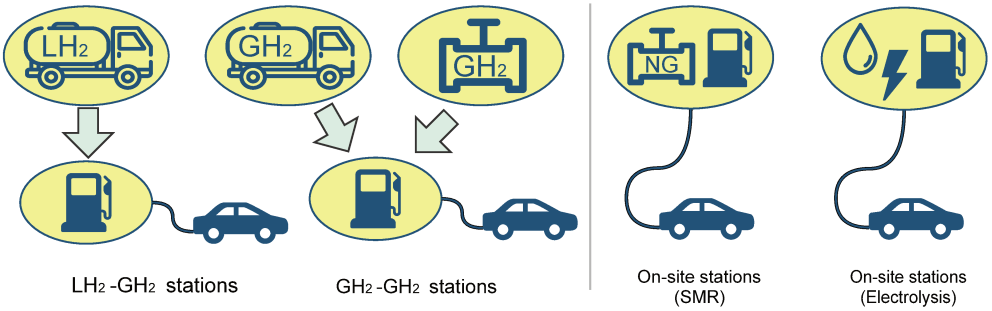

Figure 2.6: Two basic types of hydrogen refueling stations

2.4.6/ SUMMARY

It can be concluded that most of hydrogen facilities, technologies, and their combinations have been well-considered and represented in the HSCND models. However, there are specific factors that have been ignored. For instance, feedstock problems deserve further attention, and hydrogen terminals and seasonal storage should be included in the models. Moreover, for the entire delivery system, modeling an HSCN based on "alternative hydrogen carriers" (such as metal hydrids, chemical hydrids, high surface area carbon sorbents, and liquid-phase hydrocarbons) is encouraged. Although these alternative carriers have not been put into practical use, they certainly have high potentials. Compared with some technico-economic analyses, which limit the research area within the delivery system (Hooks, 2008; Reuß et al., 2017), the HSCND models could provide more insights into the gains and losses when an alternative carrier is utilized.

2.5/ MODELING AND SOLUTION METHODS

2.5.1/ DECISIONS AND PLANNING TIME HORIZON

In the supply chain management, planning decisions can be categorized into three levels called (i) strategic, (ii) tactical, and (iii) operational, depending on the time horizon (Mula et al., 2010). Strategic decisions refer to the location of facilities, the capacity of these facilities, the geographical customer areas to serve, as well as the transportation means (ships, trucks, railway, etc.) to use. Given the structure of the supply chain, tactical planning (also known as *master planning*) determines the most efficient approach to fulfill demand forecasts over a medium-term planning interval, which often covers a full seasonal cycle (Stadtler, 2005). Operational decisions are short-term decisions which are adjusted more frequently in correspondence with the current external and internal conditions (Yue et al., 2014).

The HSCND decisions belong to the first category (strategic-level) because they must be made immediately (Klibi et al., 2010) and cannot be changed in the short term. A planning interval of several years or decades may be assumed when designing the HSCN. Therefore the HSCND decisions have long-term effects on the entire supply chain.

2.5.1.1/ STRATEGIC DECISIONS IN THE HSCND

An overview of strategic decision variables in the HSCND models reported by the reference papers is presented in Fig. 2.7. Facility location decisions perform a critical function in the strategic SCND (Melo et al., 2009). In the HSCND models, location decisions are often represented by the number (integer variable) of a certain type of facility in each region (grid).

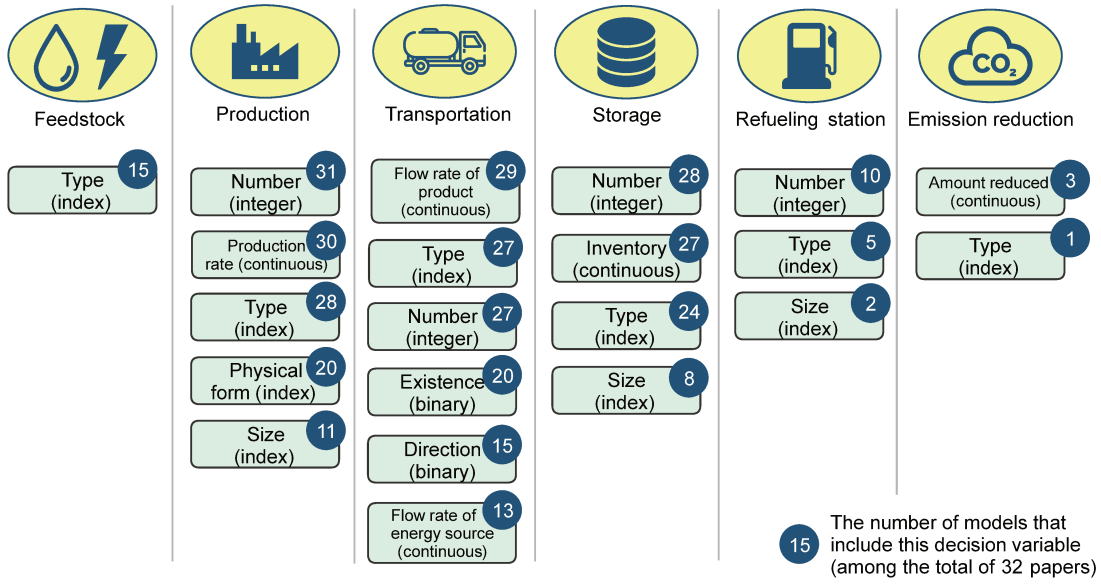

Figure 2.7: Strategic decision variables in HSCND models

Melo et al. (2009) indicated the importance of explicitly integrating the raw material problems into the SCND. This aspect, however, has not received sufficient attention. In several HSCND models, the type of feedstock is preselected according to the production technology examined (Almansoori et al., 2009). A mechanism should be developed to mathematically select the best type of feedstock, its quantity, and the distribution within the network; only a few studies introduced such a mechanism (Almansoori et al., 2009, 2012; Almaraz et al., 2014; Kim et al., 2017; Parker et al., 2010; Woo et al., 2016). According to these studies, the feedstock problem includes two essential aspects: feedstock availability and transportation.

In a significant portion of the studies, the decision to base a HSCN is based on liquid

hydrogen (LH_2) or gaseous hydrogen (GH_2) is determined subjectively through the definition of scenarios or configurations. The studies of Agnolucci et al. (2013a) and Han et al. (2012) are the only two investigations in which the separation between LH_2 and GH_2 is determined endogenously (i.e., acting as a decision variable in the model) rather than assumed exogenously (i.e., a priori).

Less than a third of the studies reported by the reference papers considered decision variables that are related to refueling station problems. Among those studies, only four determined the number of refueling stations (Almansoori et al., 2012; Almaraz et al., 2014, 2015; Nunes et al., 2015), three considered the number and type of stations (Kim et al., 2017; Konda et al., 2011; Moreno-Benito et al., 2017), and two included the three properties of a refueling station, i.e., number, type, and size (Agnolucci et al., 2013a; Woo et al., 2016). The International Energy Agency (2015) argued that identifying the optimal size of a station is a critical step. Certainly, the problem of station size is related to the utilization rate, which is undeniably important to the financial viability of a station, especially in the initial deployment phase. As proposed by the International Energy Agency (2015), considerably smaller stations might be necessary in the initial phase to achieve extensive coverage, as they could satisfy basic necessities while avoiding excessive underutilization.

It should be emphasized that no reference paper has ever reported on the facility location problem of refueling stations. This is possibly because the spatial scales considered in the studies are different. The reference papers report on whole nations or large regions, whereas the refueling station location problem typically focuses on a city or a relatively small area. Another explanation may be that the bases of hydrogen demand estimation differ. The studies reported by the reference papers consider the population and the penetration of the fuel cell electric vehicles (FCEVs) as the base material to estimate and allocate hydrogen demand. On the other hand, the refueling station location problem generally estimates hydrogen demand according to the traffic volume and its distribution (Kuby et al., 2009; De Vries et al., 2017).

2.5.1.2/ MULTI-PERIOD MODEL AND CAPACITY EXPANSION

Multi-period planning problems have been proposed to address situations in which parameters predictably change over the time. The objective is to adapt the configuration of facilities to these parameters. Thereby, a planning horizon that is divided into several time periods is usually considered (Melo et al., 2009). The model established by Almansoori et al. (2006), which is regarded as a seminal work, is mono-period (snapshot). In their subsequent studies, Almansoori et al. (2009, 2012) extended the model to the multi-period case. As listed in Table 2.9, half of the models choose the mono-period option;

the remaining half of the models select the multi-period one. Because the amount of hydrogen demand in each area changes over time, the ability to evolve is indispensable in an HSCN. Moreover, the multi-period model enables the consideration of the reduction in the cost of production and transportation technologies by considering the experience accumulated with time (known as the learning rate) (Almansoori et al., 2012; Brey et al., 2006).

Table 2.9: Distribution of studies in reference papers with respect to the objective and the period

Mono-period/Mono-objective	(1), (2), (6), (8), (11), (13), (14), (15), (17), (22), (27) (31), (32)
Mono-period/Multi-objective	(3), (12), (16)
Multi-period/Mono-objective	(9), (18), (23), (24), (25), (26), (28), (29), (30)
Multi-period/Multi-objective	(4), (5), (7), (10), (19), (20), (21)

(1), (Almansoori et al., 2016); (2), (Almansoori et al., 2006); (3), (Almaraz et al., 2013); (4), (Almaraz et al., 2014); (5), (Almaraz et al., 2015); (6), (Biqué et al., 2018c); (7), (Brey et al., 2006); (8), (Cho et al., 2016); (9), (Dayhim et al., 2014); (10), (Guillén-Gosálbez et al., 2010); (11), (Han et al., 2012); (12), (Han et al., 2013); (13), (Hwangbo et al., 2017); (14), (Johnson et al., 2012); (15), (Kamarudin et al., 2009); (16), (Kim et al., 2008b); (17), (Kim et al., 2008a); (18), (Kim et al., 2016); (19), (Ogumerem et al., 2018); (20), (Sabio et al., 2010); (21), (Sabio et al., 2012); (22), (Woo et al., 2016); (23), (Agnolucci et al., 2013a); (24), (Almansoori et al., 2009); (25), (Moreno-Benito et al., 2017); (26), (Konda et al., 2011); (27), (Kim et al., 2017); (28), (Samsatli et al., 2016); (29), (Almansoori et al., 2012); (30), (Nunes et al., 2015); (31), (Parker et al., 2010); (32), (Won et al., 2017).

It must be emphasized that the adoption of a multi-period method may introduce a few contradictions. For example, the work of Almaraz et al. (2014), which is a protracted multi-period problem (2020-2050, divided into four periods), is examined. It has been noted that the integration of the four time periods leads to a high cost by 2020. This may be viewed as prohibitive and thus may hinder hydrogen deployment in the region. One explanation is that a multi-period model aims at identifying network strategies that could satisfy the overall demand throughout the entire horizon. This means that, the model is prone to select larger production plants to cover demand increments, which incur a high cost in the initial phase. A possible solution to this problem is to introduce the assumption of *capacity expansions*. This means that the network design (e.g., plant size) can be adapted to variations in demand (i.e., network capacities are no longer fixed at the beginning, but could be extended within a certain limit). Capacity expansion problems have been studied in the SCM domain since the early 1960s (Julka et al., 2007). Some of the SCND models consider capacity expansion as a continuous variable (Verter et al., 1995). However, other ones more realistically consider discrete facility capacity options (Paquet et al., 2004; Amiri, 2006). Only one of the reference papers (Sabio et al., 2010)

has reported on the capacity expansion approach (with a discrete variable). Therefore, it is recommended that more future studies introduce this method into multi-period models.

Although the time used in most multi-period models spans several decades, some studies that focus on the integration of renewable source into the HSCN set one year of 12 periods (months) as the time horizon (Kim et al., 2016; Won et al., 2017; Woo et al., 2016). When a renewable source is considered, the variation in the availability of source in a year should be taken into account. For example, the production capacity of a wind-based HSCN would change at different months because of the uneven distribution of wind power during a year (Kim et al., 2017). Similarly, transport demand has seasonal variations. Statistics show that the fuel demand peaks during summer months and declines during winter (Samsatli et al., 2015). In the work of Woo et al. (2016), the conflict between the fluctuations in biomass availability and hydrogen demand has been investigated in a monthly analysis.

2.5.1.3/ INTERTEMPORAL INTEGRATION AND CROSS-LAYER FLOW

One crucial aspect in the SCM refers to intertemporal integration planning, which incorporates various activities over strategic, tactical, and operational planning horizons (Shapiro, 2006). Vehicle routing and inventory decisions are considered within the tactical or operational level. Nevertheless, for both location/routing and location/inventory problems, it has been shown empirically that the facility location (strategic) decisions that would be made apart from other decisions are different from those that would be made by considering routing or inventory (Daskin et al., 2005). Although the simultaneous involvement of strategic and operational planning is encouraged in the SCND (Yue et al., 2014; Daskin et al., 2005), only a few related studies on the SCM could be found. This is because their integration leads to extremely complex models with large problem sizes (Melo et al., 2009); no HSCND model has ever considered the intertemporal integration. Therefore, it is anticipated that future studies will take this problem into consideration.

In a typical HSCN (depicted in Fig. 2.2), hydrogen flows from production plants to terminals and then from terminals to refueling stations. The flow has to conform to the established hierarchy, which means that flow is not allowed from production plants directly to refueling stations in cases where terminals exist. In the SCM domain, such a direct flow is referred to as cross-layer (or cross-echelon) flow (Melo et al., 2009). Another similar concept refers to intra-layer flow, which means that flow occurs within the same layer. In the HSCN, the intra-layer flow may occur when the transportation of feedstock and hydrogen is allowed between different production plants. To date, neither the cross-layer flow nor the intra-layer flow has been modeled in the HSCND models; therefore, it could be an interesting area for future research.

2.5.2/ HSCN PERFORMANCE MEASURES

2.5.2.1/ COST

Cost is the most frequently used performance measure (model objective) in the HSCND. The cost incurred in each part of the HSCN (except feedstock) consists of the capital and operating costs (Fig. 2.8). The capital and operating costs of production, storage, refueling station, and emission reduction are grouped as facility capital and operating costs. The definitions and formulations related to the cost objective established by Almansoori et al. (2006) have been adopted by several authors. To obtain more rigorous results, the authors have expended efforts to include more details into the cost definition. One example pertains to the cost of the plant site. Typically, as indicated by Kim et al. (2008a), such a cost is assumed to be 5% of the total process unit cost. However, because land prices in different regions vary significantly, Han et al. (2012); Kim et al. (2008a, 2016) estimated the plant site cost according to the land price in each region. Apart from the definition, other factors that can significantly influence the cost include financial assumptions, such as cost discounting (Konda et al., 2011). As in multi-period models, it is more reasonable to add the cost of each period that has been discounted back to a common period; this avoids adding costs that have been sustained during different time periods (Dagdougui, 2012). Another example pertains to the remaining value. Agnolucci et al. (2013a) considered the remaining value of the hydrogen infrastructure, which was subtracted from the total cost.

Although several multi-period models account for the time value of money over the lifetime of the project, no strict analysis on discounted cash flow is employed. It is also noted that profit maximization has received extremely less attention, as only two of the reference papers report profit as the HSCN performance measure (Parker et al., 2010; Han et al., 2012).

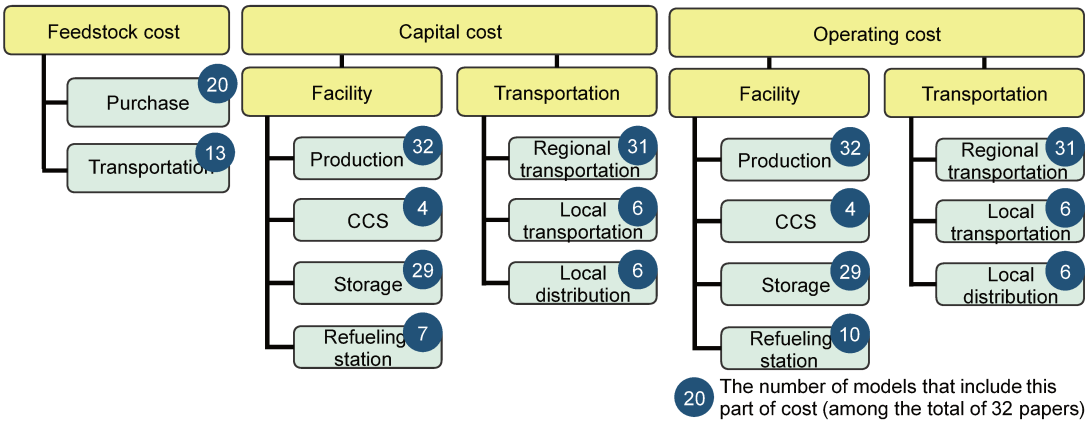

Figure 2.8: Composition of cost objective

2.5.2.2/ ENVIRONMENTAL IMPACTS

Which environmental factors should be examined? How can they be quantified? How can they be integrated into mathematical models? Based on our review, two solutions are identified: emission measurement (Almaraz et al., 2013, 2014, 2015; Han et al., 2013) and life-cycle assessment (LCA) indicators (Guillén-Gosálbez et al., 2010; Sabio et al., 2012). Environmental impact (in emission measurement method) is expressed by the global warming potential (GWP). This is an indicator of the overall effect of the process related to the heat radiation absorption of the atmosphere because of the greenhouse gas emissions (CO_2-equivalent) of the network (Almaraz et al., 2013). However, Sabio et al. (2012) argued that a single environmental metric is inadequate because it neglects the inclusion of relevant environmental criteria into the analysis. Therefore, the adoption of the LCA should consider several environmental indicators, which could evaluate the environmental impact on several aspects. In the work of Han et al. (2013), it is further noted that the environmental objective is represented by the cost rather than environmental indicators. The total mitigation cost of CO_2 is composed of emissions and CCS-related costs; it serves as the criterion of environmental performance.

2.5.2.3/ SAFETY

Hydrogen is not more dangerous than other flammable fuels, such as gasoline and natural gas. Nevertheless, under specific conditions, hydrogen can react dangerously: the burning or explosion of hydrogen can cause extremely fatal accidents (Kim et al., 2008b). Consequently, for the HSCND, safety considerations are paramount. Several papers have discussed risk assessment approaches for hydrogen infrastructures (Markert et al., 2017; Oyama et al., 2017; Kim et al., 2011). Kim et al. (2008b) proposed a framework for the HSCND risk analysis, which consists of the following steps: hazard identification, consequence and frequency analyses, risk evaluation, and the development of a relative risk index. With the support of the risk index system, the risk level of different parts of the HSCN could be evaluated. Consequently, different scenarios and pathways could be compared in the aspect of safety performance (total relative risk index). It should be noted that there is no clear and comprehensive consensus on the definition of the supply chain risk (Govindan et al., 2017). Here, the risk assessment is associated with the safety of hydrogen infrastructure systems.

2.5.2.4/ MULTI-OBJECTIVE MODEL

As can be observed in the list of Table 2.10, most of the models that are reported by the reference papers are mono-objective. The single objective is the minimization of the

total cost of the network—capital and operating costs. Dagdougui (2012) argued that minimizing only the total cost may lead to solutions that are inadequate for some other aspects, such as environmental and safety. For instance, it can be observed in some mono-objective model results (Almansoori et al., 2009, 2012) that long transportation links are installed between regions when hydrogen demand is relatively small because such an option is cheaper than building a new production facility. The safety level of such a configuration is unavoidably low because transportation mainly contributes to the risk index. The ubiquitous trade-off among the different criteria could be overcome through multi-objective models, which evaluate actions from multiple perspectives. As an example, let us consider the work of Guillén-Gosálbez et al. (2010). Their results demonstrate that a multi-objective model could identify that the most potential alternative (to achieve significant environmental savings without excessively compromising the total cost of the network) is to replace steam reforming with biomass gasification. However, this is not to suggest that a mono-objective model could not cope with trade-off problems; this is because other criteria (e.g., environmental impact) could also be represented in terms of cost. Although the model in the work of Almansoori et al. (2016) is mono-objective, it has accomplished a valuable investigation on both cost and environment.

Table 2.10: Distribution of studies in reference papers with respect to the three objectives

Cost	(1), (2), (6), (8), (9), (11), (13), (14), (15), (17), (18), (22), (23), (24), (25), (26), (27), (28), (29), (30), (31), (32)
Cost/Environment	(10), (19), (21)
Cost/Safety	(16), (20)
Cost/Environment/Safety	(3), (4), (5), (12)

(1), (Almansoori et al., 2016); (2), (Almansoori et al., 2006); (3), (Almaraz et al., 2013); (4), (Almaraz et al., 2014); (5), (Almaraz et al., 2015); (6), (Biqué et al., 2018c); (8), (Cho et al., 2016); (9), (Dayhim et al., 2014); (10), (Guillén-Gosálbez et al., 2010); (11), (Han et al., 2012); (12), (Han et al., 2013); (13), (Hwangbo et al., 2017); (14), (Johnson et al., 2012); (15), (Kamarudin et al., 2009); (16), (Kim et al., 2008b); (17), (Kim et al., 2008a); (18), (Kim et al., 2016); (19), (Ogumerem et al., 2018); (20), (Sabio et al., 2010); (21), (Sabio et al., 2012); (22), (Woo et al., 2016); (23), (Agnolucci et al., 2013a); (24), (Almansoori et al., 2009); (25), (Moreno-Benito et al., 2017); (26), (Konda et al., 2011); (27), (Kim et al., 2017); (28), (Samsatli et al., 2016); (29), (Almansoori et al., 2012); (30), (Nunes et al., 2015); (31), (Parker et al., 2010); (32), (Won et al., 2017).

Almaraz et al. (2013, 2014) analyzed the differences between mono and multi-objective approaches. The change from a centralized to a decentralized supply chain is the primary difference observed when the three criteria are considered in the optimization phase compared to the minimum cost network. One explanation for this phenomenon is that the model tends to reduce the necessity of transportation when a relatively high safety level is set (Kim et al., 2008b). Moreover, in production plants, the mono-objective model has only

resulted in the SMR type of technology. However, when a multi-objective optimization is performed, a combination of technologies are involved—SMR and biomass gasification.

2.5.3/ UNCERTAINTY

Galbraith (1977) defined uncertainty as one of the differences between the amount of required information and available information to execute a task. In this regard, although the deterministic models provide a solid foundation for the SCND, any design obtained based on these models has no guaranteed potential future performance. These models do not handle uncertainties and imperfect information concerning expected plausible future business environments (Klibi et al., 2010). Therefore, uncertainty is one of the most difficult but essential problems in the SCM (Sabri et al., 2000).

2.5.3.1/ UNCERTAINTY SOURCES

Corresponding to the levels of planning decisions, uncertainties could also be broadly categorized into strategic and operational levels (Yue et al., 2014). Similar to the biomass supply chain network discussed in (Yue et al., 2014), the most significant type of strategic uncertainty for the HSCN may be associated with government incentives and policies, as well as the market share of the fuel cell electric vehicles (FCEVs). Moreover, technology evolution is an essential type of strategic uncertainty. It may be necessary to determine whether mature technologies with minimal chances of improvement or nascent technologies with considerable potentials have to be employed. Operational uncertainties refer to those ones that necessitate consideration on a more frequent basis. The fluctuation in short-term hydrogen demand, volatility in prices and costs, and bills for utilities are types of operational uncertainties. Half of the studies reported by the reference papers considered uncertainty. The uncertainty sources considered in each model are summarized in Table 2.11. It is evident that a large portion of the studies introduced only the uncertainty of the FCEV's market share. Only one of the papers reported uncertainty as related to operating costs.

2.5.3.2/ UNCERTAINTY TYPES AND MODELING APPROACHES

Several studies discussed the taxonomy of uncertainty types in the SCND (Klibi et al., 2010; Bairamzadeh et al., 2018; Govindan et al., 2017). Here, the taxonomy summarized by Bairamzadeh et al. (2018) is adopted. It is based on the amount of available information in decision-making situations. The three types of uncertainties are randomness, epistemic, and depth.

Table 2.11: Uncertainty sources

Planning level	Source of uncertainty	Corresponding uncertain parameter	Reference papers
Strategic uncertainty	Government incentives and policies	- Policies related to emissions reduction percentage	
	Hydrogen demand	- FCEV market share	(4), (8), (9), (11), (13), (16), (17), (18), (23), (26), (27), (29), (30)
	Technology evolution	- Conversion rate of feedstock to hydrogen	
	Feedstock supply	- Feedstock availability	
	Cost	- Capital costs	
Operational uncertainty	Hydrogen demand	- Short-term hydrogen demand fluctuation	
	Prices	- Feedstock purchasing price - Hydrogen selling price - Byproducts selling price	
	Costs	- Operating costs - Feedstock supply costs	(20)

(4), (Almaraz et al., 2014); (8), (Cho et al., 2016); (9), (Dayhim et al., 2014); (11), (Han et al., 2012); (13), (Hwangbo et al., 2017); (16), (Kim et al., 2008b); (17), (Kim et al., 2008a); (18), (Kim et al., 2016); (20), (Sabio et al., 2010); (23), (Agnolucci et al., 2013a); (26), (Konda et al., 2011); (27), (Kim et al., 2017); (29), (Almansoori et al., 2012); (30), (Nunes et al., 2015).

The parameters associated with *randomness* are considered as random variables with known probability distributions. The joint events associated with the possible values of random variables can be considered as plausible future scenarios; each with a probability of occurrence (Klibi et al., 2010). As reported by the reference papers, scenario analysis is adopted in several studies to overcome the market share uncertainty of the FCEV by investigating the hydrogen demand in optimistic, neutral, and pessimistic scenarios. Another way to cope with randomness is by stochastic programming (Eppen et al., 1989; Sen et al., 1999). Half of the studies reported by the reference papers that consider the uncertainty problem adopted the two-stage stochastic programming. In this two-stage model, the decisions associated with the first-stage are made before the realization of uncertainty. These decisions are usually referred to as “here-and-now” decisions, such as the number and type of production plants and storage facilities. Future decisions correspond to those that are made after the realization of uncertainty; these are typically known as “wait-and-see” decisions, such as the number and type of transportation units

(Almansoori et al., 2012; Kim et al., 2008b). Therefore, the objective of a cost-oriented multi-stage modeling under uncertainty is to identify the optimal decision variables that minimize the cost of the first stage and expected cost of subsequent stages (Almansoori et al., 2012). The problem here is the exponential growth of the model size if there are several potential outcomes (scenarios) in each period of the multi-period model. Instead of simultaneously considering all scenarios, a representative subset could be generated by the sample average approximation (SAA) method (Santoso et al., 2005). With the support of the SAA, Dayhim et al. (2014) demonstrated that 15 scenarios are sufficient to obtain reasonably good solutions.

The *epistemic uncertainty* is related to the deficiency of knowledge pertaining to input data, which are often presented in the form of linguistic attributes or judgmental data that can be extracted from relevant experts (Bairamzadeh et al., 2018). For example, electricity generated by renewable energy can be treated as fuzzy numbers such that the corresponding possibility distribution is extracted based on an expert's estimation and knowledge. Hence, fuzzy programming could be employed to cope with epistemic uncertainty.

Deep uncertainty is characterized by the lack of information to estimate scenario probabilities. In this case, robust optimization approaches can be used. The robust optimization approach proposed by Mulvey et al. (1995) can be regarded as an extension of stochastic programming. However, it can be used with a min-max regret criterion, which would be applied in the case of deep uncertainty (Klibi et al., 2010). As mentioned above, the uncertainty of hydrogen demand (the FCEV market share) is treated as a random uncertainty as reported by several of the reference papers. However, the necessary information to derive the probability distribution for hydrogen demand values as well as various fluctuating factors that influence demand is insufficient. Accordingly, it is more realistic to characterize the hydrogen demand by deep uncertainty which is expressed as a known interval without assuming a specific probability of occurrence of possible values.

The summary in Table 2.12 indicates that the reference papers reported only random uncertainty. Half of the studies employed the scenario analysis, whereas the other half adopted stochastic programming. The epistemic and deep uncertainties, and the corresponding modeling approach, have not been considered in the HSCND models.

2.5.4/ MODEL CONSTRAINTS AND SPATIAL-BASED APPROACH

According to Almansoori et al. (2009), and Parker et al. (2010), the constraints for the HSCND model could be categorized according to capacity, flow conservation, time evolution, and non-negativity constraints. Correctly involving constraints is an essential part of the modeling work. The constraints imposed by national or regional policies and regu-

Table 2.12: Uncertainty types and corresponding modeling approaches

Type of uncertainty	Uncertainty modeling approach	Reference papers
Randomness	Scenario analysis	(4), (8), (11), (16) (18), (23), (26), (27)
	Stochastic programming	(9), (13), (29) (17), (20), (30)
Epistemic	fuzzing programming	
Deep uncertainty	Robust optimization	

(4), (Almaraz et al., 2014); (8), (Cho et al., 2016); (9), (Dayhim et al., 2014); (11), (Han et al., 2012); (13), (Hwangbo et al., 2017); (16), (Kim et al., 2008b); (17), (Kim et al., 2008a); (18), (Kim et al., 2016); (20), (Sabio et al., 2010); (23), (Agnolucci et al., 2013a); (26), (Konda et al., 2011); (27), (Kim et al., 2017); (29), (Almansoori et al., 2012); (30), (Nunes et al., 2015).

lations should also be taken into consideration. For example, the pipeline network design should exhibit conformity to government regulations and planning. Similar to the work of Johnson et al. (2012), pipeline design in southwestern California follows the existing pipeline rights-of-way as defined by the US National Pipeline Mapping System (NPMS) dataset. Other examples abound. Kim et al. (2017) considered the importance of adhering to government regulations on land use in relation to energy production when attempting to model a wind-based HSCN.

Several papers reported the importance of modeling within real geographic regions and utilized geographic information system (GIS) database in modeling (Almaraz et al., 2015; Johnson et al., 2012; Parker et al., 2010). For instance, the road network employed by Parker et al. (2010) is the “California base” network from the California Department of Transportation, which consists of all interstates, major highways, and urban arterial roads. The International Energy Agency (2015) argued that, hydrogen transportation and distribution are costly and strongly dependent on transport distance. Accordingly, a more robust T&D (transport and distribution) cost estimation can only be realistically provided if knowledge on geographical parameters is available. On the one hand, real geographic constraints could be introduced and built on a GIS database (Geographical Information System) before optimization. On the other hand, the GIS tools could be applied to validate the feasibility of results in the final HSCN structure (Almaraz et al., 2015).

2.5.5/ SOLUTION METHODS

2.5.5.1/ MONO-OBJECTIVE PROBLEMS

Solution approaches for the mono-objective SCND problems can be classified into two categories: problems solved with a general purpose software (either commercial or non-

commercial) and those solved with a specially tailored algorithm (Melo et al., 2009). Within each class, two further cases are identified: exact and heuristic solutions. The description of this classification is summarized in Table 2.13. All the studies in the reference papers are within the *General solver* category, either with the exact solution or heuristic solution. In 2010, Klibi et al. (2010) noted that most of the static and deterministic SCND models could be solved efficiently with different versions of commercial solvers, such as CPLEX, available at that time. This explains why all the HSCND models run the CPLEX solver, which is accessed via the General Algebraic Modeling System (GAMS) (Rosenthal, 2014). When solving large-scale problems with a high number of time periods and potential locations (and therefore a high number of integer and binary variables), specially tailored algorithms are preferred because they could provide near-optimal solutions with reasonable CPU times. Copado-Méndez et al. (2013) developed an algorithm for the HSCND problem that combines the strengths of the standard branch-and-cut techniques with the efficiency of the large neighborhood search (LNS) algorithm. Computational results show that the proposed hybrid algorithm achieves near-optimal solutions in less time than the CPLEX does. Furthermore, this method identifies feasible solutions even in cases where the CPLEX fails to converge (Copado-Méndez et al., 2013).

Table 2.13: Solution methods for mono-objective models (adapted from Melo et al. (2009))

- Specific algorithm/ exact solution	- Special-purpose techniques such as branch-and-bound, branch-and-cut, column generation, and decomposition methods.
- Specific algorithm/ heuristic solution	- Lagrangian relaxation, linear programming based heuristics, and meta-heuristics.
- General solver/ exact solution	- Refers to the use of mathematical programming software to solve a problem either to optimality or until a solution is obtained within a pre-specified gap reflecting the ”worst” quality accepted by the decision-maker.
- General solver/ heuristic solution	- Off-the-shelf solver run until a given time limit is reached.

2.5.5.2/ MULTI-OBJECTIVE PROBLEMS

Solution approaches for the multi-objective problems can be classified as the a priori, a posteriori, and hybrid methods (Yann et al., 2004). The summary in Table 2.14 shows that, the ϵ-constraint method dominates the studies reported in the reference papers. The value of using this type of a posteriori method is that it generates the full set of trade-off solutions. The trade-offs can be investigated further and a particular strategy that satisfies the decision-maker's willingness to compromise according to a set of generated

alternatives is selected (Hugo et al., 2005). The ϵ-constraint method is based on the minimization of one objective function while considering the other objectives as constraints bounded by certain allowable levels (known as utopia and nadir points, which are presumed to be challenging to determine). Consequently, the ϵ-constraint is often combined with an a priori method (lexicographic), because the latter could serve as an approach to construct the payoff table using only efficient solutions (Almaraz et al., 2014).

Table 2.14: Solution methods for multi-objective models

A priori preference methods	
- Weighted sum	
- Lexicographic	
A posteriori preference methods	
- Meta-heuristic methods	
- ϵ-constraint	(3), (5), (10), (16), (20), (21)
Hybrid methods	
Lexicographic + ϵ-constraint	(4)

(3), (Almaraz et al., 2013); (4), (Almaraz et al., 2014); (5), (Almaraz et al., 2015); (10), (Guillén-Gosálbez et al., 2010); (16), (Kim et al., 2008b); (20), (Sabio et al., 2010); (21), (Sabio et al., 2012).

Several studies (Guillén-Gosálbez et al., 2010; Sabio et al., 2010; Agnolucci et al., 2013a; Moreno-Benito et al., 2017) have implemented a two-step hierarchical procedure to speed up the solving, by exploiting the fact that the relaxation of the integer variables of the full-space model tends to be considerably tight in practical problems. By doing such, the CPU times could obtain a certain degree of reduction as the presence of integer variables is mostly reduced. In the work of Robles et al. (2016), the potential of genetic algorithms (GA) via a variant of the non-dominated sorting genetic algorithm II (NAGA-II) (Deb et al., 2002) was explored to cope with the multi-objective formulation. Results show that the solutions obtained by the genetic algorithm exhibited the same order of magnitude as those achieved by the CPLEX.

2.6/ PRE-OPTIMIZATION PREPARATION WORKS

In this current study, pre-optimization preparation works refer to those that serve as a basis for modeling and optimization. Although these works are significant, they have not been given sufficient attention in previous review papers. Then we set out to complete the literature review with an analysis of the sources and types of input data for supply chain optimization models. In this section, we report on the three primary preparation works are discussed: data collection, geographic division, and estimation of hydrogen demand.

2.6.1/ DATA COLLECTION

The data-intensive nature of optimization methods makes the modeling work challenging and time-consuming. This situation is worse in hydrogen energy-related problems because of the lack of historical data. We conducted here a review of the data-related work reported in the reference papers. The review includes the data source (publisher), and data type (statistics, report, book, dataset, or website); it also identifies the part of the HSCN where these ones are used (demand, feedstock, production, storage, transportation, environment, or safety). It should be noted that journal papers are not considered as data sources here, although they are commonly used for this purpose. The focus is set on the external (or original) sources to make a reference list of the data sources for future research. As shown in Fig. 2.9, reports and statistics constitute a substantial portion of the data source.

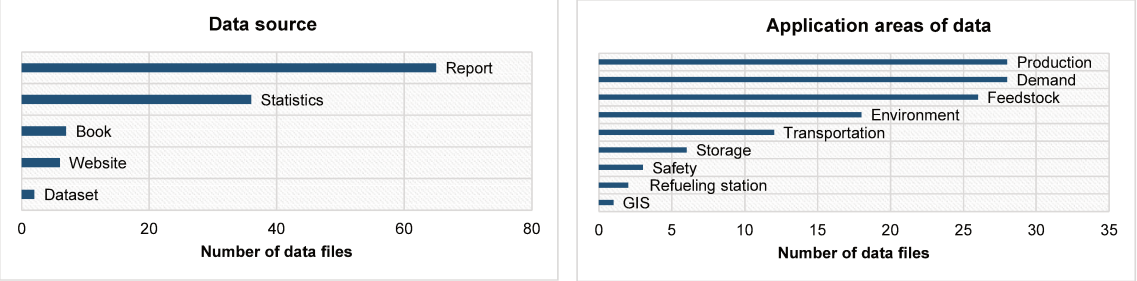

Figure 2.9: Data source and application areas

Reports from government agencies and international organizations, such as the U.S. Department of Energy, European Commission, the IEA, and Intergovernmental Panel on Climate Change provide substantial information on hydrogen demand, production, and T&D cost based on a broad range of techno-economic analysis. Statistics is another vital part of the data resource. The statistics on energy prices, road traffic, greenhouse gas emissions, population data, land use, and neighborhood are indispensable to the HSCND database. Figure 2.9 illustrates that data are more frequently used in the production, demand, and feedstock domains.

2.6.2/ GEOGRAPHIC DIVISION

The modeling of an HSCN is usually conducted within a relatively large area (i.e., a country or a region). It is necessary to divide this vast area into subregions, each one with its own hydrogen demand and initial production ability. The spatial decisions associated with the optimization of an HSCN are the answers to the two following questions: (i) in which subregion should a hydrogen production plant (or other hydrogen infrastructure) be built? (ii) how is the transportation network arranged among these subregions?

A country (or a region) could be divided into rectangular grids, administrative segments, or demand clusters; these are the three divisions adopted by the studies reported in the reference papers. The rectangular grid was mainly used by Almansoori et al. (2006, 2009, 2012). In their studies, Great Britain was divided into 34 grid squares of equal size. Administrative segmentation was used to obtain a realistic path between districts with the existence of the main roads and to estimate the potential demand from local statistics (Almaraz et al., 2014). This was the division method adopted by most authors. Konda et al. (2011), Johnson et al. (2012), and Parker et al. (2010) accomplished their geographic division by demand clusters. Konda et al. (2011) argued that the presence of population clusters usually warrants a reasonable hydrogen demand. Therefore, several clusters of the length and breadth of the country were chosen to represent the spatial dispersion of the demand vector.

2.6.3/ HYDROGEN DEMAND

As a key input, hydrogen demand estimation plays an essential role in the pre-optimization preparation works. Moreover, the change in hydrogen demand has a major impact on the structure of a hydrogen supply system. For example, the hydrogen demand of a subregion can be satisfied through inputs from adjacent areas or by building a plant. The optimal decision is obtained according to the amount of demand. The HSCN that is investigated and reported in the reference papers is established with the goal of transitioning to hydrogen-based mobility. Therefore, the hydrogen demand depends on the number of the FCEVs. The common method for the estimation of hydrogen demand reported in the reference papers is schematized in Fig. 2.10. The key step in this process depends on the estimation of hydrogen penetration. Based on the review, three approaches are identified and illustrated in Fig. 2.11.

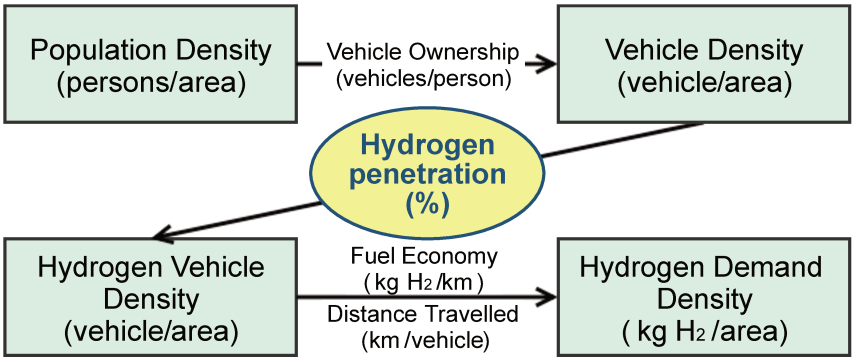

Figure 2.10: Common method for hydrogen demand estimation

Agnolucci et al. (2013b) noted that the adoption of hydrogen is expected to follow a logistic, S-shaped curve, which is similar to that observed in most of the new technologies.

Three parameters describing the logistic substitution curve are the saturation point, “anchoring” date (the start of the transition), and transition duration. Almansoori et al. (2009) explained the S-shaped curve: during the introductory stage of a hydrogen economy, the demand would be limited to a fleet of vehicles with a fixed daily route and regular refueling intervals at specific locations, e.g., buses. When the manufacturing cost of the FCEVs becomes affordable, and constraints, such as onboard storage, are overcome, the demand trajectory might sharply increase. Eventually, as the market arrives at a state of saturation, the demand trajectory will level off. Although several authors adopted the logistic substitution curve, it was usually based on subjective assumptions, which means that it was assumed outside of any mathematical model.

Melendez et al. (2008) proposed a framework for examining whether a particular market can potentially transition to hydrogen-based mobility by evaluating the socio-economic factors. As described in Fig. 2.11, nine key attributes that influence hydrogen penetration into the consumer market are identified. By mapping the value of these socio-economic factors at the local level, an idea of the geographical and temporal evolution of hydrogen demand can be acquired within a particular national context (Agnolucci et al., 2013b). Each geographic area is scored according to each attribute. Thereafter, these scores are added to obtain the final score. This final score identifies areas where hydrogen demand is presumed to be promising. Only two studies (Dayhim et al., 2014; Moreno-Benito et al., 2017) that consider the socio-economic analysis are reported in the reference papers.

The third method of linking the energy system model with an HSCN model mainly refers to a MARKAL/TIMES model as mentioned in section 2.3.1. One of the fundamental characteristics of a MARKAL/TIMES model is that both supply and demand are integrated; one automatically responds as the other changes. Considering this feature, it is possible to achieve a hydrogen demand profile by feeding MARKAL/TIMES model with a technico-economic specification. The method of linking the energy system model with an HSCN model is schematized in Fig. 2.11.

Agnolucci et al. (2013b) noted that apart from studies that use energy system models, most of the studies dealing with the modeling of an HSC assumed an exogenous trajectory of hydrogen demand. Moreover, several studies do not consider the evolution of a system over time. Only one study implemented a comparatively comprehensive estimation of the hydrogen demand that considered logistic substitution curve, socio-economic analysis, and energy system model (Agnolucci et al., 2013a). The estimation process is schematized in Fig. 2.12. Firstly, a hydrogen demand scenario (the HyWay European Hydrogen) (European Research Area, 2015) defined two of the parameters that describe a logistic substitution curve: saturation point and transition duration. Thereafter, the authors adopted an energy system model (named UK MARKAL) to indicate when hydrogen may be introduced to make the transition consistent with the broader analysis of cost-optimal

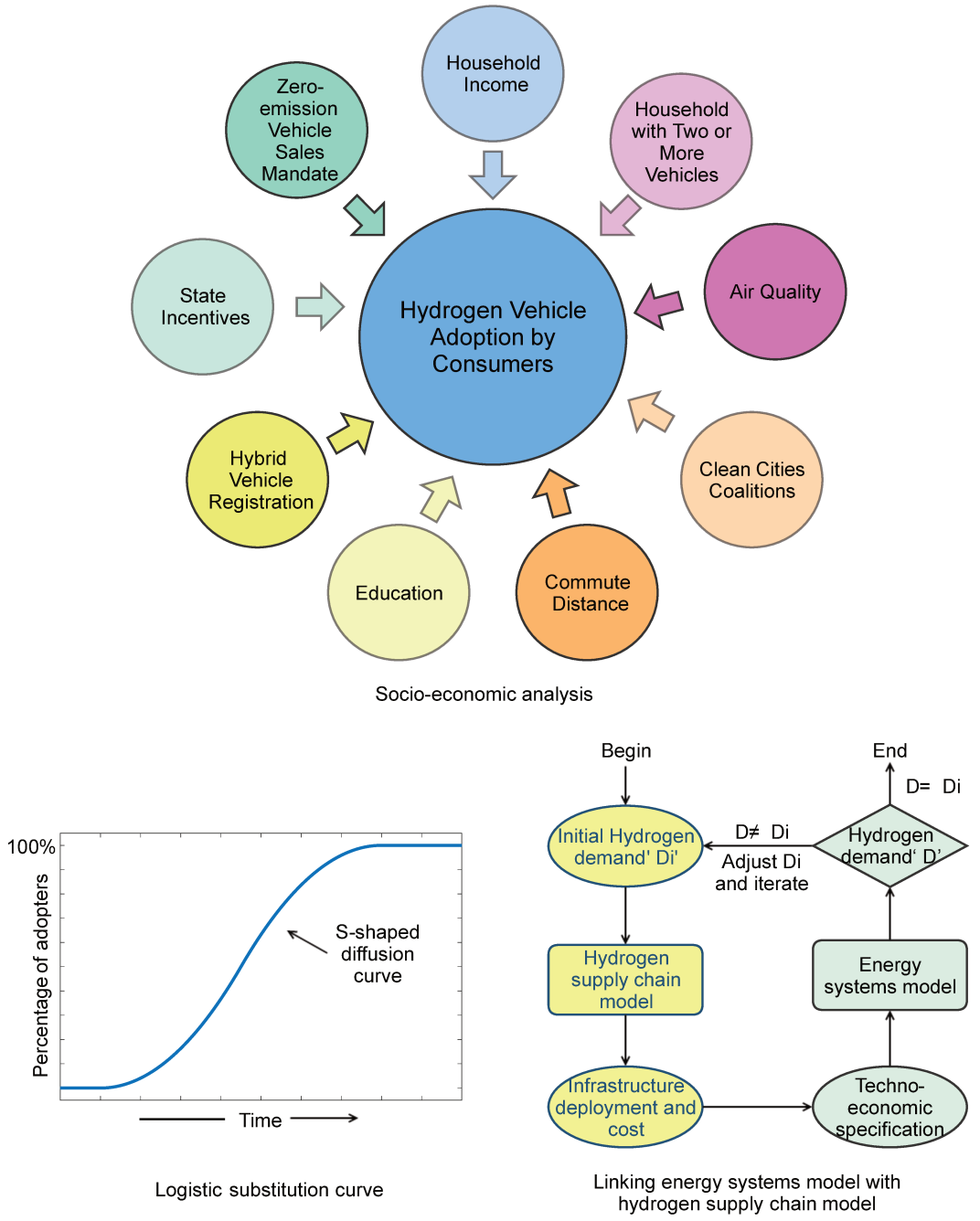

Figure 2.11: Three approaches to determine hydrogen penetration

decarbonization trajectories (known as “anchoring” date). Afterwards, a socio-economic analysis was conducted to identify the spatial distribution of hydrogen demand, specifically, the transition order of subregions. In this way, a set of several diffusion curves was assigned to the geographical area. By stacking these curves and considering a typically faster diffusion rate in regions that are slow to adopt, a profile of the hydrogen penetration was purchased.

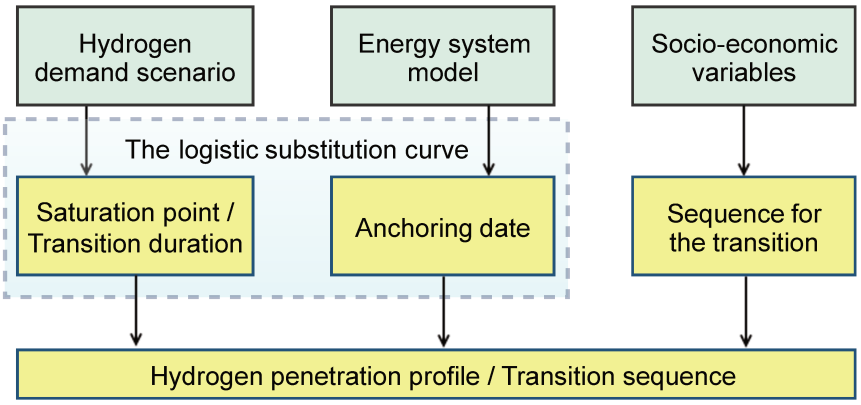

Figure 2.12: Demand forecasting process in the work of Agnolucci et al. (2013a)

2.7/ CONCLUSIONS

This chapter presented an overview of the research development regarding the use of optimization methods for the hydrogen supply chain network design (HSCND). Dedicated sections analyzed and classified the selected papers according to system analysis, decision variables, performance measures, uncertainties, and solution approaches.

The HSCN in the transportation sector is a complex system. It includes various components from feedstock supply sites to hydrogen refueling stations. Because of the inherent characteristics of a supply chain, each part of HSCN is interconnected rather than isolated. The selection of feedstock, production and refueling technologies, location of hydrogen facilities, and other major decisions make up a vast “pool” of pathways. Decision-makers require a comprehensive optimization model to help them making intelligent decisions. To our knowledge, such a model, which covers the entire HSCN (from feedstock supply to refueling stations), has not been proposed in previous researches. In addition to the problem of coverage upstream and downstream of the supply chain, other lacks were also identified: feedstock transportation, representation/estimation of the hydrogen demand, consideration of fixed-location demands (this one being ignored in all the reviewed papers)... Thus, the intercomponent integration planing of HSCND which considers various components within a single framework needs to be developed. This will be our first contribution detailed in the next chapter.

The intertemporal integration planning, which includes various activities over strategic and tactical planning horizons, has been overlooked in the HSCND models. It is suggested that the location/routing problem is the most relevant subject for future studies of the HSCND because the major trade-off in it is between the transportation cost, and capital and production costs of manufacturing facilities. Moreover, the strategic decisions that would be made in isolation might be different from those that would be made by tak-

ing into account the routing problem. This means that intertemporal integration planning could help researchers to gain further insight on the HSCND.

Fig. 2.13 illustrates the positioning of our works within the literature, as well as the detail of our contributions which are reported in the two following chapters.

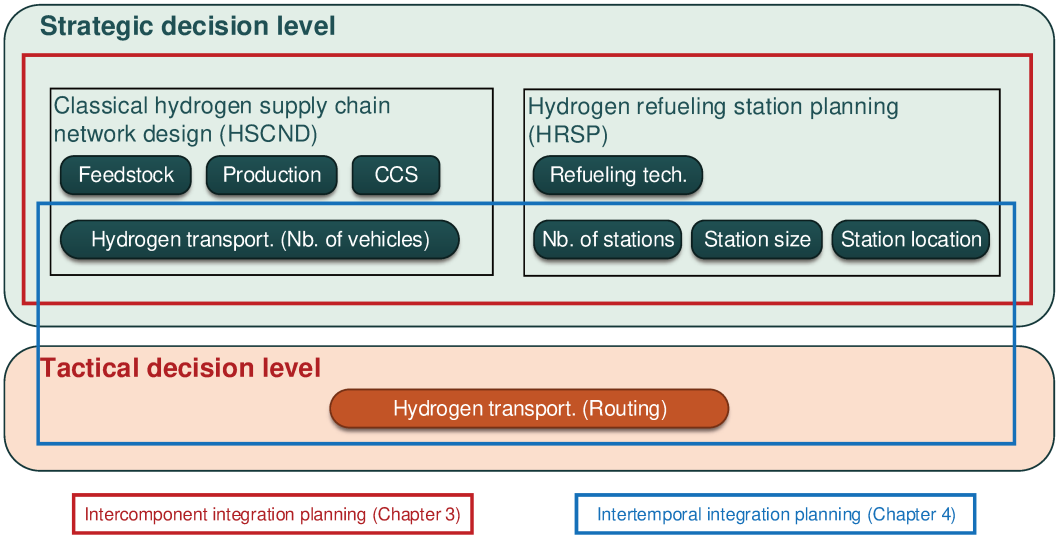

Figure 2.13: Our positioning in the literature

II

CONTRIBUTIONS

3

A MILP MODEL FOR THE INTERCOMPONENT INTEGRATION PLANNING OF HSCND

This chapter addresses the intercomponent integration planning of HSCND. Here, our main contribution is to develop a mathematical exact model that covers the entire hydrogen supply network. The classical hydrogen supply chain network design (HSCND) model is integrated with the hydrogen refueling station planning (HRSP) model to generate a new formulation. The proposed model considers the feedstock supply, the installation and operation of hydrogen facilities, the operation of transportation technologies, and the carbon capture and storage (CCS) system. Two primary hydrogen refueling technologies, namely on-site refueling (hydrogen is produced on-site) and standard refueling (hydrogen is delivered by road), are considered. The problem is formulated as a mixed-integer linear programming (MILP) model that minimizes the least cost of hydrogen (LCOH). The advantages of considering various components within a single framework are demonstrated through a case study in Franche-Comté, France. The role of each key model component (such as the refueling technology, feedstock transportation, and CCS system) is analyzed. The proposed model is able to study the interactions that exist between different components of a hydrogen supply network. Consequently, more comprehensive construction plans are guaranteed for the HSCN.

Contents

PUBLICATIONS

JOURNAL ARTICLES

- Li, L., Manier, H., and Manier, M.-A., (2020). Integrated optimization model for hydrogen supply chain network design and hydrogen fueling station planning. *Computers & Chemical Engineering (CACE)* 134, 106683, DOI:10.1016/j.compchemeng.2019.106683

NATIONAL CONFERENCES

- Li, L., Manier, H., and Manier, M.-A., Un modèle d'optimisation intégré pour la conception de la chaîne d'approvisionnement en hydrogène. *20ème congrès annuel de la société Française de Recherche Opérationnelle et d'Aide à la Décision (ROADEF 2019).* Le Havre, Normandie, France, February 19-21, 2019.

INVITED COMMUNICATIONS

- Li, L., Manier, H., and Manier, M.-A., Conception de la chaîne logistique de l'hydrogène, *Journée Industrielle du GDR RO sur le thème du Management de l'Energie*, IHP Paris, France, June 14, 2019.
- Li, L., Manier, H., and Manier, M.-A., Design and optimization of the hydrogen supply chain, *Research seminary*, Chang'an University, Xi'an, China, February 26, 2019.

SEMINARS

- Li, L., Manier, H., and Manier, M.-A., Design and optimization of the hydrogen supply chain, *DocTalks 2019, DOCEO*, Université de Technologie de Belfort-Montbéliard, Sévenans, France, March 28, 2019.
- Li, L., Manier, H., and Manier, M.-A., Conception de la chaîne d'approvisionnement en hydrogène, *IngéDoc 2018, journée des jeunes chercheurs de l'UTBM*, poster session, Université de Technologie de Belfort-Montbéliard, Sévenans, France, November 15, 2018.

3.1/ INTRODUCTION

The transportation sector is one of the most significant contributors to greenhouse gas (GHG) emissions. It accounted for 26% of EU, 28% of U.S., and 23% worldwide of total GHG emissions in recent years (Environmental Protection Agency, U.S., 2018; European Environment Agency, 2017; Sims et al., 2014). Within the sector, road transportation is by far the largest category, contributing approximately three-quarters of all emissions (International Energy Agency, 2015). Aggressive and sustained mitigation strategies are essential if deep GHG reduction ambitions, such as the two-degree scenario, are to be achieved. For this goal, the equivalent of 160 million low-emission vehicles will need to be on the roads by 2030, according to International Energy Agency (2017).

It is widely accepted that hydrogen is a critical element in the decarbonization of the transportation sector, which still relies almost exclusively on oil (McKinsey & Company, 2017). Hydrogen can be used in electric vehicles (EVs) equipped with hydrogen fuel cells (FCEV). FCEVs are a necessary complement to battery electric vehicles (BEVs) as FCEVs add convenience for consumers with long ranges and fast refueling times. FCEVs can also provide potentially very low carbon emissions (International Energy Agency, 2015). In terms of cost per mile, FCEVs will need tax credits or other subsidies to be

competitive with conventional cars and other types of alternative fuel vehicles during the early stages of commercial implementation (M. Ruth, T.A. Timbario et al., 2011). However, significant cost reduction can be realized by scaling up manufacturing of FCEVs and hydrogen refueling infrastructures (McKinsey & Company, 2017).

Although the potential environmental benefits of hydrogen in the transportation sector are promising, the shift towards a hydrogen economy is challenging. Currently, the sales of FCEVs look bleak. In the U.S., only about 1,800 Mirai (a mid-size FCEV manufactured by Toyota) have been shipped in 2017. In contrast, 60 times as many Priuses (a hybrid electric vehicle) have been sold, and Tesla has also delivered more than 50,000 electric vehicles (Carsalesbase, 2018). The sluggish pace of sales for FCEVs is in part explained by the fact that only 65 hydrogen refueling stations were available in 2017, compared to more than 20,000 charging stations across the U.S. (Department of Energy, U.S., 2018a). This situation is often described as a “chicken-and-egg” problem (Achtnicht et al., 2012). Investments in refueling infrastructures pay off only if the vehicle number grows, but developing, building, and marketing vehicles are viable only with adequate refueling stations (McKinsey & Company, 2017).

One way to solve this dilemma is to coordinate the roll-out of vehicles and infrastructure development. Let us suppose that automobile manufacturers have chosen specific cities or areas as a target. Fuel providers would need to create a construction plan to realize the coordination. Such a plan involves two essential characteristics: (i) it should focus on planning the initial development of infrastructures while accounting for the full range of local factors, such as geographic distribution of feedstocks for hydrogen production and anticipated hydrogen demand at the refueling stations; (ii) it should be an integrated plan, which means that all types of infrastructures (hydrogen production plants, refueling stations, and CO_2 storage sites) are considered simultaneously. A simple example of a hydrogen supply network is illustrated in Fig. 3.1.

Hydrogen is produced at a plant using biomass that is transported from a biomass warehouse. The CO_2 emissions from hydrogen production are captured and transported to a CO_2 storage site. Hydrogen is delivered to refueling stations and other types of consumers (e.g., a fleet of buses or stationary applications). There are also refueling stations that run autonomously as they produce hydrogen on-site, thus they do not rely on delivery. The construction plan is responsible for answering the following questions:

- What is the hydrogen demand?
- where is this demand located?
- What kind of feedstock and technology should be selected to produce hydrogen?
- Will hydrogen be produced on-site or be delivered from production plants?

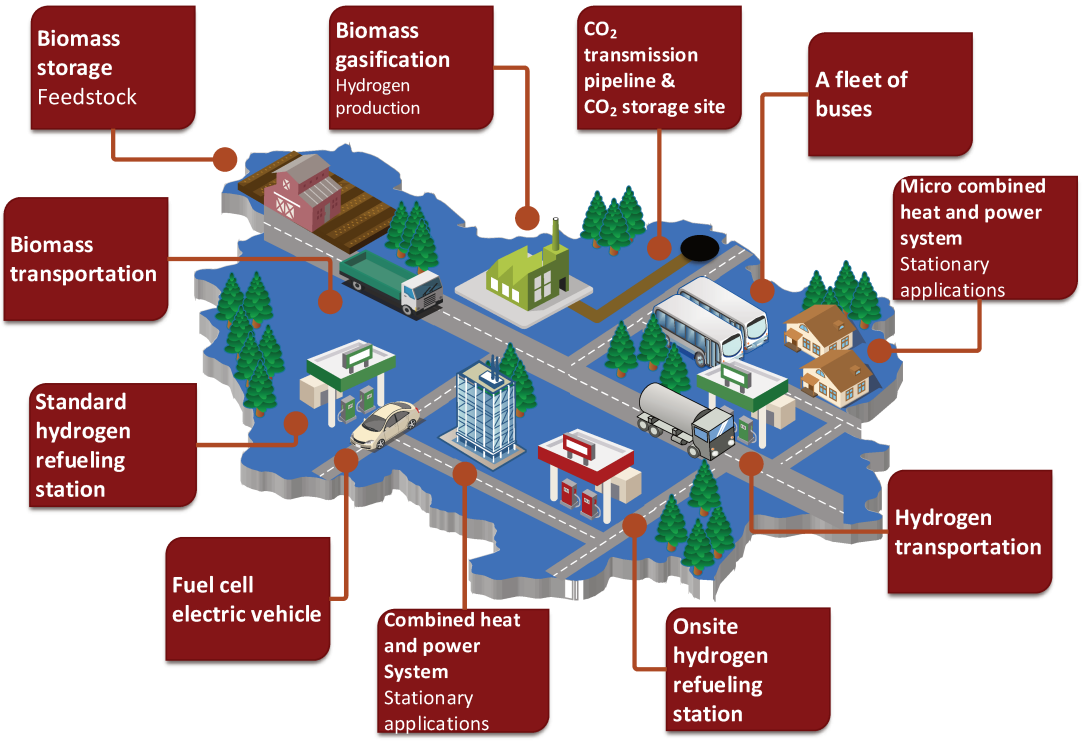

Figure 3.1: A simple example of hydrogen supply network

- How many production plants and refueling stations are needed, and where will they be located?
- What are the most suitable types of transportation (either for hydrogen or for feedstock)?

These questions are difficult to answer without using mathematical models because technological and spatial interactions exist between the different parts of the network. As discussed in Chapter 2, several models for hydrogen networks have been developed, and they typically fall into one of the following two categories:

- Hydrogen supply chain network design (HSCND) models: these models include multiple components such as feedstock, production, storage, and transportation. They focus on long-term planning and usually run on a national scale.
- Hydrogen refueling station planning (HRSP) models: these models determine the optimal location of hydrogen refueling stations. They focus on the initial development of infrastructures and are generally applied at a city or regional level.

Unfortunately, neither the HSCND nor the HRSP models are qualified to develop the construction plan described above. The main reason is that none of them considers the entire

hydrogen supply network. Most of HSCND models involve no decision variables related to refueling station issues. Those ones, which do consider refueling infrastructures, determine only the number, type (gaseous or liquefied hydrogen), and size of the stations. On the other hand, the HRSP models do not answer questions like “where will the hydrogen come from?”. They are less concerned with the technologies of the stations, and therefore do not include upstream infrastructure issues. Thus, it is reasonable to combine these two types to build a new model that can cover all types of infrastructures within the hydrogen supply network. In addition, the time horizon and geographic scale should be carefully selected to coordinate the characteristics of these two model classes. In light of these concerns, the main contributions of this chapter are:

- Propose for the first time a mathematical model that covers the entire hydrogen supply network (from feedstock supply to refueling stations).
- Demonstrate the advantages of considering all the relevant components within a single framework.

The remainder of this chapter is divided into six main sections. Section 3.2 analyzes the relevant scientific literature. Section 3.3 provides the problem description. Section 3.4 presents our proposed mathematical model. Section 3.5 describes the setup of instances as well as the input data. Section 3.6 presents the results and discussions. Finally, Section 3.7 provides the conclusions and outlines some plans for future developments.

3.2/ LITERATURE REVIEW

The relevant literature in both the fields of hydrogen supply network design and refueling station planning are reviewed in Chapter 2. The following provides some supplements.

3.2.1/ HYDROGEN SUPPLY CHAIN NETWORK DESIGN (HSCND)

Melo et al. (2009) highlighted the importance of explicitly integrating the feedstock issues into SCND. However, less than half of the reference papers reviewed in Chapter 2 involves the feedstock and its logistics into modeling, as shown in Table 3.1. It is also noted that few reference papers consider the possible adoption of a CCS (carbon capture and storage) system, which is of great importance to meet specific carbon targets when fossil energy is chosen as the feedstock. Moreover, little attention has been paid to the strategic decisions related to the refueling station in HSCND models. Neither the location problem nor the technology selection (i.e., standard or on-site) have been investigated. It is noteworthy that whether an HSCN is based on liquid hydrogen (LH_2) or gaseous hydrogen

(GH_2) is determined subjectively through the definition of scenarios or configurations in most of the models.

Table 3.1: Strategic decisions in main HSCND models

Papers	Feed.	Prod.	Transp.	CCS	Refueling station			
					Nb.	Lo.	Size	Tech.
Agnolucci et al.		✔	✔	✔	✔		✔	
Almansoori et al.		✔	✔					
Almansoori et al.	✔	✔	✔					
Cho et al.	✔	✔	✔					
Copado-Méndez et al.		✔	✔					
Almaraz et al.	✔	✔	✔		✔			
Guillén-Gosálbez et al.		✔	✔					
Hwangbo et al.		✔	✔					
Johnson et al.		✔	✔	✔				
Kim et al.		✔	✔					
Kim et al.		✔	✔					
Konda et al.		✔	✔	✔	✔			
Moreno-Benito et al.	✔	✔	✔	✔	✔			
Ogumerem et al.	✔	✔	✔					
Parker et al.	✔	✔	✔					
Samsatli et al.	✔	✔	✔					
Van Den Heever et al.		✔	✔					
Won et al.		✔	✔					
Woo et al.	✔	✔	✔		✔		✔	
Our study	✔	✔	✔	✔	✔	✔	✔	✔

Feed.: Feedstock and its transportation; Prod.: Hydrogen production; Transp.: Hydrogen transportation; CCS: Carbon capture and storage; Nb.: Number; Lo.: Location; Tech.: Technology.

3.2.2/ HYDROGEN REFUELING STATION PLANNING (HRSP)

Most papers published in this field concentrate on the location-allocation problem of refueling stations. Optimization-based approaches for locating refueling stations are divided into two main groups depending on the geometric representation of demands, which are models for node-based and flow-based demands (Hosseini et al., 2015).

The node-based demand models consider each node as a demand point, and drivers would have to make specific trips to join the facilities and obtain services. The main advantage of using these models is the relatively easy access to data, such as population and spatial information (Hwang et al., 2015). Nicholas et al. (2004) and Nicholas et al. (2006) employed the p-median model, which is one of the node-based demand models, to locate refueling stations that minimize a weighted sum of driving times to the closest station. Lin et al. (2008b) also applied the p-median model to the fuel-travel-back concept and proposed a MILP formulation that minimizes the total fuel-travel-back time. Another

example refers to the California Hydrogen Infrastructure Tool (CHIT), which is a geospatial analysis tool to identify the areas with the greatest need for refueling infrastructure based on a gap analysis between a projected market and current infrastructure (California Air Resources Board, 2018).

Many researchers argue that for refueling stations, as well as other service stations such as automatic teller machines, customer demand does not occur entirely at points, because people commonly will not make a trip solely for such a service (Jung et al., 2014). It may be more realistic to model the demands as *flows* on the network, which are served "on the way". This consideration leads to the development of flow-based models (Huang et al., 2015). First developed by Berman et al. (1992) and Hodgson (1990), the Flow-Capturing Location Model (FCLM) is a maximum coverage model that entails facility locations to serve passing flows, which are considered as captured if a facility is located on the flow paths. The basic model locates p facilities to capture as much flow as possible. Many modifications have been made to extend the original FCLM, such as introducing budget constraints (Shukla et al., 2011), considering the limited driving range of vehicles (Kuby et al., 2005, 2009; Lim et al., 2010), relaxing the assumption that all flows are on the shortest path between Origin–Destination pairs (Berman et al., 1995; Kim et al., 2012, 2013), and introducing refueling capacities (Hosseini et al., 2017b,a; Upchurch et al., 2009). Apart from the FCLM, there is another series of flow-based models that aim to satisfy all travel demands by deploying the least number of refueling stations (Wang et al., 2009, 2010, 2013).

While considerable attention has been paid to the location problem of refueling stations, the influence of refueling technology on location decisions has not received the attention it needs. It will be demonstrated in the following sections that the refueling network is deeply impacted by the selection of refueling technology (on-site or standard). It must also be noted that, for many flow-based models, the relationship between the captured flow and the refueling capacity has been neglected. In short, models cited above could tell "where" to locate the station, but neither the information on "what it is" (the refueling technology) nor "how big it is" (the size) is provided.

3.2.3/ LITERATURE SUMMARY

The existing literature reveals a gap in the development of comprehensive hydrogen supply network models. Some researchers have already noticed this issue. He et al. (2017) and Sun et al. (2017) have proposed hydrogen station location optimization models, which focus on the stage of hydrogen source-hydrogen station. Their models optimize the number and locations of stations, hydrogen source selection for the stations, and method of transportation to minimize the hydrogen life cycle cost. However, the capacity of each

station is pre-defined. Furthermore, the feedstock and its logistics, as well as a CCS system, have not been considered in the models. There is no decision variable relating to refueling technologies.

It is the primary purpose of this chapter to fill the research gap by integrating the hydrogen supply chain network design and hydrogen refueling station planning. Also, feedstock and CCS issues are involved, and the model can decide the refueling technology and refueling capacity of service stations.

3.3/ PROBLEM STATEMENT

Our model was developed to solve the problem summarized below. First, we assume to be given the following data:

- The estimated total amount of hydrogen consumed by FCEVs within a region, and spatial description of the region represented by an undirected graph. Each node denotes a city or a large town. It is a potential location for any type of component of the supply chain. It may be characterized by:
  - Demographic metrics (see Section 3.5) enabling to determine the hydrogen demand...
  - Availability of each type of feedstock (the upper and lower limit of supply capacity)
  - Existence of a potential CO_2 storage site and its processing capacity
  - Existence of fixed-location demand and its amount

  The nodes are connected with edges in the associated network graph. The edges represent the main roads of the geographical zone of the study. They are valued with distances between cities.
- A set of feedstocks, with each feedstock having the following properties:
  - Unit cost associated with its purchase
  - Corresponding production technology and transportation technology (if needed)
  - Number of units for producing 1 kg of hydrogen
- A set of production technologies, each is characterized by its:
  - Product form (gaseous or liquid hydrogen)
  - Capital, operating costs, and production capacity

  - Upstream emission factor, related to the emissions produced by the feedstock consumed and other energy inputs during their upstream processing (i.e., extraction, production, and transportation)
  - On-site emission factor, related to the emissions from the production procedure
  - Emission capture efficiency, the percentage of on-site emissions that can be captured if a CCS system is employed
- A set of refueling technologies (standard and on-site), each is characterized by:
  - Form of hydrogen it receives (standard refueling)
  - Corresponding type of feedstock (on-site refueling)
  - Feedstock demand (on-site refueling)
  - Minimum and maximum refueling capacity
  - Capital, operating costs, and emission factor
- A set of transportation technologies, each is defined by:
  - The cargo (hydrogen, feedstock, or CO_2), and the transportation capacity
  - Capital, operating costs, and emission factor (for hydrogen transportation)

Knowing such data, our goal is to determine:

- The feedstock supply and CCS system:
  - Which nodes are selected as feedstock supply sites?
  - What type of feedstock does each selected node supply and in what quantity?
  - Which nodes are selected to build the CO_2 storage sites?
  - The processing rate of each storage site
- The installation and operation of hydrogen facilities:
  - The number, location, size, and technology of production plants and refueling stations
  - Whether the network runs on gaseous or liquid hydrogen
  - Whether a CCS system is employed at each production plant
  - The production rate and refueling rate
- The operation of the transportation technology:
  - The rate of transportation of each type of cargo (hydrogen, feedstock, and CO_2) via each transportation mode between all locations.

Subject to

- The feedstock availability, the maximum capacity of technologies (production, refueling, CO_2 processing, and transportation), and the satisfaction of all fixed-location demands and a given percentage of FCEV's demand,

In order to

- Minimize the least cost of hydrogen (LCOH), which includes the contribution of capital investment, feedstock purchase, operating cost, and emission cost.

From a system modeling viewpoint, the hydrogen supply network design falls within the general category of strategic supply chain management problems (Mula et al., 2010). In terms of the structural features of the supply chain, the model that we propose is a single-commodity (hydrogen), mono-period, deterministic model with four location layers (feedstock, production, refueling station, and CO_2 storage). In addition to the typical location-allocation decisions, this model also involves decisions related to capacity, production, and transportation modes.

3.4/ MATHEMATICAL MODEL

Considering the problem characteristics, we developed a Mixed Integer Linear Program (MILP) for the studied problem. The notations are shown below, followed by the model assumptions. The objective function and constraints are characterized subsequently.

3.4.1/ NOTATIONS

3.4.1.1/ SETS

$e \in E$	feedstock types
$f \in F$	transportation mode of feedstock
$h \in H$	transportation mode of hydrogen
$i \in I$	hydrogen physical forms
$j \in J$	refueling facility sizes
$k \in K$	production facility sizes
$n, m \in N$	nodes
N_q	nodes on shortest path of OD (Origin–Destination) pair q
$o \in O$	on-site refueling technologies
$p \in P$	production technologies

$q \in Q$	OD (Origin–Destination) flow pairs
$s \in S$	standard refueling technologies

3.4.1.2/ SUBSETS

$(e,f) \in EF \subseteq E \times F$	combinations of feedstock types and transportation modes
$(e,o) \in EO \subseteq E \times O$	combinations of feedstock types and on-site refueling technologies
$(e,p) \in EP \subseteq E \times P$	combinations of feedstock types and production technologies
$(i,h) \in IH \subseteq I \times H$	combinations of hydrogen physical forms and transportation modes

3.4.1.3/ PARAMETERS

α	annual network operating period, d/y
β	payback period of capital investment, y
γ^e_{sij}	standard refueling station emission factor, kg CO_2/kg H_2
γ^e_{oj}	on-site refueling station emission factor, kg CO_2/kg H_2
γ^e_h	emission factor of hydrogen transportation mode h, kg CO_2/L fuel
γ^c_{pik}	production emission capture efficiency
γ^{eo}_{pik}	production on-site emission factor, kg CO_2/kg H_2
γ^{eu}_{pik}	production upstream emission factor, kg CO_2/kg H_2
$\delta_{(e,o)}$	conversion rates of feedstock to hydrogen (for on-site refueling stations), unit feedstock/kg H_2
$\delta_{(e,p)}$	conversion rates of feedstock to hydrogen (for hydrogen production plants), unit feedstock/kg H_2
ϵ	a small positive number
$ccap^{max}_n$	upper limit of CO_2 processing capacity, kg CO_2/d
$ccap^{min}_n$	lower limit of CO_2 processing capacity, kg CO_2/d
ccc	capital cost of a CO_2 storage site, €
coc	operating cost of CO_2 processing, €/kg CO_2
cp	carbon price, €/kg CO_2
$cpcc$	capital cost of CO_2 pipeline, €/km
$dem^{h,exp}$	percentage of hydrogen demand flow that expected to be captured, %
$dem^{h,A}_{ni}$	fixed-location hydrogen demand (Type A) of each node, kg H_2/d
$dem^{h,B}_{ni}$	fixed-location hydrogen demand (Type B) of each node, kg H_2/d
dw_h	driver wage of hydrogen transportation mode h, €/h
dw_f	driver wage of feedstock transportation mode f, €/h
$ecap^{max}_{ne}$	upper limit of feedstock supply capacity at each node, unit feedstock/d
$ecap^{min}_{ne}$	lower limit of feedstock supply capacity at each node, unit feedstock/d
eoc_e	operating cost of a feedstock site, €/d

euc_e	feedstock unit cost, €/unit feedstock
$fcap_{sij}^{max}$	upper limit of standard refueling capacity, kg H_2/d
$fcap_{sij}^{min}$	lower limit of standard refueling capacity, kg H_2/d
$fcap_{oj}^{max}$	upper limit of on-site refueling capacity, kg H_2/d
$fcap_{oj}^{min}$	lower limit of on-site refueling capacity, kg H_2/d
fcc_{sij}	capital cost of a standard refueling station, €
fcc_{oj}	capital cost of an on-site refueling station, €
fe_h	fuel economy of hydrogen transportation mode h, km/L fuel
fe_f	fuel economy of feedstock transportation mode f, km/L fuel
f_n^{node}	hydrogen refueling demand flow of each node, kg H_2/d
foc_{sij}	operating cost of a standard refueling station, €/kg H_2
foc_{oj}	operating cost of an on-site refueling station, €/kg H_2
fp_h	fuel price of hydrogen transportation mode h, €/L fuel
fp_f	fuel price of feedstock transportation mode f, €/L fuel
f_q^{pair}	hydrogen refueling demand flow of each OD (Origin–Destination) pair, kg H_2/d
ge_h	general expense of hydrogen transportation mode h, €/d
ge_f	general expense of feedstock transportation mode f, €/d
$id_n^{h,A}$	equals 1 if there exists fixed-location hydrogen demand (Type A) at this node (0 otherwise)
$id_n^{h,B}$	equals 1 if there exists fixed-location hydrogen demand (Type B) at this node (0 otherwise)
l_{nm}	the shortest distance between two different nodes, km
lut_h	load/unload time of hydrogen transportation mode h, h
lut_f	load/unload time of feedstock transportation mode f, h
me_h	maintenance expense of hydrogen transportation mode h, €/km
me_f	maintenance expense of feedstock transportation mode f, €/km
$pcap_{pik}^{max}$	upper limit of production capacity, kg H_2/d
$pcap_{pik}^{min}$	lower limit of production capacity, kg H_2/d
pcc_{pik}	capital cost of a production plant, €
poc_{pik}	operating cost of a production plant, €/kg H_2
sp_h	speed of hydrogen transportation mode h, km/h
sp_f	speed of feedstock transportation mode f, km/h
$tcap_h$	capacity of hydrogen transportation mode h, kg H_2
$tcap_f$	capacity of feedstock transportation mode f, unit feedstock
$tcap_h^{max}$	upper limit of hydrogen transportation capacity between two nodes, kg H_2/d
$tcap_f^{max}$	upper limit of feedstock transportation capacity between two nodes, unit feedstock/d
$tcap_h^{min}$	lower limit of hydrogen transportation capacity between two nodes, kg H_2/d
$tcap_f^{min}$	lower limit of feedstock transportation capacity between two nodes,

	unit feedstock/d
$tcap^{max}$	upper limit of CO_2 transportation capacity, kg CO_2/d
$tcap^{min}$	lower limit of CO_2 transportation capacity, kg CO_2/d
tcr_h	vehicle rental cost of hydrogen transportation mode h (for each vehicle), €/d
tcr_f	vehicle rental cost of feedstock transportation mode f (for each vehicle), €/d
tma_h	availability of hydrogen transportation mode h, h/d
tma_f	availability of feedstock transportation mode f, h/d

3.4.1.4/ CONTINUOUS VARIABLES

CC	total daily capital cost, €/d
CR	total processing rate of CO_2, kg CO_2/d
CR_n	CO_2 processing rate of a CO_2 storage site, kg CO_2/d
$DEM^{h,cap}$	percentage of hydrogen demand flow that could be captured, %
EC	daily feedstock purchasing cost, €/d
EMC	daily emission cost, €/d
ER	total emission rate, kg CO_2/d
ESR_e	total feedstock supply rate of feedstock sites, unit feedstock/d (feedstock type e)
FCC	daily facility capital cost, €/d
FFC	daily feedstock transportation fuel cost, €/d
FGC	daily feedstock transportation general cost, €/d
FLC	daily feedstock transportation labor cost, €/d
FMC	daily feedstock transportation maintenance cost, €/d
FOC	daily facility operating cost, €/d
FR_{noj}	refueling rate of an on-site refueling station, kg H_2/d (refueling technology o, size j)
FR_{nsij}	refueling rate of a standard refueling station, kg H_2/d (refueling technology s, hydrogen form i, size j)
FR_{oj}	total refueling rate of on-site refueling stations, kg H_2/d (refueling technology o, size j)
FR_{sij}	total refueling rate of standard refueling stations, kg H_2/d (refueling technology s, hydrogen form i, size j)
FRC	daily feedstock transportation vehicle rental cost, €/d
$FTOC$	daily feedstock transportation operating cost, €/d
HFC	daily hydrogen transportation fuel cost, €/d
HGC	daily hydrogen transportation general cost, €/d
HLC	daily hydrogen transportation labor cost, €/d
HMC	daily hydrogen transportation maintenance cost, €/d

HRC daily hydrogen transportation vehicle rental cost, €/d
$HTOC$ daily hydrogen transportation operating cost, €/d
$LCOH$ least cost of hydrogen, €/kg H_2
OC total daily operating cost, €/d
$OESR_{ne}$ feedstock supply rate for the on-site refueling station at node n, unit feedstock/d (feedstock type e)
$OFER$ total emission rate of on-site refueling stations, kg CO_2/d
PER total production emission rate, kg CO_2/d
PER^c total emission rate of production plants where emissions are captured, kg CO_2/d
PER^c_n emission rate of a production plant where emissions are captured, kg CO_2/d
$PESR_{ne}$ feedstock supply rate for production plants at node n or built at other nodes, unit feedstock/d, (feedstock type e)
PR^c_{npik} production rate of a production plant where emissions are processed, kg H_2/d
PR_{npik} production rate of a production plant, kg H_2/d (production technology p, hydrogen form i, size k)
PR_{pik} total production rate of production plants, kg H_2/d (production technology p, hydrogen form i, size k)
Q_{fnm} feedstock transportation flux from node n to m, unit feedstock/d (transportation mode f)
Q_{hnm} hydrogen transportation flux from node n to m, kg H_2/d (transportation mode h)
Q_{nm} CO_2 transportation flux from node n to m, kg CO_2/d
$SFER$ total emission rate of standard refueling stations, kg CO_2/d
TCC daily CO_2 transportation capital cost, €/d
TDC total daily cost, €/d
TER total emission rate of hydrogen transportation, kg CO_2/d
THD the amount of hydrogen delivered per day, kg H_2/d

3.4.1.5/ INTEGER VARIABLES

NE_e number of feedstock supply sites (for hydrogen production plants) (feedstock type e)
NF_{sij} number of standard refueling stations (refueling technology s, hydrogen form i, size j)
NF_{oj} number of on-site refueling stations (refueling technology o, size j)
NP_{pik} number of production plants (production technology p, hydrogen form i, size k)
NR number of CO_2 storage reservoirs
NV_h number of hydrogen transportation vehicles

NV_f number of feedstock transportation vehicles

3.4.1.6/ BINARY VARIABLES

IC_q 1 if hydrogen refueling demand flow pair q is captured
IE_n 1 if the node is chosen as a feedstock supplier of production plants
IE_{ne} 1 if the node is chosen as a feedstock supplier of production plants (feedstock type e)
IF_n 1 if there is a refueling station at this node
IF_{no} 1 if there is an on-site refueling station at this node (refueling technology o)
IF_{nsij} 1 if there is a standard refueling station at this node (refueling technology s, hydrogen form i, size j)
IF_{noj} 1 if there is an on-site refueling station at this node (refueling technology o, size j)
IM_n 1 if the emission of production plant at this node is processed
IP_n 1 if there is a production plant at this node
IP_{npik} 1 if there is a production plant at this node (production technology p, hydrogen form i, size k)
IR_n 1 if there is a CO_2 storage site at this node
OIF_n 1 if there is an on-site refueling station at this node
SIF_n 1 if there is a standard refueling station at this node
X_{fnm} 1 if feedstock is to be transported from node n to m in transportation mode f
X_{hnm} 1 if hydrogen is to be transported from node n to m in transportation mode h
X_{nm} 1 if CO_2 is to be transported through pipeline from node n to m

3.4.2/ MODEL ASSUMPTIONS

The study is based on the following assumptions:

- The length of the shortest path between each pair of nodes is regarded as the distance between the two nodes, which is given as input data;
- Two types of fixed-location demand are considered: Type A refers to stationary applications such as combined heat and power system, and Type B refers to fleet vehicles. For the former, one needs only to deliver the required amount of hydrogen, while for the latter, in addition to meeting the fixed-location demand, one should also build a standard refueling station to satisfy the refueling demand at that node;

- The vehicles required to deliver hydrogen and feedstock are rented;
- The potential locations where the CO_2 storage sites could be built are given as model inputs;
- Only the CO_2 emission of the hydrogen production plants could be captured and processed by the CCS system;
- The total amount of CO_2 emission of the HSCN could be zero or negative depending on the type of feedstock selected and whether a CCS system is adopted (e.g., when biomass is selected as feedstock and a CCS system is also applied). Negative emissions generate revenue. For simplicity, the carbon price remains the same for both positive and negative emissions.

3.4.3/ OBJECTIVE FUNCTION

The optimization framework seeks to minimize the least cost of hydrogen ($LCOH$) in €/kg H_2, which is attained by dividing the total daily cost (TDC) by the amount of hydrogen delivered per day (THD):

$$Minimize \quad LCOH \tag{3.1}$$

$$LCOH = \frac{TDC}{THD} \tag{3.2}$$

The total daily cost (TDC) consists of the contribution of capital cost (CC), feedstock purchasing cost (EC), operating cost (OC), and emission cost (EMC):

$$TDC = CC + EC + OC + EMC \tag{3.3}$$

The amount of hydrogen delivered per day (THD) is given by

$$THD = \sum_{q \in Q} f_q^{pair} * IC_q + \sum_{n \in N, i \in I} (dem_{ni}^{h,A} + dem_{ni}^{h,B}) \tag{3.4}$$

The first term on the right-hand-side of Eq. (3.4) refers to the hydrogen demand of FCEVs, where f_q^{pair} is the amount of hydrogen refueling demand flow of OD (Origin–Destination) flow pair q, and IC_q equals 1 if flow pair q is captured. The second term refers to the fixed-location demand, and $dem_{ni}^{h,A}$ and $dem_{ni}^{h,B}$ represent the fixed demand at node n (in hydrogen form i) of Type A and Type B, respectively.

3.4.3.1/ DAILY CAPITAL COST (CC)

The capital cost is composed of facility capital cost (FCC) and CO_2 transportation capital cost (TCC):

$$CC = \frac{1}{\alpha * \beta}(FCC + TCC) \tag{3.5}$$

The right-hand-side of Eq. (3.5) is divided by the annual network operating period (α) and the payback period of capital investment (β) to find the cost per day.

- Facility capital cost (FCC)

$$\begin{aligned} FCC = \sum_{p\in P, i\in I, k\in K} NP_{pik} * pcc_{pik} + \sum_{s\in S, i\in I, j\in J} NF_{sij} * fcc_{sij} \\ + \sum_{o\in O, j\in J} NF_{oj} * fcc_{oj} + NR * ccc \end{aligned} \tag{3.6}$$

where NP_{pik} represents the number of production plants of technology p, hydrogen form i, and size k. pcc_{pik} is the capital cost of one plant of this type. NF_{sij} denotes the number of standard refueling stations of technology s, hydrogen form i, and size j. fcc_{sij} is the capital cost of one station of this type. NF_{oj} gives the number of on-site refueling stations of technology o and size j. fcc_{oj} is the capital cost of one station of this type. NR represents the number of CO_2 storage sites and ccc is the capital cost of one site.

- CO_2 transportation capital cost (TCC)

The TCC is obtained by multiplying the unit capital cost of CO_2 pipeline ($cpcc$) by the pipeline length:

$$TCC = cpcc * \sum_{n,m\in N} X_{nm} * l_{nm} \tag{3.7}$$

where X_{nm} equals 1 if CO_2 is transported from node n to m, and l_{nm} is the shortest distance between the two nodes.

3.4.3.2/ DAILY FEEDSTOCK PURCHASING COST (EC)

$$EC = \sum_{e\in E} ESR_e * euc_e \tag{3.8}$$

where euc_e is the unit cost of the feedstock of type e, and ESR_e is the total supply rate of the feedstock of type e, given by

$$ESR_e = \sum_{n \in N} (PESR_{ne} + OESR_{ne}) \tag{3.9}$$

where $PESR_{ne}$ is the supply rate of a feedstock site at node n that supplies feedstock of type e to hydrogen production plants (plants at the same node or built at other nodes). $OESR_{ne}$ is the feedstock supply rate of a feedstock site at node n that supplies feedstock of type e only to the on-site refueling station built at the same node.

3.4.3.3/ DAILY OPERATING COST (OC)

The operating cost (OC) includes the facility operating cost (FOC), the operating cost associated with hydrogen, and feedstock transportation ($HTOC, FTOC$):

$$OC = FOC + HTOC + FTOC \tag{3.10}$$

- Facility operating cost (FOC)

$$FOC = \sum_{e \in E} NE_e * eoc_e + \sum_{p \in P, i \in I, k \in K} PR_{pik} * poc_{pik} + \sum_{s \in S, i \in I, j \in J} FR_{sij} * foc_{sij} + \sum_{o \in O, j \in J} FR_{oj} * foc_{oj} + CR * coc \tag{3.11}$$

where NE_e represents the number of feedstock supply sites that supply feedstock of type e to hydrogen production plants. eoc_e is the operating cost of one site of this type. PR_{pik} gives the total production rate of the production plants of technology p, hydrogen form i, and size k. poc_{pik} is the unit operating cost (per kg H_2) of this type of plant. FR_{sij} denotes the total refueling rate of standard refueling stations of technology s, hydrogen form i, and size j. foc_{sij} is the unit operating cost (per kg H_2) of this type of station. FR_{oj} represents the total refueling rate of on-site refueling stations of technology o and size j. foc_{oj} is the unit operating cost (per kg H_2) of this type of station. CR (defined in Eq. (3.63)) gives the total processing rate of CO_2. coc is the unit operating cost (per kg CO_2).

- Hydrogen transportation operating cost ($HTOC$)

$$HTOC = HFC + HLC + HMC + HGC + HRC \tag{3.12}$$

the five items on the right-hand-side are the fuel cost, labor cost, maintenance cost, general cost, and vehicle rental cost of hydrogen transportation, respectively. They are defined in Eqs. (3.13) - (3.17):

$$HFC = \sum_{h\in H,n,m\in N} fp_h * \frac{2 * l_{nm} * Q_{hnm}}{fe_h * tcap_h} \tag{3.13}$$

$$HLC = \sum_{h\in H,n,m\in N} dw_h * \frac{Q_{hnm}}{tcap_h} * (\frac{2 * l_{nm}}{sp_h} + lut_h) \tag{3.14}$$

$$HMC = \sum_{h\in H,n,m\in N} me_h * \frac{2 * l_{nm} * Q_{hnm}}{tcap_h} \tag{3.15}$$

$$HGC = \sum_{h\in H,n,m\in N} ge_h * \frac{Q_{hnm}}{tma_h * tcap_h} * (\frac{2 * l_{nm}}{sp_h} + lut_h) \tag{3.16}$$

$$HRC = \sum_{h\in H} NV_h * tcr_h \tag{3.17}$$

In these equations, fp_h, dw_h, me_h, ge_h, and tcr_h represent the fuel price (per liter fuel), driver wage (per hour), maintenance expense (per km), general expense (per day), and vehicle rental cost (per vehicle) of hydrogen transportation mode h, respectively. fe_h, sp_h, $tcap_h$, tma_h, and lut_h denote the fuel economy, speed, capacity, availability (hours per day), and load/unload time of hydrogen transportation mode h, respectively. Q_{hnm} represents the hydrogen transportation flux (in mode h) from node n to m, and l_{nm} is the shortest distance between the two nodes. NV_h denotes the number of hydrogen transportation vehicles of mode h and is calculated by the following:

$$NV_h \geqslant \sum_{n,m\in N} \frac{Q_{hnm}}{tma_h * tcap_h} * (\frac{2 * l_{nm}}{sp_h} + lut_h), \quad \forall h \in H \tag{3.18}$$

- Feedstock transportation operating cost ($FTOC$)

$$FTOC = FFC + FLC + FMC + FGC + FRC \tag{3.19}$$

The five items on the right-hand-side are the fuel cost, labor cost, maintenance cost, general cost, and vehicle rental cost of feedstock transportation, respectively. Their definitions and calculation of the number of feedstock transportation vehicles have the same forms as those of the hydrogen transportation operating cost (Eqs. (3.13) - (3.18)).

3.4.3.4/ DAILY EMISSION COST (EMC)

$$EMC = ER * cp \tag{3.20}$$

where cp is the carbon price and ER is the total emission rate, which is given by

$$ER = (PER - PER^c) + SFER + OFER + TER \tag{3.21}$$

PER is the production emission rate, which is obtained by

$$PER = \sum_{n\in N, p\in P, i\in I, k\in K} PR_{npik} * (\gamma^{eu}_{pik} + \gamma^{eo}_{pik}) \tag{3.22}$$

In the equation, PR_{npik} denotes the production rate of a production plant of technology p, hydrogen form i, and size k. γ^{eu}_{pik} and γ^{eo}_{pik} are the production upstream and on-site emission factors of this type of plant, respectively.

PER^c is the total emission rate of production plants where emissions are processed, given by

$$PER^c = \sum_{n\in N} PER^c_n \tag{3.23}$$

where PER^c_n is the emission rate of a production plant at node n, where emissions are processed, given by

$$PER^c_n = \sum_{p\in P, i\in I, k\in K} PR^c_{npik} * \gamma^{eo}_{pik} * \gamma^c_{pik} \tag{3.24}$$

where PR^c_{npik} represents the production rate of a production plant of technology p, hydrogen form i, and size k, and where emissions are processed (see Eq. (3.65)), and γ^c_{pik} is the production emission capture efficiency of this type of plant.

Refueling emission rates are obtained by Eqs. (3.25) and (3.26):

$$SFER = \sum_{s\in S, i\in I, j\in J} FR_{sij} * \gamma^e_{sij} \tag{3.25}$$

$$OFER = \sum_{o\in O, j\in J} FR_{oj} * \gamma^e_{oj} \tag{3.26}$$

$SFER$ and $OFER$ are the total emission rates of the standard and on-site refueling stations, respectively. FR_{sij} represents the total refueling rate of standard refueling stations of technology s, hydrogen form i, and size j. γ^e_{sij} is the emission factor of this type of station. FR_{oj} denotes the total refueling rate of on-site refueling stations of technology o and size j. γ^e_{oj} is the emission factor of this type of station.

The emission rates related to hydrogen transportation (TER) depend on fuel usage, given by

$$TER = \sum_{h \in H, n,m \in N} \gamma_h^e * \frac{2 * l_{nm} * Q_{hnm}}{fe_h * tcap_h} \tag{3.27}$$

where γ_h^e is the emission factor of hydrogen transportation, which represents the volume of emissions due to the unit fuel usage. Q_{hnm} represents the hydrogen transportation flux (in mode h) from node n to m, and l_{nm} is the shortest distance between the two nodes. fe_h and $tcap_h$ are the fuel economy and capacity of hydrogen transportation mode h. The emissions results from feedstock transportation are included in the upstream emission of hydrogen production, therefore do not need to be calculated separately.

3.4.4/ CONSTRAINTS

3.4.4.1/ MASS BALANCE CONSTRAINTS

- Hydrogen

The hydrogen mass balance is defined at each node n, and for each hydrogen form i, such that the hydrogen production (PR_{npik}) and input from other nodes m (Q_{hmn}) meets the refueling demand (FR_{nsij}), the fixed-location demand ($dem_{ni}^{h,A}, dem_{ni}^{h,B}$) of this node n, and the hydrogen output to other nodes m (Q_{hnm}), as follows:

$$\sum_{p \in P, k \in K} PR_{npik} + \sum_{m \in N, h:(i,h) \in IH} Q_{hmn} = \sum_{m \in N, h:(i,h) \in IH} Q_{hnm} + \sum_{s \in S, j \in J} FR_{nsij} + dem_{ni}^{h,A} + dem_{ni}^{h,B}, \quad \forall n \in N, i \in I \tag{3.28}$$

- Feedstock

For feedstock consumed by hydrogen production plants, the feedstock mass balance is defined at each node n, for each combination of feedstock types and production technologies (e, p), such that the feedstock supply ($PESR_{ne}$) and input from other nodes m (Q_{fmn}) meets the consumption of feedstock, which is calculated by multiplying the production rate at that node (PR_{npik}) by the corresponding conversion rate ($\delta_{(e,p)}$), and the feedstock output to other nodes m (Q_{fnm}), as follows:

$$PESR_{ne} + \sum_{m\in N, f:(e,f)\in EF} Q_{fmn} = \sum_{m\in N, f:(e,f)\in EF} Q_{fnm} + \sum_{i\in I, k\in K} PR_{npik} * \delta_{(e,p)}, \quad \forall n \in N, (e,p) \in EP \tag{3.29}$$

For feedstock consumed by on-site refueling stations, the feedstock mass balance is given:

$$OESR_{ne} = \sum_{j\in J} FR_{noj} * \delta_{(e,o)}, \quad \forall n \in N, (e,o) \in EF \tag{3.30}$$

In the equation, $OESR_{ne}$ represents the feedstock supply rate. FR_{noj} denotes the refueling rate and $\delta_{(e,o)}$ is the conversion rate of feedstock (type e) to hydrogen at on-site stations.

- CO_2

The CO_2 mass balance should be likewise satisfied at each node n to quantify the infrastructure needs for a CCS system.

$$PER_n^c + \sum_{m\in N} Q_{mn} = \sum_{m\in N} Q_{nm} + CR_n, \quad \forall n \in N \tag{3.31}$$

In the equation, PER_n^c represents the emission rate of a production plant at node n, where emissions are processed. Q_{mn} is the CO_2 transportation flux from node m to n, whereas Q_{nm} is the flux from node n to m. CR_n is the CO_2 processing rate.

3.4.4.2/ FEEDSTOCK CONSTRAINTS

The feedstock supply rate ($PESR_{ne}$, $OESR_{ne}$) cannot exceed certain limits:

$$IE_{ne} * ecap_{ne}^{min} \leqslant PESR_{ne} \leqslant IE_{ne} * ecap_{ne}^{max}, \quad \forall n \in N, e \in E \tag{3.32}$$

$$IF_{no} * ecap_{ne}^{min} \leqslant OESR_{ne} \leqslant IF_{no} * ecap_{ne}^{max}, \quad \forall n \in N, (e,o) \in EO \tag{3.33}$$

$$PESR_{ne} + OESR_{ne} \leqslant ecap_{ne}^{max}, \quad \forall n \in N, e \in E \tag{3.34}$$

IF_{no} equals 1 if there is an on-site refueling station of technology o at node n, and is defined by

$$IF_{no} = \sum_{j \in J} IF_{noj}, \quad \forall n \in N, o \in O \tag{3.35}$$

The number of feedstock supply sites that supply feedstock of type e to hydrogen production plants (NE_e) is defined as

$$NE_e = \sum_{n \in N} IE_{ne}, \quad \forall e \in E \tag{3.36}$$

In Eqs. (3.32) - (3.36), IE_{ne} equals 1 if node n is chosen as a feedstock supplier (type e) of production sites. IF_{noj} equals 1 if there is an on-site refueling station of technology o and size j at node n. The bounds of feedstock supply capacity are denoted by $ecap$.

3.4.4.3/ PRODUCTION CONSTRAINTS

The production rate (PR_{npik}) cannot exceed certain limits:

$$IP_{npik} * pcap_{pik}^{min} \leqslant PR_{npik} \leqslant IP_{npik} * pcap_{pik}^{max}, \quad \forall n \in N, p \in P, i \in I, k \in K \tag{3.37}$$

The number of production plants (NP_{pik}) is given by

$$NP_{pik} = \sum_{n \in N} IP_{npik}, \quad \forall p \in P, i \in I, k \in K \tag{3.38}$$

The total production rate of production plants (PR_{pik}) is defined as

$$PR_{pik} = \sum_{n \in N} PR_{npik}, \quad \forall p \in P, i \in I, k \in K \tag{3.39}$$

In Eqs. (3.37) - (3.39), IP_{npik} equals 1 if there is a production plant at node n, of technology p, hydrogen form i, and size k. The bounds of production capacity are represented by $pcap$.

3.4.4.4/ REFUELING STATION CONSTRAINTS

The refueling rate (FR_{nsij}, FR_{noj}) cannot exceed certain limits:

$$IF_{nsij} * fcap_{sij}^{min} \leqslant FR_{nsij} \leqslant IF_{nsij} * fcap_{sij}^{max}, \quad \forall n \in N, s \in S, i \in I, j \in J \tag{3.40}$$

$$IF_{noj} * fcap_{oj}^{min} \leqslant FR_{noj} \leqslant IF_{noj} * fcap_{oj}^{max}, \quad \forall n \in N, o \in O, j \in J \tag{3.41}$$

The total refueling rates (FR_{sij}, FR_{oj}) are defined as

$$FR_{sij} = \sum_{n \in N} FR_{nsij}, \quad \forall s \in S, i \in I, j \in J \tag{3.42}$$

$$FR_{oj} = \sum_{n \in N} FR_{noj}, \quad \forall o \in O, j \in J \tag{3.43}$$

The number of refueling stations (NF_{sij}, NF_{oj}) are given by

$$NF_{sij} = \sum_{n \in N} IF_{nsij}, \quad \forall s \in S, i \in I, j \in J \tag{3.44}$$

$$NF_{oj} = \sum_{n \in N} IF_{noj}, \quad \forall o \in O, j \in J \tag{3.45}$$

In Eqs. (3.40) - (3.45), IF_{nsij} equals 1 if there is a standard refueling station at node n, of technology s, hydrogen form i, and size j. IF_{noj} equals 1 if there is an on-site refueling station at node n, of technology o and size j. The bounds of refueling capacity are denoted by $fcap$.

If fixed-location hydrogen demand of Type B exists at node n (means $id_n^{h,B}$ equals 1), a standard refueling station should also be built at this node:

$$SIF_n \geqslant id_n^{h,B}, \quad \forall n \in N \tag{3.46}$$

SIF_n equals 1 if there is a standard refueling station at node n.

3.4.4.5/ TRANSPORTATION CONSTRAINTS

The transportation flux of hydrogen, feedstock, and CO_2 (Q_{hnm}, Q_{fnm}, Q_{nm}) cannot exceed certain limits:

$$X_{hnm} * tcap_h^{min} \leqslant Q_{hnm} \leqslant X_{hnm} * tcap_h^{max}, \quad \forall h \in H, n, m \in N \tag{3.47}$$

$$X_{fnm} * tcap_f^{min} \leqslant Q_{fnm} \leqslant X_{fnm} * tcap_f^{max}, \quad \forall f \in F, n, m \in N \tag{3.48}$$

$$X_{nm} * tcap^{min} \leqslant Q_{nm} \leqslant X_{nm} * tcap^{max}, \quad \forall n, m \in N \tag{3.49}$$

In Eqs. (3.47) - (3.49), X_{hnm}, X_{fnm}, and X_{nm} are binary variables that take the value of 1 if transportation links are established from node n to m. The bounds of transportation capacity are represented by $tcap$.

Transportation between different nodes can only occur in one direction:

$$X_{hnm} + X_{hmn} \leqslant 1, \quad \forall h \in H, n, m \in N \tag{3.50}$$

$$X_{fnm} + X_{fmn} \leqslant 1, \quad \forall f \in F, n, m \in N \tag{3.51}$$

$$X_{nm} + X_{mn} \leqslant 1, \quad \forall n, m \in N \tag{3.52}$$

A node can only export hydrogen when there is a production plant at this node:

$$IP_n \geqslant X_{hnm}, \quad \forall h \in H, n, m \in N \tag{3.53}$$

where IP_n equals 1 if there is a production plant (of any technology, any hydrogen form, and any size) at this node. The following equation ensures that only one plant could be installed at each node.

$$IP_n = \sum_{p \in P, i \in I, k \in K} IP_{npik}, \quad \forall n \in N \tag{3.54}$$

where IP_{npik} equals 1 if there is a production plant at node n, of technology p, hydrogen form i, and size k.

Hydrogen is imported into the nodes that have standard refueling stations or fixed-location demand of Type A, or both:

$$SIF_n + id_n^{h,A} \geqslant X_{hmn}, \quad \forall h \in H, n, m \in N \tag{3.55}$$

where SIF_n equals 1 if there is a standard refueling station (of any technology, any hydrogen form, and any size) at this node. $id_n^{h,A}$ indicates whether node n has fixed-location demand of Type A.

A node cannot export feedstock when there is no feedstock supplier of hydrogen production plants (of any type of feedstocks) at this node (implies IE_n equals to 0):

$$IE_n \geqslant X_{fnm}, \quad \forall f \in F, n, m \in N \tag{3.56}$$

where IE_n is defined as

$$IE_n = \sum_{e \in E} IE_{ne}, \quad \forall n \in N \tag{3.57}$$

where IE_{ne} equals 1 if node n is chosen as a feedstock supplier that supplies feedstock of type e to production plants.

The end of the feedstock transportation link can only be the production plants:

$$IP_n \geqslant X_{fmn}, \quad \forall f \in F, n, m \in N \tag{3.58}$$

where IP_n equals 1 if there is a production plant at node n.

A node can only export CO_2 when the emission of the production plant at this node is processed (means IM_n equals 1):

$$IM_n \geqslant X_{nm}, \quad \forall n, m \in N \tag{3.59}$$

The CO_2 transportation link ends only at the nodes where CO_2 storage sites are located (means IR_n equals 1):

$$IR_n \geqslant X_{mn}, \quad \forall n, m \in N \tag{3.60}$$

3.4.4.6/ EMISSION CONSTRAINTS

The production emission of a node cannot be processed if there is no plant at this node:

$$IM_n \leqslant IP_n, \quad \forall n \in N \tag{3.61}$$

where IP_n denotes whether node n has a production plant, and IM_n takes the value of 1 if the emission of the plant at that node is processed.

The CO_2 processing rate (CR_n) cannot exceed certain limits:

$$IR_n * ccap_n^{min} \leqslant CR_n \leqslant IR_n * ccap_n^{max}, \quad \forall n \in N \tag{3.62}$$

where IR_n equals 1 if there is a CO_2 storage site at node n. The bounds of CO_2 processing

capacity are represented by $ccap$.

The total processing rate of CO_2 (CR) is given by

$$CR = \sum_{n \in N} CR_n \tag{3.63}$$

where CR_n is the CO_2 processing rate of a CO_2 storage site at node n.

The number of CO_2 storage sites (NR) is defined as

$$NR = \sum_{n \in N} IR_n \tag{3.64}$$

The production rate of a production plant where emissions are processed (PR^c_{npik}) can be obtained by the following equation:

$$PR^c_{npik} = IM_n * PR_{npik}, \quad \forall n \in N, p \in P, i \in I, k \in K \tag{3.65}$$

where PR_{npik} represents the production rate of a production plant at node n, and IM_n denotes whether the emission of this plant is processed.

The Eq. (3.65) is nonlinear and can be linearized by the following constraints:

$$PR^c_{npik} \leqslant IM_n * pcap^{max}_{pik}, \quad \forall n \in N, p \in P, i \in I, k \in K \tag{3.66}$$

$$PR^c_{npik} \leqslant PR_{npik}, \quad \forall n \in N, p \in P, i \in I, k \in K \tag{3.67}$$

$$PR^c_{npik} \geqslant PR_{npik} - (1 - IM_n) * pcap^{max}_{pik}, \quad \forall n \in N, p \in P, i \in I, k \in K \tag{3.68}$$

where $pcap^{max}_{pik}$ is the upper limit of production capacity.

3.4.4.7/ DEMAND CONSTRAINTS

The percentage of hydrogen refueling demand flow that can be captured ($DEM^{h,cap}$) should be equal to the number given as input ($dem^{h,exp}$):

$$DEM^{h,cap} = dem^{h,exp} \tag{3.69}$$

Because hydrogen refueling demand flow of OD (Origin–Destination) flow pairs are dis-

crete values, the following constraints to replace the Eq. (3.69) are introduced:

$$dem^{h,exp} \leqslant DEM^{h,cap} \leqslant dem^{h,exp} + \epsilon \tag{3.70}$$

where ϵ is a small positive number, which is set to 0.01 in this study, and $DEM^{h,cap}$ is defined by

$$DEM^{h,cap} = \frac{\sum_{q \in Q} f_q^{pair} * IC_q}{\sum_{q \in Q} f_q^{pair}} * 100 \tag{3.71}$$

where f_q^{pair} is the amount of hydrogen refueling demand flow of OD flow pair q, and IC_q equals 1 if flow pair q is captured.

A hydrogen refueling demand flow is captured if there is at least one refueling station (of any technology and any size) on one of the nodes that lie on the shortest path of this flow pair:

$$\sum_{n \in N_q} IF_n \geqslant IC_q, \quad \forall q \in Q, \tag{3.72}$$

where IF_n equals 1 if there is a refueling station (standard or on-site) at this node. The following equations ensure that only one refueling station could be installed at each node.

$$IF_n = SIF_n + OIF_n, \quad \forall n \in N \tag{3.73}$$

$$SIF_n = \sum_{s \in S, i \in I, j \in J} IF_{nsij}, \quad \forall n \in N \tag{3.74}$$

$$OIF_n = \sum_{o \in O, j \in J} IF_{noj}, \quad \forall n \in N \tag{3.75}$$

where SIF_n equals 1 if there is a standard refueling station at node n, and OIF_n equals 1 if there is an on-site refueling station at this node. IF_{nsij} equals 1 if there is a standard refueling station at node n, of technology s, hydrogen form i, and size j. IF_{noj} equals 1 if there is an on-site refueling station at node n, of technology o and size j.

The refueling rate at node n (FR_{nsij}, FR_{noj}) should be able to cover the amount of hydrogen refueling demand flow captured by the refueling station established at that node:

$$\sum_{s \in S, i \in I, j \in J} FR_{nsij} \geqslant SIF_n * f_n^{node}, \quad \forall n \in N \tag{3.76}$$

$$\sum_{o\in O, j\in J} FR_{noj} \geqslant OIF_n * f_n^{node}, \quad \forall n \in N \tag{3.77}$$

where f_n^{node} is the hydrogen refueling demand flow of node n.

3.4.5/ SOME ELEMENTS FOR COMPLEXITY

Considering $|E|$ as the number of elements in the set E, it is possible to determine the number of continuous, integer and binary variables as well as the number of constraints.

Number of decision variables:

- continuous:

  $|x_1| = 30 + |E| + |O| \cdot |J| + |S| \cdot |I| \cdot |J| + |P| \cdot |I| \cdot |K|$
  $+|N| \cdot (2 + 2 \cdot |E| + |O| \cdot |J| + |S| \cdot |I| \cdot |J| + 2 \cdot |P| \cdot |I| \cdot |K|)$
  $+|N|^2 \cdot (1 + |H| + |F|)$
  If we consider only the independent variables, the number is :
  $|x_1| = 2 + |E|$
  $+|N| \cdot (1 + |E| + |O| \cdot |J| + |S| \cdot |I| \cdot |J| + 2 \cdot |P| \cdot |I| \cdot |K|)$
  $+|N|^2 \cdot (1 + |H| + |F|)$

- integer:

  $|x_2| = 1 + |E| + |F| + |H| + |O| \cdot |J| + |S| \cdot |I| \cdot [J| + |P| \cdot |I| \cdot |K|$
  Only NV_h and NV_f are integer independent variables
  $|x_2| = |F| + |H|$

- binary:

  $|x_3| = |Q|$
  $+|N| \cdot (7 + |E| + |O| + |O| \cdot |J| + |S| \cdot |I| \cdot [J| + |P| \cdot |I| \cdot |K|)$
  $+|N|^2 \cdot (1 + |H| + |F|)$
  If we consider only the independent variables, the number is :
  $|x_3| = |Q|$
  $+|N| \cdot (2 + |E| + |O| \cdot |J| + |S| \cdot |I| \cdot [J| + |P| \cdot |I| \cdot |K|)$
  $+|N|^2 \cdot (1 + |H| + |F|)$

- global:

$|x| = |x_1| + |x_2| + |x_3| = 31 + 2 \cdot |E| + |F| + |H| + |Q| + 2 \cdot |O| \cdot |J| + 2 \cdot |S| \cdot |I| \cdot [J| + 2 \cdot |P| \cdot |I| \cdot |K|$
$+|N| \cdot (9 + 3 \cdot |E| + |O| + 2 \cdot |O| \cdot |J| + 2 \cdot |S| \cdot |I| \cdot |J| + 3 \cdot |P| \cdot |I| \cdot |K|)$
$+2 \cdot |N|^2 \cdot (1 + |H| + |F|)$
the total number of independant variables is :
$|x| = |x_1| + |x_2| + |x_3| = 2 + |E| + |F| + |H| + |Q|$
$+|N| \cdot (3 + 2 \cdot |E| + 2 \cdot |O| \cdot |J| + 2 \cdot |S| \cdot |I| \cdot |J| + 3 \cdot |P| \cdot |I| \cdot |K|)$
$+2 \cdot |N|^2 \cdot (1 + |H| + |F|)$

If the number of nodes in the graph is very large, with
$9 + 3 \cdot |E| + |O| + 2 \cdot |O| \cdot |J| + 2 \cdot |S| \cdot |I| \cdot |J| + 3 \cdot |P| \cdot |I| \cdot |K| << |N|$, then the total number of decision variables is equivalent to : $2 \cdot |N|^2 \cdot (1 + |H| + |F|)$

Number of constraints:

$|cst| = 36 + |E| + |Q| + 2 \cdot |O| \cdot |J| + 2 \cdot |S| \cdot |I| \cdot [J| + 2 \cdot |P| \cdot |I| \cdot |K|)$
$+|N| \cdot (11 + |I| + 2 \cdot |E| + |O| + |E| \cdot |P| + |E| \cdot |F| + |E| \cdot |O| + |O| \cdot |J| + |S| \cdot |I| \cdot |J| + 4 \cdot |P| \cdot |I| \cdot |K|)$
$+4 \cdot |N|^2 \cdot (1 + |H| + |F|)$

If the number of nodes in the graph is very large, with
$11 + |I| + 2 \cdot |E| + |O| + |E| \cdot |P| + |E| \cdot |F| + |E| \cdot |O| + |O| \cdot |J| + |S| \cdot |I| \cdot |J| + 4 \cdot |P| \cdot |I| \cdot |K| << |N|$,
then the total number of constraints is equivalent to : $4 \cdot |N|^2 \cdot (1 + |H| + |F|)$

It should be specified that these elements of complexity are theoretical: they represent the maximal number of variables and constraints used to solve the problem. For example, $|E| \cdot |F|$ is greater than the possible combinations of feedstock types and transportation modes.

To validate our exact model and confirm its interest compared to existing optimization models, we considered a real case, the one of the Franche-Comté region, for which we aimed to evaluate the deployment of a hydrogen supply chain. The approach that we followed for the experimentation phase and that we detailed in the two following sections is as follows:

- elaboration of the network graph for this region;
- estimation and representation of hydrogen demand;
- description of the components of the supply chain and associated characteristics;

- generation of several sets of instances based on the regional case study;
- solving of the generated instances using our exact model;
- analysis of the results and discussion about the contribution of the proposed model.

3.5/ CASE STUDY: FRANCHE-COMTÉ REGION, FRANCE

3.5.1/ NETWORK DESCRIPTION

Franche-Comté is a region in eastern France (since 2016, it is part of the new region Bourgogne Franche-Comté.). Its total area is 16,202 km^2. In 2016, its population was 1,180,397 persons.The 31 most populous cities in the studied region are selected as network nodes. Demographic data of each city are collected based on the *commune*[1] in which the city is located. The most populous city is Besançon, the capital of the region. There are several large cities in the northeast, including Belfort, Montbéliard and Valentigney. Other major cities include Vesoul in the north, Dole in the west, and Pontarlier in the south. The main roads (including highways, national roads, and departmental roads) connecting the cities are selected as network edges. There are 65 edges. Length data are acquired from Google Maps^{TM}. The length of the network's edges and the distances between different cities are given in appendix A. The network generated is presented in Fig. 3.2 - (a).

Three types of feedstock are considered in this study: natural gas, electricity, and biomass. Natural gas can be supplied only in cities that are covered by the natural gas network. According to GRTgaz (2019, 2017)[2], 23 cities have access to the natural gas network, as shown in Fig. 3.2 - (b). The maximum supply capacity of natural gas is fixed at 30,000 Nm^3/d (normal cubic meter per day). Electricity is available in all cities (see Fig. 3.2 - (c)). The maximum supply capacity is fixed at 300,000 kWh/d (kilo watt hour per day). It is assumed that two cities (Luxeuil-les-Bains in the north and Valdahon in the center) could supply biomass, and the maximum supply capacity is fixed at 70,000 kg/d (kilos per day). The feedstock prices are shown in Table 3.8.

It is assumed that a potential CO_2 storage site is located at Morteau and its maximum processing capacity is 200,000 kg CO_2/d (see Fig. 3.2 - (d)). Other CCS system inputs can be found in Table 3.8. It is also assumed that the fixed-location demand of Type A (stationary application type) exists at Saint-Claude, the amount of hydrogen demand is 500 kg/d. Fixed-location demand of Type B (fleet vehicules type) exists at Pontarlier, the amount of demand is 500 kg/d (see Fig. 3.2 - (e)).

[1] The commune is a level of administrative division in France.
[2] GRTgaz is a French natural gas transmission system operator.

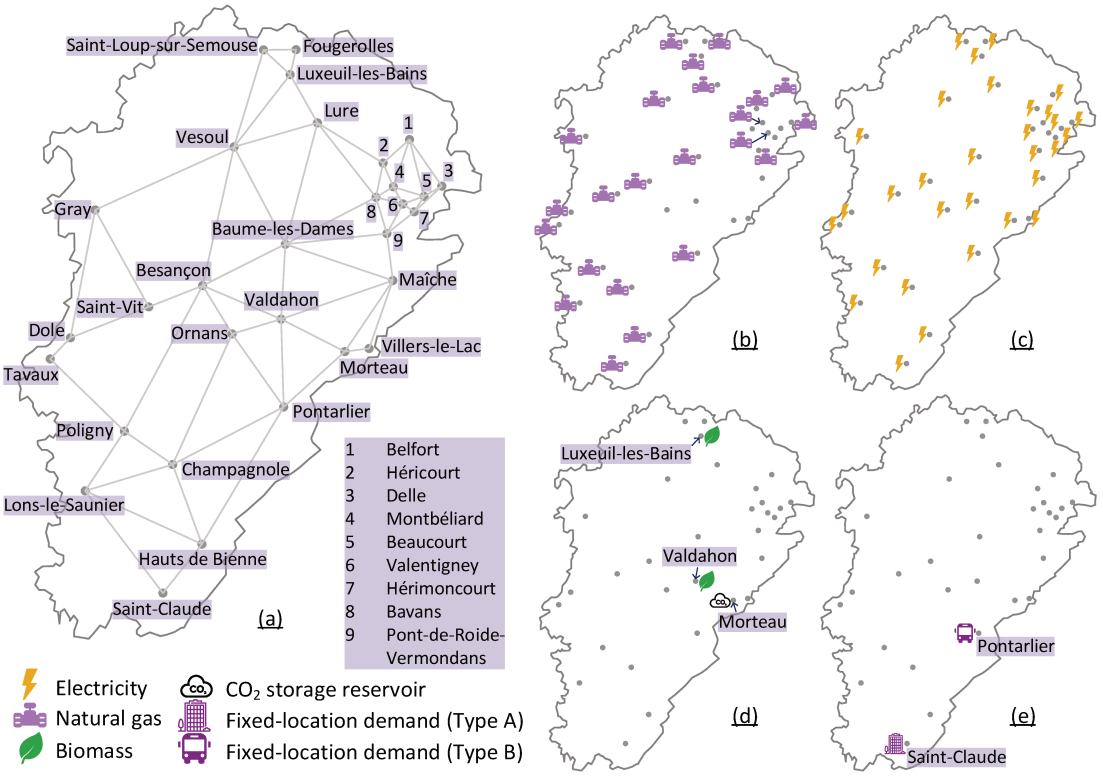

Figure 3.2: Franche-Comté network: (a) Basic network; (b) Natural gas distribution; (c) Electricity distribution; (d) Biomass distribution and location of a potential CO_2 storage site; (e) Location of fixed-location demands

3.5.2/ HYDROGEN REFUELING DEMAND

The proposed model satisfies two major types of hydrogen demand: fixed-location demand (node-based) and refueling demand of FCEVs (flow-based). This section explains how the refueling demand of FCEVs is represented by the flow-based demand. The classical Flow-Capturing Location Model (FCLM) defines only the locations of the service facilities. Decision-makers receive no references on the required service capacity to satisfy part or all of the "flow captured". It is obvious that the relationship between the "flow captured" and the service capacity should be built before the capacity-related decision variables are introduced into the model. In the context of refueling station deployment, such a relationship is often established between the refueling demand and the road traffic flow. The underlying assumption is that all units of traffic flow within the region (between different origins and destinations) contribute equally to the refueling demand. Considering that most of the vehicles on the road still rely on gasoline or diesel, this assumption is reasonable when deploying traditional refueling stations. However, this same assumption becomes questionable when the problem has been changed to hydrogen refueling station planning. It is mainly due to uneven distribution of FCEVs within the region's traffic flow. Therefore, the concept of hydrogen refueling demand flow is introduced, which is a

modified traffic flow that involves the influences of potential FCEV owner-ships in different cities or towns. The refueling capacity of a hydrogen refueling station is therefore defined by the hydrogen refueling demand flow that has been captured by the station.

It is assumed that hydrogen refueling demand flow is more likely to appear between two closer cities with higher FCEV ownerships. The potential FCEV ownership is related not only to the population but also to several demographic metrics. Melendez et al. (2008) proposed nine metrics that influence FCEV adoption by consumers. Given the availability of statistics, the following four ones are chosen for this study:

- *Vehicle*[3]*:* Households with multiple vehicles are more likely to adopt hydrogen vehicles.
- *Income*[4]*:* Higher incomes lead to earlier adoption of FCEV.
- *Education*[5]*:* Higher education leads to earlier adoption.
- *Commute*[6]*:* Commuting with private vehicles interests consumers in newer and more efficient vehicles.

Table A.1 (in appendix A) provides the population size and four demographic metrics for each city. Data are collected from INSEE (L'Institut national de la statistique et des études économiques (2018a,b, 2015a,b)[7]).

Considering all five factors, we first defined and employed a "scoring system" similar to the one used by Melendez et al. (2006) but extended to the distribution of the demand in flows. In this "scoring system", data in each column are first normalized in the range of 1-100 to compute the score of each city on each item:

$$Score_x = 1 + 99 * \frac{Value_x - Value_{min}}{Value_{max} - Value_{min}} \tag{3.78}$$

Then the final score of each city is obtained by a linear combination of the five obtained scores, as shown in Eq. (3.79). The weights are chosen according to the importance of each metric. The sum of those weights equals 1.

$$\begin{aligned} Score_{final} = Score_{Population} * 0.6 + Score_{Vehicle} * 0.1 + Score_{Income} * 0.1 \\ + Score_{Education} * 0.1 + Score_{Commute} * 0.1 \end{aligned} \tag{3.79}$$

[3]The ratio of households with two or more vehicles.
[4]Yearly household income.
[5]Share of persons whose highest degree is a bachelor's degree in the out-of-school population aged 15 or over.
[6]Share of persons who use private vehicles for commuting.
[7]National Institute of Statistics and Economic Studies

The final score represents the relative potential FCEV ownership of each city. If one considers the final score as the *weight* of each city, then a network with weight values of cities could be obtained, as presented in Fig. 3.3 - (a). The radius of circles at city nodes is visually proportional to these weights. The plot of Fig. 3.3 - (b) is the weighted network based only on population. It can be seen that after considering the influence of the four additional demographic metrics, some cities with smaller populations have gained greater weights. For example, Villers-le-lac has the highest score of "Income", Gray has the highest score of "Vehicle", and Bavans has higher scores in both "Vehicle" and "Commute". It can also be found that, although Besançon is still the city with the largest weight, the urban agglomerations in the northeast have gathered several cities with relatively high weights.

After computing the demand level for the 31 considered cities, the potential flow of FCEVs on the roads of the network should be determined. First, the gravity model (Haynes et al., 1985) is used to quantitatively measure the possibility that an Origin-Destination (OD) pair flow becomes a hydrogen refueling demand flow. As shown in Eq. (3.80), the possibility (P_q) of an OD pair (q) that links two cities n and m can be expressed as a ratio of the multiplied final scores (weights of cities obtained above) over the distance between this pair of cities.

$$P_q = \frac{Score_{final,city_n} * Score_{final,city_m}}{l_{nm}} \tag{3.80}$$

The obtained results can be regarded as "weights" of origin–destination (OD) pairs, with which the value of hydrogen refueling demand flow of each pair is determined. Based on the report of L'Association Française pour l'Hydrogène et les Piles à Combustible (2018)[8], it is estimated that the potential hydrogen demand of FCEV in Franche-Comté in 2030 will be 4,378 kg/d[9]. This total demand is distributed between the OD pairs according to their "weights" obtained by Eq. (3.80). In this way, the hydrogen refueling demand is linked to the OD flow pairs, and the resulting demand flow network is presented in Fig. 3.3 - (c). The larger the radius of the circle, the higher the refueling demand in the city. The wider the edge, the greater the refueling demand flow carried by that edge. Comparing this flow network with the one based only on population (Fig. 3.3 - (d)), the common element is the region's east-west traffic artery–A36 (Montbéliard-Besançon-Dole), which carries the largest hydrogen refueling demand in both networks. However, one can observe the following differences:

[8]The French Association for Hydrogen and Fuel Cells

[9]The report provides only the total hydrogen demand of FCEV in France in 2030 (89,000 kg/d). The value for Franche-Comté is obtained by multiplying the total demand with the proportion of province (Franche-Comté) population to France population (1.80% (L'Institut national de la statistique et des études économiques, 2015b))

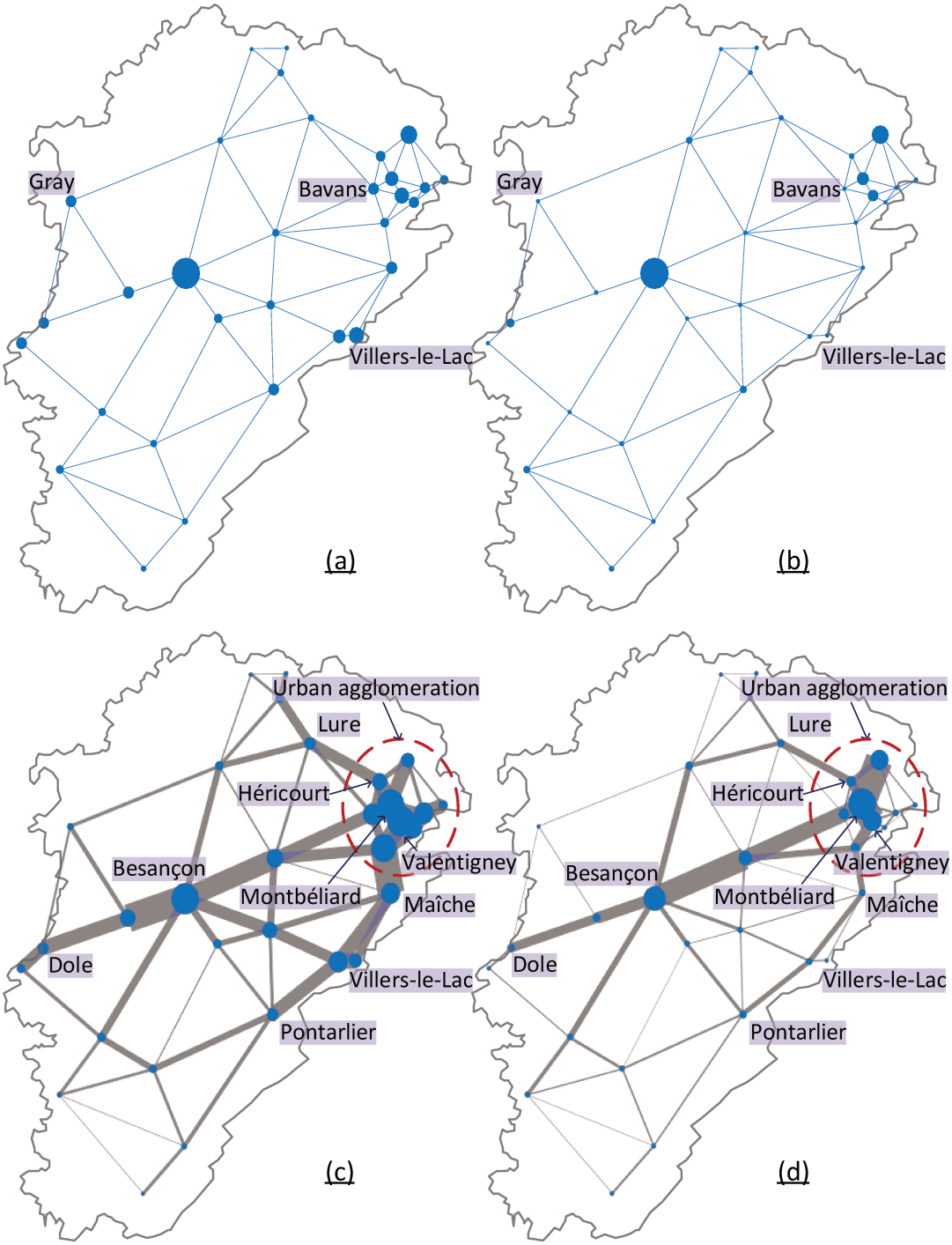

Figure 3.3: Hydrogen refueling demand flow: (a) Weighted network; (b) Weighted network based only on population; (c) Hydrogen refueling demand flow network; (d) Hydrogen refueling demand flow network based only on population

- The hydrogen refueling demand flow between the eastern urban agglomerations has increased significantly. This can be explained as follows: According to the gravity model, greater weight and closer distance result in larger interaction. The

urban agglomerations formed by several cities with large weights have reasonably more interactions with each other.

- In the east, the flow through Lure, Héricourt, Valentigney, Maîche, Pontarlier has increased significantly. This can be explained by the fact that small cities like Villers-le-lac, Maîche, and Bavans have higher weights.

3.5.3/ HYDROGEN SUPPLY NETWORK

3.5.3.1/ PRODUCTION PLANTS

Corresponding to three types of feedstock, three types of production technologies are set up: steam methane reforming (SMR), electrolysis, and biomass gasification (BG). The production plant has three sizes (small, medium, and large), with production capacity ranging from 1,000 kg/d to 5,000 kg/d. Each type of plant has sets of data for the production of gaseous hydrogen and liquid hydrogen. Data are collected mainly from the Hydrogen Analysis (H2A) project conducted by the U.S. Department of Energy (Department of Energy, U.S., 2018c, 2010, 2018d,b). Tables 3.2, 3.3, and 3.4 present the capital cost, operating cost, production capacity, emission factor, and emission capture efficiency for each type of production technology. Attention has been directed to use the local emission factor of electricity that is obtained from EDF (Électricité de France (2018)[10]). The conversion rates of production technologies can be found in Table 3.8.

3.5.3.2/ REFUELING STATIONS

The refueling capacity ranges from 50 kg/d to 1,200 kg/d, divided into four sizes - small, medium, large, and extra-large[11]. Standard refueling stations are divided into two subtypes according to the hydrogen form they receive, and the cost and emission data are shown in Table 3.5. The on-site refueling stations consist of on-site-SMR and on-site-electrolysis. The cost and emission data are presented in Table 3.6 (Melaina et al., 2013).

3.5.3.3/ HYDROGEN AND FEEDSTOCK TRANSPORTATION

Gaseous hydrogen is conveyed via tube trailers whereas liquefied hydrogen is transported in tanker trucks. For feedstock, this study considers only the transportation of biomass via trucks. The cost and emission data are presented in Table 3.7.

[10] A French electric utility company
[11] The refueling capacity of “extra-large” stations is twice that of “large” ones

Table 3.2: Production technology - steam methane reforming (SMR)

	Hydrogen form:	Gaseous			Liquid			Source
	Facility size:	Small	Medium	Large	Small	Medium	Large	
Capital cost	million €	1.05	1.70	2.28	10.62	16.70	21.78	(1)
Operating cost	€/kg H_2	0.34	0.31	0.30	2.65	2.15	1.93	(2)
Maximum capacity	1,000 kg/d	2.00	3.50	5.00	2.00	3.50	5.00	
Minimum capacity	1,000 kg/d	1.00	2.50	4.00	1.00	2.50	4.00	
Upstream emission factor	kg CO_2/kg H_2	2.40	2.40	2.40	3.07	3.00	2.97	(3)
On-site emission factor	kg CO_2/kg H_2	8.66	8.66	8.66	8.66	8.66	8.66	(4)
Emission capture efficiency		0.90	0.90	0.90	0.90	0.90	0.90	(5)

Source: (1), (2), (4) - (Department of Energy, U.S., 2018c, 2010); (3) - (Department of Energy, U.S., 2018c, 2010; Électricité de France, 2018); (5) - (Department of Energy, U.S., 2018b).
Note: The costs of liquid production (capital and operating) are obtained by adding the cost of liquefier to gaseous production.

Table 3.3: Production technology - Electrolysis

	Hydrogen form:	Gaseous			Liquid			Source
	Facility size:	Small	Medium	Large	Small	Medium	Large	
Capital cost	million €	1.74	2.62	3.92	11.32	17.62	23.43	(1)
Operating cost	€/kg H_2	0.17	0.14	0.11	2.48	1.98	1.74	(2)
Maximum capacity	1,000 kg/d	2.00	3.50	5.00	2.00	3.50	5.00	
Minimum capacity	1,000 kg/d	1.00	2.50	4.00	1.00	2.50	4.00	
Upstream emission factor	kg CO_2/kg H_2	1.96	1.57	1.26	2.63	2.17	1.83	(3)
On-site emission factor	kg CO_2/kg H_2	-	-	-	-	-	-	
Emission capture efficiency		0.90	0.90	0.90	0.90	0.90	0.90	(4)

Source: (1), (2) - (Department of Energy, U.S., 2018d, 2010); (3) - (Department of Energy, U.S., 2018d, 2010; Électricité de France, 2018); (4) - (Department of Energy, U.S., 2018b).
Note: The costs of liquid production (capital and operating) are obtained by adding the cost of liquefier to gaseous production;
Because lack of information, the upstream emission factor of "Medium" and "Large" (gaseous production) are obtained by multiplying the value of "Small" with 0.8 and 0.64, respectively.

Table 3.4: Production technology - biomass gasification (BG)

	Hydrogen form:	Gaseous			Liquid			Source
	Facility size:	Small	Medium	Large	Small	Medium	Large	
Capital cost	million €	4.09	7.03	9.64	13.67	22.03	29.15	(1)
Operating cost	€/kg H_2	4.01	2.48	1.90	6.32	4.33	3.52	(2)
Maximum capacity	1,000 kg/d	2.00	3.50	5.00	2.00	3.50	5.00	
Minimum capacity	1,000 kg/d	1.00	2.50	4.00	1.00	2.50	4.00	
Upstream emission factor	kg CO_2/kg H_2	-22.26	-22.26	-22.26	-21.59	-21.66	-21.69	(3)
On-site emission factor	kg CO_2/kg H_2	24.00	24.00	24.00	24.00	24.00	24.00	(4)
Emission capture efficiency		0.90	0.90	0.90	0.90	0.90	0.90	(5)

Source: (1), (2), (4) - (Department of Energy, U.S., 2018b, 2010); (3) - (Department of Energy, U.S., 2018b, 2010; Électricité de France, 2018); (5) - (Department of Energy, U.S., 2018b).
Note: The costs of a liquid production plant (capital and operating) are obtained by adding the cost of a liquefier to a gaseous production plant.
The upstream emission factors are negative because the plants that are the source of biomass capture a certain amount of CO_2 through photosynthesis while they are growing.

Table 3.5: Standard refueling technology

	Hydrogen form:	Gaseous				Liquid				Source
	Facility size:	Small	Medium	Large	Extra-large	Small	Medium	Large	Extra-large	
Capital cost	million €	1.08	1.87	2.10	4.21	1.16	1.52	1.57	3.14	(1)
Operating cost	€/kg H_2	3.28	2.20	1.28	1.28	5.39	2.66	1.45	1.45	(2)
Maximum capacity	1,000 kg/d	0.15	0.30	0.60	1.20	0.15	0.30	0.60	1.20	(3)
Minimum capacity	1,000 kg/d	0.05	0.15	0.30	0.60	0.05	0.15	0.30	0.60	(4)
Emissions factor	kg CO_2/kg H_2	2.34	2.07	1.59	1.59	0.42	0.41	0.41	0.41	(5)

Source: (1), (2), (5) - (Department of Energy, U.S., 2010); (3), (4) - (L'Association Française pour l'Hydrogène et les Piles à Combustible, 2018).

Table 3.6: On-site refueling technologies

	On-site refueling techn.:	On-site-SMR				On-site-electrolysis				Source
	Facility size:	Small	Medium	Large	Extra-large	Small	Medium	Large	Extra-large	
Capital cost	million €	1.26	2.18	2.59	5.19	1.32	2.27	2.75	5.50	(1)
Operating cost	€/kg H_2	4.57	3.31	2.21	2.21	4.15	2.97	1.79	1.79	(2)
Maximum capacity	1,000 kg/d	0.15	0.30	0.60	1.20	0.15	0.30	0.60	1.20	(3)
Minimum capacity	1,000 kg/d	0.05	0.15	0.30	0.60	0.05	0.15	0.30	0.60	(4)
Emissions factor	kg CO_2/kg H_2	19.49	16.25	13.54	13.54	5.34	4.45	3.71	3.71	(5)

Source: (1), (2) - (Melaina et al., 2013; Department of Energy, U.S., 2018c,d); (3), (4) - (L'Association Française pour l'Hydrogène et les Piles à Combustible, 2018); (5) - (Department of Energy, U.S., 2018c,d; Électricité de France, 2018).
Note: The costs of an on-site station (capital and operating) are obtained by adding the cost of on-site production to a gaseous standard station.
Due to lack of information, the emission factor of "Medium" and "Small" are obtained by multiplying the value of "Large" with 1.2 and 1.44, respectively.

Table 3.7: Hydrogen and feedstock transportation: cost and emission data

		Hydrogen		Biomass	Source
		Tube trailer	Tanker truck	Truck	
Driver wage	€/h	20.47	20.47	20.47	(1)
Fuel economy	km/L	2.55	2.55	2.55	(2)
Fuel price	€/L	1.46	1.46	1.46	(3)
General expenses	€/d	7.32	7.32	7.32	(4)
Load/unload time	h	2.00	2.00	2.00	(5)
Maintenance expenses	€/km	0.09	0.09	0.09	(6)
Average speed	km/h	55.00	55.00	55.00	(7)
Availability	h/d	18.00	18.00	18.00	(8)
Emissions factor	kg CO_2/L	2.68	2.68	2.68	(9)
Capacity	1,000 kg	0.18	4.08	8.00	(10)
Vehicle rental cost	€/d	71.20	89.00	44.50	(11)
Maximum transport capacity	1,000 kg/d	5.00	5.00	69.40	
Minimum transport capacity	1,000 kg/d	0.05	0.05	8.00	

Source: (1), (2), (4), (5), (6), (7), (8) - (Almansoori et al., 2006); (3) - (GlobalPetrolPrices, 2019); (9) - (Almansoori et al., 2016); (10) - (Almansoori et al., 2006; RentalYard, 2018); (11) - (RentalYard, 2018).
Note: The maximum transport capacity is based on the assumption that individual modes cannot transport more than what is produced by a large production facility.

Table 3.8: Feedstock prices, conversion rates, and CCS system inputs

Parameter		Value	Source
Natural gas price	€/Nm^3	0.36	(1)
Electricity price	€/kWh	0.10	(2)
Biomass price	€/kg	0.05	(3)
Conversion rate (SMR)	Nm^3 Natural gas/kg H_2	4.61	(4)
Conversion rate (Electrolysis)	kWh Electricity/kg H_2	54.60	(5)
Conversion rate (BG)	kg Biomass/kg H_2	13.88	(6)
CCS capital cost	million €	2.03	(7)
CO_2 pipeline capital cost	million €/km	0.08	(8)
CO_2 processing cost	€/kg	0.09	(9)
CO_2 transport capacity (Max)	1,000 kg/d	500.00	
CO_2 transport capacity (Min)	1,000 kg/d	-	

Source: (1) - (Statista, 2019b); (2) - (Statista, 2019a); (3), (6) - (National Renewable Energy Laboratory, U.S., 2011); (4) - (Department of Energy, U.S., 2018c); (5) - (Department of Energy, U.S., 2018d); (7), (8), (9) - (Department of Energy, U.S., 2018b)

3.5.4/ INSTANCES GENERATION

One of the primary purposes of this study is to demonstrate the advantages of integrating all possible components within a single framework. The influence of any component on

the HSCN can be identified only by comparing and analyzing the model results with and without this component. Based on this principle, seven groups of instances have been designed, each of which corresponds to a component composition, as shown in Table 3.9.

Table 3.9: Groups of instances

	Model components				
	On-site station	Standard station	Feedstock transportation	CCS system	Fixed-location demand
Group A	✔				
Group B		✔			
Group C	✔	✔			
Group D		✔	✔		
Group E		✔		✔	
Group F		✔			✔
Group G	✔	✔	✔	✔	✔

- *Group A:* Only on-site stations are used to satisfy refueling needs. This can be seen as a simple upgrade of the classical FCLM (Flow-Capturing Location Model). The main mission is to locate on-site stations under the constraints of feedstock availabilities. In addition, the model needs to select a proper size for each on-site station.

- *Group B:* Only standard stations are employed to satisfy refueling needs. The model needs to locate standard stations as well as production plants, as the former can only receive hydrogen produced by the latter. In this group of instances, feedstock transportation is forbidden. Therefore, a plant can use only the feedstock supplied by the city where it is located. Plants and standard stations are linked by hydrogen transportation. Group B integrates the HSCND model and the HRSP model, and covers the whole hydrogen supply chain, from feedstock to refueling stations.

- *Group C:* Based on Group B, with the addition of on-site stations. The introduction of on-site stations allows the model to choose between two completely different refueling technologies. It is reasonable to assume that “mix” may provide more interesting configurations. By comparing the results of instances of Group A, Group B, and Group C, one could learn how refueling technologies impact HSCN.

- *Group D:* Based on Group B, but allowing feedstock transportation. The introduction of feedstock transportation provides the model with the capability to examine the trade-off between the transportation of feedstock and hydrogen. By comparing the results of instances of Group B and Group D, one examines the advantages of integrating feedstock transportation into the model.

- *Group E:* Based on Group B, and involving a CCS system. Although the adoption of a CCS system could greatly reduce the CO_2 emission of HSCN, it yields huge expenses. The introduction of a CCS system makes the model capable of studying the trade-off between considerable emission costs and establishment of a CCS system. In addition, the model examines the trade-off among the transportation of hydrogen, feedstock, and CO_2 when locating production plants. By comparing the results of instances of Group B and Group E, one reviews the advantages of integrating a CCS system into the model.

- *Group F:* Based on Group B, adding fixed-location demand. The purpose of this group is to verify that the model can meet other hydrogen demand requirements while satisfying the refueling demands. By comparing the results of instances of Group B and Group F, one can observe how fixed-location demand changes the configuration of HSCN.

- *Group G:* All model components are involved. The model will be able to compare all possible configurations together and to consider various trade-offs to find the optimal result.

Within each group of instances, one or several sets are defined. The sets of a given group differ by the feedstock type or the hydrogen form, as shown in Table 3.10.

Table 3.10: Sets of instances within each group

	Feedstock			Hydrogen form	
	Electricity	Natural gas	Biomass	Gaseous	Liquid
Set A1	✔			N/A	N/A
Set A2		✔		N/A	N/A
Set B1		✔		✔	
Set B2		✔			✔
Set B3			✔	✔	
Set C		✔		✔	
Set D			✔	✔	
Set E1		✔		✔	
Set E2			✔	✔	
Set F		✔		✔	
Set G	✔	✔	✔	✔	✔

The model proposed in this study is mono-objective. The environmental impact of the HSCN is represented by the contribution of emission cost in the LCOH (least cost of hydrogen, expressed in €/kg H_2). Therefore, the value of the carbon price has a significant influence on the model results. Two levels of carbon price are set to observe the changes in configuration, especially the model's behavior toward a CCS system. Based on the estimation of carbon price in Europe from various institutions (Chestney, 2018; Carbon

Tracker, 2018; World Bank et al., 2018), the low level of carbon price (LC) is set to 0.05 €/kg CO_2, and the high level (HC) is set to 0.27 €/kg CO_2.

The potential hydrogen refueling demand is represented by "flow". It may not necessarily be "captured" totally. Decision-makers can decide freely the percentage of flow that needs to be captured. For a specific percentage of flow, the model provides the optimal HSCN configuration that satisfies these demands and the resulting LCOH. Fig. 3.4 presents the value of LCOH and number of refueling stations for each percent of flow captured of Set A1 with LC (low carbon price), from 1% to 100%. It can be seen that the LCOH curve appears U-shaped. A small refueling demand flow requires at least one station to be satisfied. Therefore, the contribution of capital cost to LCOH will be extremely high. Thus, for less than 10%, the smaller the percentage of flow captured, the higher the LCOH. At the other side, for a captured flow greater than 90%, the model needs to build more stations to approach 100%. This is because the places that are more efficient in flow capturing have already been chosen. The "extra" expenditure in capital cost causes the curve to rise sharply. So we can deduce that, at least for such an instance, and for decision-makers, less than 10% and higher than 90% are areas of less interest. Therefore, three levels of refueling demand are set, 10% for low demand (LD), 50% for medium demand (MD), and 90% for high demand (HD). Then we have generated 66 instances. The name of each instance is formatted as "Set-N-C-D", where "N" is the name of the 11 sets defined in Table 3.10, "C" is the carbon price level (LC for low one or HC for high one), and "D" represents the refueling demand level (LD, MD, or HD, respectively for low, medium and high, as defined above).

Each instance is solved to obtain its optimal LCOH value and associated network configuration. Fig. 3.5 illustrates the configuration and captured hydrogen refueling demand flow for Set-A1-LC-MD. It is shown that three on-site stations are located at Besançon, Champagnole, and Valentigney. The captured flow is indicated in red. Based on the model's assumptions, a refueling station could capture all refueling demand of the node at which it is located. Correspondingly, all edges' flow directly linked to this node is also captured. This explains why the three cities and their surrounding roads are all red. Flows in areas with no stations are less captured, as in the northern area. For all the instances analyzed in the following section, we will provide such figures to allow a visual representation of the captured hydrogen refueling demand flow.

3.6/ RESULTS AND DISCUSSION

Our model is solved by CPLEX 12.7 for the defined instances on a computer equipped with a 3.2 GHz i5-6500 and 16 GB of RAM. The corresponding computational statistics are summarized in Table 3.11 which illustrates the complexity of each instances'group.

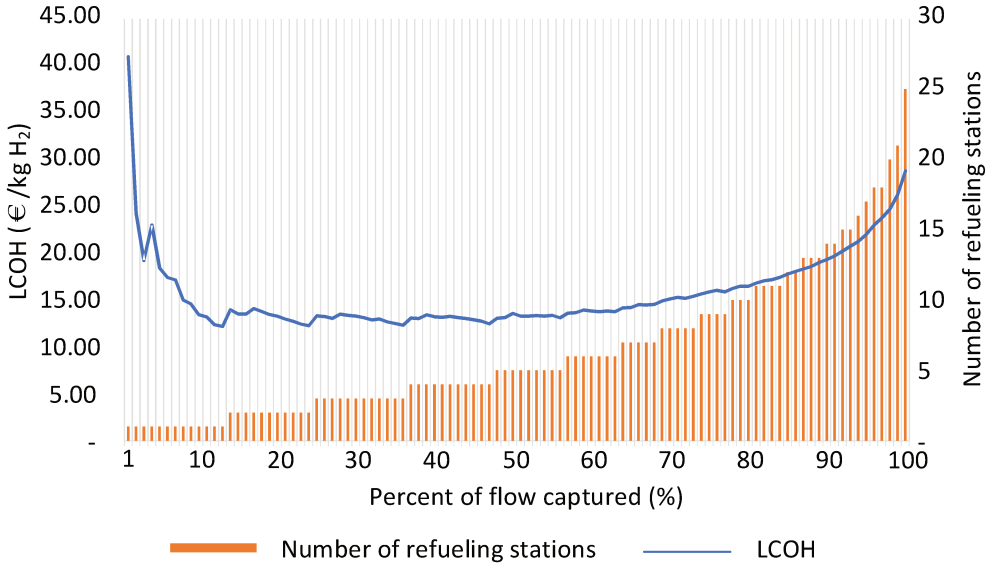

Figure 3.4: The value of LCOH and number of refueling stations for each percent of flow captured for Set A1 with LC (low carbon price), from 1% to 100%

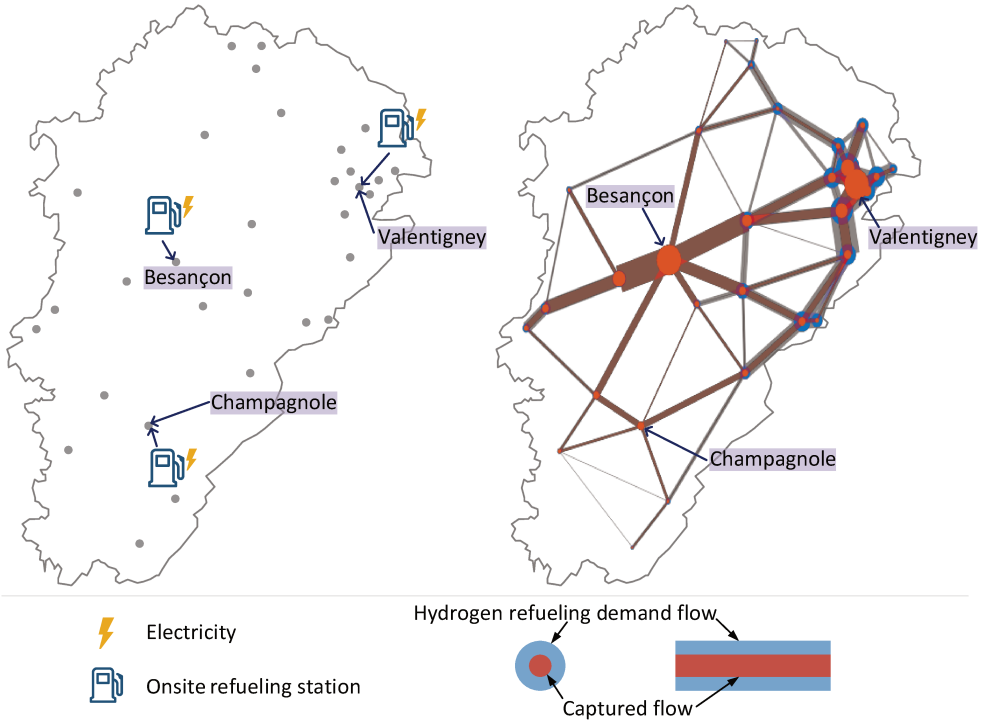

Figure 3.5: Configuration and captured hydrogen refueling demand flow for Set-A1-LC-MD

Fig. 3.6 provides a comparison between the results obtained in terms of LCOH. Detailed results of our 66 generated instances are presented in appendix B.

Table 3.11: Size of the instances

Instance group	A	B	C	D	E	F	G
Number of constraints	932	10,761	11,226	15,598	15,969	11,722	24,526
Number of binary variables	682	2,728	2,914	3,720	3,751	2,728	5,735
Number of integer variables	-	2	2	3	2	2	3
Number of continuous variables	155	2,170	2,325	3,131	3,255	2,170	5,673
Maximum CPU time (s)	1	7,567	16	407	144	11	539

3.6.1/ ROLE OF FEEDSTOCK AVAILABILITIES

It is known that on-site-electrolysis stations have a higher capital cost than on-site-SMR, as shown in Table 3.6. Therefore, in most situations, instances of Set A1 obtain a higher LCOH than instances of Set A2 (see Fig. 3.6 - (a)). As the emission factor of on-site-SMR is higher than that of on-site-electrolysis, the impact of emission costs will be more important as the carbon price is high. The gap between the two sets shrinks when carbon price increases, and this gap may even reverse for instances A_i-HC-HD.

Fig. 3.7 illustrates the differences between the supply chain structures obtained with our model for Set A1 and A2. Only the results for the high carbon price scenario are presented here. For the two sets of instances, we obtain the same number and locations of on-site stations at low (LD) and medium (MD) demands. It must be noted that Set A2 can only install on-site-SMR stations at cities that are covered by a natural gas network, which means that the model cannot locate stations considering only the efficiency of refueling demand flow capturing. Consequently, at high demand, Set A2 results in more stations and higher LCOH than Set A1.

3.6.2/ ROLE OF HYDROGEN FORMS

Fig. 3.6 - (b) shows that HSCN based on liquid hydrogen is more expensive at all three demand levels. The high cost is due to the need for liquefaction devices, which incur a high capital cost. Moreover, liquefaction requires a large amount of power consumption, increasing operating costs. We can notice that the gap between gaseous and liquid is shrinking when hydrogen demand rises. This can be explained by the advantage of liquid hydrogen in transportation. The number of vehicles required to transport the same amount of liquid hydrogen is smaller than for gaseous hydrogen because the capacity of a tanker truck (for liquid hydrogen) is nearly 23 times as large as a tube trailer (for gaseous hydrogen). Although the advantage in transportation cannot offset the high cost of lique-

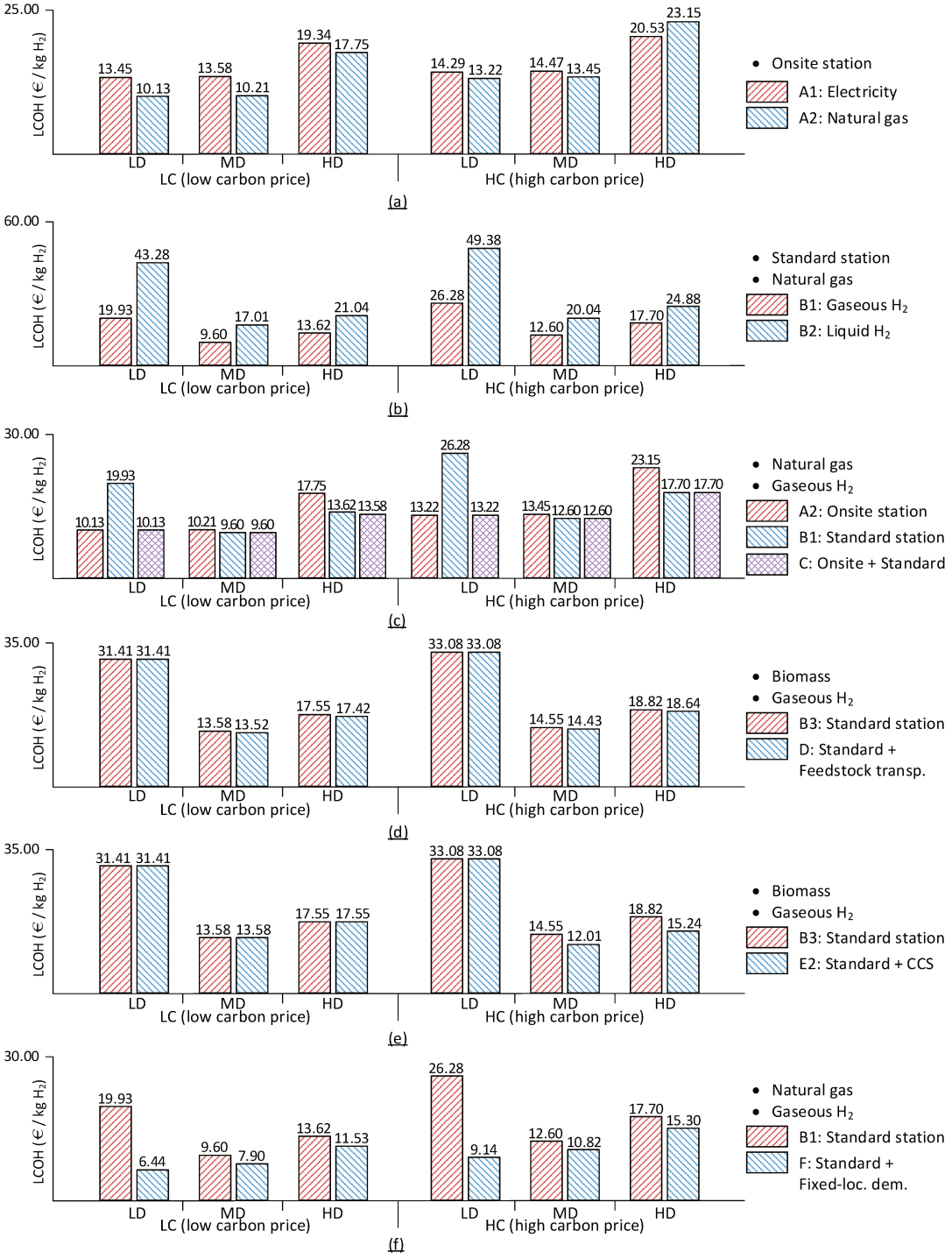

Figure 3.6: Obtained LCOH: (a) Set A1 vs. Set A2; (b) Set B1 vs. Set B2; (c) Set A2 vs. Set B1 vs. Set C; (d) Set B3 vs. Set D; (e) Set B3 vs. Set E2; (f) Set B1 vs. Set F

faction at low demand (i.e., when only a small number of vehicles are required), HSCN based on liquid hydrogen may be attractive when the demand of hydrogen increases.

In Fig. 3.8, we observe that, at medium and high demand, results for Set B2 involve fewer

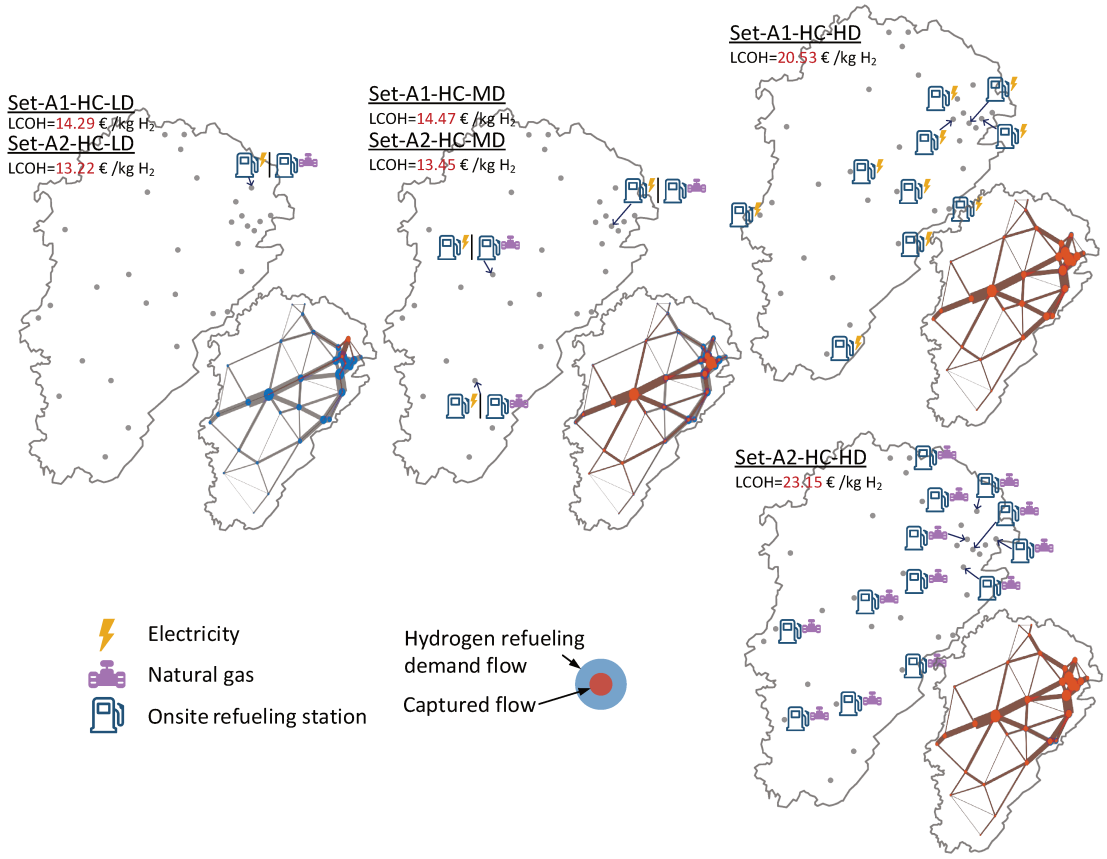

Figure 3.7: Configurations for Set A1 and A2 with high carbon price

plants, and are more dependent on hydrogen transportation. This can reduce the disadvantages of high costs of liquefaction and take advantage of transportation. Therefore, it can be concluded that HSCN based on liquid hydrogen prefers centralized production.

3.6.3/ Role of refueling technologies

First, let us observe Set A2 (on-site station only) and Set B1 (standard station only) in Fig. 3.6 - (c). It is shown that at low demand, Set B1 has higher LCOH. Indeed, any standard station requires to be supplied by a production plant, which increases the cost. At medium demand, the advantage of centralized production makes Set B1 reach lower LCOH than Set A2, and this advantage is even more obvious at high demand. The involvement of different refueling technologies provides the model with the ability to consider the trade-off between a centralized solution (with standard stations) and a decentralized configuration (with on-site stations).

It is reasonable to assume that “mix” could bring even better results (lower LCOH), and Set C is therefore introduced, as shown by the obtained solutions illustrated in Fig. 3.9. At low demand, Set C has the same configuration and LCOH as Set A2. At medium

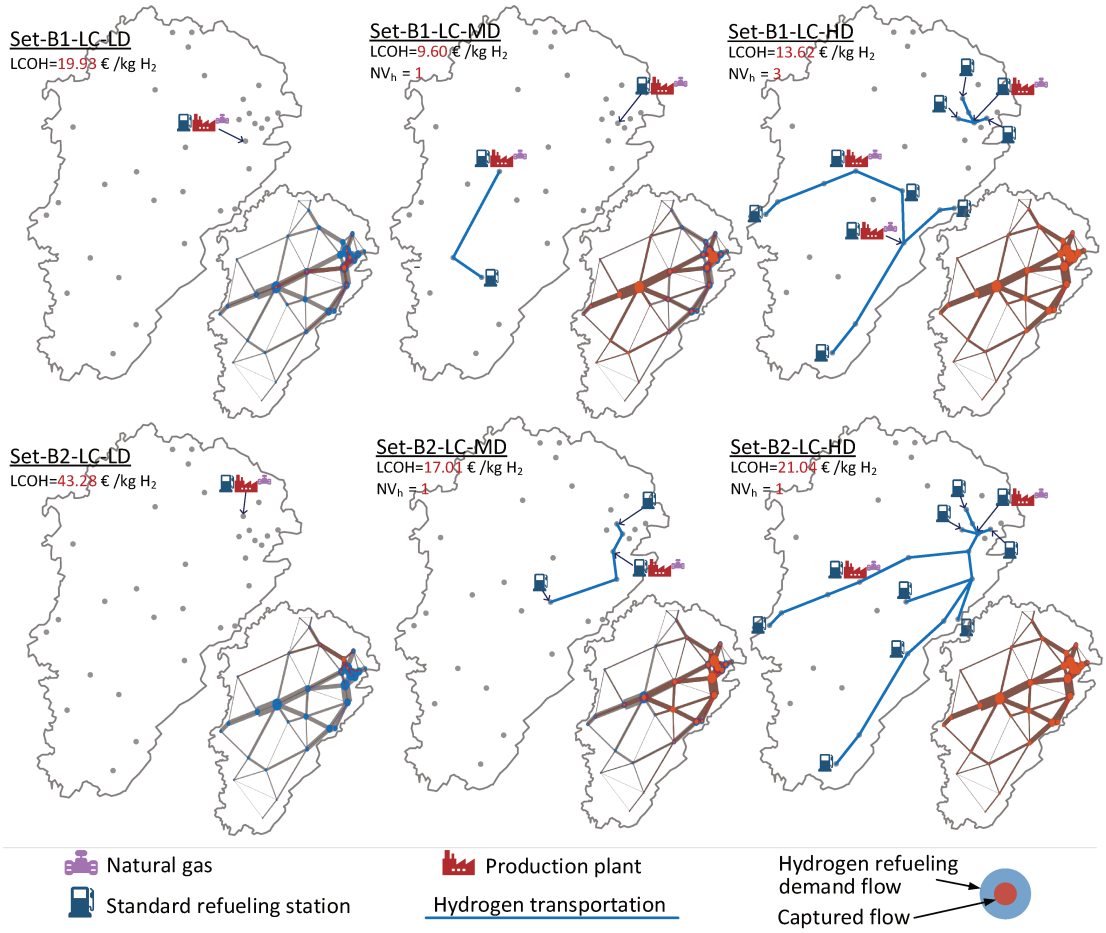

Figure 3.8: Configurations for Set B1 and B2 with low carbon price

demand, Set C has the same results as Set B1. At high demand, Set C obtains the lowest LCOH. Although the instance Set-C-LC-HD has the same number of refueling stations as Set-B1-LC-HD, the former achieves lower LCOH by adopting both on-site and standard stations. In Set-C-LC-HD, the model chooses to install an on-site station at Champagnole. The introduction of an on-site station reduces the demand for hydrogen produced by production plants. Therefore Set-C-LC-HD has one less plant than Set-B1-LC-HD. Although these structural changes result in only a slight drop in LCOH, it proves that it is indeed possible to find a supply chain configuration with lower LCOH by allowing the model to consider both refueling technologies. Let us notice that in high carbon price scenarios, not illustrated here but observable in Fig. 3.6 - (c), Set C and Set B1 have the same LCOH and configuration at high demand. The reason why Set C does not choose a “mix” solution in the high carbon price scenario can be explained by the fact that the emission factor of on-site-SMR is approximately seven times greater than the gaseous standard station emission factor. Therefore on-site stations are less attractive when carbon price rises.

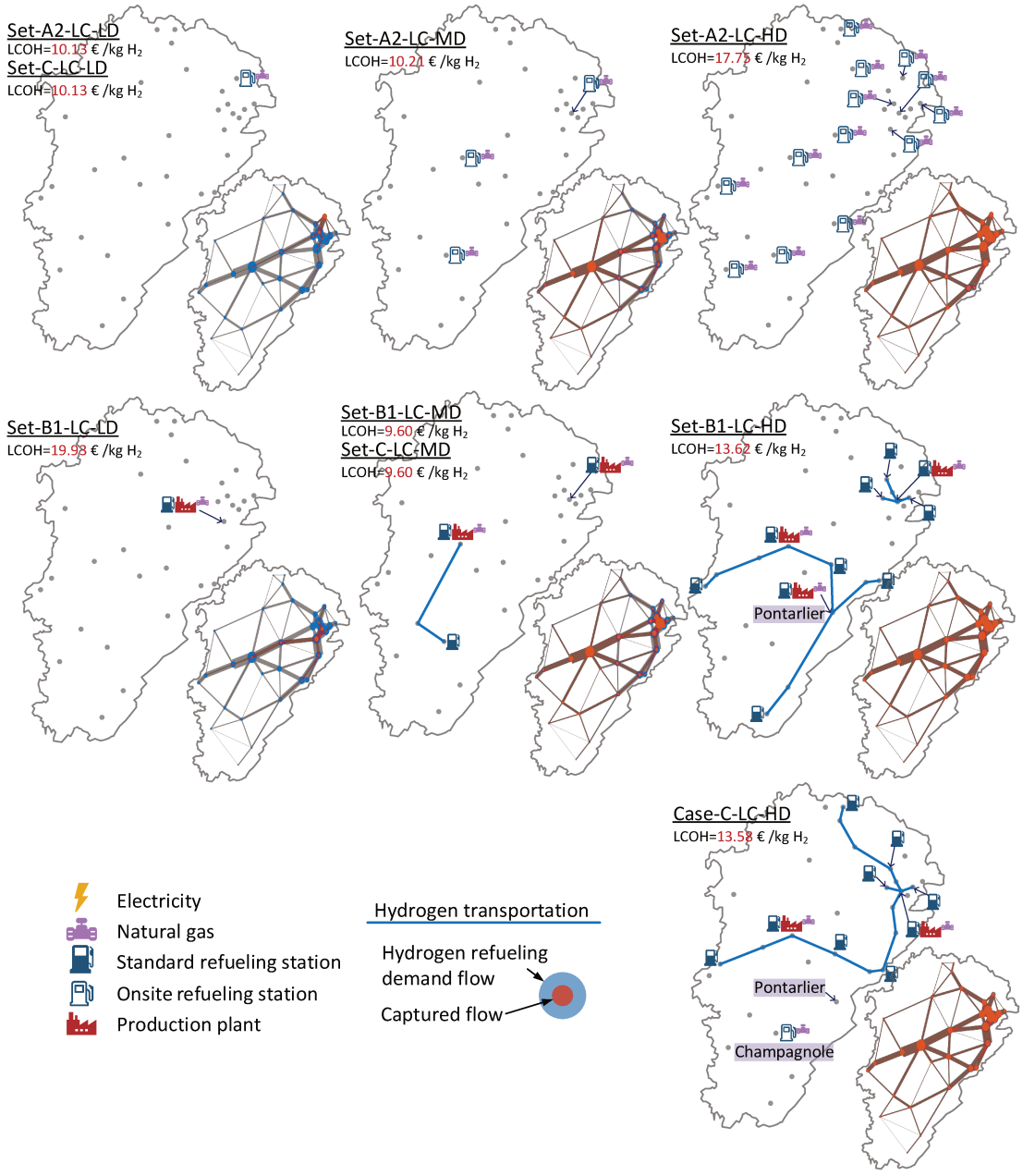

Figure 3.9: Configurations for Set A2, B1 and C with low carbon price

3.6.4/ ROLE OF FEEDSTOCK TRANSPORTATION

For this part, high carbon price does not bring changes in configuration (Fig. 3.6 - (d)). Only the results for low carbon price are discussed. We notice that at low demand, our model obtains the same LCOH for Set D and B3. At medium and high demand, one obtains slightly different values of LCOH. That is because Set D uses feedstock transportation, and therefore finds lower LCOH. The comparison of Set-D-LC-HD and Set-B3-LC-HD serves as a good example to show how feedstock transportation could help the

model to find a better configuration (Fig. 3.10). Based on case input, biomass is supplied only at Luxeuil-les-Bains and Valdahon. In Set-B3-LC-HD, as feedstock transportation is not allowed, the model has to put two BG plants at the two cities. Notice that four refueling stations are located in the urban agglomerations in the northeast. It is reasonable to assume that lower LCOH could be reached if the BG plant at Luxeuil-les-Bains is relocated within or near the urban agglomerations, and hydrogen transportation is replaced by feedstock transportation. This assumption is verified with the instance Set-D-LC-HD. For the two instances, one obtains the same number and locations of refueling stations. The change in LCOH results only from the involvement of feedstock transportation.

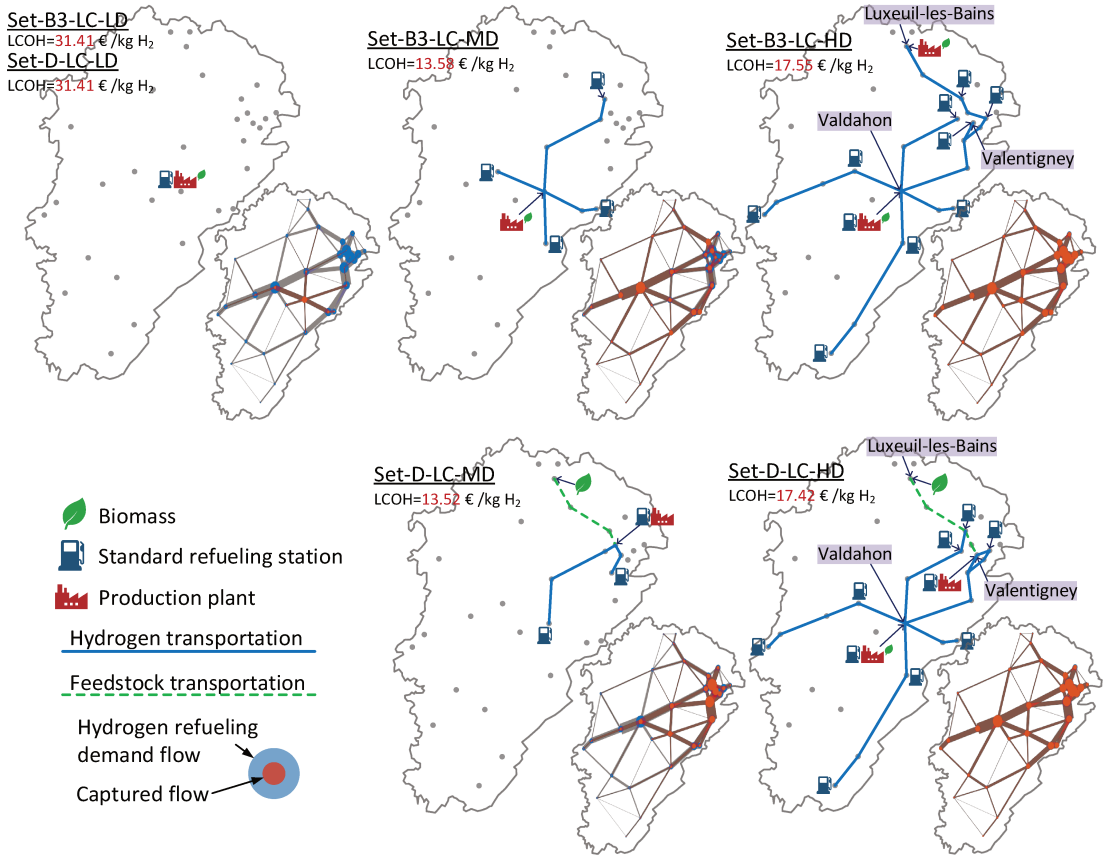

Figure 3.10: Configurations for Set B3 and D with low carbon price

3.6.5/ ROLE OF CCS SYSTEM

The feedstock type and the value of carbon price are two key factors that influence the choice of a CCS system. The optimal solution provided by the model does not include a CCS system in both low and high carbon price scenarios when natural gas is selected as feedstock (Set B1 vs. Set E1). It can be explained by the fact that the reduction in emission cost is not comparable to the expenses of a CCS system. The characteristic

of biomass is that its upstream emission factor is negative. If a BG plant adopts a CCS system, 90% of its on-site emission will be captured so that the plant's CO_2 emissions are negative for every 1 kg of hydrogen produced using biomass. Hydrogen production plant emissions account for most of the total emissions of HSCN. Therefore, the entire system's emissions would likely be negative, and the system gains revenue because of negative emissions.

Fig. 3.6 - (e) provides obtained values of our objective LCOH for Set B3 and E2. The model employs a CCS system only at medium and high demand in the high carbon price scenario. Analyzing the composition of LCOH shows that, although the adoption of a CCS system greatly increases the capital and operating costs, the negative emission reduces the overall cost, which makes the LCOH smaller. The obtained configurations are illustrated in Fig. 3.11. Notice that at high demand, only emission of the BG plant at Valdahon is captured, whereas emission of another BG plant at Luxeuil-les-Bains is not captured. This could be explained as Luxeuil-les-Bains is too far from Morteau, where the CO_2 storage site is located. If the model resulted in capturing emissions of the BG plant at Luxeuil-les-Bains, a 127 km CO_2 pipeline should be installed, adding a huge capital cost of 10.16 million euros. It can be concluded that a CCS system is attractive only at a high level of hydrogen demand and in high carbon price scenarios. Only when using biomass as feedstock, benefits resulting from the reduction of emissions can outweigh the huge expenses of adopting a CCS system.

Apart from carbon price, another leading strategy to promote CO_2 emission reductions is the maximum CO_2 emission constraint. The French government has set the carbon budget (CO_2 emission constraint) for the transport sector in 2029–2033 as 94 million metric tons per year (CO_2 equivalent) (Ministère de la Transition écologique et solidaire, 2018). Generally, the emission contributions of light duty vehicles (LDVs) account for 60% in the transport sector, which represents 56.4 million metric tons per year in France. Multiplying this value with the proportion of province (Franche-Comté) population to France population (1.8%), we obtain the maximum emission of LDVs in Franche-Comté as 1 million metric tons per year. Assuming that the share of FCEVs in LDVs in Franche-Comté in 2030 will be 2%, the maximum allowable emission limit for the HSCN designed in this study is 54,970 kg CO_2/d. A new parameter er^{max} is used to represent this upper bound and a new constraint is introduced:

$$ER \leqslant er^{max} \tag{3.81}$$

where ER is the total emission rate (kg CO_2/d) of the entire network.

The new constraint is imposed to Set E1 and E2 in order to observe the changes in network configuration under the simultaneous influences of carbon price and maximum

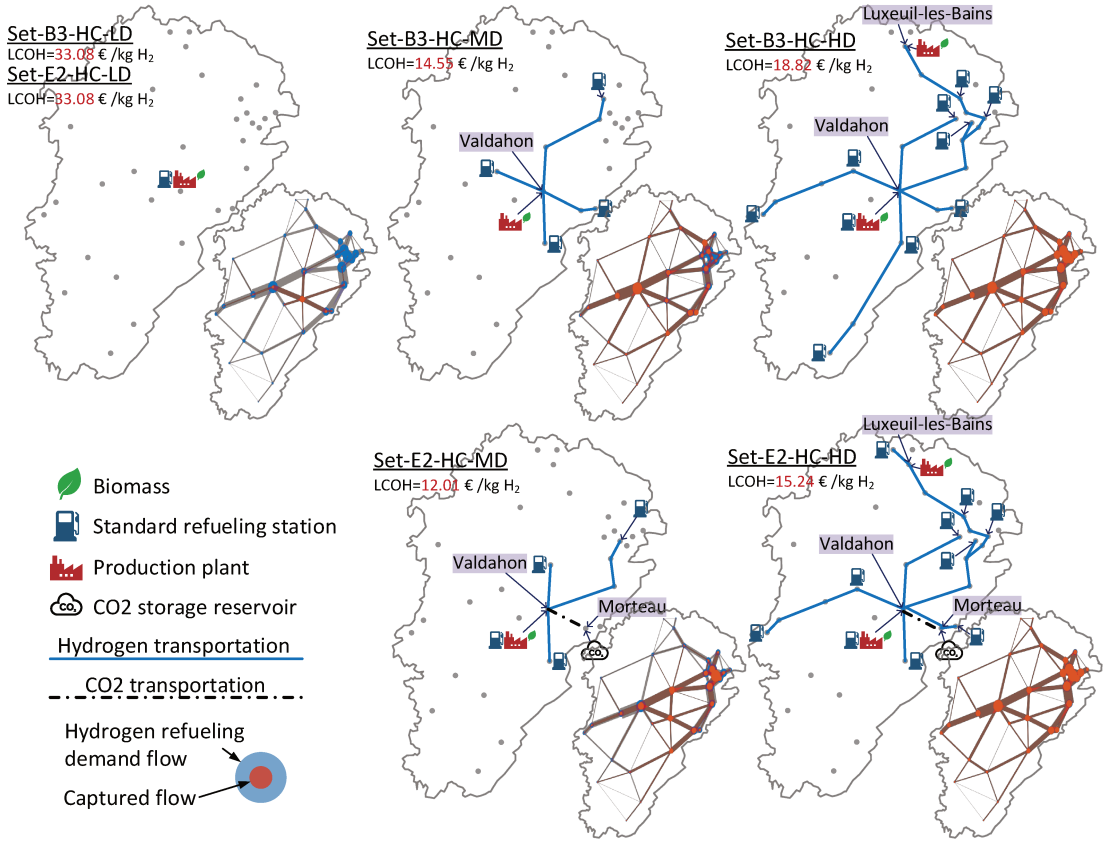

Figure 3.11: Configurations for Set B3 and E2 with high carbon price

emission constraint. It is found that configuration changes only occur in Set-E1-LC-HD and Set-E1-HC-HD. These two instances have the same ER (before the new constraint is applied) equal to 73,096 kg CO_2/d, which is larger than the maximum allowable emission limit. Fig. 3.12 illustrates these configuration changes. Notice that before the new constraint is introduced, Set-E1-LC-HD and Set-E1-HC-HD have the same configurations. They both have ten standard refueling stations and three production plants, respectively located in Besançon (production rate: 1,704 kg H_2/d), Valentigney (2,991 kg H_2/d), and Pontarlier (1,000 kg H_2/d). After the maximum emission constraint is applied, both instances adopt a CCS system. In addition, the production capacity has been re-deployed, and the hydrogen transportation has been re-organized. In the low carbon price scenario, the model chooses to capture the emission of the plant at Pontarlier. To capture sufficient emissions to reduce the total emissions below er^{max}, Besançon's plant has been closed, and its production capacity is transferred to the plant at Pontarlier. The reduction in the number of plants has made the system more dependent on hydrogen transportation, and the number of hydrogen transportation vehicles has increased from three to five. In the high carbon price scenario, the model chooses to capture even more emissions through centralized production. A large plant is located at Pont-de-Roide-Vermondans, where 49% of total emissions of the entire supply network are captured and processed. This

value is only 28% in the low carbon price scenario. Although this results in long CO_2 pipeline distance (52 km compared to 29 km in the low carbon price scenario), the cost savings from further reduction of emissions outweighs the increased capital cost. Based on this observation, it can be concluded that the maximum emission constraint forces instances where ER (before the new constraint is applied) is larger than er^{max} to adopt a CCS system. In the low carbon price scenario, the model only captures a small portion of emissions to satisfy the new constraint. In the high carbon price scenario, the model chooses to capture more emissions to reduce the carbon cost.

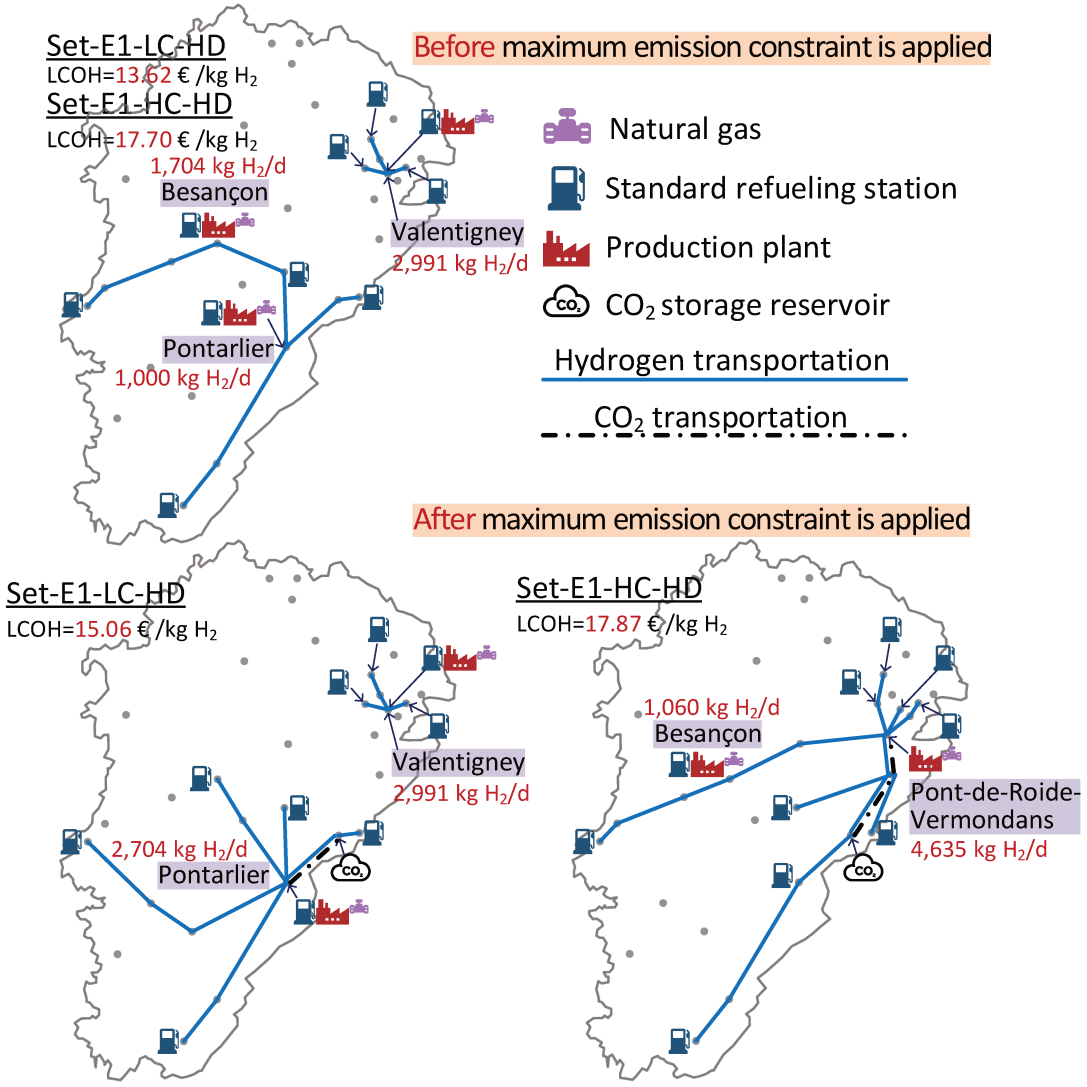

Figure 3.12: Configuration changes for Set-E1-LC(HC)-HD after the introduction of a maximum emission constraint

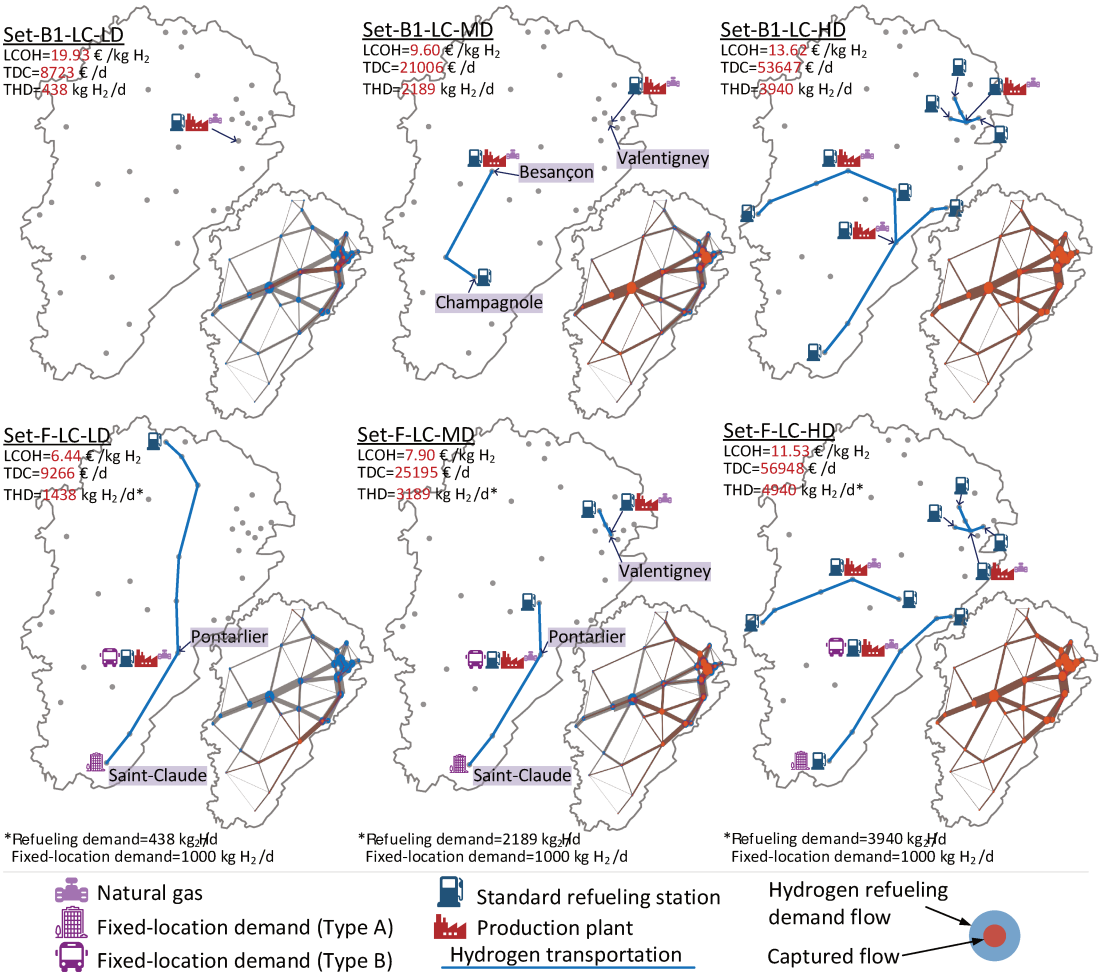

Figure 3.13: Configuration for Set B1 and F with low carbon price

3.6.6/ ROLE OF FIXED-LOCATION DEMAND

Fig. 3.13 shows the supply chain configurations provided by running our exact model with associated instances. To satisfy the fixed-location demand, instances in Set F have to build more facilities than those in Set B1. Take the medium-demand scenario as an example, Set B1 installs three refueling stations at three major cities - Valentigney, Besançon, and Champagnole, and two production plants at Valentigney and Besançon. Let us remember that fixed-location demands can be supplied only by production plants. Set F builds a plant at Pontarlier, which facilitates the supply for fixed-location demand of Type A at Saint-Claude and fixed-location demand of Type B at Pontarlier. For Set F, a standard refueling station is installed at Pontarlier because there exists fixed-location demand of Type B. However, the refueling demand flow captured by this station is less than that of major cities. Therefore, the model has to build an additional station to capture 50% of refueling demand flow. Fig. 3.6 - (f) compares the values of LCOH for those two sets. Although the total daily cost for Set F is higher than for Set B1, Set F obtains lower

LCOH because a higher amount of hydrogen is sold.

3.6.7/ SYNTHESIS

As a synthesis and based on the above tests, some following conclusions can be drawn:

- Feedstock availabilities have an impact on the location of on-site refueling stations, as our model cannot locate on-site stations only according to the efficiency of refueling demand flow capturing;
- When the total hydrogen demand level is low (as the case of Franche-Comté), the advantage in hydrogen transportation cannot offset the high cost of hydrogen liquefaction;
- The involvement of different refueling technologies provides the model with the ability to consider the trade-off between a centralized solution (with standard stations) and a decentralized configuration (with on-site stations). “Mixed solutions” (have both type of refueling stations) have been found in some results, as they obtained lower LCOH compared to single type station instances;
- The involvement of feedstock transportation helps the model to find lower LCOH by replacing hydrogen transportation by feedstock transportation in our case study;
- A CCS system is attractive only at a high level of hydrogen demand and in high carbon price scenarios. Only when using biomass as feedstock, benefits resulting from the reduction of emissions can outweigh the huge expenses of adopting a CCS system;
- Instances with fixed-location demand have to build more facilities than those without. Although the daily cost for the former ones are higher, they obtains lower LCOH because a higher amount of hydrogen is sold.

Then the last step of our experimentation is to validate our model on the last and more complete set of instances, belonging to Set G.

3.6.8/ THE CONSTRUCTION PLAN FOR FRANCHE-COMTÉ

Group G provides the complete instances in which all types of components are available to design the Franche-Comté hydrogen supply chain. Fig. 3.14 illustrates the optimal configurations obtained in low and high carbon price scenarios. Let us notice that no on-site station is installed in the presented configurations. This can be explained by the existence of fixed-location demand, which relies on hydrogen delivered by production

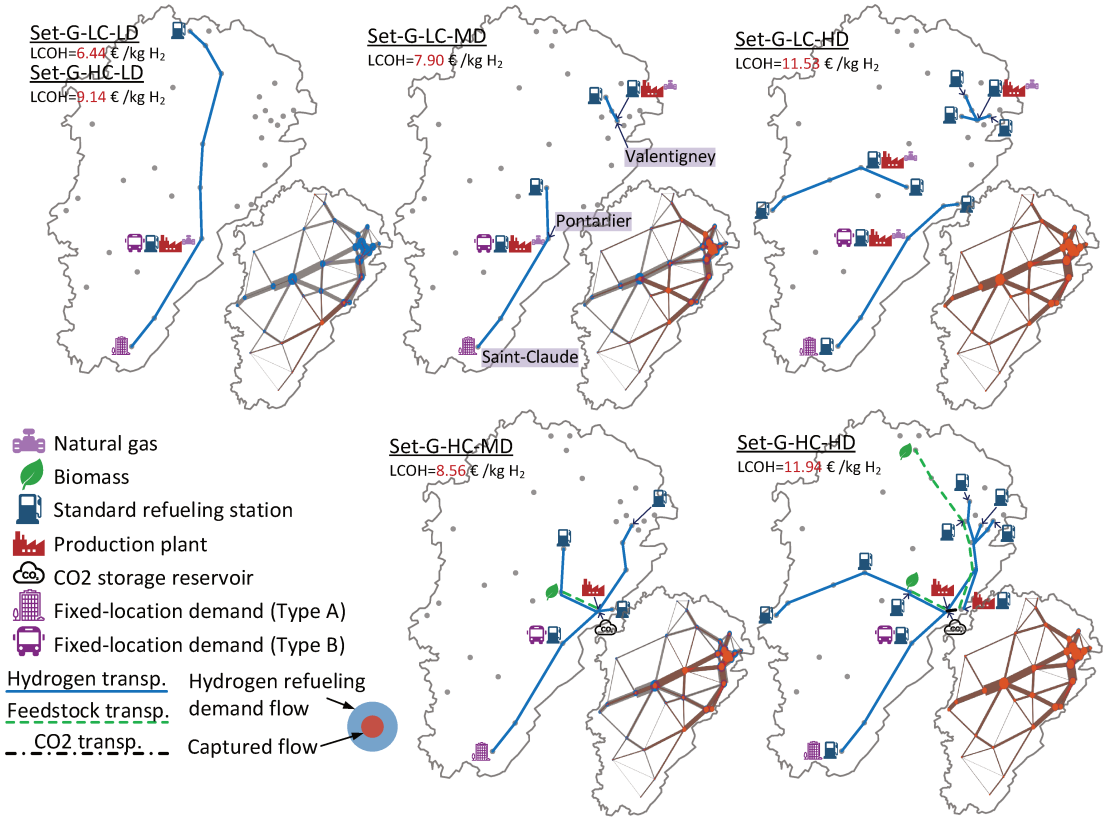

Figure 3.14: Configurations for Set G

plants. In the low carbon price scenario, the model selects SMR because the production technology such as SMR plants is less expensive in capital cost, and the HSCN is built on gaseous hydrogen. The observed differences between the configurations obtained for the two scenarios are that a CCS system has been adopted at medium and high demand and that BG plants are chosen instead of SMR plants. It is noteworthy that CO_2 emissions of the two BG plants at high demand are all captured by the CCS system. The model chooses to install the two BG plants near the CO_2 storage site and accepts the long distances of feedstock transportation.

To conclude this experimentation part, and beyond the results corresponding to the particular case of the Franche-Comté region, the configurations that we obtained show that:

- Our exact model is well capable of solving the integrated problem under consideration;
- All the components of the supply chain, from feedstock to service stations, effectively participate in the quality of the chain built and in obtaining a trade-off in terms of the possible choices, with the aim of minimising the ”Pump price”, which is the objective retained for our study (LCOH). Not considering all of these components, and therefore these choices, calls into question the overall balance sought, and can

have a strong impact on the construction of the chain, as shown by the resolution of degraded instances of the full instance G.

3.7/ CONCLUSION

The hydrogen supply chain network in the transportation sector is a complex system. It includes various components from feedstock supply sites to hydrogen refueling stations. Because of the inherent characteristics of a supply chain, each part of HSCN is interconnected rather than isolated. The selection of feedstock, production and refueling technology, locations of hydrogen facilities, and other major decisions make up a vast "pool" of pathways, each of which has a different value of LCOH and network configuration. For decision-makers, it is challenging to make intelligent designs without support from optimization models.

In this chapter, an intercomponent integration planning of HSCND was proposed. Specifically, a mathematical optimization model was developed, which integrates the hydrogen supply chain network design (HSCND) and hydrogen refueling station planning (HRSP). In particular, our model satisfies two major types of hydrogen demand: fixed-location demand (node-based) and refueling demand of FCEVs (flow-based). To represent the refueling demand of FCEVs, we have introduced the concept of hydrogen refueling demand flow, which is a modified traffic flow that involves the influences of potential FCEV ownerships in different cities or towns. The developed model was applied to Franche-Comté. For this case study, we have generated 66 instances to learn the role of each key model component. A deep analysis of the numerous results confirmed the interest of proposing a more complete model than those ones in the literature.

Our exact model has both advantages and drawbacks. It could first constitute a solid base for further developments, which means that we could extend it to include other aspects such as multiple objectives to optimize. Another research direction could also be to develop a heuristic approach to solve the same problem. Indeed, like for many other optimization problems, the studied one is complex and an exact model generally fails to solve large size problems in reasonable time. It is all the more true when changing the problem scale and envisaging to address it at a national level for example. Those few possible perspectives still remain in a strategic decision level. Rather than keeping on focusing on the strategic planning horizon, where no tactical activities are involved, we decided to study the intertemporal integration planning of HSCND, simultaneously considering location decisions of hydrogen facilities (strategic level) and routing decisions of hydrogen transportation vehicles (tactical level). This is the subject of our second main contribution which is reported in the next chapter.

4

A LOCATION ROUTING MODEL AND TWO METAHEURISTIC APPROACHES FOR THE INTERTEMPORAL INTEGRATION PLANNING OF HSCND

In this chapter, the intertemporal integration planning of HSCND is introduced. Specifically, a location routing approach is presented to determine simultaneously siting of hydrogen refueling stations (HRSs) and the routing decisions for hydrogen delivery trucks. The model is proposed to overcome barriers to the deployment of HRSs. The hydrogen supply network is determined while maximizing the refueling demand flow captured and minimizing the total daily cost. Two metaheuristic algorithms are proposed to solve the problem, including adaptive large neighborhood search (ALNS) and genetic algorithm (GA). The developed model and algorithms are applied to Bourgogne-Franche-Comté, a region in France. Results show that the simultaneous involvement of strategic (location decisions) and tactical (routing decisions) planning improves understanding of decision-makers about various components within hydrogen supply network, and provides useful managerial insights regarding the role of fleet composition and physical forms of hydrogen.

Contents

PUBLICATIONS

WORKING PAPERS

- Li, L. ,Al Chami, Z., Manier, H., and Manier, M.-A., Incorporating fuel delivery in network design for hydrogen refueling stations: formulation and two metaheuristic approaches. Submitted to *Omega*, February, 2020.

4.1/ INTRODUCTION

The total stock of FCEVs exceeded 12,900 vehicles as at the end of 2018 showing 80% increase in 2018 (International Energy Agency, 2019a)[1]. According to L'Association Française pour l'Hydrogène et les Piles à Combustible (2018)[2], there were only 324 FCEVs in France at the end 2018. Many governments and associations have announced targets, visions and projections on FCEVs. The Hydrogen Council estimated that hydrogen will power more than 400 million cars in 2050 (McKinsey & Company, 2017). France will have 5,000 FCEVs in 2023 and this number may rise to 50,000 in 2028 (L'Association Française pour l'Hydrogène et les Piles à Combustible, 2018).

The most significant challenge to meet these targets is the roll-out of hydrogen refueling stations (HRS) (International Energy Agency, 2019b, 2015; McKinsey & Company, 2017). For consumers, the coverage provided by hydrogen refueling networks is a pre-requisite for the adoption of FCEVs. Besides, car manufacturers can be attracted to the market only if a minimal number of hydrogen refueling stations (HRSs) is available or will be installed soon in a given region. France needs to build up 100 HRSs by 2023, and at the end of 2028, this number should rise up to 1,000. Until 15 June 2019, there were 23 HRS in operation in France, in which 15 are non-public and 12 are public (L'Association Française pour l'Hydrogène et les Piles à Combustible, 2018). Non-public HRSs serve dedicated

[1] Advanced Fuel Cells Technology Collaboration Program
[2] The French Association for Hydrogen and Fuel Cells

fleet vehicles (such as urban buses, taxis, and handling vehicles). They provide support for market introduction of FCEVs. Public HRS play a more significant role because largely self-sustained market is based on massive adoption of FCEVs by average consumers. The number and locations of public HRSs determine the fuel accessibility in a given region. In addition, the deployment of public HRSs has a major impact on hydrogen fuel prices (European Union, 2014).

Land requirements and hydrogen sources are the two principal barriers to a deployment of public HRSs. Public HRSs need to be installed within or near urban areas to ensure the fuel accessibility (Melaina et al., 2012). However, most cities, especially major ones, face the problem of urban land scarcity. In addition, the hazardous zone or risk contour related to a HRS intensifies the difficulty of land requirements (Lototskyy et al., 2019; Sun et al., 2014). Even if there is suitable land, skyrocketing land prices will raise the hydrogen fuel prices and hinder the adoption of FCEVs. The hydrogen sources should be taken into account at the very beginning of HRS deployment. Two major propositions provided by academics and practitioners are: hydrogen is produced in a newly built centralized production plant and delivered to HRS using tube tailors or tanker trucks; or hydrogen is produced on-site through small scale of electrolysis or steam methane reforming, as discussed in Chapter 3.

In this chapter, another possible solution is discussed which consists of:

- installing hydrogen dispenser in existing gasoline stations;
- and making use of surplus hydrogen as sources which are obtained from existing petroleum refineries, chemical complexes, or other industrial plants that have excess hydrogen production.

Apart from installation of new HRSs, the conversion of existing gasoline stations to HRS is also regarded as a possible scenario (Scipioni et al., 2017). European Research Area (2015) estimated that many HRS will be placed on already existing conventional refueling stations, because there the basic infrastructure is already in place and because hydrogen retailers are expected to be linked to today's petrol retailing players. Rebuilding existing gasoline stations into gasoline-hydrogen stations could solve the land requirement problem. Besides, the consumer refueling behavior will not be changed, and a "good" refueling experience is guaranteed through familiar settings (a hydrogen bay in an existing gasoline station) (Nicholas et al., 2004, 2010). Adding onsite small-scale hydrogen generator to existing gasoline stations are discussed in (Forsberg et al., 2007; Katikaneni et al., 2014; Bersani et al., 2009). Sun et al. (2017) investigated the way of installing hydrogen dispenser in existing gasoline stations along the expressway, and noted that great reduction in the cost of building and operating a hydrogen station can be achieved. However, not all existing gasoline stations are qualified for this rebuilding. Brown et al. (2013) pointed

that the required footprint for potential station expansion may be prohibitive with respect to space available at existing gasoline stations. Thus there will be a limited number of existing sites that could possibly be used for dispensing hydrogen (National Research Council, U.S., 2015).

The volume of surplus hydrogen from industry is significant. Hydrogen losses in industrial waste gas streams have been estimated to be 10 billion Nm^3/y (Nm^3 per year) in Europe (Maisonnier et al., 2007). In Shanghai, there is an estimated 3,600 metric tons/y of excess hydrogen production capacity (Weinert et al., 2007). Within a more sustainable framework, this surplus hydrogen could be used as fuel for transportation (Yáñez et al., 2018). Several studies (Konda et al., 2011; Almansoori et al., 2009, 2012) demonstrated by mathematical modeling that the use of surplus hydrogen could reduce the capital needs, while facilitating a seamless transition to hydrogen mobility, especially in the early stages. In 2010, a FCEV demonstration was conducted during the World Expo Shanghai, including a coking factory which serves as hydrogen source. The industrial plant that has excess hydrogen production (hydrogen source) and existing gasoline stations which are chosen to install hydrogen dispensers (HRS) are linked through hydrogen delivery based on road transportation. The proposed solution is designed to tie hydrogen infrastructure into existing energy and industrial infrastructure where possible. It is especially attractive when oil companies represent one of the major stakeholders of hydrogen production.

Let us assume that an oil company plans to deploy hydrogen refueling network in a given region, based on an existing refinery plant and several gasoline stations owned by this company. Decision makers thus have to choose on which gasoline stations a hydrogen dispensing equipment will be placed (European Research Area, 2015). Criteria include economic consideration and coverage (to reach as many customers as possible). Besides, under these circumstances, hydrogen delivery cost will become significant and account for around one-fifth of the total hydrogen cost (€/kg) (Weinert et al., 2007) . A sub-optimal delivery system may lead to the consequence that the cost advantages of surplus hydrogen will be outweighed by the distribution cost. Thus, decision makers should also take the delivery plan into consideration.

These first elements provide an inventory of the current situation or one envisaged by the public authorities and operators in the field. Let us now try to re-situate the positioning of these findings in the context of the thesis and the work reported in Chapter 3. The first discussions above may suggest that the two problems that we have dealt with are independent. In reality this is not the case. In a classic decision-making scheme, the strategic level HSCND (including the HSRP part) makes it possible to choose, locate and size all the components of the supply chain, from feedstock to refueling stations. These components can be selected from existing and operational sites (for example gasoline

stations delivering hydrogen, or stations delivering gasoline but which could be extended to the distribution of hydrogen), and/or new potential sites to set up. The results of our optimization model then constitute constraints for the lower decision level which is the tactical level. It will then be a question of defining the transport services associated with the supply chain, in particular to supply the selected refueling stations by optimizing a new cost function. Here we are faced with vehicle routing problems. However, if the solution provided by the first decision level is optimized, that resulting from the second level is only optimal in the context imposed by the strategic level. It can therefore generate additional costs compared to another solution allowing a total or at least partial modification of the previous decisions. At this stage, two possibilities are open to us:

- either we question everything: this amounts to considering a fully integrated strategic/tactical problem. It is clear that although optimal, this solution would be at the cost of an untractable complexity, including by approximate methods;
- or we authorize a partial questioning: this is the approach we have chosen here, considering the last level of the supply chain, that is to say the refueling stations, assuming that the characteristics of the components upstream (production,. ..) cannot be changed. The problem of HSCND is reduced then to a problem of HRS location, which will therefore be combined with vehicle routing problems.

Let us note that in a backtrack loop of the decision chain (from the strategic level to the tactical level), the new modified choices may be evaluated by our HSCND model, in particular to measure the gap in term of LCOH with the initial solution. Fig. 4.1 illustrates the sequencing and interaction between our two contributions.

Then in this chapter and considering this background, we have developed an intertemporal integration planning approach, which simultaneously considers location and routing decisions, by combining the two above optimization problems. First, the hydrogen refueling demand flow network is generated, which is based on traffic flow and demographic metrics of the region. Then, the model determines which existing gasoline stations are selected to be expanded into HRSs, and their refueling capacities. In addition, the model determines which vehicles (among a vehicle fleet) will be used to deliver hydrogen and for each vehicle, the HRSs assigned to it as well as the vehicle routes. The network configuration is determined while both maximizing the refueling demand flow captured and minimizing the total daily cost. For this bi-objective problem, the generated Pareto solutions will provide decision makers with abundant valuable references. Decision makers can query the least cost to obtain a certain amount of coverage. They can also demand the maximum coverage that can be achieved with a predefined budget. Furthermore, the Pareto front composed of these solutions represents different possible refueling network configurations, thus it allows the decision makers to choose the optimal solution based

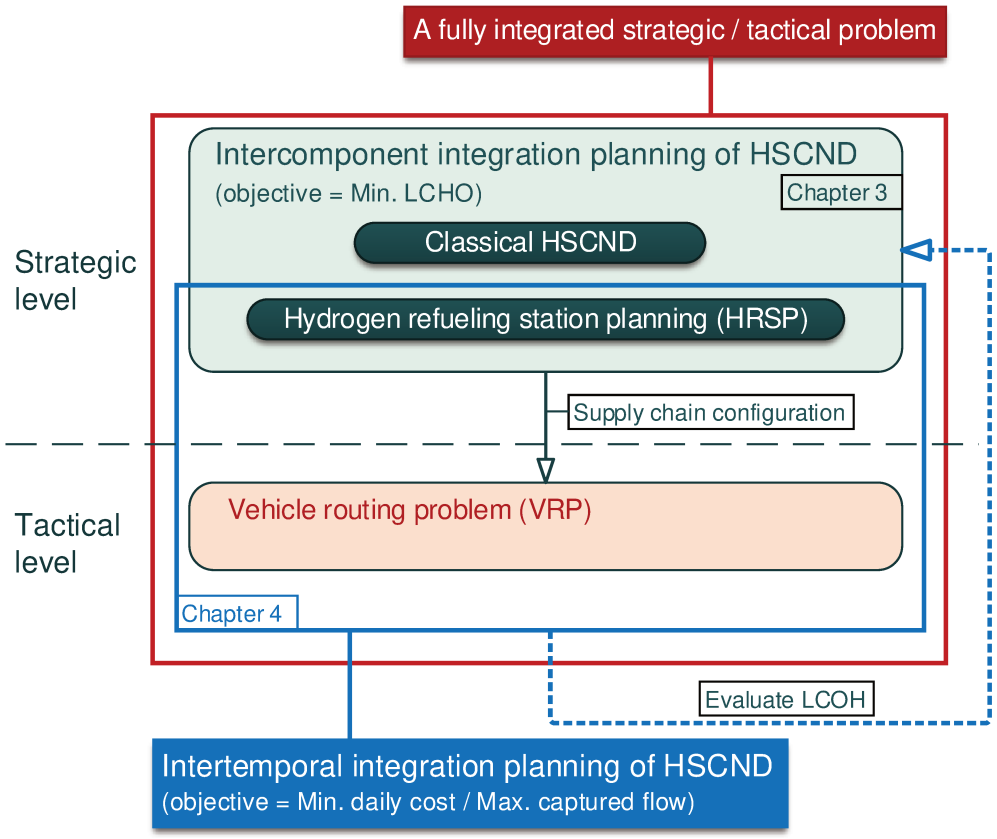

Figure 4.1: Strategic and tactical decision levels of the hydrogen supply chain

on their interests. To solve the studied problem, we have elaborated two metaheuristic algorithms, including Adaptive Large Neighborhood Search (ALNS) and Genetic Algorithm (GA). The developed model and algorithms are applied to Bourgogne-Franche-Comté, France.

4.2/ LITERATURE REVIEW

The existing researches on hydrogen refueling station planning (HRSP) were reviewed in Chapter 2 and Chapter 3. In this section, we firstly present some near problems encountered in the installation of charging infrastructure for electric vehicles.

To find the optimal location of electric vehicle fast charging stations, Cruz-Zambrano et al. (2013) proposed an extension of FCLM (Flow Capture Location Model) including distribution network and location costs. The authors explained the reason why the interdependencies with electricity supply is involved as: building up the grid tie to electricity distribution network is one of the main costs of the fast charging stations commissioning, and

that fast charging stations have a significant impact on the distribution network. Scheiper et al. (2019) presented an integrated planning approach to locate charging infrastructure for battery electric vehicles considering interactions with the electrical grid. The interactions have been examined through combining a charging station location model and a power flow model with integrated energy stores. He et al. (2017) and Sun et al. (2017) created a HRS siting optimization model which involves hydrogen source planning and hydrogen station planning. Their model optimizes the number and locations of stations, the hydrogen source selection for the stations, and the way of transportation to minimize the hydrogen life cycle cost.

For exact solutions, Arslan et al. (2016) used Benders decomposition algorithm to solve the charging station location problem with plug-in hybrid electric vehicles. Yıldız et al. (2016) proposed a Branch&Price algorithm for solving the HRSP with routing. Göpfert et al. (2019) proposed a Branch&Cut approach for the planning of recharging and refueling infrastructure. For heuristic solutions, Lim et al. (2010) developed heuristic algorithms for solving the Flow Refueling Location Model (FRLM), which included greedy, greedy-adding with substitution, and genetic algorithms. Kim et al. (2013) presented a heuristic algorithm based on the network transformation to solve the deviation FRLM. Hosseini et al. (2017a) developed a heuristic method based on Lagrangian relaxation to solve an extension of FRLM.

Let us note that the main difference between FRLM and FCLM is the following one: FRLM (Flow Refueling Location Model) can be viewed as an extension of Flow Capture Location Model (FCLM) where the vehicles autonomy is taken into account, for example in terms of the round trip distance between two stations. Then FCLM should be efficient for small distances (for example regional level) whereas FRLM should be more adapted for greater distances travelled by users (national area).

In the quoted papers, two problems are to be solved: the location of charging sites and the way to supply them. These two problems are similar to the joint location problem (HRSP) and routing problem (VRP) in the studied hydrogen supply chain. In the literature about optimization, the problem addressed in this chapter falls into the category of location routing problems (LRPs). Indeed, the classical LRP simultaneously locates depots and determines vehicle routes supplying customers from these depots (Prodhon et al., 2014). However, in the definition of LRP, what must be located are the upstream depots, for a set of customers a priori defined. In our case, it is the opposite: the origin of the transport is defined, these are the production plants (eventually located by the HSCND model), while we search to locate and size the ”customers”, that is to say stations, among a set of possible locations. Our problem can nevertheless be seen as a particular variant of multi-objective Capacited LRP (multi-objective CLRP).

In addition to the classical variants of LRP, (Drexl et al., 2015) enumerates some atypical

variants, summarized in Table 4.1. The first one, called planar LRP, does not apply in our case, because the possible locations of ”depots” (production plants) are known in advance in our case. In the arc-routing LRP variant, the demand is located on the edges of the graph, which is not the case for hydrogen: indeed, although we are talking about flow, the demand will always be localized at a node. In the same way, our problem is not a LRP with outsourcing because we do not consider subcontractors. As for the prize-collecting LRP, which can be considered as a selective variant, it could have matched with our problem in the sense as all the possible places for stations are not supplied. But the main difference is that customers are independent, whereas in our case, when a station is chosen, it is no more useful to deliver the neighbour locations, as the flow is captured and so adding a new station would bring nothing more for the flow coverage. This flow capture notion also constitutes the main difference with classical LRPs, in which we search to minimize a total cost (often expressed as a totally traveled distance), to satisfy all the demands of customers. In the hydrogen supply chain, we also aim at minimizing a cost, but in order to guarantee a given coverage rate (not of customers but of the considered geographical area).

Table 4.1: Particular identified LRP variants (adapted from (Drexl et al., 2015))

LRP variants	Brief description	Ref.
Planar LRP	facility locations are not restricted to a discrete set, but facilities may be located freely in the plane	(1), (2)
Arc-routing LRP	consider service requirements along the edges of a network	(3)
LRP with outsourcing	subcontracted facilities are available that serve assigned customers at a route-independent cost given by the subcontractor (*particularly adapted for multi-echelon cases*)	(4)
Prize-collecting LRP	a profit is collected when visiting a customer and penalties are incurred for each unvisited customer	(5)
Generalized LRP	customers are clustered into disjoint groups; objective: find routes in which exactly one customer from each group is visited exactly once	(6)

(1), (Schwardt et al., 2009); (2), (Manzour-al Ajdad et al., 2012); (3), (Doulabi et al., 2013); (4), (Stenger et al., 2012); (5), (Ahn et al., 2012); (6), (Glicksman et al., 2008).

In conclusion and although we did not find an existing scheme characterizing our study, we will consider in the following that we must solve a particular (new?) variant of multi-objective Capacited LRP (multi-objective CLRP). The next section sets out the hypotheses and the framework of our study, as well as proposes a mathematical formulation. Then two heuristic algorithms will be developed and their performance will be evaluated

on a new case study.

4.3/ THE LOCATION ROUTING PROBLEM IN HYDROGEN SUPPLY CHAIN

In the present problem, we consider a single depot (hydrogen production plant) in a fixed location, and the model needs to locate customers (HRSs) and determine vehicle routes for hydrogen delivery. Moreover, this optimization problem has two objectives, maximizing the refueling demand flow captured and minimizing the total daily cost.

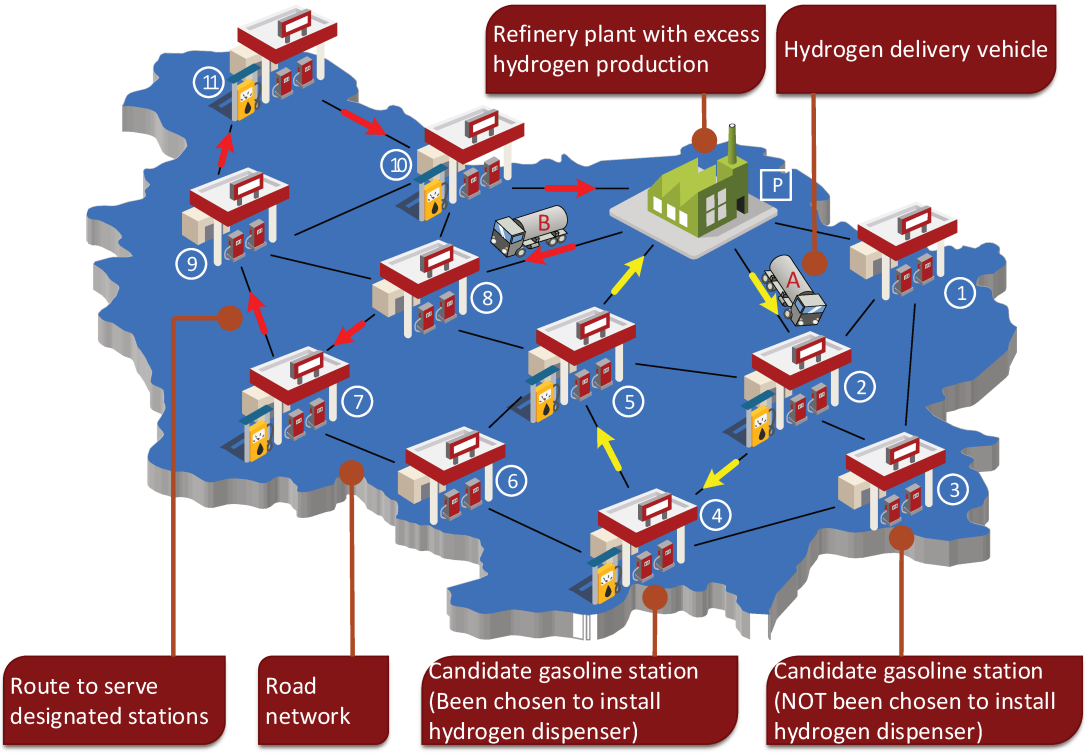

Figure 4.2: A schematic example of the location routing problem in hydrogen supply chain

Fig. 4.2 is a schematic example of the location routing problem in hydrogen supply chain. Within the road network, a single node represents the hydrogen plant (P), and all other nodes represent candidate existing gasoline stations that are qualified to be expanded (1, 2, 3,. . .). Each couple of nodes make up an Origin-Destination (OD) pair, and there is an amount of hydrogen refueling demand flow corresponding to each OD pair. If a candidate gasoline station has been chosen to install hydrogen dispenser, then this station becomes an *opened station*; otherwise it is *non-opened*. Based on the concept of flow capturing, any combination of opened stations corresponds to a specific value of *flow*

captured (or *percentage of flow captured* when divided by the total amount of pairs flow). Each delivery vehicle starts from the hydrogen plant, travels a route to serve designated opened stations, and returns to the plant. In Fig. 4.2 for example, Vehicle B serves three opened stations - 7, 10, and 11, it follows the route: P → 8 → 7 → 9 → 11 → 10 → P. Notice that stations 8 and 9 are not served by Vehicle B, even if they are on the route. These non-opened stations that are just visited (but not served) by delivery vehicles are called *transit stations*. The model aims to determine which candidate gasoline stations are opened, their hydrogen refueling capacities, and the most efficient vehicle routes to maximize the refueling demand flow captured and to minimize the total daily cost which includes the cost related to hydrogen production, delivery, and dispensing.

The road network is described by an undirected graph $G(N, E)$, where N is the set of nodes and E is the set of edges. The node set N is composed of the node of hydrogen plant P and the set of candidate gasoline stations S. The edge set E represents road segments linking nodes in network. In this regard, the assumption, notations, and proposed model are as follows:

4.3.1/ Assumptions

- For each OD pair, the path linking the nodes from origin to destination follows the principle of the shortest path, and the nodes on that path is known;
- Each candidate station has a known hydrogen refueling demand. It is calculated by gathering all refueling demand flows that pass through the associated node;
- The production capacity of the hydrogen plant is sufficient even when all candidate stations are opened;
- There are several available delivery vehicles with different capacities, and the total capacity of the fleet is sufficient even when all candidate stations are opened;
- Each opened station belongs to one route, and each route is served by one vehicle;
- For each route, the path linking the adjacent hydrogen plant and opened stations or the adjacent two opened stations follows the principle of the shortest path.

4.3.2/ Notations

4.3.2.1/ Sets

$q \in Q$	OD (Origin-Destination) pairs
$s \in S$	set of candidate gasoline stations

p	hydrogen production plant
$i, j \in N = S \cup p$	set of all nodes
$k \in K$	set of all hydrogen delivery vehicles
N_q	set of nodes on the shortest path for OD pair q

4.3.2.2/ PARAMETERS

f_q	hydrogen refueling demand flow of each OD pair q, kg H_2/d
h_s	hydrogen refueling demand of candidate station s, kg H_2/d (sum of all the refueling demand flows f_q that pass through this station)
pcc	daily cost of the production plant, €/d
scc_s	daily cost of making a candidate station s opened, €/d
g^k	fixed daily cost of using delivery vehicle k, €/d
c_{ij}	cost of traveling from node i to node j, €
u^k	capacity of vehicle k, kg H_2
u^{max}	the maximum capacity of vehicles, kg H_2

4.3.2.3/ DECISION VARIABLES

IC_q	1 if hydrogen refueling demand flow of OD pair q is captured, 0 otherwise
IS_s	1 if the candidate station s is opened, 0 otherwise
X_{ij}^k	1 if vehicle k travels from i to j, 0 otherwise
Y^k	1 if vehicle k is assigned to a route, 0 otherwise
R_s	an auxiliary continuous variable, (it can be seen as the amount of hydrogen held by the vehicle after its visit of station s)

4.3.3/ MATHEMATICAL FORMULATION

$$Maximize \quad OBJ1 = \frac{\sum_{q \in Q} IC_q * f_q}{\sum_{q \in Q} f_q} \tag{OBJ1}$$

$$Minimize \quad OBJ2 = pcc + \sum_{s \in S} IS_s * scc_s + \sum_{k \in K} Y^k * g^k + \sum_{i \in N, j \in N, k \in K} X_{ij}^k * c_{ij} \tag{OBJ2}$$

Subject to:

$$\sum_{i \in N_q : i \neq p} IS_i \geqslant IC_q, \quad \forall q \in Q \tag{4.1}$$

$$\sum_{k\in K, i\in N: i\neq s} X_{is}^{k} = IS_s, \quad \forall s \in S \tag{4.2}$$

$$\sum_{i\in N: i\neq j} X_{ij}^{k} - \sum_{i\in N: i\neq j} X_{ji}^{k} = 0, \quad \forall j \in N, k \in K \tag{4.3}$$

$$\sum_{s\in S} X_{sp}^{k} = Y^{k}, \quad \forall k \in K \tag{4.4}$$

$$\sum_{s\in S} X_{ps}^{k} = Y^{k}, \quad \forall k \in K \tag{4.5}$$

$$\sum_{i\in N, s\in S: s\neq i} h_s * X_{is}^{k} \leqslant u^{k} * Y^{k}, \quad \forall k \in K \tag{4.6}$$

$$R_{s'} + h_{s'} * X_{ss'}^{k} - u^{max} * (1 - X_{ss'}^{k}) \leqslant R_s, \quad \forall s, s' \in S : s' \neq s, k \in K \tag{4.7}$$

$$0 \leqslant R_s \leqslant u^{max} - h_s, \quad \forall s \in S \tag{4.8}$$

$$X_{ij}^{k} = 0, 1 \quad \forall i, j \in N, k \in K \tag{4.9}$$

$$Y^{k} = 0, 1 \quad \forall k \in K \tag{4.10}$$

$$IC_q = 0, 1 \quad \forall q \in Q \tag{4.11}$$

$$IS_s = 0, 1 \quad \forall s \in S \tag{4.12}$$

OBJ1 maximizes the percentage of flow captured. OBJ2 minimizes the total daily cost, in which the first term is the cost of hydrogen production plant, and the second term relates to the cost of opened stations. The third and fourth terms denote the fixed and variable transportation costs, respectively. Constraints (4.1) indicate that a hydrogen refueling demand flow is captured because there is at least one opened station on the nodes which lies on the shortest path of this flow pair. Constraints (4.2) state that every opened station must be on exactly one route. Constraints (4.3) are flow conservation constraints. Constraints (4.4) and (4.5) ensure that if vehicle k is assigned to a route, then one link

goes into the plant and one leaves the plant. Constraints (4.6) are the vehicle capacity constraints. Constraints (4.7) are the continuity and sub-tour elimination constraints, ensuring that the solution contains no sub-tour disconnected from the plant, and that the vehicle's available capacity is a non-increasing step function in accordance with the refueling demand of the opened stations that are on the route of the vehicle. Constraints (4.8) are capacity bounding constraints which restrict the upper and lower bounds of R_s. Finally, constraints (4.9) - (4.12) are the integrality constraints.

In terms of complexity of this proposed model, and for a large number of nodes $|N|$ in the graph, the number of decision variables is equivalent to : $|N|^2 \cdot |K|$, and the number of constraints is equivalent to : $2 \cdot |N|^2 \cdot |K|$.

4.4/ METAHEURISTIC APPROACHES

Exact methods present many limitations when trying to solve multi-objective optimization problems. Indeed, solving large instances may not be achieved in a reasonable time and taking several objectives can further complicate the resolution. Therefore, several researchers decided to use approximate methods, especially the metaheuristic ones. These latter are widely used techniques to tackle optimization problems and they are characterized by their capabilities to find good solution in a reasonable time, even for large instances. Over the last years, researchers have introduced hundreds of those methods but generally they can be divided into two categories: the trajectory-based methods and the population-based methods. In this study, two of the most famous metaheuristics are chosen: Adaptive Large Neighborhood Search (ALNS) described in subsection 4.4.1 and Genetic Algorithm (GA) presented in subsection 4.4.2. This choice can be explained by the commitment to test the two different categories of those approaches in order to show some advantages and drawbacks of each one.

4.4.1/ ADAPTIVE LARGE NEIGHBORHOOD SEARCH

The ALNS belongs to the category of trajectory-based methods and was first introduced in Ropke et al. (2006). It can be considered as an improved version of the Large Neighborhood Search (LNS) approach introduced in Shaw (1998) to solve a variant of Vehicle Routing Problem. In LNS, destroy and repair operators are respectively applied to an initial solution to improve it. The chosen operators are randomly selected from a set of defined destroy and repair operators. This totally random selection presents the big drawback of the LNS approach. Therefore, the ALNS has overcome this problem by prioritizing best operators to be selected. The idea of this approach is to give a score for each operator which will be then adjusted regarding its performance in the past iterations.

Algorithm 1 illustrates the global framework of the ALNS approach. The W1 and W2 parameters are used to adjust the scores of operators after each iteration. Let us note that in this study, the ALNS implementation slightly differs from the standard one regarding that a multi-objective problem is treated. Subsequently, each part of this algorithm will be explained in detail.

Algorithm 1: ALNS approach

```
Generate initial solutions;
Insert the generated solutions into a list of non-dominated solutions LONS;
Nb_iter=0;
while Nb_iter < Nb_iter_max do
    Start_Solution = Choose starting solution from LONS;
    Select a destroy operator according to its score;
    Select a repair operator according to its score;
    Apply chosen operators on Start_Solution to generate a new solution New_S;
    if one or several solutions from LONS are dominated by New_S || New_S is a new
     non-dominated solution then
        Increase scores of chosen operators using W1 parameter;
        Nb_iter=0;
    else
        if New_S has the same cost and coverage of Start_Solution then
            Replace Start_Solution by New_S in LONS;
        else
            Decrease scores of chosen operators using W2 parameter;
            Nb_iter++;
        end
    end
end
```

4.4.1.1/ GENERATION OF INITIAL SOLUTIONS

A solution of our problem is composed of one or several routes, each route being associated with a used vehicle. A route is an ordered list of opened stations. The classical trajectory-based methods are often used to solve mono-objective problem. Therefore, one initial solution is generated in a way that it has a good quality regarding this objective. This is not the case in our study as a multi-objective variant is considered, a list of three initial solutions is then generated. Each of those solutions aims at representing a part of the Pareto-front. Hence, they are respectively characterized by a coverage range of [0.01;33.99], [34.00, 66.99] and [67.00, 100.00].

The generation of each solution goes through two steps: the first step chooses the stations to open whereas the second one aims at designing the hydrogen delivery routes. The overall procedure used to generate initial solutions is described in algorithm 2.

Algorithm 2: Generate an initial solution in the coverage range [LB;UB]

Step 1 :
Generate a list L with all non-opened stations in descending order of their coverage contributions (OBJ1 in the model);
Open one or several stations from the top of the list to obtain a solution coverage in the range [LB;UB];
Step 2 :
Generate a list L' with all non-used vehicles in ascending order of their using cost;
Flag1 : Start the first route using the first vehicle in L' by inserting the plant ;
Reference point = plant;
Flag2 : Insert the closest station (from the opened stations in step 1) to the reference point;
if the insertion is feasible **then**
    Reference point = new inserted station;
    Goto Flag2;
else
    if the route contains only the plant **then**
        Remove the plant from the route;
        Repeat from Flag1 using the next vehicle in L';
    else
        End the route by inserting the plant;
        Remove used vehicle from L';
    end
end

As shown in this algorithm, the goal of step 1 is to minimize the number of stations that gives the desired coverage to the solution. It is done by adopting a list with all non-opened stations in descending order of their coverage contributions [3]. Then, step 2 builds the delivery routes by inserting at each time the closest station to the last inserted point, according to the nearest neighbour heuristic, which has the advantage of being very fast. Let us note that each generated solution will be inserted into the list of non-dominated solutions (LONS) if it is not dominated by any other solution already inserted.

4.4.1.2/ CHOICE OF THE STARTING SOLUTION

As the LONS may contain up to three different initial solutions, the selection of starting one can significantly impact the final results of the approach. Therefore, it is decided to start with the solution having the smallest ratio of cost over coverage. Over the iterations, this latter can be removed from LONS and/or new non-dominated solutions can be inserted, which gives the possibility for other solutions to be selected as the current one.

[3] Suppose that the coverage value obtained by all opened stations is a (when there is no opened station, $a = 0$), and the new coverage value obtained by all opened stations plus any non-opened station (now is assumed to be opened) is b, then the *coverage contribution* of this non-opened station is $b - a$.

4.4.1.3/ DESTROY OPERATORS

To destroy a part of the current solution, each operator uses a specific strategy to remove either a station or a complete route (composed of one or many stations). Six destroy operators are involved in ALNS and can be described as follows:

1. **Remove the most expensive station:** this operator removes temporarily and alternatively each station and then computes the total cost of the reduced solution. Then, the most expensive station will be removed. Once the station is removed and to maintain a valid route, the two stations that surrounded the deleted station will be directly linked.
2. **Remove the most expensive route:** The route having the most expensive cost will be removed.
3. **Remove the least coverage station:** The same process as for the first operator will be applied. Then, the station having the lower contribution in the total coverage will be deleted. Let us note that removing a station may not impact the total coverage, if the flows captured by this station are also captured by other near opened stations (redondancy in the flow capture).
4. **Remove the least coverage route:** This operator removes each route from the solution, then the coverage is computed. So in this way, we can remove the route with the least coverage contribution.
5. **Remove randomly a station:** A randomly chosen station is removed from the solution.
6. **Remove randomly a route:** This operator erases a randomly chosen route.

It is clearly shown that all six destroy operators are used for diversification purposes. The first four operators are used to destroy parts of the solution which directly impact one of the two considered objectives. Whereas, the last two random operators are not dedicated to destroy any specific part of the solution but can help to avoid looping in a local optimum.

4.4.1.4/ REPAIR OPERATORS

Once a destroy operator is selected, the algorithm chooses one of the four repairing operators to be applied on the destroyed solution.

1. **Add the most coverage station:** This operator tries to add the station which contributes the most in increasing the solution coverage. If this station is one of the

transit stations (one of the nodes on the shortest path linking two opened stations) and it can be opened (the capacity of the vehicle remains respected), the station is opened in its current position. In this case, the total cost of the solution is increased only by adding the opening cost of the added station. If the desired station is not a transit one, the procedure added it in the first possible position. Moreover, if the station cannot be added (all used vehicle cannot handle its hydrogen demand), the second station which contributes the most will be inserted and so on. Once an insertion is done, the process stops.

2. **Add the most coverage route:** The aim of this operator is to add a complete route to the solution. For that, the procedure firstly chooses the vehicle characterized by the bigger capacity (from the list of non-used vehicle). Then, the algorithm tries to insert into the route of this vehicle the station having the higher coverage contribution. If the insertion is feasible, the contribution of remaining stations is updated. Then the new most contributed station is added and so on until an unfeasible insertion is obtained. Let us note that if all available vehicle are used, this operator will not change anything in the solution.

3. **Add the least expensive station:** The goal is to add the least expensive station to the current solution. But, the impact of adding a new station on the total solution cost depends on two elements: the opening cost and the routing cost. This latter is directly linked to the position of the added station. Therefore, the procedure should test all possible positions for all non-opened stations. A long solving time is then needed to find the real least expensive station. Hence, a heuristic method is proposed (see algorithm 3), which rapidly chooses the station in a way that it slightly increases the total cost.

   As shown in algorithm 3, the operator firstly tests to open a transit station because such opening will not impact the routing cost. If any transit stations cannot be opened due to vehicles capacities, the process defines a score for each of non-opened stations. This score is based on the opening cost and the increasing in routing cost caused by adding a non-opened station into its future position (as mentioned in algorithm 3). Finally, the station having the lower score will be inserted.

4. **Add the least expensive route:** This operator uses the least expensive non-used vehicle, then it computes a score for each non-opened station. This score is the sum of opening cost and the routing cost for serving this station. Station having lower score will be finally inserted into the route.

We notice that all repair operators are used for intensification purposes. In other words, they try to generate a final solution with a lower additional cost or bigger coverage.

Algorithm 3: Add the least expensive station

```
if one or several transit stations can be opened then
    Open the one having the minimal opening cost;
else
    for each station s in the list of non-opened station do
        if the station s can not be delivered by any vehicle then
            Increasing cost of s=∞;
        else
            s' = the closed station to s from the list of opened stations in vehicles
             which can deliver s;
            Position of s = test to add s before and after s' and take the best position;
            Increasing cost of s = cost after adding s - cost before adding s;
            Final score of s = opening cost of s + increasing cost of s
        end
    end
    Add the station having the lower final score into its position;
end
```

4.4.1.5/ SELECTION BASED ON SCORES

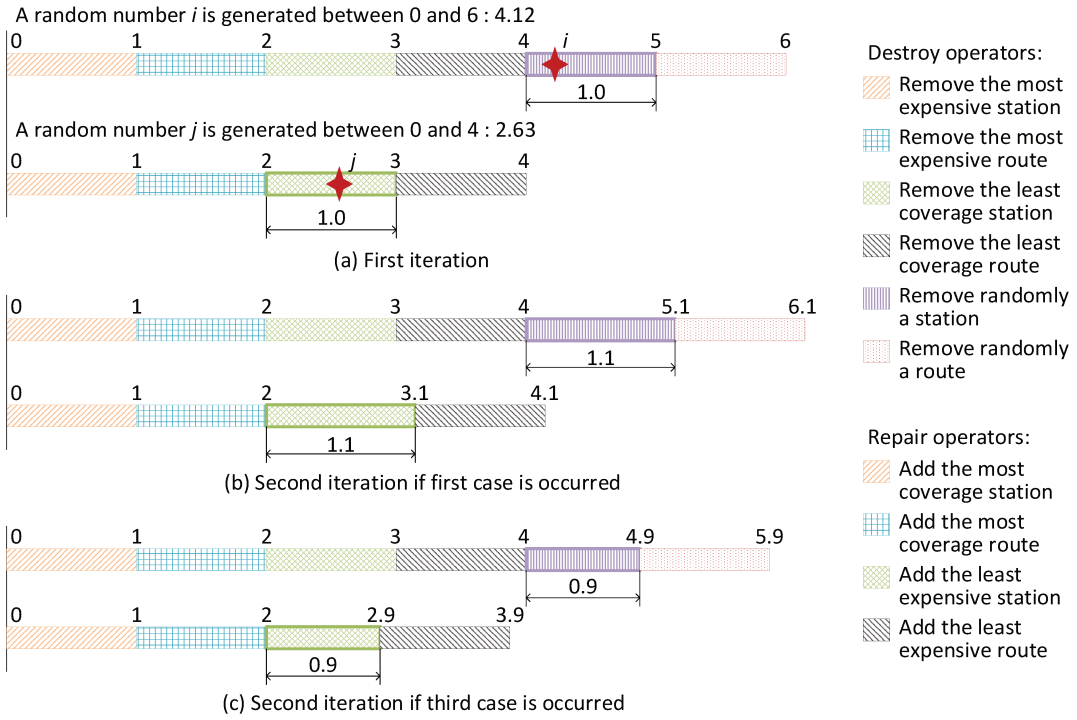

Figure 4.3: Selection and scores evolution

As already indicated, the improvement brought by ALNS is that the operators are not totally randomly selected. But the selection depends on their past performances. At

the beginning of the approach, all operators have a score of 1 (i.e. they have the same chance to be selected). Then two successive selections are done to choose respectively the destroy and repair operators. For each selection, a random number is generated between 0 and the sum of scores for each set. Depending on this number, an operator will be selected. Fig. 4.3 presents an example of the selection at the first iteration. Here, the random numbers are respectively 4.12 and 2.63, then the chosen operators are: "Remove randomly a station" and "Add the least expensive station". Once the operators are applied, three cases can occur:

- In the first one, the new obtained solution dominates [4] one or several solutions from LONS (here, the dominated solutions are removed from LONS).Or, the new solution is a new non-dominated solution. In this first case, the new solution will be inserted into LONS and the scores of the chosen operator will be increased by multiplying the old score by W1.
- In the second case, the new solution has the same cost and coverage as the starting solution. The process replaces then the old one by the new one in LONS without changing the scores of chosen operators. This procedure can bring some diversification to the research trajectory.
- In the last case, the new solution is dominated by at least one solution of LONS. Then, the score of chosen operators should be decreased by multiplying by W2.

It is clear that W1 (W2) should be bigger (smaller) than 1. Fig. 4.3 also shows the new scores at the second iteration, if the first or third cases are occurred. In this example, W1=1.1 and W2=0.9.

In this part, the based-trajectory method ALNS was introduced and the obtained results will be discussed in section 4.5. In the next part, a genetic algorithm, which belongs to the based-population metaheuristics category, will be introduced.

4.4.2/ GENETIC ALGORITHM

Genetic algorithms, firstly introduced in Holland (1973), are widely used methods in the operations research literature. They are based on genetic-inspired operators as the crossover and the mutation. This part will be dedicated to explain the genetic algorithm implementation used to tackle the considered problem.

[4] For two solutions A et B, A dominates B in one of these 3 cases: (1): Coverage(A) > coverage(B) and cost(A) == cost(B); (2): Coverage(A) == coverage(B) and cost(A) < cost(B); (3): Coverage(A) > coverage(B) and cost(A) < cost(B)

4.4.2.1/ CHROMOSOMAL REPRESENTATION

Each solution is represented under the shape of a chromosome composed of a sequence of genes. Each one is associated with a vehicle and contains its routing itinerary. Then each gene is composed of an ordered sequence of integers which are indices of the HRSs assigned to the same vehicle, except the first and last elements which represent the production plant (P). The number of genes per chromosome is equal to the maximum number of available vehicles. Figure 4.4 gives an example of a chromosome with 3 vehicles. Among those vehicles, the first two are used to deliver hydrogen to stations $\{6;7\}$ and $\{5;3;2\}$ respectively. The last vehicle is not used as shown in this solution.

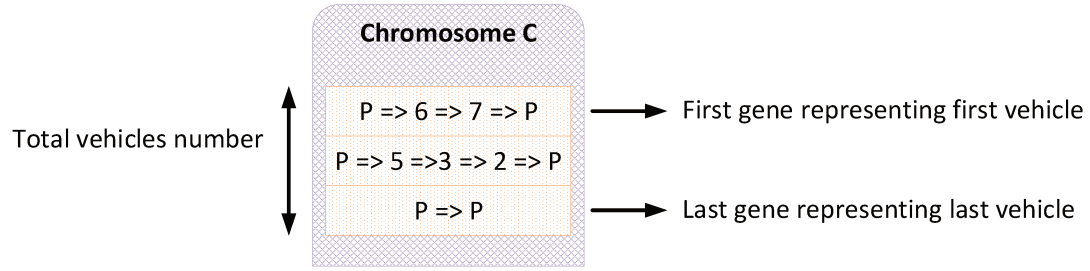

Figure 4.4: Chromosomal representation

Let us note that the routes generated by the model, and appearing in the chromosome, are only composed of opened stations, even if the determination of the distances with a shortest path algorithm enables to identify the transit stations on each route.

4.4.2.2/ INITIAL POPULATION

Generating the initial population of chromosomes is the first step in all genetic algorithms and it may significantly impact the final results. In the implementation, two categories of chromosomes are generated: the first one contains 11 greedy chromosomes and the second category is composed of (NBS-11) randomly generated chromosomes. NBS is a parameter of the approach, which gives the number of chromosomes in the initial population.

The greedy chromosomes belongs to the following ranges of coverage: [0;0], [0.01;9.99], [10.00;19.99], [20.00;29.99], [30.00;39.99], [40.00;49.99], [50.00;59.99], [60.00;69.99], [70.00;79.99], [80.00;89.99], [90.00;100.00]. They are generated using algorithm 2 described in 4.4.1.1. For each randomly generated chromosome, we start by randomly generating a number NRS between 0 and the total number of stations. Then, NRS stations are picked from the list of non-opened stations in a random manner. Finally, step 2 in algorithm 2 is applied to generate the delivery routes. Figure 4.5 gives a small example

with NBS=15.

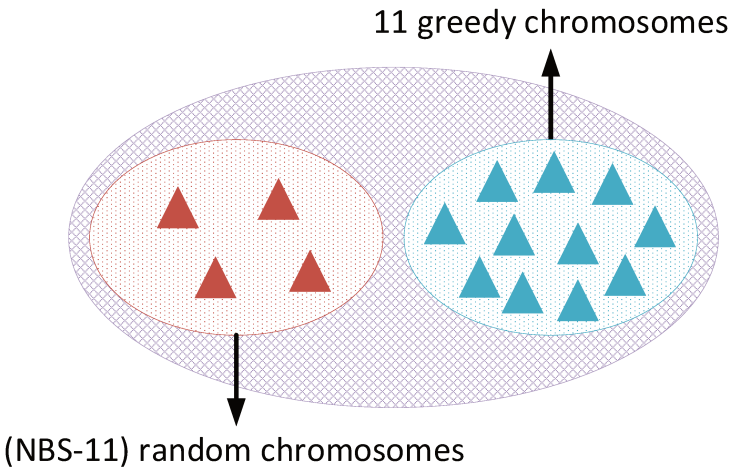

Figure 4.5: Initial population

4.4.2.3/ CHROMOSOMES EVALUATION

As this study deals with a bi-objective variant with no prioritized objective, the evaluation of chromosomes should probably be based on the Pareto dominance theory. Therefore, a rank is calculated for each chromosome by using NSGA (Non-dominated Sorting Genetic Algorithm) introduced in Srinivas et al. (1994). This technique is used to classify the population based on the dominance degree of each chromosome.

The NSGA is based on several layers of classification. In the first one, all non-dominated solutions are associated with a rank R equal to 1. Then this layer of solutions will be temporarily removed from the population. The new layer of non-dominated chromosomes is then assigned with a rank equal to (R+1) and so on. The process will be repeated to classify all chromosomes. Fig. 4.6 gives an evaluation example for a small population of six chromosomes.

Chromosome	Cost (Units)	Coverage (%)	Rank
1	180	80	1
2	170	52	1
3	160	25	1
4	170	38	2
5	160	18	2
6	160	10	3

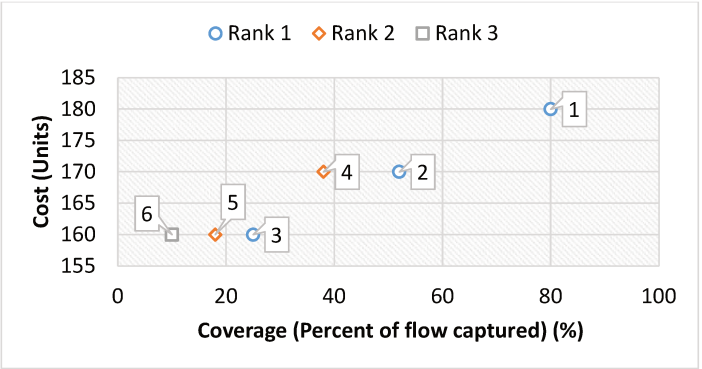

Figure 4.6: Example of ranking function

4.4.2.4/ SELECTION

Once the population is evaluated, the selection of two parents is mandatory to apply the crossover operator. This selection is done using a tournament procedure. For each parent, two chromosomes are randomly chosen from the current population. Then, the one with the lower rank is kept. If the two chromosomes have the same rank, a random one will be kept as described in Fig. 4.7.

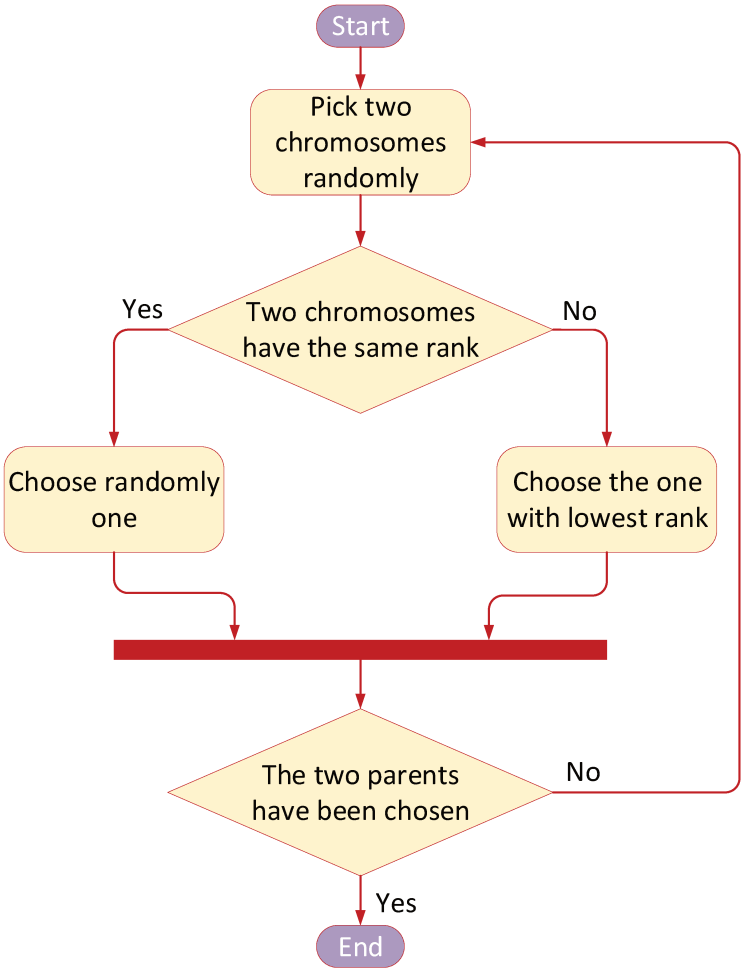

Figure 4.7: Selection procedure

4.4.2.5/ CROSSOVER

The crossover operator is applied on the two chosen parents to obtain two children. The principle of the operator is that the first and second child will respectively heritage the best genes in terms of cost and coverage. For the first child, the procedure begins by comparing the first gene of the two parents. The gene with the lowest cost will be copied as the first gene of this child. Then, the second gene is determined in the same way from

the second genes of the parents, and so on until all genes are filled. In the first gene of second child, the process copies the gene (from the first genes of the parents) which mostly contributes to the coverage while considering that no station is opened yet. Then, the other genes are copied but this time one should take for each new gene the already inserted stations into consideration.

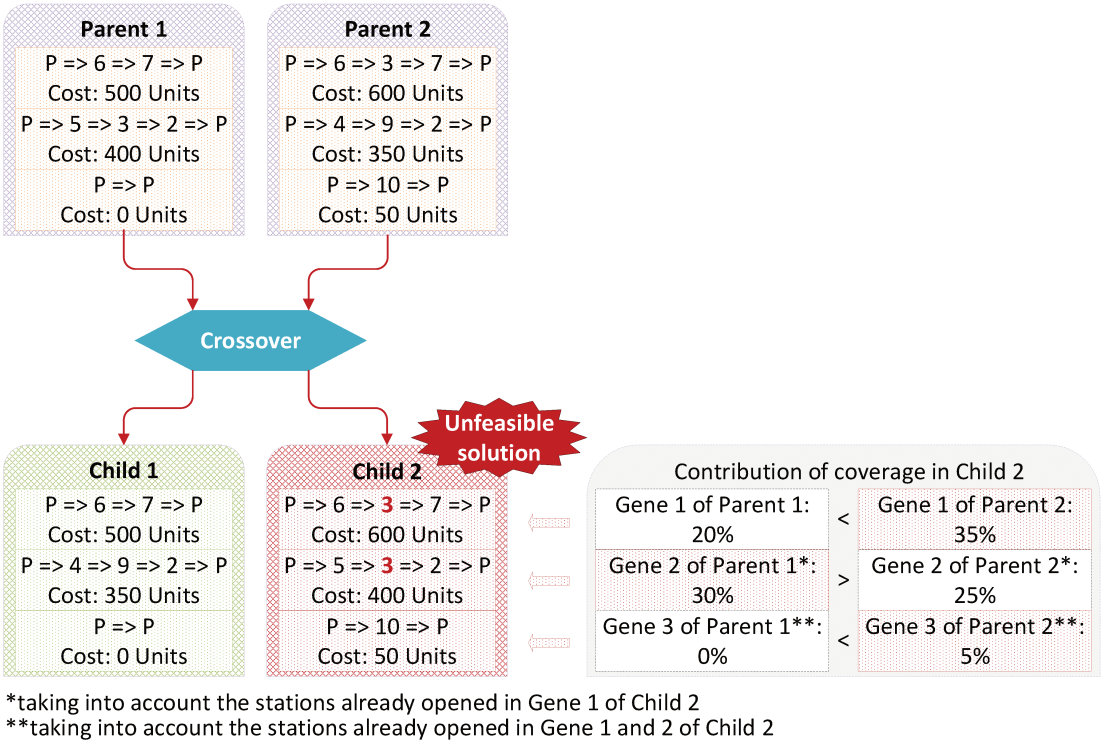

Figure 4.8: Crossover procedure

Fig. 4.8 gives an example of applying the crossover operator on two parents. It is clearly shown that the second child in this example represents an unfeasible solution because station 3 is served by more than one vehicle. Therefore, a repairing procedure should be applied on the two generated children to ensure their feasibility. This procedure is described in algorithm 4. Fig. 4.9 shows the application of this repairing procedure on the second child.

Algorithm 4: Repairing procedure

```
if one of the duplicated stations is the only station visited in one route then
    Remove this station (then the route is automatically removed);
else
    Remove each duplicated station and compute the resulting cost of the route;
    Keep the station in the gene which minimizes the total cost;
end
```

After applying the repairing procedure on the generated children, an insertion function

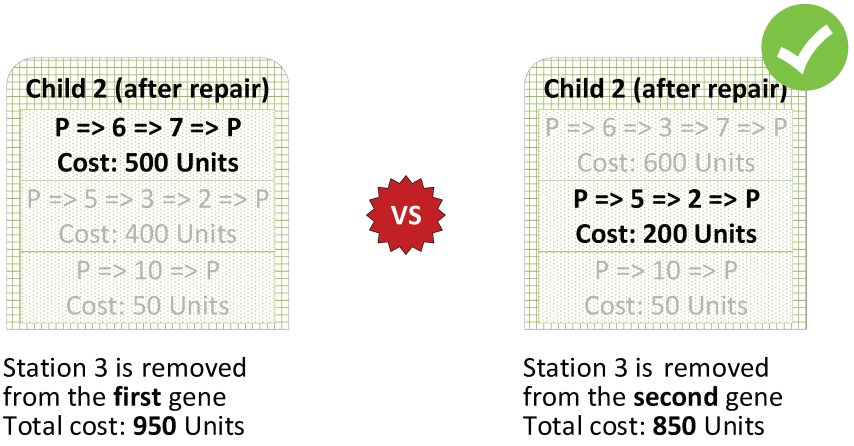

Figure 4.9: Repairing example

will be applied to the second child only. It tries to increase its coverage by inserting a non-opened station into its genes. The process starts by listing all non-opened stations in decreasing order regarding their coverage contributions. Then, if the capacity constraints remain feasible, the first station is inserted into its transit position; else, we try all possible positions in the used vehicles (genes having at least one station). When a feasible insertion is found, the process stops. Otherwise, if no feasible insertion can be found, the process is repeated, but this time by using the second most contributing station and so on until a station is successfully inserted. The choice of using this procedure on the second child is justified by the fact that this latter is dedicated to get the best genes in terms of coverage.

4.4.2.6/ MUTATION

The mutation is applied on the children in order to improve their quality. It involves three operators: Stations_Rearrange, Station_Shift and Station_Exchange. They aim at minimizing the total cost of each child. Algorithm 5 describes the mutation process where Max_M fixes the maximal number of iterations without improvement.

The three operators are described as follows:

1. Stations_Rearrange: this operator is applied on a randomly chosen gene of the child by swapping two randomly selected stations. If this gene contains less than two stations, this operator can not be applied.

2. Stations_Shift: two genes should be randomly selected. Then, one station will be removed from the first gene and inserted into the second one. The operator tests all positions to find the best one for inserting the station. Note that one of the two

Algorithm 5: Mutation procedure

```
Input: i=0; Child C;
Output: Child C';
while i < Max_M do
    C' = Apply randomly one of the three operators on C;
    if C' is feasible and Cost(C') < Cost (C) then
        C = C';
        i = 0;
    else
        i++;
    end
end
```

genes should have at least one station.

3. Stations_Exchange: this operator also randomly chooses two genes but it exchanges two randomly selected stations between them. The first (second) one will be removed from the first (second) gene and inserted into the other one. Here, the two chosen genes should have at least one station.

4.4.2.7/ OVERALL ALGORITHM

After the application of the mutation on the two children, a test of dominance is done for each child by comparing it to its parents. If a child dominates at least one of its parents, it will be inserted into the population. Otherwise, it will be removed. When a new child is inserted, it should be verified that the size of population does not exceed the limit fixed by the parameter Max_Pop. If this limit is exceeded, the solutions having the highest ranks are removed from the population until this one obtains a size equal to Max_Pop. All the steps of the algorithm are repeated Max_iter times, as illustrated in figure 4.10.

4.5/ CASE STUDY: BOURGOGNE-FRANCHE-COMTÉ, FRANCE

The proposed model and algorithms are applied to Bourgogne-Franche-Comté, a region of east-central France. Region Bourgogne-Franche-Comté is composed of two former administrative regions of Bourgogne and Franche-Comté. Its total area is 47,784 km^2, and has a population of 2,816,814 persons.

Totally 62 major cities are selected as network nodes. The most populous cities are Dijon and Besançon, the capitals of the two former region. There are several large cities including Belfort, Chalon-sur-Saône, Auxerre, Nevers, Mâcon, Sens and Montbéliard. The main roads (including highways, national roads, and departmental roads) connecting

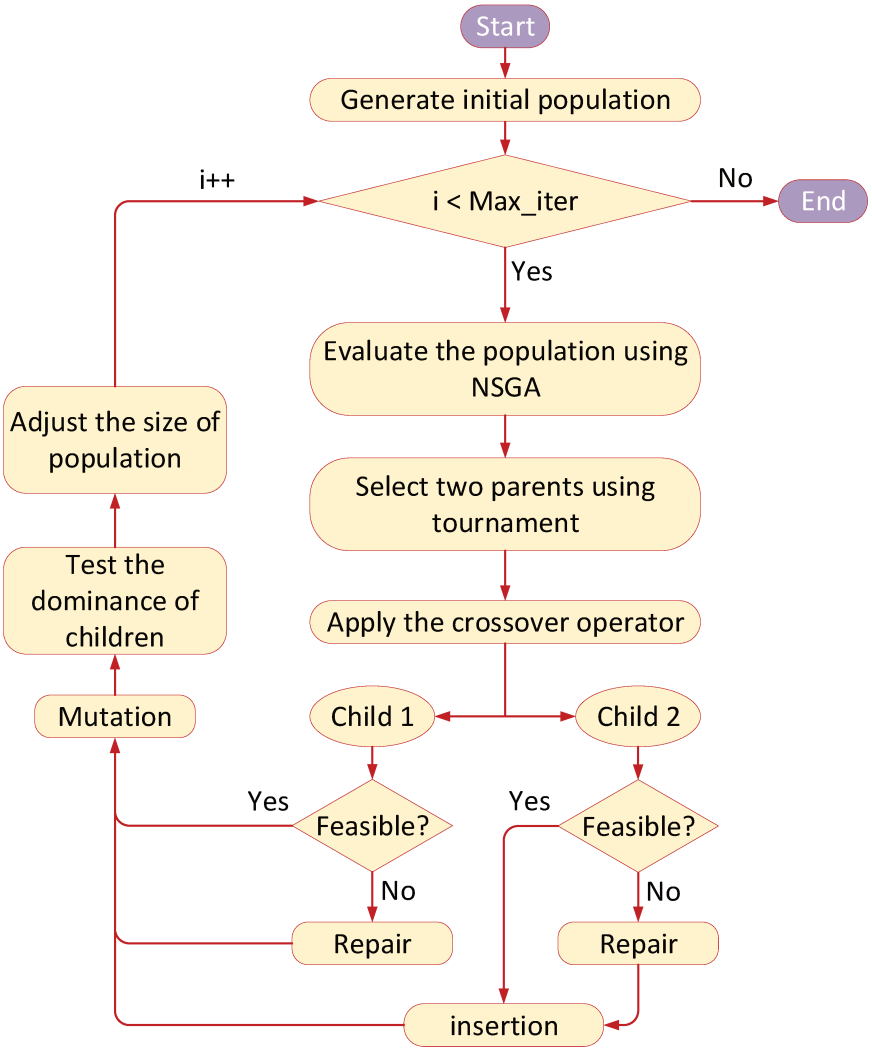

Figure 4.10: Our genetic algorithm scheme

the cities are selected as network edges. There are totally 137 edges. Length data are acquired from Google Maps^{TM}. The length of the network's edges and the distances between different cities are given in appendix A. The network generated is presented in Fig. 4.11 - (a).

The hydrogen refueling demand flow network is based on traffic flow network. By incorporating the potential FCEV ownership of each city, the refueling demand of FCEVs is represented by the flow-based demand. The generation process is detailed in Chapter 3. The resulting flow network is presented in Fig. 4.11 - (b). The larger the radius of the circle, the higher the refueling demand in the city. The wider the edge, the greater the refueling demand flow carried by that edge.

Region Bourgogne-Franche-Comté has a large chemical plant - Solvay-Inovyn, which is

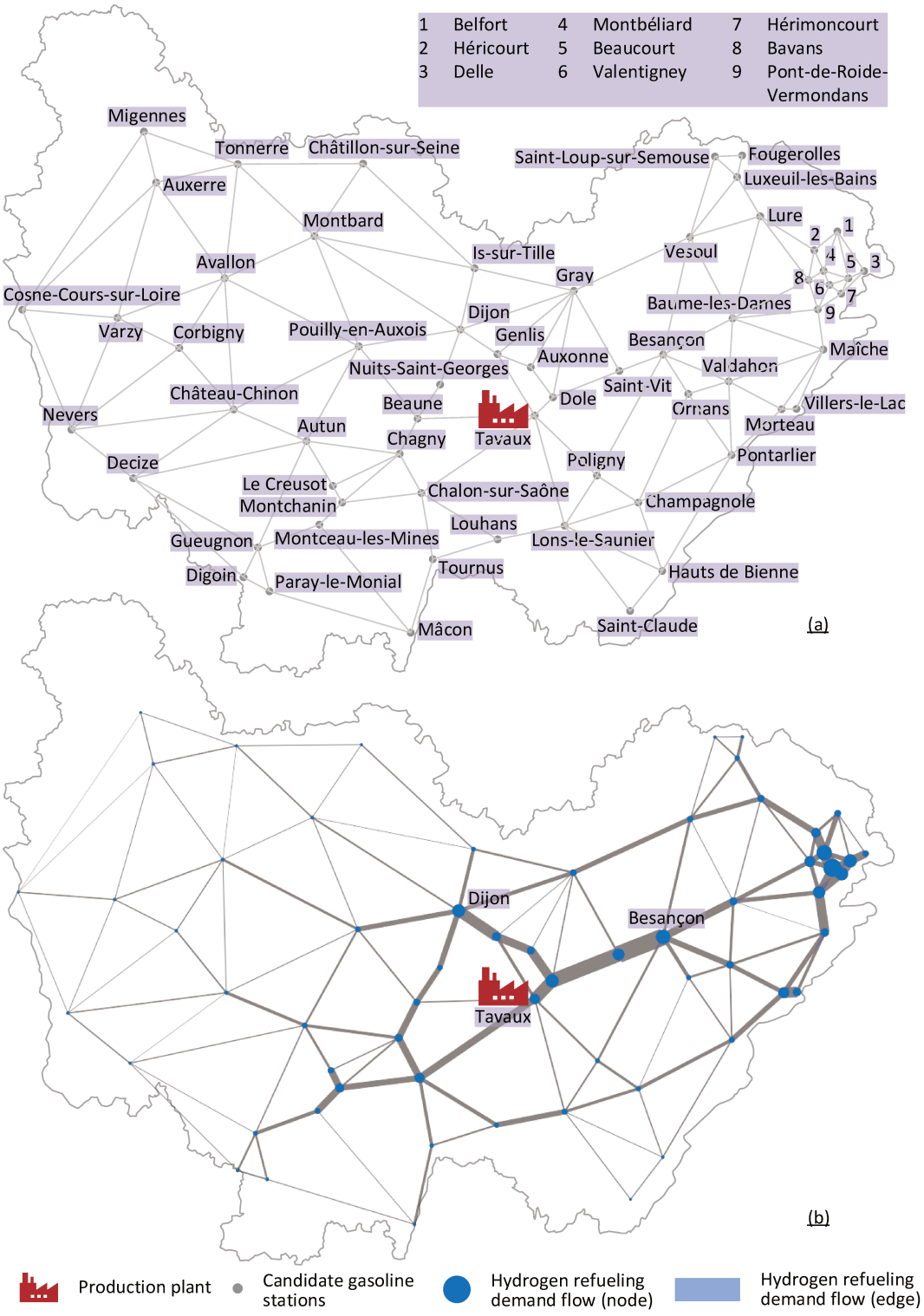

Figure 4.11: Bourgogne-Franche-Comté network: (a) Basic network; (b) Hydrogen refueling demand flow network

located at Tavaux. Solvay-Inovyn extracts salt by hydrolysis and electrolysis. It produces 700,000 metric tons/y of salt and converts it into a number of industrial chemical deriva-

tives. It is estimated that this plant holds 10,000 metric tons/y of excess hydrogen production capacity, sufficient to cover the hydrogen refueling demand of the region (Association de préfiguration de l'Institut de stockage de l'hydrogène, 2019). Therefore Tavaux serves as hydrogen plant and all other nodes (cities) are seen as candidate stations.

Two hydrogen delivery scenarios are defined - gaseous and liquid. In the gaseous scenario, hydrogen is compressed at the plant, and then loaded onto tube trailers. Refueling stations take delivered compressed gas hydrogen and fill the onboard storage tank in a vehicle. In the liquid scenario, hydrogen is liquified at the plant, and then loaded onto tanker trucks. Refueling stations receive delivered liquid hydrogen and charge gaseous hydrogen to a users'vehicles (FCEVs). The costs related to hydrogen liquifier and compressor are shown in Table 4.2. In the gaseous scenario, there exist tube trailers of three different sizes (300kg, 600kg, and 1,100kg). In the liquid scenario, tanker trucks of three different sizes are available (1,100kg, 2,000kg, and 3,500kg). The related fixed daily costs and variable operating costs are listed in Table 4.3. In both gaseous and liquid scenario, there are three sizes of stations with different refueling capacities (300 kg/d, 600 kg/d, and 1,100 kg/d). The related capital costs, operating costs, and resulting daily costs are shown in Table 4.4. It is assumed that, if the model chose to open a candidate station, the least refueling capacity that can cover the demand of that node should be selected.

Table 4.2: Hydrogen production

Parameter		Value		Source
Gaseous scenario				
Compressor capacity	kg H_2/d	14,000.00	21,000.00	(2)
Capital cost	million €	3.90	4.97	(1)
Operating cost	million €/y	0.40	0.54	(1)
Daily cost (pcc)	€/d	3,232.88	4,202.74	(2)
Liquid scenario				
Liquefier capacity	kg H_2/d	14,000.00	21,000.00	(2)
Capital cost	million €	51.00	66.87	(1)
Operating cost	million €/y	5.90	7.94	(1)
Daily cost (pcc)	€/d	44,109.59	58,394.52	(2)

(1) (Department of Energy, U.S., 2010)
(2) our choice

It is demonstrated through case study that the model proposed is capable to improve understanding of decision-makers about various components within the hydrogen supply network. Specifically, the role of fleet composition and delivery scenario are analyzed. In other words, the model is to answer questions like:

- Compared to a homogeneous fleet, whether a heterogeneous one can obtain a lower cost under the same coverage?
- Which scenario is more economical, gaseous or liquid?

Table 4.3: Hydrogen delivery

Parameter		Value	Source
Gaseous scenario			
Tube trailer capacity	kg H_2	300.00	(Weinert et al., 2007)
Tube trailer cost	million €	0.19	(Weinert et al., 2007)
Truck cost	1,000 €	75.00	(Weinert et al., 2007)
General expenses	€/d	7.22	(Almansoori et al., 2006)
Fixed daily cost (g^k)	€/d	152.43	
Liquid scenario			
Tanker truck capacity	kg H_2	3,500.00	(Amos, 1999)
Tanker truck cost	million €	0.31	(Amos, 1999)
Truck cab	1,000 €	79.00	(Amos, 1999)
Truck undercarriage	1,000 €	53.00	(Amos, 1999)
General expenses	€/d	7.22	(Almansoori et al., 2006)
Fixed daily cost (g^k)	€/d	249.41	
Variable Operating cost			
Fuel economy	km/L	2.55	(Amos, 1999)
Fuel price	€/L	1.46	(GlobalPetrolPrices, 2019)
Maintenance expense	€/km	0.086	(Almansoori et al., 2006)
Variable Operating cost	€/km	0.66	

Note: Because lack of information, the fixed daily costs of tube trailer with capacity of 600 and 1,100 kg are obtained by multiplying the value of the tube trailer with capacity of 300 with 1.8 and 3.24, respectively; the fixed daily costs of tanker truck with capacity of 600 and 300 kg are obtained by multiplying the value of the tanker truck with capacity of 3,500 with 0.56 and 0.31, respectively.

Table 4.4: Hydrogen refueling station

Parameter		Value			Source
Gaseous scenario					
Refueling capacity	kg H_2/d	300.00	600.00	1,100.00	(2)
Capital cost	million €	1.87	2.10	4.21	(1)
Operating cost	€/kg H_2	2.20	1.28	1.28	(1)
Daily cost (scc_s)	€/d	1,519.66	1,726.68	3,394.85	(2)
Liquid scenario					
Refueling capacity	kg H_2/d	300.00	600.00	1,100.00	(2)
Capital cost	million €	1.52	1.57	3.14	(1)
Operating cost	€/kg H_2	2.66	1.45	1.45	(1)
Daily cost (scc_s)	€/d	1,431.38	1,512.77	2,953.05	(2)

(1) (Department of Energy, U.S., 2010)
(2) our choice

- What are the differences in network configurations between the two delivery scenarios under the same coverage?

- In addition, whether the answers to the above questions are related to the size of the studied area?

To respond all these concerns, eight instances are generated based on different combinations of the studied area, delivery scenario, and fleet composition. Detailed information of each instance is listed in Table 4.5. It should be noted that Franche-Comté is a former administrative region which comprises 32 major cities (Tavaux included) of Region Bourgogne-Franche-Comté. Franche-Comté is therefore suitable to be adopted as a relatively small study area.

Table 4.5: Instances

Instance*	Quantity of candidate stations	Delivery scenario	Fleet composition (vehicle capacity * quantity)
FC-G-Ho	30	Gaseous	1100 *18
FC-G-He	30	Gaseous	300*9/600*9/1100*9
FC-L-Ho	30	Liquid	3500*7
FC-L-He	30	Liquid	1100*4/2000*4/3500*4
BFC-G-Ho	61	Gaseous	1100*28
BFC-G-He	61	Gaseous	300*15/600*15/1100*15
BFC-L-Ho	61	Liquid	3500*10
BFC-L-He	61	Liquid	1100*5/2000*5/3500*5

* Explanation for the name of instance X-Y-Z:
part X: equals FC (Franche-Comté) or BFC (Bourgogne-Franche-Comté);
part Y: equals G (Gaseous) or L (Liquid);
part Z: equals Ho (Homogeneous fleet) or He (Heterogeneous fleet).

4.6/ RESULTS AND DISCUSSION

4.6.1/ PARAMETERS TUNING

Each of the two proposed metaheuristics uses many parameters that should be initialized. Tuning parameters must be carefully done because it may have an important influence on the effectiveness and the efficiency of the search. Fixing the value of each parameter depends on the considered problem and the resolution time needed to solve this problem (El-Ghazali, 2009). Therefore, a simple tuning methodology is proposed to initialize the parameters. It must be noted that the proposed metaheuristics were coded in C++ on an Intel Core i7 with 2.60 GHz speed and 64 GB RAM. The proposed tuning technique involves testing many values for each parameter on the tested instance (which involve 120 OD pairs, 15 candidate gasoline stations, and four delivery vehicles with the same capacity). Each configuration was run 5 times. Then we compute the average gap between the obtained Pareto front after each run (generated by GA or ALNS) and the optimal one (generated using CPLEX). Finally the configurations, which give the best average gaps, are chosen (as shown in table 4.6). All preliminary experiments are accessible via this link: http://bit.ly/2SxDNM5.

Table 4.6: Parameters configurations

GA				ALNS		
Max_iter	Max_M	NBS	Max_pop	Nb_iter_max	W1	W2
150	12	50	100	150	1.3	0.9

4.6.2/ PERFORMANCE OF THE METAHEURISTIC APPROACHES

This section provides a synthesis of the whole results obtained which are detailed in appendix C (costs, coverage rates, CPU times, opened stations, routes...). The two proposed approaches were run on the 8 generated instances using the parameters configurations as discussed in subsection 4.6.1. As already mentioned, ALNS is an adaptive approach in which the score of each operator depends on their past performances. To illustrate this phenomenon, figure 4.12 gives the evolution of all probabilities over the iterations for instance FC-L-Ho. In this example, the score of "Add the most coverage route" operator increases significantly in the first iterations but then one can remark that it gives bad performances, which reflects a decreasing in its score. Concerning the destroy operators, it is clear that the "remove randomly a station" is the best one in the first iterations. Let us note that all the scores converge to zero because they cannot improve more the obtained solutions.

It is to note that this analysis cannot lead to a general conclusion on possible best destroy and repair operators. As can be seen through Fig. 4.12 and Fig. 4.13, the performance of the operators depends on the tested instance. Then it justifies to keep all the proposed operators, to efficiently tackle the various kinds of instances as well as to provide some diversity in the explored solutions of the search space.

Table 4.7 and 4.8 summarize the obtained results for each method. Table 4.7 gives the CPU time in seconds, and the number of non-dominated solutions (in the Pareto front). The average gap between the generated Pareto front by each approach and the one obtained using CPLEX is also reported. Indeed, for each solution (Coverage C1, Cost C2) obtained by one of the metaheuristics, our exact model implemented in CPLEX is run by adding a constraint that forces the coverage to be equal to C1. Then the gap between C2 and the cost founded by CPLEX is calculated. A time limit of two hours per solution is configured in CPLEX, if this time interval expired without finding the optimal cost, we take the last found (feasible) cost into account to compute the gap. Once each solution gap is found, an average gap can be then calculated for the whole front.

Firstly, it should be noted that the metaheuristics are always faster than CPLEX, which seems logical mainly because of the obligation for running CPLEX several times in order to generate the Pareto front. But as shown in table 4.7, it is clear that GA is faster than ALNS for all tested instances. This difference in time can be mainly remarked on big instances, where it can be up to several hours. But, the average gap of GA is bigger

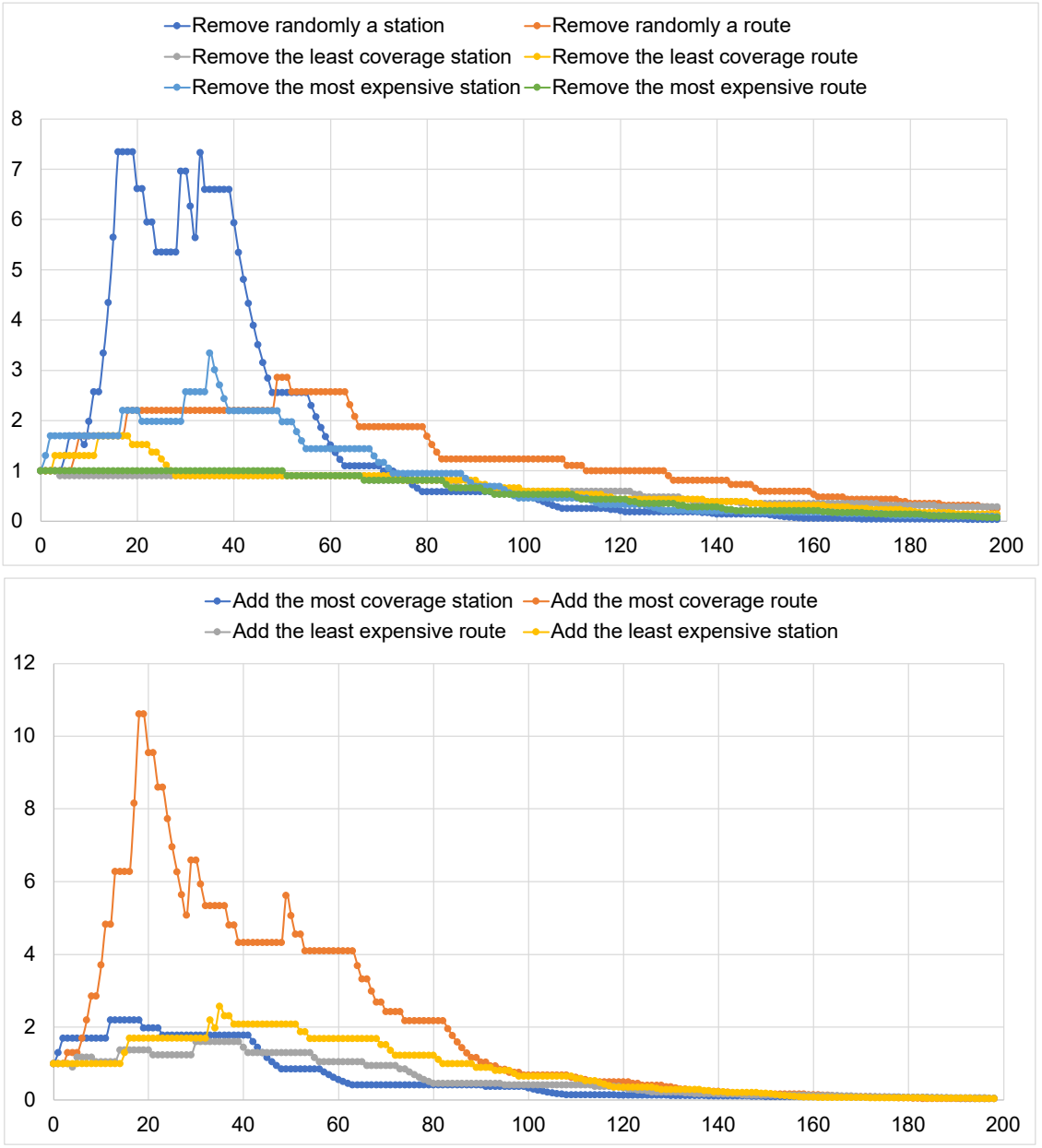

Figure 4.12: Example of scores evolution for instance FC-L-Ho

than the one of our ALNS one for all instances. This may be explained if we compare the number of solutions obtained by each metaheuristic. Indeed, GA generates more solutions than the ALNS approach, which increases the possibility of getting a solution with higher gap and therefore a higher average gap. Two main reasons may be behind this difference in the number of obtained solutions. Firstly, 39 random and 11 greedy chromosomes are generated in the initial population of the GA. A number of these initial chromosomes may survive and compose a part of the final solutions. Secondly, the random aspect in the selection procedure (see 4.4.2.4) may help to diversify the research procedure and then to find more solutions. On the contrary, the selection of solution at

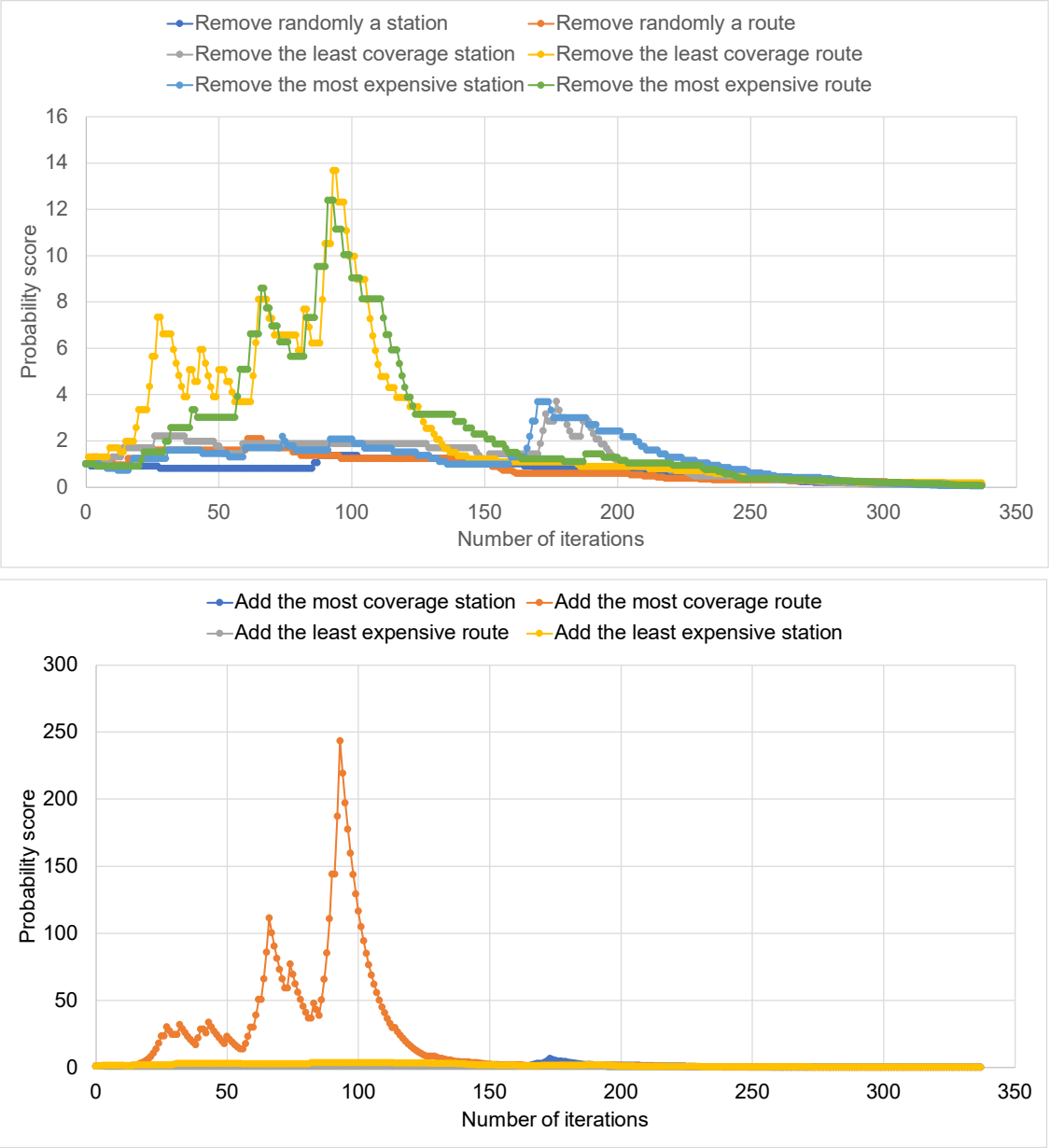

Figure 4.13: Example of scores evolution for instance BFC-L-He

each iteration in ALNS is based on a fixed criterion (see 4.4.1.2).

Moreover, an important aspect in comparing two multi-objectives approaches is by studying the distribution of the obtained solutions over the Pareto front. Table 4.8 gives for each instance: the minimal and maximal coverages obtained with each approach. In addition, it illustrates the maximum difference “Max dif” in terms of coverage between two adjacent solutions (in terms of coverage rates). This last value may be helpful to understand more how the solutions are distributed. Indeed, a smaller value reflects a more complete distribution. Let us note that in the “Min” column, the minimal coverage different from zero is reported.

Table 4.7: Performance of the two proposed approaches

Instance	ALNS			GA		
	CPU time (s)	Nb of solutions*	average gap (%)	CPU time (s)	Nb of solutions	average gap** (%)
FC-G-Ho	2,472	4	2.25	225	19	13.83
FC-G-He	2,145	4	2.59	259	20	11.41
FC-L-Ho	1,122	17	3.55	353	22	5.18
FC-L-He	1,577	20	3.54	261	23	6.74
BFC-G-Ho	21,193	13	8.36	1,582	29	20.51
BFC-G-He	19,435	6	6.14	1,811	19	14.38
BFC-L-Ho	28,764	13	2.49	1,399	20	9.49
BFC-L-He	7,026	12	3.28	1,379	23	7.43

* *number of non dominated solutions (Pareto front)*
** *average gap in terms of costs obtained with CPLEX for the same coverage rates*

Table 4.8: The distribution of the obtained solutions

Instance	ALNS			GA		
	Min	Max	Max dif	Min	Max	Max dif
FC-G-Ho	24.21	68.57	24.21	13.64	100.00	16.21
FC-G-He	24.21	68.57	24.21	13.64	100.00	13.64
FC-L-Ho	47.09	100.00	47.09	8.77	100.00	14.83
FC-L-He	24.21	100.00	24.20	13.64	100.00	22.88
BFC-G-Ho	3.03	68.43	13.68	6.40	100.00	13.60
BFC-G-He	3.03	68.43	27.41	6.40	100.00	15.79
BFC-L-Ho	41.02	90.73	41.02	9.88	100.00	15.79
BFC-L-He	41.02	89.12	41.02	6.39	100.00	11.80

Table 4.8 shows that GA outperforms ALNS regarding the distribution of solutions, because the interval of coverages [Min coverage, Max coverage] is larger using GA for all tested instances. In addition, the Max-dif per instance is always smaller than the one obtained using ALNS. An example for the application of two approaches on the instance "FC-L-Ho" is illustrated in figure 4.14.

Finally, the two proposed approaches have their advantages and limitations. On the one hand, ALNS is characterized by a better average gap comparing to GA. On the other hand, GA outperforms ALNS in terms of solving time and number of solutions. In addition, GA gives a better distribution of solutions compared with ALNS.

4.6.3/ MANAGERIAL INSIGHTS

In this part, the questions raised in Section 4.5 are replied based on instance results. To facilitate our analysis, three representative levels of coverage are chosen to compare results for different instances: low, medium, and high coverage which correspond to approximate 10%, 50%, and 90% of hydrogen demand flow captured.

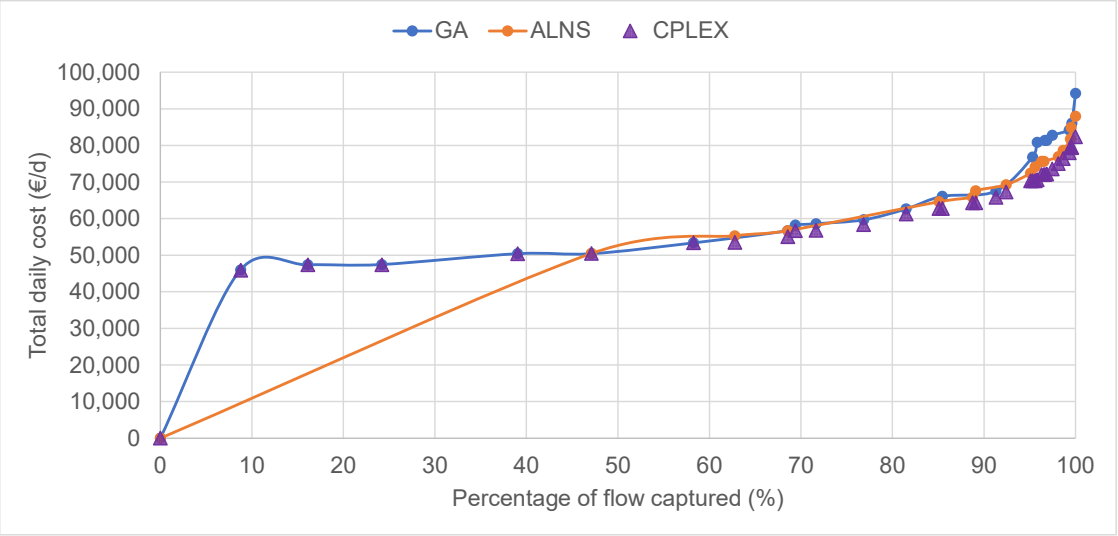

Figure 4.14: Example of obtained solutions for instance “FC-L-Ho”

4.6.3.1/ ROLE OF FLEET COMPOSITION

Overall, a heterogeneous fleet has almost the same performance as a homogeneous one in the case study. As shown in Fig. 4.15 - (a), FC-G-He obtains the same total daily cost as FC-G-Ho for medium and high coverage. Only for low coverage, FC-G-He reaches a cost value slightly lower than that of FC-G-Ho. Both FC-G-Ho and FC-G-He choose to open a candidate station at Poligny and Saint-Vit to obtain the coverage value of 16.12%. The difference is that FC-G-Ho adopts a single tube trailer with capacity of 1,100 kg, and FC-G-He employs one vehicle with capacity of 300 kg and another of 600 kg. Fig. 4.15 - (b) illustrates that in liquid delivery scenario, the heterogeneous fleet has the same cost value as the homogeneous one for high coverage, and slightly lower values for low and medium coverages. The configuration differences between FC-L-Ho and FC-L-He with 47.09% coverage are detailed in Fig. 4.15 - (c). For the larger studied area (that of Bourgogne Franche-Comté), similar results are obtained. Therefore a conclusion can be drawn that, in the regional level, a heterogeneous fleet cannot obtain much better economic performance than a homogeneous one. Only in low and medium levels of coverage can a heterogeneous fleet find a slightly cheaper solution. Taking into account the convenience of management, decision-makers are recommended to adopt the homogeneous fleet in the regional level deployment of hydrogen supply network. It is important to note that this conclusion is based on the assumptions that multi-visit is not allowed (an opened station can be visited by only one delivery vehicle).

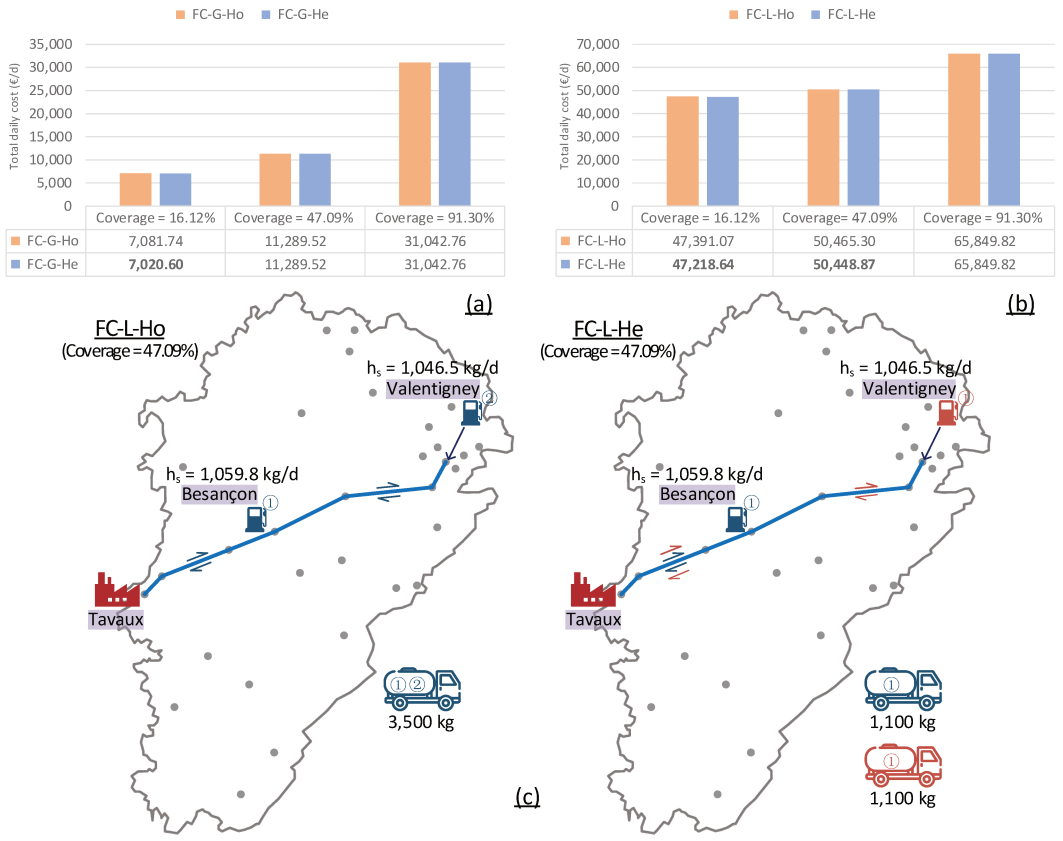

Figure 4.15: Cost values and configurations of Franche-Comté instances: (a) cost values of FC-G-Ho and FC-G-He; (b) cost values of FC-L-Ho and FC-L-He; (c) configuration of FC-L-Ho and FC-L-He with 47.09% coverage

4.6.3.2/ ROLE OF PHYSICAL FORMS OF HYDROGEN

Since it is already found that there is no great difference between heterogeneous and homogeneous fleet instances, here only homogeneous fleet instances in different physical forms of hydrogen are analyzed. In general, a gaseous scenario is more economical than a liquid scenario for all levels of coverage for both Franche-Comté and Bourgogne Franche-Comté, as shown by the column charts in Fig. 4.16. The high cost of liquid delivery scenario is due to the need of liquefaction devices, which incurs a high capital cost. Moreover, liquefaction requires a large amount of power consumption, increasing operating cost. It is also due to one of model's assumptions that the production capacity of the hydrogen plant should be sufficient even when all candidate stations are opened. We can notice that the gap between the total daily cost of gaseous and liquid scenario is shrinking when the coverage rises.

If we divide the total daily cost by the daily hydrogen demand, we obtain the least cost of hydrogen (LCOH). Using the LCOH as an indicator, it is more obvious that the gap between gaseous and liquid is narrower for higher levels of coverage, as shown by the

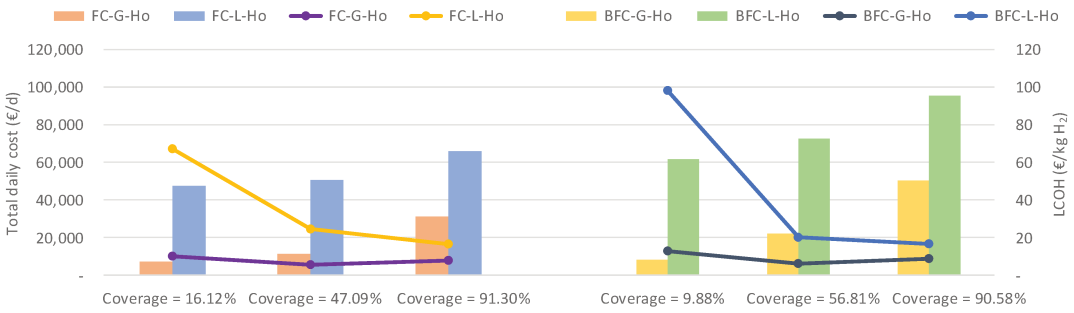

Figure 4.16: Cost values for homogeneous fleet instances

line charts in Fig. 4.16. This can be explained by the advantage of liquid hydrogen in transportation. The number of vehicles required to transport the same amount of liquid hydrogen is smaller than for gaseous hydrogen because the capacity of a tanker trucker is 3 times as large as a tube trailer in the case study. The supply network is more dependent on hydrogen transportation when coverage rises and therefore the advantage in transportation of liquid scenario narrows the cost gap with gaseous scenario. Even if the same trend of results are found in the two studied areas, a small difference is worth being noted: the gaps of LCOH between gaseous and liquid scenario are smaller for medium and high coverage for Bourgogne-Franche-Comté than for Franche-Comté. This can also be explained by the advantage of liquid hydrogen in transportation, since Bourgogne-Franche-Comté is two times as large as Franche-Comté. Therefore such an advantage is more obvious as the distance of hydrogen transportation increases. It can be estimated that the liquid delivery scenario may be economical and attractive when the supply network covers a larger area and when the hydrogen refueling demand increases.

Two representative examples are presented to illustrate the differences in network configurations between gaseous and liquid scenarios for the same level of coverage. Fig. 4.17 shows that, for the same coverage (91.30%), FC-G-Ho and FC-L-Ho both have the same number of opened stations and locations. The former uses six tube trailers with capacity of 1,100 kg and the latter adopts two tanker truck with capacity of 3,500 kg. Due to the capacity limit, a tube trailer can satisfy only one or two stations with high refueling demand. A tanker truck, on the other side, is capable to supply five stations. For the coverage of 56.81%, the network configurations of BFC-G-Ho and BFC-L-Ho show more differences. As shown in Fig. 4.18 - (a), BFC-G-Ho has eight opened stations and BFC-L-Ho has only six. It is reasonable that the model tries to make the best use of each vehicle's capacity by supplying as many stations as possible to increase the value of coverage. A tube trailer has only 1,100 kg of capacity, it can supply one station with high demand or several (2-3) stations with relatively low demand. It turns out that BFC-G-Ho selects the latter strategy. For the liquid scenario, a tanker truck could satisfy several stations with high demand due

to its large capacity. Consequently, BFC-L-Ho opens several stations with high demand (e.g., Dijon, Besançon, and Valentigney), and achieved the same coverage as BFC-G-Ho with fewer opened stations. Although the two instances have the same value of coverage, they actually have different displays in the captured hydrogen refueling demand flow network, as described in Fig. 4.18 - (b). This kind of figure could provide a visual representation of the captured hydrogen refueling demand flow, and therefore increase the understanding of decision-makers about the model results.

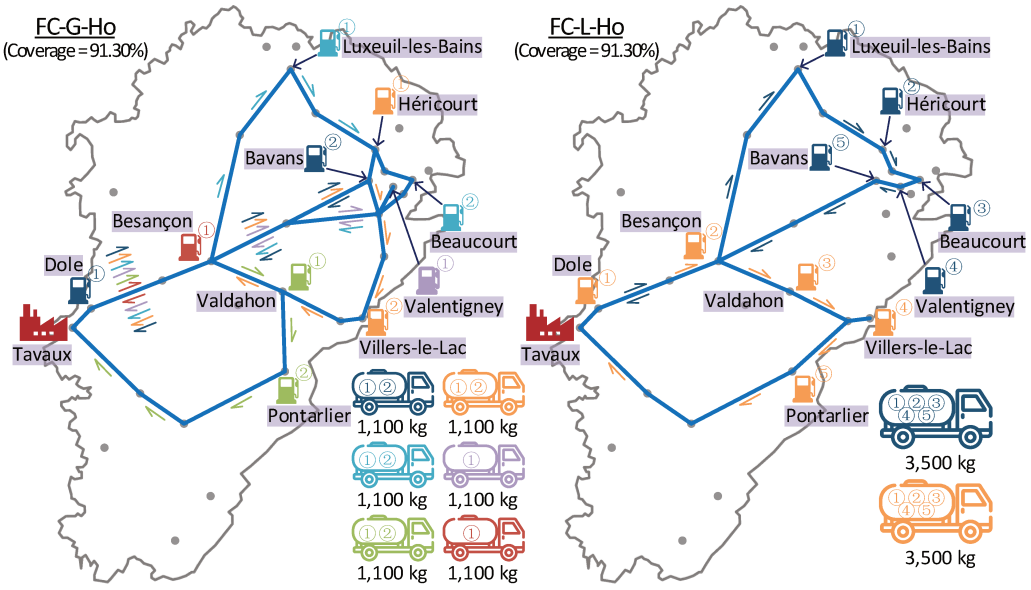

Figure 4.17: Configuration of FC-G-Ho and FC-L-Ho with 91.30% coverage

4.7/ CONCLUSIONS

In this chapter, the intertemporal integration planning of HSCND, a location routing approach, was presented. The proposed model enabled us to determine a hydrogen supply network configuration, which satisfies the refueling demand of FCEVs, while maximizing the flow coverage and minimizing the total daily cost. Two metaheuristic algorithms, ALNS and GA, were developed to solve this model. Results of the model and performances of the metaheuristic approaches were discussed for two real case studies (Franche-Comté and Bourgogne-Franche-Comté, France), through eight instances generated based on different combinations of study area, delivery scenario, and fleet composition. It has been found that GA is faster than ALNS for all tested instances, though ALNS is characterized by a better average gap in terms of cost, compared with the optimal solutions provided by our exact model. It is also worth noting that GA provides more non dominated solutions and a better distribution of them. Managerial insights regarding the role of fleet

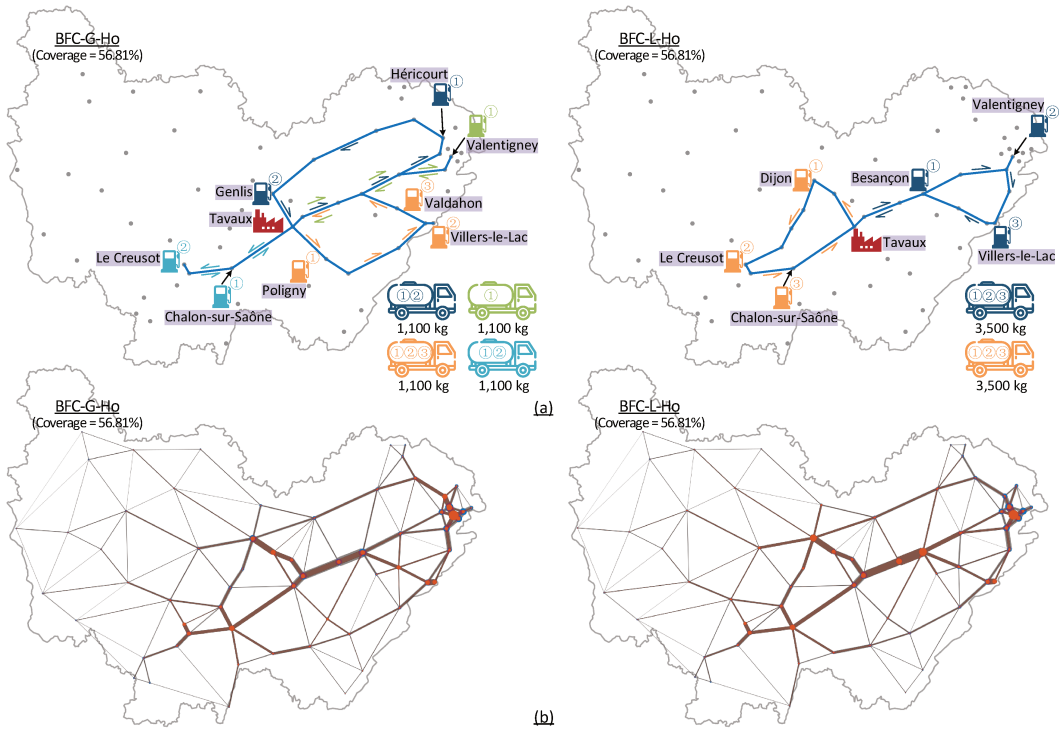

Figure 4.18: Configuration and captured hydrogen refueling demand flow of BFC-G-Ho and BFC-L-Ho with 56.81% coverage: (a) network configuration; (b) captured hydrogen refueling demand flow

composition and physical forms of hydrogen were also derived. At a regional level, a heterogeneous fleet cannot obtain much better economic performance than a homogeneous one. Only for low and medium levels of coverage can a heterogeneous fleet find a slightly cheaper solution. In general, a gaseous scenario is more economical than a liquid scenario for all levels of coverage for both Franche-Comté and Bourgogne-Franche-Comté. However, it can be estimated that the liquid delivery scenario may be economical and attractive when the supply network covers a larger area and when the hydrogen refueling demand increases.

These first results and analyses are very encouraging as they show that our model and algorithms can successfully address the both HRSP and VRP problems identified respectively at strategic and tactical levels. Of course, extensions should deserve to be envisaged in future works to consider more general problems (for example with several production plants) as well as other optimization methods.

III

CONCLUSION

5

GENERAL CONCLUSION

5.1/ SYNTHESIS OF THE PHD THESIS CONTRIBUTIONS

As an energy carrier, hydrogen is thought to bring viable, financially attractive, and socially beneficial answers to the challenges to transitioning towards low-carbon form of energy, and improving air quality in cities. Its putative success relies not only on breakthroughs in key technologies (such as fuel cells), but also on holistic designs that take various factors into account. The modeling of supply chain network based on mathematical programming methods is becoming one of the primary approaches in the design of hydrogen and other energy supply chains. Optimization models, of which the main representative is the mixed-integer linear programming model, can give rise to optimal solutions through operations research methods, while at the same time taking into account numerous constraints.

The main objective of the thesis was to promote the hydrogen infrastructure deployment by providing new strategies based on optimization approaches. To this end, firstly an overview of the research development regarding the use of optimization methods for the HSCND has been presented. The deep analysis and classification conducted in chapter 3 have allowed us to identify in particular two primary research gaps: the lack of a comprehensive optimization model which covers entire HSCN (from feedstock supply to refueling stations), and the lack of the integration of activities over strategic, tactical, and operational planning horizons. Then the classical HSCND model has been extended by intercomponent and intertemporal integration plannings, respectively in chapters 3 and 4.

Chapter 3 has filled the first gap by addressing the intercomponent integration planning of HSCND. The classical hydrogen supply chain network design (HSCND) model was integrated with the hydrogen refueling station planning (HRSP) model to generate a new formulation in the form of a MILP model. This one aims at solving the “chicken-and-egg” dilemma by coordinating the roll-out of hydrogen vehicles and infrastructure development. A construction plan could be drawn through solving the model to determine: the hydrogen demand distribution, the type of feedstock and technology to produce hydrogen, the fu-

eling technology (standard or on-site), the number, size and location of production plants and refueling stations, and the most suitable types of transportation (for hydrogen and for feedstock). One of the advantages of the intercomponent integration planning is its ability to investigate the interaction among HSCN components. This ability was demonstrated through the case study of Franche-Comté, France, derived in 66 instances that we have generated.

Chapter 4 has dealt with the second research gap by introducing an intertemporal integration planning of HSCND. A particular variant of location routing problem (LRP) was solved to determine simultaneously the siting of hydrogen refueling stations (HRSs) and the routing decisions for hydrogen delivery trucks. The developed exact model provides the solution to overcome the two primary barriers of deployment of HRSs: land requirements and hydrogen sources, under some assumptions about existing stations and the source of delivered hydrogen. Considering a bi-objective approach led us to develop two metaheuristic solving algorithms based on Adaptive Large Neigborhood Search (ALNS) and Genetic Algorithm (GA). Our model and algorithms were evaluated and compared through 8 instances that we have generated, representing the region Bourgogne-Franche-Comté, France. Managerial insights regarding the role of fleet composition and physical forms of hydrogen were derived. Decision-makers were also recommended to adopt the homogeneous fleet in regional level deployment of hydrogen supply network. Besides, the liquid delivery scenario becomes interesting for high levels of hydrogen demand and coverage and for a larger region.

5.2/ PERSPECTIVES

Numerous perspectives may be suggested to improve and extend the proposed work. Among them, the following ones seem particularly attractive to us.

Obviously, in the point of view of the optimization tools, we could improve the solving of the two dealt problems, for example by elaborating metaheuristic approaches dedicated to the HSCND, in particular to solve larger size instances and to optimize several objectives in addition to the LCOH. The metaheuristic algorithms already developed for the second problem (LRP) may also be improved, both in terms of efficiency and to deal with extended problems, like the one considering more than one production plant. This one would amount to considering another variant of LRP (with several origin depots to assign and several destination sites (HRSs) to select).

In the point of view of the considered application of supply chain design, we would like to find other real life instances. But we have realized that it is not so easy as we already spent much time to collect the necessary data on the Bourgogne Franche-Comté

region. Nevertheless this approach seems essential to us to test the limits of our models and methods. We have already been able to do this on an instance in the Ile de France region for which the resolution of the intertemporal integration planning problem has been complicated (instance with 28,920 OD pairs, 240 candidate stations, and 93 delivery vehicles, compared to instance Bourgogne Franche-Comté with 1,891 OD pairs, 61 candidate stations, and 45 delivery vehicles). This makes all the more important to improve our optimization methods, so as to give them a good scalability.

To complete our work and to show even more the interest of the two planning models which we proposed, we should confirm their interaction and their potential exploitation by applying them in a sequential and interactive way, as in the loop procedure illustrated by the Fig. 4.1.

We could also consider the evolution of the HSCN over time, rather than a snapshot of the network at one point in time. In real-world conditions, the formation of the hydrogen energy market and the construction of the hydrogen energy supply network usually span decades. The hydrogen fueling demand will probably increase gradually over the time. Therefore the construction plan of the HSCN should be designed in stages corresponding to successive periods. In fact we have already extended our HSCND model to deal with this new problem. The idea is that, at each period T, the model is run with a given objective for this period, while considering the decisions taken in the previous periods as constraints (hydrogen sources, opened HRS,...). Fig. 5.1 illustrates the kind of results we have obtained for the Franche-Comté region, with a 10-year projection cut into 5 periods

Another perspective would be to consider the interactions between the hydrogen supply (hydrogen facilities) and demand (FCEV potential buyers). In the present study, the hydrogen fueling demand flow is pre-defined, and it will not be impacted by the hydrogen supply system. The influence of the hydrogen supply on demand has been ignored. The model will be improved by converting the hydrogen demand from model input to a decision variable to endogenously forecast hydrogen demand while optimizing the hydrogen supply network.

The emergency to confront with climate change calls for sustainable supply chain design. We have already worked on this issue, trying to involve the life cycle assessment (LCA) into HSCND. Specifically, we made proposals about how to perform life cycle costing (LCC) and life cycle inventory (LCI) analysis for HSCND models. The next step will be to integrate these approaches into our main model, and to evaluate the influence of sustainable performance measures on the configuration of HSCN.

Another aspect that requires more attention is the uncertainty. Uncertainty sources, such as government incentives and policies, technology evolution, capital cost, as well as the operational uncertainties are ignored in previous HSCND models. Concerning uncertainty types and modeling approaches, the inclusion of epistemic uncertainty, deep un-

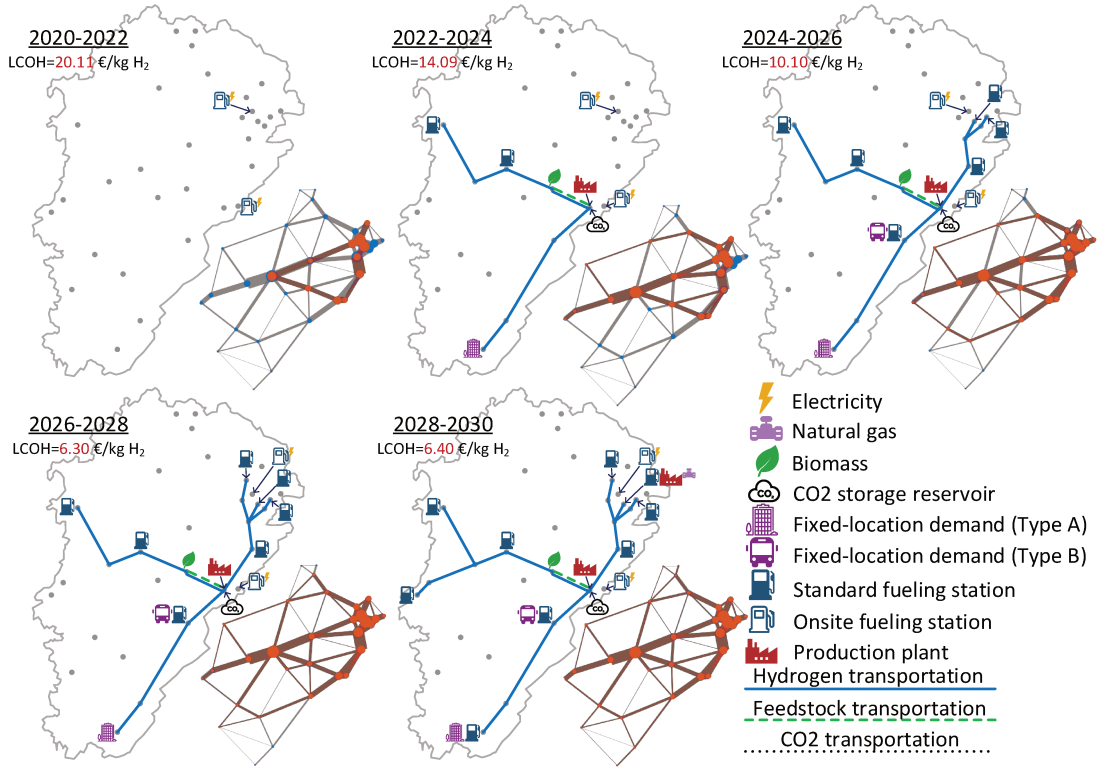

Figure 5.1: The multi-period (2020-2030) construction plan of HSCN for Franche-Comté (High carbon price scenario)

certainty, and corresponding modeling approaches, particularly robust optimization, is a future direction to improve our present work.

Finally a hydrogen supply system is not isolated; it is an integral part of the entire energy system. A broader perspective may offer more suitable solutions. Its integration with other supply chains is another important research direction. The critical factor for such an integration is to identify the appropriate “insertion points” through which two supply chains are connected. For the HSCN, such “insertion points” are not difficult to identified. Several previous studies could serve as good examples. In the work of Cho et al. (2016); Parker et al. (2010), and Woo et al. (2016), the modeling and optimization of a HSCN is conducted with a biomass supply chain. Kim et al. (2017) discussed the integration of a HSCN with a wind power generation system. In the work of Hwangbo et al. (2017), the HSCN was associated with a utility supply network, and the SMR process was used as a linkage (insertion point) between the two networks. Furthermore, Biqué et al. (2018b) developed an MILP model for the integration of hydrogen and CO_2 supply chains, and the production of methanol links the two networks together. Beyond that, other feedstocks (e.g., electricity from solar energy or nuclear energy), byproducts (e.g., oxygen from electrolysis), and final products (hydrogen for other uses, e.g., industry or “Power to Gas” project (Welder et al., 2018)) could serve as “insertion points” to conduct

more integrations. Therefore, there remain several areas for integrating present HSCND modeling work with other networks and systems.

BIBLIOGRAPHY

Abbasi, T., et Abbasi, S. (2011). **'Renewable' hydrogen: Prospects and challenges**. *Renewable and Sustainable Energy Reviews*, 15(6):3034–3040.

Achtnicht, M., Bühler, G., et Hermeling, C. (2012). **The impact of fuel availability on demand for alternative-fuel vehicles**. *Transportation Research Part D: Transport and Environment*, 17:262–269.

Agnolucci, P., Akgul, O., McDowall, W., et Papageorgiou, L. G. (2013a). **The importance of economies of scale, transport costs and demand patterns in optimising hydrogen fuelling infrastructure: An exploration with shipmod (spatial hydrogen infrastructure planning model)**. *International Journal of Hydrogen Energy*, 38(26):11189–11201.

Agnolucci, P., et McDowall, W. (2013b). **Designing future hydrogen infrastructure: Insights from analysis at different spatial scales**. *International Journal of Hydrogen Energy*, 38(13):5181–5191.

Ahn, J., De Weck, O., Geng, Y., et Klabjan, D. (2012). **Column generation based heuristics for a generalized location routing problem with profits arising in space exploration**. *European Journal of Operational Research*, 223(1):47–59.

Alazemi, J., et Andrews, J. (2015). **Automotive hydrogen fuelling stations: An international review**. *Renewable and Sustainable Energy Reviews*, 48:483–499.

Almansoori, A., et Betancourt-Torcat, A. (2016). **Design of optimization model for a hydrogen supply chain under emission constraints-A case study of Germany**. *Energy*, 111:414–429.

Almansoori, A., et Shah, N. (2006). **Design and operation of a future hydrogen supply chain: Snapshot model**. *Chemical Engineering Research and Design*, 84(6):423–438.

Almansoori, A., et Shah, N. (2009). **Design and operation of a future hydrogen supply chain: Multi-period model**. *International Journal of Hydrogen Energy*, 34(19):7883–7897.

Almansoori, A., et Shah, N. (2012). **Design and operation of a stochastic hydrogen supply chain network under demand uncertainty**. *International Journal of Hydrogen Energy*, 37(5):3965–3977.

Almaraz, S. D.-L., Azzaro-Pantel, C., Montastruc, L., et Boix, M. (2015). **Deployment of a hydrogen supply chain by multi-objective/multi-period optimisation at regional and national scales**. *Chemical Engineering Research and Design*, 104:11–31.

Almaraz, S. D.-L., Azzaro-Pantel, C., Montastruc, L., et Domenech, S. (2014). **Hydrogen supply chain optimization for deployment scenarios in the Midi-Pyrénées region, France**. *International Journal of Hydrogen Energy*, 39(23):11831–11845.

Almaraz, S. D.-L., Azzaro-Pantel, C., Montastruc, L., Pibouleau, L., et Senties, O. B. (2013). **Assessment of mono and multi-objective optimization to design a hydrogen supply chain**. *International Journal of Hydrogen Energy*, 38(33):14121–14145.

Amiri, A. (2006). **Designing a distribution network in a supply chain system: Formulation and efficient solution procedure**. *European Journal of Operational Research*, 171(2):567–576.

Amoo, L. M., et Fagbenle, R. L. (2014). **An integrated impact assessment of hydrogen as a future energy carrier in Nigeria's transportation, energy and power sectors**. *International Journal of Hydrogen Energy*, 39(24):12409–12433.

Amos, W. A. (1999). **Costs of storing and transporting hydrogen**. Technical Report, National Renewable Energy Laboratory, U.S.

André, J., Auray, S., Brac, J., De Wolf, D., Maisonnier, G., Ould-Sidi, M.-M., et Simonnet, A. (2013). **Design and dimensioning of hydrogen transmission pipeline networks**. *European Journal of Operational Research*, 229(1):239–251.

André, J., Auray, S., De Wolf, D., Memmah, M.-M., et Simonnet, A. (2014). **Time development of new hydrogen transmission pipeline networks for France**. *International Journal of Hydrogen Energy*, 39(20):10323–10337.

Arslan, O., et Karaşan, O. E. (2016). **A Benders decomposition approach for the charging station location problem with plug-in hybrid electric vehicles**. *Transportation Research Part B: Methodological*, 93:1339–1351.

Association de préfiguration de l'Institut de stockage de l'hydrogène (2019). **Grand Dole - Cluster hydrogène**. Accessed: 27 December 2019.

Bairamzadeh, S., Saidi-Mehrabad, M., et Pishvaee, M. S. (2018). **Modelling different types of uncertainty in biofuel supply network design and planning: A robust optimization approach**. *Renewable Energy*, 116:500–517.

Ball, M., Wietschel, M., et Rentz, O. (2007). **Integration of a hydrogen economy into the German energy system: An optimising modelling approach**. *International Journal of Hydrogen Energy*, 32(10):1355–1368.

Balta-Ozkan, N., et Baldwin, E. (2013). **Spatial development of hydrogen economy in a low-carbon UK energy system**. *International Journal of Hydrogen Energy*, 38(3):1209–1224.

Banos, R., Manzano-Agugliaro, F., Montoya, F., Gil, C., Alcayde, A., et Gómez, J. (2011). **Optimization methods applied to renewable and sustainable energy: A review**. *Renewable and Sustainable Energy Reviews*, 15(4):1753–1766.

Baufumé, S., Hake, J.-F., Linssen, J., et Markewitz, P. (2011). **Carbon capture and storage: A possible bridge to a future hydrogen infrastructure for Germany?** *International Journal of Hydrogen Energy*, 36(15):8809–8821.

Berman, O., Bertsimas, D., et Larson, R. C. (1995). **Locating discretionary service facilities II: Maximizing market size, minimizing inconvenience**. *Operations Research*, 43:623–632.

Berman, O., Larson, R. C., et Fouska, N. (1992). **Optimal location of discretionary service facilities**. *Transportation Science*, 26:201–211.

Bersani, C., Minciardi, R., Sacile, R., et Trasforini, E. (2009). **Network planning of fuelling service stations in a near-term competitive scenario of the hydrogen economy**. *Socio-Economic Planning Sciences*, 43(1):55–71.

Biqué, A. O., Maia, L. K., La Mantia, F., Manca, D., et Zondervan, E. (2018a). **Balancing costs, safety and CO_2 emissions in the design of hydrogen supply chains**. In *Computer Aided Chemical Engineering*, volume 43, pages 603–608. Elsevier.

Biqué, A. O., Nguyen, T. B., Leonzio, G., Galanopoulos, C., et Zondervan, E. (2018b). **Integration of carbon dioxide and hydrogen supply chains**. In *Computer Aided Chemical Engineering*, volume 43, pages 1413–1418. Elsevier.

Biqué, A. O., et Zondervan, E. (2018c). **An outlook towards hydrogen supply chain networks in 2050—Design of novel fuel infrastructures in Germany**. *Chemical Engineering Research and Design*, 134:90–103.

Brey, J., Brey, R., Carazo, A., Contreras, I., Hernandez-Diaz, A., et Gallardo, V. (2006). **Designing a gradual transition to a hydrogen economy in Spain**. *Journal of Power Sources*, 159(2):1231–1240.

Brey, J., Carazo, A., et Brey, R. (2012). **Using AHP and binary integer programming to optimize the initial distribution of hydrogen infrastructures in Andalusia**. *International Journal of hydrogen energy*, 37(6):5372–5384.

Brown, T., Schell, L. S., Stephens-Romero, S., et Samuelsen, S. (2013). **Economic analysis of near-term California hydrogen infrastructure**. *International Journal of Hydrogen Energy*, 38(10):3846–3857.

Brugier, C., et Langevin, A. W. (2017). **New "Hydrogen Council" launches in Davos — Air Liquide**. Accessed: 26 December 2019.

California Air Resources Board (2018). **2018 Annual evaluation of fuel cell electric vehicle deployment and hydrogen fuel station network development**. Technical Report, California Environmental Protection Agency.

Cany, C., Mansilla, C., da Costa, P., et Mathonnière, G. (2017). **Adapting the French nuclear fleet to integrate variable renewable energies via the production of hydrogen: Towards massive production of low carbon hydrogen?** *International Journal of Hydrogen Energy*, 42(19):13339–13356.

Carbon Tracker (2018). **EU carbon prices could double by 2021 and quadruple by 2030**. Accessed: 26 December 2019.

Carsalesbase (2018). **Automotive industry analysis, opinions and data**. Accessed: 26 December 2019.

Chattanathan, S. A., Adhikari, S., et Abdoulmoumine, N. (2012). **A review on current status of hydrogen production from bio-oil**. *Renewable and Sustainable Energy Reviews*, 16(5):2366–2372.

Chestney, N. (2018). **European Union carbon prices climb to 10-year high**. Accessed: 26 December 2019.

Cho, S., Woo, Y.-b., Kim, B. S., et Kim, J. (2016). **Optimization-based planning of a biomass to hydrogen (B2H2) system using dedicated energy crops and waste biomass**. *Biomass and Bioenergy*, 87:144–155.

Contaldi, M., Gracceva, F., et Mattucci, A. (2008). **Hydrogen perspectives in Italy: Analysis of possible deployment scenarios**. *International Journal of Hydrogen Energy*, 33(6):1630–1642.

Contreras, A., Guervós, E., et Posso, F. (2009). **Market penetration analysis of the use of hydrogen in the road transport sector of the Madrid region, using MARKAL**. *International Journal of Hydrogen Energy*, 34(1):13–20.

Copado-Méndez, P. J., Blum, C., Guillén-Gosálbez, G., et Jiménez, L. (2013). **Large neighbourhood search applied to the efficient solution of spatially explicit strategic supply chain management problems**. *Computers & Chemical Engineering*, 49:114–126.

Cruz-Zambrano, M., Corchero, C., Igualada-Gonzalez, L., et Bernardo, V. (2013). **Optimal location of fast charging stations in Barcelona: A flow-capturing approach**. In *International Conference on the European Energy Market, EEM*, pages 1–6. IEEE.

Dagdougui, H. (2012). **Models, methods and approaches for the planning and design of the future hydrogen supply chain**. *International Journal of Hydrogen Energy*, 37(6):5318–5327.

Dagdougui, H., Ouammi, A., et Sacile, R. (2012). **Modelling and control of hydrogen and energy flows in a network of green hydrogen refuelling stations powered by mixed renewable energy systems**. *International Journal of Hydrogen Energy*, 37(6):5360–5371.

Daskin, M. S., Snyder, L. V., et Berger, R. T. (2005). **Facility location in supply chain design**. In *Logistics systems: Design and optimization*, pages 39–65. Springer.

Dayhim, M., Jafari, M. A., et Mazurek, M. (2014). **Planning sustainable hydrogen supply chain infrastructure with uncertain demand**. *International Journal of Hydrogen Energy*, 39(13):6789–6801.

De Meyer, A., Cattrysse, D., Rasinmäki, J., et Van Orshoven, J. (2014). **Methods to optimise the design and management of biomass-for-bioenergy supply chains: A review**. *Renewable and Sustainable Energy Reviews*, 31:657–670.

De Vries, H., et Duijzer, E. (2017). **Incorporating driving range variability in network design for refueling facilities**. *Omega*, 69:102–114.

Deb, K., Pratap, A., Agarwal, S., et Meyarivan, T. (2002). **A fast and elitist multiobjective genetic algorithm: NSGA-II**. *IEEE transactions on evolutionary computation*, 6(2):182–197.

Department of Energy, U.S. (2010). **H2A: Delivery components model version 2.0**. Accessed: 26 December 2019.

Department of Energy, U.S. (2018a). **Alternative fuels data center**. Accessed: 26 December 2019.

Department of Energy, U.S. (2018b). **H2A: Hydrogen analysis production case studies - future central hydrogen production via biomass gasification version 3.2018**. Accessed: 26 December 2019.

Department of Energy, U.S. (2018c). **H2A: Hydrogen analysis production case studies - future distributed hydrogen production from natural gas (1,500 kg per day) version 3.2018**. Accessed: 26 December 2019.

Department of Energy, U.S. (2018d). **H2A: Hydrogen analysis production case studies - future distributed hydrogen production from PEM electrolysis version 3.2018**. Accessed: 26 December 2019.

Dincer, I., et Acar, C. (2015). **Review and evaluation of hydrogen production methods for better sustainability**. *International Journal of Hydrogen Energy*, 40(34):11094–11111.

Diwekar, U. (2008). **Introduction to applied optimization**, volume 22. Springer Science & Business Media.

Dominković, D., Bačeković, I., Pedersen, A. S., et Krajačić, G. (2017). **The future of transportation in sustainable energy systems: Opportunities and barriers in a clean energy transition**. *Renewable and Sustainable Energy Reviews*.

Doulabi, S. H. H., et Seifi, A. (2013). **Lower and upper bounds for location-arc routing problems with vehicle capacity constraints**. *European Journal of Operational Research*, 224(1):189–208.

Drexl, M., et Schneider, M. (2015). **A survey of variants and extensions of the location-routing problem**. *European Journal of Operational Research*, 241(2):283–308.

El-Ghazali, T. (2009). **Metaheuristics: From design to implementation**. John Wiley & Sons.

Électricité de France (2018). **Emissions de gaz à effet de serre : Le relevé mensuel d'EDF**. Accessed: 26 December 2019.

Elgowainy, A., Krishna, R., Mintz, M., et Brown, D. (2015). **H2A delivery scenario analysis model version 3.0 (HDSAM 3.0) user's manual**. Technical Report, Argonne National Laboratory, Pacific Northwest National Laboratory, U.S.

Endo, E. (2007). **Market penetration analysis of fuel cell vehicles in Japan by using the energy system model MARKAL**. *International Journal of Hydrogen Energy*, 32(10):1347–1354.

Environmental Protection Agency, U.S. (2018). **Fast Facts: U.S. transportation sector GHG emissions (1990-2016)**. Technical Report, Environmental Protection Agency, U.S.

Eppen, G. D., Martin, R. K., et Schrage, L. (1989). **OR practice—a scenario approach to capacity planning**. *Operations Research*, 37(4):517–527.

Eskandarpour, M., Dejax, P., Miemczyk, J., et Péton, O. (2015). **Sustainable supply chain network design: An optimization-oriented review**. *Omega*, 54:11–32.

European Environment Agency (2017). **Greenhouse gas emissions from transport**. Technical Report, European Environment Agency.

European Research Area (2015). **HyWays, The European hydrogen roadmap**. Technical Report, European Commission.

European Union (2014). **Directive 2014/94/EU of the European parliament and the council**.

Forsberg, P., et Karlström, M. (2007). **On optimal investment strategies for a hydrogen refueling station**. *International Journal of Hydrogen Energy*, 32(5):647–660.

Galbraith, J. R. (1977). **Organization design**. Addison Wesley Publishing Company.

Garfield, E., et Pudovkin, A. I. (2004). **The HistCite system for mapping and bibliometric analysis of the output of searches using the ISI Web of Knowledge**. In *Proceedings of the 67th annual meeting of the American society for information science and technology*, pages 12–17.

Gim, B., Boo, K. J., et Cho, S. M. (2012). **A transportation model approach for constructing the cost effective central hydrogen supply system in Korea**. *International Journal of Hydrogen Energy*, 37(2):1162–1172.

Glicksman, H., et Penn, M. (2008). **Approximation algorithms for group prize-collecting and location-routing problems**. *Discrete Applied Mathematics*, 156(17):3238–3247.

GlobalPetrolPrices (2019). **France diesel prices**. Accessed: 15 April 2019.

Göpfert, P., et Bock, S. (2019). **A Branch&Cut approach to recharging and refueling infrastructure planning**. *European Journal of Operational Research*, 279(3):808–823.

Govindan, K., Fattahi, M., et Keyvanshokooh, E. (2017). **Supply chain network design under uncertainty: A comprehensive review and future research directions**. *European Journal of Operational Research*, 263(1):108–141.

GRTgaz (2017). **GRTgaz et les territoires**. Technical Report, GRTgaz.

GRTgaz (2019). **Un réseau de transport au cœur des flux gaziers Européens**. Accessed: 26 December 2019.

Guillén-Gosálbez, G., Mele, F. D., et Grossmann, I. E. (2010). **A bi-criterion optimization approach for the design and planning of hydrogen supply chains for vehicle use**. *AIChE Journal*, 56(3):650–667.

Gül, T., Kypreos, S., Turton, H., et Barreto, L. (2009). **An energy-economic scenario analysis of alternative fuels for personal transport using the Global Multiregional MARKAL model (GMM)**. *Energy*, 34(10):1423–1437.

Hajimiragha, A., Fowler, M. W., et Canizares, C. A. (2009). **Hydrogen economy transition in Ontario – Canada considering the electricity grid constraints**. *International Journal of Hydrogen Energy*, 34(13):5275–5293.

Han, J.-H., Ryu, J.-H., et Lee, I.-B. (2012). **Modeling the operation of hydrogen supply networks considering facility location**. *International Journal of Hydrogen Energy*, 37(6):5328–5346.

Han, J.-H., Ryu, J.-H., et Lee, I.-B. (2013). **Multi-objective optimization design of hydrogen infrastructures simultaneously considering economic cost, safety and CO_2 emission**. *Chemical Engineering Research and Design*, 91(8):1427–1439.

Haynes, K. E., et Fotheringham, A. S. (1985). **Gravity and spatial interaction models**. SAGE Publications.

He, C., Sun, H., Xu, Y., et Lv, S. (2017). **Hydrogen refueling station siting of expressway based on the optimization of hydrogen life cycle cost**. *International Journal of Hydrogen Energy*, 42(26):16313–16324.

Hodgson, M. J. (1990). **A flow-capturing location-allocation model**. *Geographical Analysis*, 22:270–279.

Holland, J. H. (1973). **Genetic algorithms and the optimal allocation of trials**. *SIAM Journal on Computing*, 2(2):88–105.

Hooks, M. (2008). **Hydrogen delivery using alternative hydrogen carriers: Analysis and results**. Technical Report, TIAX LLC.

Hosseini, M., et MirHassani, S. A. (2015). **Refueling-station location problem under uncertainty**. *Transportation Research Part E: Logistics and Transportation Review*, 84:101–116.

Hosseini, M., et MirHassani, S. A. (2017a). **A heuristic algorithm for optimal location of flow-refueling capacitated stations**. *International Transactions in Operational Research*, 24:1377–1403.

Hosseini, M., MirHassani, S. A., et Hooshmand, F. (2017b). **Deviation-flow refueling location problem with capacitated facilities: Model and algorithm**. *Transportation Research Part D: Transport and Environment*, 54:269–281.

Hosseini, S. E., et Wahid, M. A. (2016). **Hydrogen production from renewable and sustainable energy resources: Promising green energy carrier for clean development**. *Renewable and Sustainable Energy Reviews*, 57:850–866.

Huang, Y., Li, S., et Qian, Z. S. (2015). **Optimal deployment of alternative fueling stations on transportation networks considering deviation paths**. *Networks and Spatial Economics*, 15:183–204.

Hugo, A., Rutter, P., Pistikopoulos, S., Amorelli, A., et Zoia, G. (2005). **Hydrogen infrastructure strategic planning using multi-objective optimization**. *International Journal of Hydrogen Energy*, 30(15):1523–1534.

Hwang, S. W., Kweon, S. J., et Ventura, J. A. (2015). **Infrastructure development for alternative fuel vehicles on a highway road system**. *Transportation Research Part E: Logistics and Transportation Review*, 77:170–183.

Hwangbo, S., Lee, I.-B., et Han, J. (2017). **Mathematical model to optimize design of integrated utility supply network and future global hydrogen supply network under demand uncertainty**. *Applied Energy*, 195:257–267.

Ingason, H. T., Ingolfsson, H. P., et Jensson, P. (2008). **Optimizing site selection for hydrogen production in Iceland**. *International Journal of Hydrogen Energy*, 33(14):3632–3643.

International Energy Agency (2007). **Hydrogen production & distribution**. Technical Report, International Energy Agency.

International Energy Agency (2015). **Technology roadmap-hydrogen and fuel cells**. Technical Report, International Energy Agency.

International Energy Agency (2016). **20 years of carbon capture and storage**. International Energy Agency.

International Energy Agency (2017). **Global EV outlook 2017: Two million and counting**. Technical Report, International Energy Agency.

International Energy Agency (2019a). **2019 Survey on the number of fuel cell vehicles, hydrogen refueling stations and targets**. Technical Report, International Energy Agency.

International Energy Agency (2019b). **Global energy & CO_2 status report: Emissions**. Technical Report, International Energy Agency.

Johnson, N., et Ogden, J. (2012). **A spatially-explicit optimization model for long-term hydrogen pipeline planning**. *International Journal of Hydrogen Energy*, 37(6):5421–5433.

Johnson, N., Yang, C., Ni, J., Johnson, J., Lin, Z., et Ogden, J. M. (2005). **Optimal design of a fossil fuel-based hydrogen infrastructure with carbon capture and**

sequestration: Case study in Ohio. Technical Report, Institute of Transportation Studies, UC Davis.

Julka, N., Baines, T., Tjahjono, B., Lendermann, P., et Vitanov, V. (2007). **A review of multi-factor capacity expansion models for manufacturing plants: Searching for a holistic decision aid**. *International Journal of Production Economics*, 106(2):607–621.

Jung, J., Chow, J. Y., Jayakrishnan, R., et Park, J. Y. (2014). **Stochastic dynamic itinerary interception refueling location problem with queue delay for electric taxi charging stations**. *Transportation Research Part C: Emerging Technologies*, 40:123–142.

Kamarudin, S. K., Daud, W. R. W., Yaakub, Z., Misron, Z., Anuar, W., et Yusuf, N. (2009). **Synthesis and optimization of future hydrogen energy infrastructure planning in Peninsular Malaysia**. *International Journal of Hydrogen Energy*, 34(5):2077–2088.

Katikaneni, S. P., Al-Muhaish, F., Harale, A., et Pham, T. V. (2014). **On-site hydrogen production from transportation fuels: An overview and techno-economic assessment**. *International Journal of Hydrogen Energy*, 39(9):4331–4350.

Kim, J., Lee, Y., et Moon, I. (2008a). **Optimization of a hydrogen supply chain under demand uncertainty**. *International Journal of Hydrogen Energy*, 33(18):4715–4729.

Kim, J., Lee, Y., et Moon, I. (2011). **An index-based risk assessment model for hydrogen infrastructure**. *International Journal of Hydrogen Energy*, 36(11):6387–6398.

Kim, J., et Moon, I. (2008b). **Strategic design of hydrogen infrastructure considering cost and safety using multiobjective optimization**. *International Journal of Hydrogen Energy*, 33(21):5887–5896.

Kim, J. G., et Kuby, M. (2012). **The deviation-flow refueling location model for optimizing a network of refueling stations**. *International Journal of Hydrogen Energy*, 37:5406–5420.

Kim, J. G., et Kuby, M. (2013). **A network transformation heuristic approach for the deviation flow refueling location model**. *Computers & Operations Research*, 40:1122–1131.

Kim, M., et Kim, J. (2016). **Optimization model for the design and analysis of an integrated renewable hydrogen supply (IRHS) system: Application to Korea's hydrogen economy**. *International Journal of Hydrogen Energy*, 41(38):16613–16626.

Kim, M., et Kim, J. (2017). **An integrated decision support model for design and operation of a wind-based hydrogen supply system**. *International Journal of Hydrogen Energy*, 42(7):3899–3915.

Klibi, W., Martel, A., et Guitouni, A. (2010). **The design of robust value-creating supply chain networks: A critical review**. *European Journal of Operational Research*, 203(2):283–293.

Konda, N. M., Shah, N., et Brandon, N. P. (2011). **Optimal transition towards a large-scale hydrogen infrastructure for the transport sector: The case for the Netherlands**. *International Journal of Hydrogen Energy*, 36(8):4619–4635.

Konda, N. M., Shah, N., et Brandon, N. P. (2012). **Dutch hydrogen economy: Evolution of optimal supply infrastructure and evaluation of key influencing elements**. *Asia-Pacific Journal of Chemical Engineering*, 7(4):534–546.

Krishnan, V., Gonzalez-Marciaga, L., et McCalley, J. (2014). **A planning model to assess hydrogen as an alternative fuel for national light-duty vehicle portfolio**. *Energy*, 73:943–957.

Krzyzanowski, D. A., Kypreos, S., et Barreto, L. (2008). **Supporting hydrogen based transportation: Case studies with Global MARKAL Model**. *Computational Management Science*, 5(3):207–231.

Kuby, M., et Lim, S. (2005). **The flow-refueling location problem for alternative-fuel vehicles**. *Socio-Economic Planning Sciences*, 39(2):125–145.

Kuby, M., Lines, L., Schultz, R., Xie, Z., Kim, J.-G., et Lim, S. (2009). **Optimization of hydrogen stations in florida using the flow-refueling location model**. *International Journal of Hydrogen Energy*, 34(15):6045–6064.

Lahnaoui, A., Wulf, C., Heinrichs, H., et Dalmazzone, D. (2018). **Optimizing hydrogen transportation system for mobility by minimizing the cost of transportation via compressed gas truck in North Rhine-Westphalia**. *Applied Energy*, 223:317–328.

L'Association Française pour l'Hydrogène et les Piles à Combustible (2018). **Mobilité hydrogène France**. Accessed: 26 December 2019.

Le Duigou, A., Bader, A.-G., Lanoix, J.-C., et Nadau, L. (2017). **Relevance and costs of large scale underground hydrogen storage in France**. *International Journal of Hydrogen Energy*, 42(36):22987–23003.

Li, Z., Gao, D., Chang, L., Liu, P., et Pistikopoulos, E. N. (2008). **Hydrogen infrastructure design and optimization: a case study of China**. *International Journal of Hydrogen Energy*, 33(20):5275–5286.

Lim, S., et Kuby, M. (2010). **Heuristic algorithms for siting alternative-fuel stations using the Flow-Refueling Location Model**. *European Journal of Operational Research*, 204:51–61.

Lin, Z., Chen, C.-W., Ogden, J., et Fan, Y. (2008a). **The least-cost hydrogen for Southern California**. *International Journal of Hydrogen Energy*, 33(12):3009–3014.

Lin, Z., Ogden, J., Fan, Y., et Chen, C.-W. (2008b). **The fuel-travel-back approach to hydrogen station siting**. *International Journal of Hydrogen Energy*, 33(12):3096–3101.

Lin, Z., Ogden, J. M., Fan, Y., et Sperling, D. (2006). **The Hydrogen Infrastructure Transition (HIT) model and its application in optimizing a 50-year hydrogen infrastructure for urban Beijing**. Technical Report, Institute of Transportation Studies, UC Davis.

L'Institut national de la statistique et des études économiques (2015a). **Fichier Mobilités professionnelles des individus - Logements, individus, activité, mobilités scolaires et professionnelles en 2012**. Accessed: 26 December 2019.

L'Institut national de la statistique et des études économiques (2015b). **Populations légales 2013**. Accessed: 26 December 2019.

L'Institut national de la statistique et des études économiques (2018a). **Comparateur de territoire**. Accessed: 26 December 2019.

L'Institut national de la statistique et des études économiques (2018b). **Statistiques locales - Indicateurs : cartes, données et graphiques**. Accessed: 26 December 2019.

Lototskyy, M., Davids, M. W., Swanepoel, D., Louw, G., Klochko, Y., Smith, F., Haji, F., Tolj, I., Chidziva, S., Pasupathi, S., et Linkov, V. (2019). **Hydrogen refuelling station with integrated metal hydride compressor: Layout features and experience of three-year operation**. *International Journal of Hydrogen Energy*.

M. Ruth, T.A. Timbario, T. T., et Laffen, M. (2011). **Methodology for calculating cost per mile for current and future vehicle powertrain technologies, with projections to 2024**. Technical Report, National Renewable Energy Laboratory, U.S.

Maisonnier, G., Perrin, J., et Steinberger, R. (2007). **European hydrogen infrastructure atlas and industrial excess hydrogen analysis**. Technical Report, European Commission.

Manzour-al Ajdad, S., Torabi, S. A., et Salhi, S. (2012). **A hierarchical algorithm for the planar single-facility location routing problem**. *Computers & Operations Research*, 39(2):461–470.

Markert, F., Marangon, A., Carcassi, M., et Duijm, N. J. (2017). **Risk and sustainability analysis of complex hydrogen infrastructures**. *International Journal of Hydrogen Energy*, 42(11):7698–7706.

Maryam, S. (2017). **Review of modelling approaches used in the HSC context for the UK**. *International Journal of Hydrogen Energy*.

McKinsey & Company (2017). **Hydrogen scaling up: A sustainable pathway for the global energy transition**. Technical Report, Hydrogen Council.

Melaina, M., Bremson, J., et Solo, K. (2012). **Consumer convenience and the availability of retail stations as a market barrier for alternative fuel vehicles**. Technical Report, National Renewable Energy Laboratory, U.S.

Melaina, M., et Penev, M. (2013). **Hydrogen station cost estimates: Comparing hydrogen station cost calculator results with other recent estimates**. Technical Report, National Renewable Energy Laboratory, U.S.

Melendez, M., et Milbrandt, A. (2006). **Geographically based hydrogen consumer demand and infrastructure analysis**. Technical Report, National Renewable Energy Laboratory, U.S.

Melendez, M., et Milbrandt, A. (2008). **Regional consumer hydrogen demand and optimal hydrogen refueling station siting**. Technical Report, National Renewable Energy Laboratory, U.S.

Melo, M. T., Nickel, S., et Saldanha-Da-Gama, F. (2009). **Facility location and supply chain management–A review**. *European Journal of Operational Research*, 196(2):401–412.

Ministère de la Transition écologique et solidaire (2018). **National low carbon strategy project**. Technical Report, Ministère de la Transition écologique et solidaire.

Moreno-Benito, M., Agnolucci, P., et Papageorgiou, L. G. (2017). **Towards a sustainable hydrogen economy: Optimisation-based framework for hydrogen infrastructure development**. *Computers & Chemical Engineering*, 102:110–127.

Mula, J., Peidro, D., Díaz-Madroñero, M., et Vicens, E. (2010). **Mathematical programming models for supply chain production and transport planning**. *European Journal of Operational Research*, 204(3):377–390.

Mulvey, J. M., Vanderbei, R. J., et Zenios, S. A. (1995). **Robust optimization of large-scale systems**. *Operations Research*, 43(2):264–281.

National Renewable Energy Laboratory, U.S. (2011). **Hydrogen production cost estimate using biomass gasification, independent review**. Technical Report, National Renewable Energy Laboratory, U.S.

National Research Council, U.S. (2004). **The hydrogen economy: Opportunities, costs, barriers, and R&D needs**. National Academies Press.

National Research Council, U.S. (2015). **Transitions to alternative transportation technologies–A focus on hydrogen**. National Academies Press.

Netinform (2018). **Hydrogen filling stations worldwide**. Accessed: 14 February 2018.

Nicholas, M., Handy, S., et Sperling, D. (2004). **Using geographic information systems to evaluate siting and networks of hydrogen stations**. *Transportation Research Record: Journal of the Transportation Research Board*, 1880:126–134.

Nicholas, M., et Ogden, J. (2006). **Detailed analysis of urban station siting for California hydrogen highway network**. *Transportation Research Record: Journal of the Transportation Research Board*, 1983:121–128.

Nicholas, M., et Ogden, J. (2010). **An analysis of near-term hydrogen vehicle rollout scenarios for Southern California**. Technical Report February, Institute of Transportation Studies, UC Davis.

Nikolaidis, P., et Poullikkas, A. (2017). **A comparative overview of hydrogen production processes**. *Renewable and Sustainable Energy Reviews*, 67:597–611.

Nunes, P., Oliveira, F., Hamacher, S., et Almansoori, A. (2015). **Design of a hydrogen supply chain with uncertainty**. *International Journal of Hydrogen Energy*, 40(46):16408–16418.

Ogumerem, G. S., Kim, C., Kesisoglou, I., Diangelakis, N. A., et Pistikopoulos, E. N. (2018). **A multi-objective optimization for the design and operation of a hydrogen network for transportation fuel**. *Chemical Engineering Research and Design*.

Oyama, S., Satoh, S., et Sakanaka, S. (2017). **HAZID for CO_2-free hydrogen supply chain FEED (Front End Engineering Design)**. *International Journal of Hydrogen Energy*, 42(11):7322–7330.

Paquet, M., Martel, A., et Desaulniers, G. (2004). **Including technology selection decisions in manufacturing network design models**. *International Journal of Computer Integrated Manufacturing*, 17(2):117–125.

Parker, N., Fan, Y., et Ogden, J. (2010). **From waste to hydrogen: An optimal design of energy production and distribution network**. *Transportation Research Part E: Logistics and Transportation Review*, 46(4):534–545.

Prodhon, C., et Prins, C. (2014). **A survey of recent research on location-routing problems**. *European Journal of Operational Research*, 238(1):1–17.

Qadrdan, M., Saboohi, Y., et Shayegan, J. (2008). **A model for investigation of optimal hydrogen pathway, and evaluation of environmental impacts of hydrogen supply system**. *International Journal of Hydrogen Energy*, 33(24):7314–7325.

Rath-Nagel, S., et Stocks, K. (1982). **Energy modelling for technology assessment: The MARKAL approach**. *Omega*, 10(5):493–505.

Ren, J., Manzardo, A., Toniolo, S., et Scipioni, A. (2013). **Sustainability of hydrogen supply chain. Part I: Identification of critical criteria and cause–effect analysis for enhancing the sustainability using DEMATEL**. *International Journal of Hydrogen Energy*, 38(33):14159–14171.

RentalYard (2018). **Chemical / acid tank trailers for rent**. Accessed: 26 December 2019.

Reuß, M., Grube, T., Robinius, M., Preuster, P., Wasserscheid, P., et Stolten, D. (2017). **Seasonal storage and alternative carriers: A flexible hydrogen supply chain model**. *Applied Energy*, 200:290–302.

Ringer, M. (2006). **H2A delivery components model version 1.1: Users guide**. Technical Report, National Renewable Energy Laboratory, U.S.

Rits, V., Kypreos, S., et Wokaun, A. (2004). **Evaluating the diffusion of fuel-cell cars in the China markets**. *IATSS Research*, 28(1):34–46.

Robles, J. O., Almaraz, S. D.-L., et Azzaro-Pantel, C. (2016). **Optimization of a hydrogen supply chain network design by multi-objective genetic algorithms**. In *Computer Aided Chemical Engineering*, volume 38, pages 805–810. Elsevier.

Ropke, S., et Pisinger, D. (2006). **An adaptive large neighborhood search heuristic for the pickup and delivery problem with time windows**. *Transportation Science*, 40(4):455–472.

Rosenberg, E., Fidje, A., Espegren, K. A., Stiller, C., Svensson, A. M., et Møller-Holst, S. (2010). **Market penetration analysis of hydrogen vehicles in Norwegian passenger transport towards 2050**. *International Journal of Hydrogen Energy*, 35(14):7267–7279.

Rosenthal, R. E. (2014). **GAMS: A user's guide**. GAMS Development Corporation.

Sabio, N., Gadalla, M., Guillén-Gosálbez, G., et Jiménez, L. (2010). **Strategic planning with risk control of hydrogen supply chains for vehicle use under uncertainty in operating costs: A case study of Spain**. *International Journal of Hydrogen Energy*, 35(13):6836–6852.

Sabio, N., Kostin, A., Guillén-Gosálbez, G., et Jiménez, L. (2012). **Holistic minimization of the life cycle environmental impact of hydrogen infrastructures using multi-objective optimization and principal component analysis**. *International Journal of Hydrogen Energy*, 37(6):5385–5405.

Sabri, E. H., et Beamon, B. M. (2000). **A multi-objective approach to simultaneous strategic and operational planning in supply chain design**. *Omega*, 28(5):581–598.

Samsatli, S., et Samsatli, N. J. (2015). **A general spatio-temporal model of energy systems with a detailed account of transport and storage**. *Computers & Chemical Engineering*, 80:155–176.

Samsatli, S., Staffell, I., et Samsatli, N. J. (2016). **Optimal design and operation of integrated wind-hydrogen-electricity networks for decarbonising the domestic transport sector in Great Britain**. *International Journal of Hydrogen Energy*, 41(1):447–475.

Santoso, T., Ahmed, S., Goetschalckx, M., et Shapiro, A. (2005). **A stochastic programming approach for supply chain network design under uncertainty**. *European Journal of Operational Research*, 167(1):96–115.

Scheiper, B., Schiffer, M., et Walther, G. (2019). **The flow refueling location problem with load flow control**. *Omega*, 83:50–69.

Schwardt, M., et Fischer, K. (2009). **Combined location-routing problems—a neural network approach**. *Annals of Operations Research*, 167(1):253.

Scipioni, A., Manzardo, A., et Ren, J. (2017). **Hydrogen economy : Supply chain, life cycle analysis and energy transition for sustainability**. Academic Press, 1st edition.

Sen, S., et Higle, J. L. (1999). **An introductory tutorial on stochastic linear programming models**. *Interfaces*, 29(2):33–61.

Sgobbi, A., Nijs, W., De Miglio, R., Chiodi, A., Gargiulo, M., et Thiel, C. (2016). **How far away is hydrogen? Its role in the medium and long-term decarbonisation of the European energy system**. *International Journal of Hydrogen Energy*, 41(1):19–35.

Shapiro, J. (2006). **Modeling the supply chain**. Nelson Education.

Shaw, P. (1998). **Using constraint programming and local search methods to solve vehicle routing problems**. In *Principles and Practice of Constraint Programming — CP98*, pages 417–431. Springer, Berlin, Heidelberg.

Shukla, A., Pekny, J., et Venkatasubramanian, V. (2011). **An optimization framework for cost effective design of refueling station infrastructure for alternative fuel vehicles**. *Computers & Chemical Engineering*, 35:1431–1438.

Sims, R., Schaeffer, R., Creutzig, F., Cruz-Núñez, X., et D'Agosto, M. (2014). **Transport. In: Climate Change 2014: Mitigation of Climate Change. Contribution of Working Group III to the Fifth Assessment Report of the Intergovernmental Panel on Climate Change**. Technical Report, Intergovernmental Panel on Climate Change.

Srinivas, N., et Deb, K. (1994). **Muiltiobjective optimization using nondominated sorting in genetic algorithms**. *Evolutionary Computation*, 2(3):221–248.

Stadtler, H. (2005). **Supply chain management and advanced planning—-basics, overview and challenges**. *European Journal of Operational Research*, 163(3):575–588.

Statista (2019a). **Industry prices for electricity in France 2008-2017**. Accessed: 26 December 2019.

Statista (2019b). **Industry prices of natural gas in France 2008-2017**. Accessed: 26 December 2019.

Stenger, A., Schneider, M., Schwind, M., et Vigo, D. (2012). **Location routing for small package shippers with subcontracting options**. *International Journal of Production Economics*, 140(2):702–712.

Stephens-Romero, S. D., Brown, T. M., Kang, J. E., Recker, W. W., et Samuelsen, G. S. (2010). **Systematic planning to optimize investments in hydrogen infrastructure deployment**. *International Journal of Hydrogen Energy*, 35(10):4652–4667.

Strachan, N., Balta-Ozkan, N., Joffe, D., McGeevor, K., et Hughes, N. (2009). **Soft-linking energy systems and GIS models to investigate spatial hydrogen infrastructure development in a low-carbon UK energy system**. *International Journal of Hydrogen Energy*, 34(2):642–657.

Sun, H., He, C., Wang, H., Zhang, Y., Lv, S., et Xu, Y. (2017). **Hydrogen station siting optimization based on multi-source hydrogen supply and life cycle cost**. *International Journal of Hydrogen Energy*, 42(38):23952–23965.

Sun, K., Pan, X., Li, Z., et Ma, J. (2014). **Risk analysis on mobile hydrogen refueling stations in Shanghai**. *International Journal of Hydrogen Energy*, 39(35):20411–20419.

The HyUnder project (2015). **Hyunder**. Accessed: 27 December 2019.

Tseng, P., Lee, J., et Friley, P. (2005). **A hydrogen economy: Opportunities and challenges**. *Energy*, 30(14):2703–2720.

Upchurch, C., Kuby, M., et Lim, S. (2009). **A model for location of capacitated alternative-fuel stations**. *Geographical Analysis*, 41:127–148.

Van Den Heever, S. A., et Grossmann, I. E. (2003). **A strategy for the integration of production planning and reactive scheduling in the optimization of a hydrogen supply network**. *Computers & Chemical Engineering*, 27:1813–1839.

Verter, V., et Dincer, M. C. (1995). **Facility location and capacity acquisition: An integrated approach**. *Naval Research Logistics*, 42(8):1141–1160.

Wang, Y.-W., et Lin, C.-C. (2009). **Locating road-vehicle refueling stations**. *Transportation Research Part E: Logistics and Transportation Review*, 45:821–829.

Wang, Y. W., et Lin, C. C. (2013). **Locating multiple types of recharging stations for battery-powered electric vehicle transport**. *Transportation Research Part E: Logistics and Transportation Review*, 58:76–87.

Wang, Y. W., et Wang, C. R. (2010). **Locating passenger vehicle refueling stations**. *Transportation Research Part E: Logistics and Transportation Review*, 46:791–801.

Weinert, J. X., Shaojun, L., Ogden, J. M., et Jianxin, M. (2007). **Hydrogen refueling station costs in Shanghai**. *International Journal of Hydrogen Energy*, 32(16):4089–4100.

Welder, L., Ryberg, D. S., Kotzur, L., Grube, T., Robinius, M., et Stolten, D. (2018). **Spatio-temporal optimization of a future energy system for power-to-hydrogen applications in Germany**. *Energy*.

Winskel, M., Markusson, N., Moran, B., et Taylor, G. (2009). **Decarbonising the UK energy system: Accelerated development of low carbon energy supply technologies**. Technical Report, Energy Research Centre, U.K.

Won, W., Kwon, H., Han, J.-H., et Kim, J. (2017). **Design and operation of renewable energy sources based hydrogen supply system: Technology integration and optimization**. *Renewable Energy*, 103:226–238.

Woo, Y.-b., Cho, S., Kim, J., et Kim, B. S. (2016). **Optimization-based approach for strategic design and operation of a biomass-to-hydrogen supply chain**. *International Journal of Hydrogen Energy*, 41(12):5405–5418.

World Bank, et Ecofys (2018). **State and trends of carbon pricing 2018**. Technical Report, World Bank and Ecofys.

Yáñez, M., Ortiz, A., Brunaud, B., Grossmann, I. E., et Ortiz, I. (2018). **Contribution of upcycling surplus hydrogen to design a sustainable supply chain: The case study of Northern Spain**. *Applied Energy*, 231:777–787.

Yang, C., et Ogden, J. M. (2013). **Renewable and low carbon hydrogen for California–Modeling the long term evolution of fuel infrastructure using a quasi-spatial TIMES model**. *International Journal of Hydrogen Energy*, 38(11):4250–4265.

Yann, C., et Siarry, P. (2004). **Multiobjective optimization: Principles and case studies**. Springer-Verlag: Berlin, Germany.

Yeh, S., Farrell, A., Plevin, R., Sanstad, A., et Weyant, J. (2008). **Optimizing US mitigation strategies for the light-duty transportation sector: What we learn from a bottom-up model**. *Environmental Science & Technology*, 42(22):8202.

Yue, D., You, F., et Snyder, S. W. (2014). **Biomass-to-bioenergy and biofuel supply chain optimization: Overview, key issues and challenges**. *Computers & Chemical Engineering*, 66:36–56.

Yıldız, B., Arslan, O., Karaşan, O. E., YIldIz, B., Arslan, O., Karaşan, O. E., Yıldız, B., Arslan, O., et Karaşan, O. E. (2016). **A branch and price approach for routing and refueling station location model**. *European Journal of Operational Research*, 248(3):815–826.

List of Figures

List of Tables

IV

Appendix

A

CASE STUDY INPUTS

A1. Population and demographic metrics values of 62 cities

City	Population (person)	Vehicle (%)	Income (€/year)	Education (%)	Commute (%)
C1 Baume-les-Dames	5,255	55.45	19,395	12.90	73.87
C2 Bavans	3,701	68.25	20,224	15.70	81.31
C3 Beaucourt	5,047	63.96	19,884	14.70	82.29
C4 Belfort	63,683	37.22	17,604	15.03	63.88
C5 Besançon	116,690	33.11	18,583	15.80	61.65
C6 Champagnole	7,908	45.91	19,059	14.10	72.08
C7 Delle	5,773	54.42	19,483	15.20	76.37
C8 Dole	23,312	46.34	18,813	15.40	71.09
C9 Fougerolles	5,504	36.90	15,679	15.80	67.62
C10 Gray	3,721	71.08	19,023	15.00	83.78
C11 Héricourt	9,967	60.50	18,630	14.00	79.25
C12 Hérimoncourt	3,635	60.87	19,600	15.50	84.24
C13 Lons-le-Saunier	17,311	34.21	18,185	17.90	63.87
C14 Lure	8,324	46.88	17,174	14.80	68.98
C15 Luxeuil-les-Bains	6,917	46.83	17,003	14.80	73.67
C16 Maîche	4,233	59.06	23,853	15.00	85.30
C17 Montbéliard	40,733	46.28	16,734	13.37	73.98
C18 Hauts de Bienne	5,457	48.44	19,561	12.80	72.18
C19 Morteau	6,827	51.62	27,219	18.50	77.14
C20 Ornans	4,329	57.94	20,775	15.50	71.81
C21 Poligny	4,146	51.53	18,975	17.00	68.40
C22 Pontarlier	17,413	45.44	21,995	16.70	71.36
C23 Pont-de-Roide-Vermondans	4,230	62.47	19,497	14.70	75.54
C24 Saint-Claude	10,096	45.11	18,032	12.40	68.70
C25 Saint-Loup-sur-Semouse	3,263	52.00	15,493	12.00	68.40
C26 Saint-Vit	4,803	60.38	20,718	16.40	83.40
C27 Tavaux	3,957	63.91	21,373	15.80	82.25
C28 Valdahon	5,344	44.76	20,614	20.20	63.22
C29 Valentigney	34,877	57.10	17,875	13.86	79.72
C30 Vesoul	15,212	34.31	17,159	14.50	66.37
C31 Villers-le-Lac	4,750	65.32	30,370	16.60	88.26
C32 Châtillon-sur-Seine	5,378	38.63	18,129	13.20	69.01
C33 Montbard	5,334	42.03	18,344	13.50	62.78
C34 Beaune	21,644	44.73	20,356	14.40	68.76
C35 Auxonne	7,683	50.82	18,762	16.40	71.89
C36 Genlis	5,350	56.34	20,235	15.60	74.14
C37 Is-sur-Tille	4,413	60.50	20,090	15.10	73.74
C38 Dijon	155,090	32.43	20,922	17.50	57.85

C39 Nuits-Saint-Georges	5,543	51.79	20,843	14.10	69.12
C40 Chagny	5,605	57.97	19,314	16.20	71.19
C41 Chalon-sur-Saône	45,446	33.16	17,879	16.00	65.40
C42 Montceau-les-Mines	18,722	51.08	17,344	14.30	82.27
C43 Louhans	6,349	42.92	19,032	13.80	79.95
C44 Tournus	5,562	44.29	19,352	15.60	67.94
C45 Mâcon	33,427	38.58	17,789	14.80	70.12
C46 Gueugnon	7,092	60.51	19,344	11.30	67.26
C47 Digoin	7,811	52.58	17,510	11.50	74.82
C48 Paray-le-Monial	9,160	48.59	19,189	14.30	77.76
C49 Autun	13,532	41.37	18,465	14.70	68.04
C50 Le Creusot	21,752	48.42	18,388	13.90	81.60
C51 Montchanin	5,098	59.32	18,145	14.60	83.90
C52 Cosne-Cours-sur-Loire	10,102	49.96	19,504	15.00	75.41
C53 Nevers	33,235	37.76	18,302	15.20	69.50
C54 Decize	5,519	48.89	19,097	16.90	67.40
C55 Migennes	7,162	45.15	16,126	13.90	70.50
C56 Auxerre	34,846	39.04	18,466	15.30	69.41
C57 Tonnerre	4,705	37.54	16,656	12.20	68.77
C58 Avallon	6,748	41.80	17,588	13.90	69.40
C59 Varzy	1,219	60.17	18,381	12.10	66.10
C60 Pouilly-en-Auxois	1,446	57.02	20,733	13.80	72.81
C61 Corbigny	1,498	53.47	19,505	15.60	76.39
C62 Château-Chinon (Ville)	2,001	39.07	16,918	19.30	52.32

A2. The length of network's edges

Edge	City	City	Length of edge km
1	Saint-Claude	Hauts de Bienne	32
2	Lons-le-Saunier	Hauts de Bienne	56
3	Hauts de Bienne	Champagnole	34
4	Champagnole	Lons-le-Saunier	37
5	Saint-Claude	Lons-le-Saunier	58
6	Lons-le-Saunier	Poligny	32
7	Poligny	Tavaux	48
8	Poligny	Champagnole	23
9	Champagnole	Pontarlier	44
10	Pontarlier	Ornans	36
11	Pontarlier	Morteau	29
12	Morteau	Villers-le-Lac	7
13	Pontarlier	Valdahon	31
14	Valdahon	Besançon	31
15	Ornans	Besançon	25
16	Poligny	Besançon	57
17	Besançon	Saint-Vit	21
18	Saint-Vit	Dole	28
19	Dole	Tavaux	11
20	Hauts de Bienne	Pontarlier	62
21	Morteau	Valdahon	32
22	Dole	Gray	45
23	Saint-Vit	Gray	40
24	Vesoul	Gray	58
25	Vesoul	Baume-les-Dames	43
26	Besançon	Baume-les-Dames	39
27	Valdahon	Baume-les-Dames	31
28	Vesoul	Lure	31
29	Luxeuil-les-Bains	Lure	20
30	Luxeuil-les-Bains	Vesoul	34
31	Luxeuil-les-Bains	Saint-Loup-sur-Semouse	13
32	Vesoul	Saint-Loup-sur-Semouse	34
33	Fougerolles	Saint-Loup-sur-Semouse	11
34	Fougerolles	Luxeuil-les-Bains	9
35	Vesoul	Besançon	49

Edge	City	City	Length of edge km
36	Ornans	Valdahon	20
37	Ornans	Champagnole	57
38	Morteau	Maîche	29
39	Villers-le-Lac	Maîche	28
40	Baume-les-Dames	Maîche	60
41	Baume-les-Dames	Lure	44
42	Héricourt	Lure	28
43	Héricourt	Belfort	18
44	Montbéliard	Belfort	20
45	Montbéliard	Héricourt	10
46	Montbéliard	Bavans	10
47	Montbéliard	Valentigney	9
48	Montbéliard	Beaucourt	14
49	Delle	Beaucourt	9
50	Hérimoncourt	Beaucourt	8
51	Hérimoncourt	Valentigney	6
52	Beaucourt	Valentigney	9
53	Delle	Belfort	23
54	Beaucourt	Belfort	24
55	Bavans	Pont-de-Roide-Vermondans	15
56	Bavans	Valentigney	12
57	Pont-de-Roide-Vermondans	Valentigney	13
58	Pont-de-Roide-Vermondans	Hérimoncourt	13
59	Delle	Hérimoncourt	17
60	Pont-de-Roide-Vermondans	Maîche	23
61	Bavans	Baume-les-Dames	43
62	Pont-de-Roide-Vermondans	Baume-les-Dames	40
63	Bavans	Lure	41
64	Valdahon	Maîche	43
65	Héricourt	Bavans	17
66	Dole	Auxonne	15
67	Gray	Auxonne	37
68	Genlis	Auxonne	15
69	Genlis	Tavaux	33
70	Genlis	Gray	47
71	Genlis	Dijon	21
72	Gray	Dijon	50

Edge	City	City	Length of edge km
73	Is-sur-Tille	Dijon	25
74	Is-sur-Tille	Gray	48
75	Is-sur-Tille	Châtillon-sur-Seine	69
76	Is-sur-Tille	Montbard	72
77	Châtillon-sur-Seine	Montbard	34
78	Châtillon-sur-Seine	Tonnerre	50
79	Montbard	Tonnerre	47
80	Auxerre	Tonnerre	36
81	Avallon	Tonnerre	46
82	Avallon	Auxerre	62
83	Migennes	Auxerre	21
84	Varzy	Auxerre	59
85	Cosne-Cours-sur-Loire	Auxerre	85
86	Cosne-Cours-sur-Loire	Migennes	97
87	Tonnerre	Migennes	46
88	Varzy	Avallon	53
89	Varzy	Cosne-Cours-sur-Loire	40
90	Nevers	Cosne-Cours-sur-Loire	51
91	Nevers	Varzy	52
92	Nevers	Corbigny	59
93	Varzy	Corbigny	33
94	Avallon	Corbigny	39
95	Avallon	Montbard	43
96	Pouilly-en-Auxois	Montbard	56
97	Dijon	Montbard	74
98	Dijon	Pouilly-en-Auxois	43
99	Dijon	Nuits-Saint-Georges	29
100	Beaune	Nuits-Saint-Georges	20
101	Beaune	Pouilly-en-Auxois	41
102	Beaune	Tavaux	63
103	Lons-le-Saunier	Tavaux	59
104	Chalon-sur-Saône	Tavaux	56
105	Louhans	Lons-le-Saunier	27
106	Louhans	Chalon-sur-Saône	39
107	Chagny	Chalon-sur-Saône	19
108	Chagny	Beaune	17
109	Chagny	Autun	42

Edge	City	City	Length of edge km
110	Chagny	Le Creusot	36
111	Chagny	Montchanin	41
112	Chalon-sur-Saône	Montchanin	35
113	Chalon-sur-Saône	Tournus	28
114	Louhans	Tournus	28
115	Mâcon	Tournus	31
116	Mâcon	Paray-le-Monial	66
117	Digoin	Paray-le-Monial	14
118	Digoin	Gueugnon	16
119	Paray-le-Monial	Gueugnon	22
120	Montceau-les-Mines	Gueugnon	28
121	Montchanin	Montceau-les-Mines	16
122	Montchanin	Le Creusot	8
123	Autun	Le Creusot	26
124	Autun	Château-Chinon (Ville)	35
125	Decize	Château-Chinon (Ville)	56
126	Nevers	Château-Chinon (Ville)	68
127	Corbigny	Château-Chinon (Ville)	39
128	Avallon	Château-Chinon (Ville)	64
129	Avallon	Pouilly-en-Auxois	66
130	Pouilly-en-Auxois	Château-Chinon (Ville)	72
131	Pouilly-en-Auxois	Autun	46
132	Gueugnon	Autun	52
133	Decize	Autun	81
134	Decize	Gueugnon	65
135	Decize	Digoin	68
136	Decize	Nevers	34
137	Montceau-les-Mines	Mâcon	65

A3. Delivery distances between different cities

(Unit: km)

	C1	C2	C3	C4	C5	C6	C7	C8	C9	C10	C11	C12	C13	C14	C15	C16	C17	C18	C19	C20	C21	C22	C23	C24	C25	C26	C27	C28	C29	C30	C31
C1	0	43	61	73	39	106	70	88	73	100	60	53	128	44	64	60	53	124	63	51	96	62	40	156	77	60	99	31	53	43	70
C2	43	0	21	30	82	140	30	131	70	130	17	18	171	41	61	38	10	158	67	94	139	96	15	190	74	103	142	74	12	72	66
C3	61	21	0	24	100	146	9	149	81	141	24	8	183	52	72	44	14	164	73	107	157	102	21	196	85	121	160	87	9	83	72
C4	73	30	24	0	112	167	23	161	75	135	18	32	201	46	66	65	20	185	94	124	169	123	42	217	79	133	172	104	29	77	93
C5	39	82	100	112	0	80	109	49	92	61	99	92	89	80	83	74	92	114	63	25	57	61	79	146	83	21	60	31	92	49	70
C6	106	140	146	167	80	0	155	82	172	127	157	138	37	150	163	102	147	34	73	57	23	44	125	66	163	101	71	75	138	129	80
C7	70	30	9	23	109	155	0	158	90	150	33	17	192	61	81	53	23	173	82	116	166	111	30	205	94	130	169	96	18	92	81
C8	88	131	149	161	49	82	158	0	141	45	148	141	70	129	132	123	141	116	112	74	59	110	128	128	132	28	11	80	141	98	119
C9	73	70	81	75	92	172	90	141	0	101	57	82	181	29	9	108	67	197	136	117	149	135	85	229	11	113	152	104	76	43	136
C10	100	130	141	135	61	127	150	45	101	0	117	142	115	89	92	135	127	161	124	86	104	122	140	173	92	40	56	92	136	58	131
C11	60	17	24	18	99	157	33	148	57	117	0	25	188	28	48	55	10	175	84	111	156	113	32	207	61	120	159	91	19	59	83
C12	53	18	8	32	92	138	17	141	82	142	25	0	175	53	73	36	15	156	65	99	149	94	13	188	86	113	152	79	6	84	64
C13	128	171	183	201	89	37	192	70	181	115	188	175	0	169	172	139	181	56	110	94	32	81	162	58	172	98	59	112	175	138	117
C14	44	41	52	46	80	150	61	129	29	89	28	53	169	0	20	79	38	168	107	95	137	106	56	200	33	101	140	75	47	31	107
C15	64	61	72	66	83	163	81	132	9	92	48	73	172	20	0	99	58	188	127	108	140	126	76	220	13	104	143	95	67	34	127
C16	60	38	44	65	74	102	53	123	108	135	55	36	139	79	99	0	45	120	29	63	125	58	23	152	112	95	134	43	36	103	28
C17	53	10	14	20	92	147	23	141	67	127	10	15	181	38	58	45	0	165	74	104	149	103	22	197	71	113	152	84	9	69	73
C18	124	158	164	185	114	34	173	116	197	161	175	156	56	168	188	120	165	0	91	91	57	62	143	32	197	135	105	93	156	163	98
C19	63	67	73	94	63	73	82	112	136	124	84	65	110	107	127	29	74	91	0	52	96	29	52	123	140	84	123	32	65	106	7
C20	51	94	107	124	25	57	116	74	117	86	111	99	94	95	108	63	104	91	52	0	80	36	86	123	108	46	85	20	99	74	59
C21	96	139	157	169	57	23	166	59	149	104	156	149	32	137	140	125	149	57	96	80	0	67	136	89	140	78	48	88	149	106	103
C22	62	96	102	123	61	44	111	110	135	122	113	94	81	106	126	58	103	62	29	36	67	0	81	94	139	82	115	31	94	105	36
C23	40	15	21	42	79	125	30	128	85	140	32	13	162	56	76	23	22	143	52	86	136	81	0	175	89	100	139	66	13	83	51
C24	156	190	196	217	146	66	205	128	229	173	207	188	58	200	220	152	197	32	123	123	89	94	175	0	229	156	117	125	188	195	130
C25	77	74	85	79	83	163	94	132	11	92	61	86	172	33	13	112	71	197	140	108	140	139	89	229	0	104	143	108	80	34	140
C26	60	103	121	133	21	101	130	28	113	40	120	113	98	101	104	95	113	135	84	46	78	82	100	156	104	0	39	52	113	70	91
C27	99	142	160	172	60	71	169	11	152	56	159	152	59	140	143	134	152	105	123	85	48	115	139	117	143	39	0	91	152	109	130
C28	31	74	87	104	31	75	96	80	104	92	91	79	112	75	95	43	84	93	32	20	88	31	66	125	108	52	91	0	79	74	39
C29	53	12	9	29	92	138	18	141	76	136	19	6	175	47	67	36	9	156	65	99	149	94	13	188	80	113	152	79	0	78	64
C30	43	72	83	77	49	129	92	98	43	58	59	84	138	31	34	103	69	163	106	74	106	105	83	195	34	70	109	74	78	0	113
C31	70	66	72	93	70	80	81	119	136	131	83	64	117	107	127	28	73	98	7	59	103	36	51	130	140	91	130	39	64	113	0
C32	217	247	258	252	178	219	267	145	218	117	234	259	207	206	209	252	244	253	241	203	196	239	257	265	209	157	148	209	253	175	248
C33	213	250	261	255	174	199	270	125	221	120	237	262	187	209	212	248	247	233	237	199	176	235	253	245	212	153	128	205	256	178	244
C34	162	205	223	234	123	134	232	74	200	99	216	215	102	188	191	197	215	158	186	148	111	178	202	160	191	102	63	154	215	157	193
C35	103	146	164	172	64	97	173	15	138	37	154	156	85	126	129	138	156	131	127	89	74	125	143	143	129	43	26	95	156	95	134
C36	118	161	179	182	79	104	188	30	148	47	164	171	92	136	139	153	171	138	142	104	81	140	158	150	139	58	33	110	171	105	149
C37	148	178	189	183	109	150	198	76	149	48	165	190	138	137	140	183	175	184	172	134	127	170	188	196	140	88	79	140	184	106	179
C38	139	180	191	185	100	125	200	51	151	50	167	192	113	139	142	174	177	159	163	125	102	161	179	171	142	79	54	131	186	108	170
C39	168	209	220	214	129	154	229	80	180	79	196	221	122	168	171	203	206	178	192	154	131	190	208	180	171	108	83	160	215	137	199
C40	174	217	235	247	135	122	244	86	217	116	233	227	85	205	208	209	227	141	195	160	117	166	214	143	208	114	75	166	227	174	202
C41	155	198	216	228	116	103	225	67	208	112	215	208	66	196	199	190	208	122	176	141	98	147	195	124	199	95	56	147	208	165	183
C42	206	249	267	279	167	154	276	118	259	163	266	259	117	247	250	241	259	173	227	192	149	198	246	175	250	146	107	198	259	216	234
C43	155	198	210	228	116	64	219	97	208	142	215	202	27	196	199	166	208	83	137	121	59	108	189	85	199	125	86	139	202	165	144
C44	183	226	238	256	144	92	247	95	236	140	243	230	55	224	227	194	236	111	165	149	87	136	217	113	227	123	84	167	230	193	172
C45	214	257	269	287	175	123	278	126	267	171	274	261	86	255	258	225	267	142	196	180	118	167	248	144	258	154	115	198	261	224	203
C46	234	277	295	307	195	182	304	146	287	191	294	287	145	275	278	269	287	201	255	220	177	226	274	203	278	174	135	226	287	244	262
C47	250	293	311	323	211	198	320	162	303	207	310	303	161	291	294	285	303	217	271	236	193	242	290	219	294	190	151	242	303	260	278
C48	256	299	317	329	217	189	326	168	309	213	316	309	152	297	300	291	309	208	262	242	184	233	296	210	300	196	157	248	309	266	269
C49	216	259	277	274	177	164	286	128	240	139	256	269	127	228	231	251	266	183	237	202	159	208	256	185	231	156	117	208	269	197	244
C50	198	241	259	271	159	146	268	110	251	152	258	251	109	239	242	233	251	165	219	184	141	190	238	167	242	138	99	190	251	208	226
C51	190	233	251	263	151	138	260	102	243	147	250	243	101	231	234	225	243	157	211	176	133	182	230	159	234	130	91	182	243	200	218
C52	341	382	393	387	302	311	402	253	353	252	369	394	274	341	344	376	379	330	365	327	304	355	381	332	344	281	256	333	388	310	372
C53	319	362	374	368	280	267	383	231	334	233	350	372	230	322	325	354	360	286	340	305	262	311	359	288	325	259	220	311	369	291	347
C54	297	340	358	355	258	245	367	209	321	220	337	350	208	309	312	332	347	264	318	283	240	289	337	266	312	237	198	289	350	278	325
C55	306	343	354	348	267	292	363	218	314	213	330	355	280	302	305	341	340	326	330	292	269	328	346	338	305	246	221	298	349	271	337
C56	296	333	344	338	257	282	353	208	304	203	320	345	270	292	295	331	330	316	320	282	259	318	336	328	295	236	211	288	339	261	327
C57	260	297	308	302	221	246	317	172	268	167	284	309	234	256	259	295	294	280	284	246	223	282	300	292	259	200	175	252	303	225	291
C58	248	289	300	294	209	234	309	160	260	159	276	301	209	248	251	283	286	265	272	234	211	270	288	267	251	188	163	240	295	217	279
C59	301	342	353	347	262	271	362	213	313	212	329	354	234	301	304	336	339	290	325	287	264	315	341	292	304	241	216	293	348	270	332
C60	182	223	234	228	143	168	243	94	194	93	210	235	143	182	185	217	220	199	206	168	145	204	222	201	185	122	97	174	229	151	213
C61	287	328	339	333	248	238	348	199	299	198	315	340	201	287	290	322	325	257	311	273	233	282	327	259	290	227	191	279	334	256	318
C62	251	294	306	300	212	199	315	163	266	165	282	304	162	254	257	286	292	218	272	237	194	243	291	220	257	191	152	243	301	223	279

	C32	C33	C34	C35	C36	C37	C38	C39	C40	C41	C42	C43	C44	C45	C46	C47	C48	C49	C50	C51	C52	C53	C54	C55	C56	C57	C58	C59	C60	C61	C62
C1	217	213	162	103	118	148	139	168	174	155	206	155	183	214	234	250	256	216	198	190	341	319	297	306	296	260	248	301	182	287	251
C2	247	250	205	146	161	178	180	209	217	198	249	198	226	257	277	293	299	259	241	233	382	362	340	343	333	297	289	342	223	328	294
C3	258	261	223	164	179	189	191	220	235	216	267	210	238	269	295	311	317	277	259	251	393	374	358	354	344	308	300	353	234	339	306
C4	252	255	234	172	182	183	185	214	247	228	279	228	256	287	307	323	329	274	271	263	387	368	355	348	338	302	294	347	228	333	300
C5	178	174	123	64	79	109	100	129	135	116	167	116	144	175	195	211	217	177	159	151	302	280	258	267	257	221	209	262	143	248	212
C6	219	199	134	97	104	150	125	154	122	103	154	64	92	123	182	198	189	164	146	138	311	267	245	292	282	246	234	271	168	238	199
C7	267	270	232	173	188	198	200	229	244	225	276	219	247	278	304	320	326	286	268	260	402	383	367	363	353	317	309	362	243	348	315
C8	145	125	74	15	30	76	51	80	86	67	118	97	95	126	146	162	168	128	110	102	253	231	209	218	208	172	160	213	94	199	163
C9	218	221	200	138	148	149	151	180	217	208	259	208	236	267	287	303	309	240	251	243	353	334	321	314	304	268	260	313	194	299	266
C10	117	120	99	37	47	48	50	79	116	112	163	142	140	171	191	207	213	139	152	147	252	233	220	213	203	167	159	212	93	198	165
C11	234	237	216	154	164	165	167	196	233	215	266	215	243	274	294	310	316	256	258	250	369	350	337	330	320	284	276	329	210	315	282
C12	259	262	215	156	171	190	192	221	227	208	259	202	230	261	287	303	309	269	251	243	394	372	350	355	345	309	301	354	235	340	304
C13	207	187	102	85	92	138	113	122	85	66	117	27	55	86	145	161	152	127	109	101	274	230	208	280	270	234	209	234	143	201	162
C14	206	209	188	126	136	137	139	168	205	196	247	196	224	255	275	291	297	228	239	231	341	322	309	302	292	256	248	301	182	287	254
C15	209	212	191	129	139	140	142	171	208	199	250	199	227	258	278	294	300	231	242	234	344	325	312	305	295	259	251	304	185	290	257
C16	252	248	197	138	153	183	174	203	209	190	241	166	194	225	269	285	291	251	233	225	376	354	332	341	331	295	283	336	217	322	286
C17	244	247	215	156	171	175	177	206	227	208	259	208	236	267	287	303	309	266	251	243	379	360	347	340	330	294	286	339	220	325	292
C18	253	233	158	131	138	184	159	178	141	122	173	83	111	142	201	217	208	183	165	157	330	286	264	326	316	280	265	290	199	257	218
C19	241	237	186	127	142	172	163	192	195	176	227	137	165	196	255	271	262	237	219	211	365	340	318	330	320	284	272	325	206	311	272
C20	203	199	148	89	104	134	125	154	160	141	192	121	149	180	220	236	242	202	184	176	327	305	283	292	282	246	234	287	168	273	237
C21	196	176	111	74	81	127	102	131	117	98	149	59	87	118	177	193	184	159	141	133	304	262	240	269	259	223	211	264	145	233	194
C22	239	235	178	125	140	170	161	190	166	147	198	108	136	167	226	242	233	208	190	182	355	311	289	328	318	282	270	315	204	282	243
C23	257	253	202	143	158	188	179	208	214	195	246	189	217	248	274	290	296	256	238	230	381	359	337	346	336	300	288	341	222	327	291
C24	265	245	160	143	150	196	171	180	143	124	175	85	113	144	203	219	210	185	167	159	332	288	266	338	328	292	267	292	201	259	220
C25	209	212	191	129	139	140	142	171	208	199	250	199	227	258	278	294	300	231	242	234	344	325	312	305	295	259	251	304	185	290	257
C26	157	153	102	43	58	88	79	108	114	95	146	125	123	154	174	190	196	156	138	130	281	259	237	246	236	200	188	241	122	227	191
C27	148	128	63	26	33	79	54	83	75	56	107	86	84	115	135	151	157	117	99	91	256	220	198	221	211	175	163	216	97	191	152
C28	209	205	154	95	110	140	131	160	166	147	198	139	167	198	226	242	248	208	190	182	333	311	289	298	288	252	240	293	174	279	243
C29	253	256	215	156	171	184	186	215	227	208	259	202	230	261	287	303	309	269	251	243	388	369	350	349	339	303	295	348	229	334	301
C30	175	178	157	95	105	106	108	137	174	165	216	165	193	224	244	260	266	197	208	200	310	291	278	271	261	225	217	270	151	256	223
C31	248	244	193	134	149	179	170	199	202	183	234	144	172	203	262	278	269	244	226	218	372	347	325	337	327	291	279	332	213	318	279
C32	0	34	131	130	115	69	94	123	148	167	186	206	195	226	188	204	210	136	162	170	170	175	197	96	86	50	77	130	90	116	141
C33	34	0	97	110	95	72	74	103	114	133	152	172	161	192	154	170	176	102	128	136	136	141	163	93	83	47	43	96	56	82	107
C34	131	97	0	85	70	74	49	20	17	36	74	75	64	95	102	118	124	59	53	58	200	162	140	190	169	144	107	160	41	133	94
C35	130	110	85	0	15	61	36	65	101	82	133	112	110	141	161	177	183	125	125	117	238	219	206	203	193	157	145	198	79	184	151
C36	115	95	70	15	0	46	21	50	87	89	140	119	117	148	162	178	184	110	123	124	223	204	191	188	178	142	130	183	64	169	136
C37	69	72	74	61	46	0	25	54	91	110	148	149	138	169	166	182	188	114	127	132	208	208	195	165	155	119	115	168	68	154	140
C38	94	74	49	36	21	25	0	29	66	85	123	124	113	144	141	157	163	89	102	107	202	183	170	167	157	121	109	162	43	148	115
C39	123	103	20	65	50	54	29	0	37	56	94	95	84	115	122	138	144	79	73	78	220	182	160	196	186	150	127	180	61	153	114
C40	148	114	17	101	87	91	66	37	0	19	57	58	47	78	85	101	107	42	36	41	189	145	123	207	186	161	124	149	58	116	77
C41	167	133	36	82	89	110	85	56	19	0	51	39	28	59	79	95	101	61	43	35	208	164	142	226	205	180	143	168	77	135	96
C42	186	152	74	133	140	148	123	94	57	51	0	90	79	65	28	44	50	50	24	16	178	127	93	232	211	195	149	157	96	124	85
C43	206	172	75	112	119	149	124	95	58	39	90	0	28	59	118	134	125	100	82	74	247	203	181	265	244	219	182	207	116	174	135
C44	195	161	64	110	117	138	113	84	47	28	79	28	0	31	107	111	97	89	71	63	236	192	170	254	233	208	171	196	105	163	124
C45	226	192	95	141	148	169	144	115	78	59	65	59	31	0	88	80	66	115	89	81	233	182	148	285	264	239	202	222	136	189	150
C46	188	154	102	161	162	166	141	122	85	79	28	118	107	88	0	16	22	52	52	44	150	99	65	231	210	197	151	151	98	126	87
C47	204	170	118	177	178	182	157	138	101	95	44	134	111	80	16	0	14	68	68	60	153	102	68	234	213	213	167	154	114	142	103
C48	210	176	124	183	184	188	163	144	107	101	50	125	97	66	22	14	0	74	74	66	167	116	82	248	227	219	173	168	120	148	109
C49	136	102	59	125	110	114	89	79	42	61	50	100	89	115	52	68	74	0	26	34	147	103	81	182	161	145	99	107	46	74	35
C50	162	128	53	125	123	127	102	73	36	43	24	82	71	89	52	68	74	26	0	8	173	129	107	208	187	171	125	133	72	100	61
C51	170	136	58	117	124	132	107	78	41	35	16	74	63	81	44	60	66	34	8	0	181	137	109	216	195	179	133	141	80	108	69
C52	170	136	200	238	223	208	202	220	189	208	178	247	236	233	150	153	167	147	173	181	0	51	85	97	85	121	93	40	159	73	112
C53	175	141	162	219	204	208	183	182	145	164	127	203	192	182	99	102	116	103	129	137	51	0	34	132	111	144	98	52	140	59	68
C54	197	163	140	206	191	195	170	160	123	142	93	181	170	148	65	68	82	81	107	109	85	34	0	166	145	166	120	86	127	93	56
C55	96	93	190	203	188	165	167	196	207	226	232	265	254	285	231	234	248	182	208	216	97	132	166	0	21	46	83	80	149	113	147
C56	86	83	169	193	178	155	157	186	186	205	211	244	233	264	210	213	227	161	187	195	85	111	145	21	0	36	62	59	128	92	126
C57	50	47	144	157	142	119	121	150	161	180	195	219	208	239	197	213	219	145	171	179	121	144	166	46	36	0	46	95	103	85	110
C58	77	43	107	145	130	115	109	127	124	143	149	182	171	202	151	167	173	99	125	133	93	98	120	83	62	46	0	53	66	39	64
C59	130	96	160	198	183	168	162	180	149	168	157	207	196	222	151	154	168	107	133	141	40	52	86	80	59	95	53	0	119	33	72
C60	90	56	41	79	64	68	43	61	58	77	96	116	105	136	98	114	120	46	72	80	159	140	127	149	128	103	66	119	0	105	72
C61	116	82	133	184	169	154	148	153	116	135	124	174	163	189	126	142	148	74	100	108	73	59	93	113	92	85	39	33	105	0	39
C62	141	107	94	151	136	140	115	114	77	96	85	135	124	150	87	103	109	35	61	69	112	68	56	147	126	110	64	72	72	39	0

C1: Baume-les-Dames;C 2: Bavans; C3: Beaucourt; C4: Belfort; C5: Besançon; C6: Champagnole; C7: Delle; C8: Dole; C9: Fougerolles; C10: Gray; C11: Héricourt; C12: Hérimoncourt; C13: Lons-le-Saunier; C14: Lure; C15: Luxeuil-les-Bains; C16: Maîche; C17: Montbéliard; C18: Hauts de Bienne; C19: Morteau; C20: Ornans; C21: Poligny; C22: Pontarlier; C23: Pont-de-Roide-Vermondans; C24: Saint-Claude;C25: Saint-Loup-sur-Semouse; C26: Saint-Vit;C 27: Tavaux; C28: Valdahon; C29: Valentigney; C30: Vesoul; C31: Villers-le-Lac; C32: Châtillon-sur-Seine; C33: Montbard; C34: Beaune; C35: Auxonne; C36: Genlis; C37: Is-sur-Tille; C38: Dijon; C39: Nuits-Saint-Georges; C40: Chagny; C41: Chalon-sur-Saône; C42: Montceau-les-Mines; C43: Louhans; C44: Tournus; C45: Mâcon; C46: Gueugnon; C47: Digoin; C48: Paray-le-Monial; C49: Autun; C50: Le Creusot; C51: Montchanin; C52: Cosne-Cours-sur-Loire; C53: Nevers; C54: Decize; C55: Migennes; C56: Auxerre; C57: Tonnerre; C58: Avallon; C59: Varzy; C60: Pouilly-en-Auxois; C61: Corbigny; C62: Château-Chinon (Ville)

B

Detailed results of case study in Chapter 3

B1. Value of LCOH and its composition, the percentage of captured hydrogen fueling demand flow, and solution time

No.	Instance	LCOH	contri_CC	contri_EC	contri_OC	contri_EMC	$DEM^{h,cap}$	SolutionTime
		€/kg H_2	€/kg H_2	€/kg H_2	€/kg H_2	€/kg H_2	%	s
1	Set-A1-LC-LD	13.45	5.73	5.66	1.86	0.19	10.01	0.17
2	Set-A1-LC-MD	13.58	5.53	5.82	2.03	0.20	50.00	0.23
3	Set-A1-LC-HD	19.34	8.48	7.89	2.70	0.27	90.01	0.30
4	Set-A1-HC-LD	14.29	5.73	5.66	1.86	1.04	10.00	0.17
5	Set-A1-HC-MD	14.47	5.53	5.82	2.03	1.09	50.00	0.27
6	Set-A1-HC-HD	20.53	8.48	7.89	2.70	1.47	90.01	0.44
7	Set-A2-LC-LD	10.13	5.41	1.72	2.29	0.70	10.01	0.14
8	Set-A2-LC-MD	10.21	5.24	1.77	2.47	0.74	50.00	0.22
9	Set-A2-LC-HD	17.75	9.41	2.94	4.18	1.23	90.00	0.09
10	Set-A2-HC-LD	13.22	5.41	1.72	2.29	3.79	10.01	0.14
11	Set-A2-HC-MD	13.45	5.24	1.77	2.47	3.97	50.00	0.17
12	Set-A2-HC-HD	23.15	9.50	2.94	4.10	6.60	90.00	0.13
13	Set-B1-LC-LD	19.93	10.97	3.79	3.72	1.44	10.01	14.88
14	Set-B1-LC-MD	9.60	5.17	1.77	1.98	0.68	50.00	5.41
15	Set-B1-LC-HD	13.62	7.41	2.40	2.87	0.93	90.01	8.27
16	Set-B1-HC-LD	26.28	10.97	3.79	3.72	7.80	10.00	7.06
17	Set-B1-HC-MD	12.60	5.17	1.77	1.98	3.68	50.00	4.80
18	Set-B1-HC-HD	17.70	7.41	2.40	2.87	5.01	90.01	9.53
19	Set-B2-LC-LD	43.28	28.72	3.79	9.39	1.39	10.00	51.21
20	Set-B2-LC-MD	17.01	10.25	1.90	4.18	0.69	50.00	784.69
21	Set-B2-LC-HD	21.04	12.50	2.40	5.26	0.87	90.01	7,567.27
22	Set-B2-HC-LD	49.38	28.72	3.79	9.39	7.49	10.00	161.68
23	Set-B2-HC-MD	20.04	10.25	1.90	4.18	3.73	50.01	1,104.37
24	Set-B2-HC-HD	24.88	12.50	2.40	5.26	4.71	90.01	1,891.06
25	Set-B3-LC-LD	31.41	17.31	1.59	12.13	0.38	10.00	0.42
26	Set-B3-LC-MD	13.58	7.32	0.79	5.25	0.22	50.01	0.73
27	Set-B3-LC-HD	17.55	9.72	1.00	6.54	0.29	90.01	0.70
28	Set-B3-HC-LD	33.08	17.31	1.59	12.13	2.05	10.00	0.51
29	Set-B3-HC-MD	14.55	7.32	0.79	5.25	1.19	50.01	0.97
30	Set-B3-HC-HD	18.82	9.72	1.00	6.54	1.55	90.01	0.78
31	Set-C-LC-LD	10.13	5.41	1.72	2.29	0.70	10.01	0.80
32	Set-C-LC-MD	9.60	5.17	1.77	1.98	0.68	50.00	6.70
33	Set-C-LC-HD	13.58	7.24	2.40	3.00	0.94	90.00	15.68
34	Set-C-HC-LD	13.22	5.41	1.72	2.29	3.79	10.01	0.92
35	Set-C-HC-MD	12.60	5.17	1.77	1.98	3.68	50.00	5.13
36	Set-C-HC-HD	17.70	7.41	2.40	2.87	5.01	90.01	12.38
37	Set-D-LC-LD	31.41	17.31	1.59	12.13	0.38	10.00	99.92
38	Set-D-LC-MD	13.52	7.32	0.79	5.20	0.21	50.00	190.04
39	Set-D-LC-HD	17.42	9.72	1.00	6.42	0.28	90.01	177.03
40	Set-D-HC-LD	33.08	17.31	1.59	12.13	2.05	10.00	47.78
41	Set-D-HC-MD	14.43	7.32	0.79	5.20	1.12	50.01	164.12
42	Set-D-HC-HD	18.64	9.79	1.00	6.44	1.40	90.01	406.52
43	Set-E1-LC-LD	19.93	10.97	3.79	3.72	1.44	10.01	11.34
44	Set-E1-LC-MD	9.60	5.17	1.77	1.98	0.68	50.01	8.70
45	Set-E1-LC-HD	13.62	7.41	2.40	2.87	0.93	90.01	11.44
46	Set-E1-HC-LD	26.28	10.97	3.79	3.72	7.80	10.00	41.93
47	Set-E1-HC-MD	12.60	5.17	1.77	1.98	3.68	50.01	16.12
48	Set-E1-HC-HD	17.70	7.41	2.40	2.87	5.01	90.01	144.35

No.	Instance	LCOH	contri_CC	contri_EC	contri_OC	contri_EMC	$DEM^{h,cap}$	SolutionTime
		€/kg H_2	€/kg H_2	€/kg H_2	€/kg H_2	€/kg H_2	%	s
49	Set-E2-LC-LD	31.41	17.31	1.59	12.13	0.38	10.00	0.52
50	Set-E2-LC-MD	13.58	7.32	0.79	5.25	0.22	50.01	0.75
51	Set-E2-LC-HD	17.55	9.72	1.00	6.54	0.29	90.01	0.77
52	Set-E2-HC-LD	33.08	17.31	1.59	12.13	2.05	10.01	1.05
53	Set-E2-HC-MD	12.01	9.24	0.81	7.54	-5.58	50.01	0.70
54	Set-E2-HC-HD	15.24	10.78	1.01	8.87	-5.42	90.00	0.73
55	Set-F-LC-LD	6.44	2.69	1.68	1.46	0.61	10.00	0.84
56	Set-F-LC-MD	7.90	3.61	1.81	1.79	0.68	50.01	7.53
57	Set-F-LC-HD	11.53	5.91	2.25	2.51	0.86	90.01	10.91
58	Set-F-HC-LD	9.14	2.69	1.68	1.46	3.30	10.00	0.75
59	Set-F-HC-MD	10.82	3.61	1.75	1.88	3.58	50.00	7.79
60	Set-F-HC-HD	15.30	5.91	2.25	2.51	4.63	90.01	7.97
61	Set-G-LC-LD	6.44	2.69	1.68	1.46	0.61	10.00	3.55
62	Set-G-LC-MD	7.90	3.61	1.81	1.79	0.68	50.01	18.12
63	Set-G-LC-HD	11.53	5.91	2.25	2.51	0.86	90.01	22.15
64	Set-G-HC-LD	9.14	2.69	1.68	1.46	3.30	10.01	44.24
65	Set-G-HC-MD	8.56	6.35	0.87	7.45	-6.11	50.00	143.56
66	Set-G-HC-HD	11.94	8.23	0.94	9.26	-6.50	90.01	538.89

LCOH: least cost of hydrogen; contri_CC: the contribution of capital cost to LCOH; contri_EC: the contribution of purchasing cost to LCOH; contri_OC: the contribution of operating cost to LCOH; contri_EMC: the contribution of to LCOH; $DEM^{h,cap}$: percentage of hydrogen demand flow that could be captured.

B2. Configuration of hydrogen supply chain network

No.1 Set-A1-LC-LD

Onsite fueling stations

City	Fueling technology	Facility size	Fueling rate (kg H_2/d)
Belfort	Onsite-electrolysis	Large	454.06

No.2 Set-A1-LC-MD

Onsite fueling stations

City	Fueling technology	Facility size	Fueling rate (kg H_2/d)
Besançon	Onsite-Electrolysis	ExtraLarge	1,059.77
Champagnole	Onsite-Electrolysis	Medium	226.70
Valentigney	Onsite-Electrolysis	ExtraLarge	1,046.54

No.3 Set-A1-LC-HD

Onsite fueling stations

City	Fueling technology	Facility size	Fueling rate (kg H_2/d)
Bavans	Onsite-Electrolysis	ExtraLarge	705.51
Beaucourt	Onsite-Electrolysis	ExtraLarge	700.74
Besançon	Onsite-Electrolysis	ExtraLarge	1,059.77
Héricourt	Onsite-Electrolysis	Large	537.75
Pontarlier	Onsite-Electrolysis	Large	384.10
Saint-Claude	Onsite-Electrolysis	Small	59.36
Tavaux	Onsite-Electrolysis	Medium	246.46
Valdahon	Onsite-Electrolysis	Large	518.01
Valentigney	Onsite-Electrolysis	ExtraLarge	1,046.54
Villers-le-Lac	Onsite-Electrolysis	Large	436.39

No.4 Set-A1-HC-LD

Onsite fueling stations

City	Fueling technology	Facility size	Fueling rate (kg H_2/d)
Belfort	Onsite-Electrolysis	Large	454.06

No.5 Set-A1-HC-MD

Onsite fueling stations

City	Fueling technology	Facility size	Fueling rate (kg H_2/d)
Besançon	Onsite-Electrolysis	ExtraLarge	1,059.77
Champagnole	Onsite-Electrolysis	Medium	226.70
Valentigney	Onsite-Electrolysis	ExtraLarge	1,046.54

No.6 Set-A1-HC-HD

Onsite fueling stations

City	Fueling technology	Facility size	Fueling rate (kg H_2/d)
Bavans	Onsite-Electrolysis	ExtraLarge	705.51
Beaucourt	Onsite-Electrolysis	ExtraLarge	700.74
Besançon	Onsite-Electrolysis	ExtraLarge	1,059.77
Héricourt	Onsite-Electrolysis	Large	537.75
Pontarlier	Onsite-Electrolysis	Large	384.10
Saint-Claude	Onsite-Electrolysis	Small	59.36
Tavaux	Onsite-Electrolysis	Medium	246.46
Valdahon	Onsite-Electrolysis	Large	518.01
Valentigney	Onsite-Electrolysis	ExtraLarge	1,046.54
Villers-le-Lac	Onsite-Electrolysis	Large	436.39

No.7 Set-A2-LC-LD

Onsite fueling stations

City	Fueling technology	Facility size	Fueling rate (kg H_2/d)
Belfort	Onsite-SMR	Large	454.06

No.8 Set-A2-LC-MD

Onsite fueling stations

City	Fueling technology	Facility size	Fueling rate (kg H_2/d)
Besançon	Onsite-SMR	ExtraLarge	1,059.77
Champagnole	Onsite-SMR	Medium	226.70
Valentigney	Onsite-SMR	ExtraLarge	1,046.54

No.9 Set-A2-LC-HD

Onsite fueling stations

City	Fueling technology	Facility size	Fueling rate (kg H_2/d)
Baume-les-Dames	Onsite-SMR	Large	597.05
Belfort	Onsite-SMR	Large	454.06
Besançon	Onsite-SMR	ExtraLarge	1,059.77
Champagnole	Onsite-SMR	Medium	226.70
Delle	Onsite-SMR	Medium	290.01
Dole	Onsite-SMR	Large	370.15
Fougerolles	Onsite-SMR	Small	92.84
Lons-le-Saunier	Onsite-SMR	Small	109.35
Lure	Onsite-SMR	Large	379.13
Montbéliard	Onsite-SMR	ExtraLarge	1,011.68
Pontarlier	Onsite-SMR	Large	384.10
Pont-de-Roide-Vermondans	Onsite-SMR	ExtraLarge	952.75
Valentigney	Onsite-SMR	ExtraLarge	1,046.54

No.10 Set-A2-HC-LD

Onsite fueling stations

City	Fueling technology	Facility size	Fueling rate (kg H_2/d)
Belfort	Onsite-SMR	Large	454.06

No.11 Set-A2-HC-MD

Onsite fueling stations

City	Fueling technology	Facility size	Fueling rate (kg H_2/d)
Besançon	Onsite-SMR	ExtraLarge	1,059.77
Champagnole	Onsite-SMR	Medium	226.70
Valentigney	Onsite-SMR	ExtraLarge	1,046.54

No.12 Set-A2-HC-HD

Onsite fueling stations

City	Fueling technology	Facility size	Fueling rate (kg H_2/d)
Baume-les-Dames	Onsite-SMR	Large	597.05
Belfort	Onsite-SMR	Large	454.06
Besançon	Onsite-SMR	ExtraLarge	1,059.77
Champagnole	Onsite-SMR	Medium	226.70
Delle	Onsite-SMR	Large	300.00
Dole	Onsite-SMR	Large	370.15
Fougerolles	Onsite-SMR	Small	92.84
Lons-le-Saunier	Onsite-SMR	Small	109.35
Lure	Onsite-SMR	Large	379.13
Montbéliard	Onsite-SMR	ExtraLarge	1,011.68
Pontarlier	Onsite-SMR	Large	384.10
Pont-de-Roide-Vermondans	Onsite-SMR	ExtraLarge	952.75
Valentigney	Onsite-SMR	ExtraLarge	1,046.54

No.13 Set-B1-LC-LD

Standard fueling stations

City	Fueling technology	Hydrogen form	Facility size	Fueling rate (kg H_2/d)
Pont-de-Roide-Vermondans	Standard	Gaseous	ExtraLarge	1,000.00

Feedstock supply sites

City	Feedstock type	Supply rate (Nm^3/d)
Pont-de-Roide-Vermondans	NaturalGas	4,610.00

Production plants

City	Production technology	Hydrogen form	Facility size	Production rate (kg H_2/d)
Pont-de-Roide-Vermondans	SMR	Gaseous	Small	1,000.00

No.14 Set-B1-LC-MD

Standard fueling stations

City	Fueling technology	Hydrogen form	Facility size	Fueling rate (kg H_2/d)
Besançon	Standard	Gaseous	ExtraLarge	1,059.77
Champagnole	Standard	Gaseous	Medium	226.70
Valentigney	Standard	Gaseous	ExtraLarge	1,046.54

Feedstock supply sites

City	Feedstock type	Supply rate (Nm^3/d)
Besançon	NaturalGas	5,930.63
Valentigney	NaturalGas	4,824.55

Production plants

City	Production technology	Hydrogen form	Facility size	Production rate (kg H_2/d)
Besançon	SMR	Gaseous	Small	1,286.47
Valentigney	SMR	Gaseous	Small	1,046.54

Hydrogen transportation Number of vehicles = 1

Hydrogen form	Origin	Destination	Hydrogen flux (kg H_2/d)
Gaseous	Besançon	Champagnole	226.70

No.15 Set-B1-LC-HD

Standard fueling stations

City	Fueling technology	Hydrogen form	Facility size	Fueling rate (kg H_2/d)
Bavans	Standard	Gaseous	ExtraLarge	705.51
Beaucourt	Standard	Gaseous	ExtraLarge	700.74
Besançon	Standard	Gaseous	ExtraLarge	1,059.77
Héricourt	Standard	Gaseous	Large	537.75
Pontarlier	Standard	Gaseous	Large	384.10
Saint-Claude	Standard	Gaseous	Small	59.36
Tavaux	Standard	Gaseous	Medium	246.46
Valdahon	Standard	Gaseous	Large	518.01
Valentigney	Standard	Gaseous	ExtraLarge	1,046.54
Villers-le-Lac	Standard	Gaseous	Large	436.39

Feedstock supply sites

City	Feedstock type	Supply rate (Nm^3/d)
Besançon	NaturalGas	7,855.85
Pontarlier	NaturalGas	4,610.00
Valentigney	NaturalGas	13,786.39

Production plants

City	Production technology	Hydrogen form	Facility size	Production rate (kg H_2/d)
Besançon	SMR	Gaseous	Small	1,704.09
Pontarlier	SMR	Gaseous	Small	1,000.00
Valentigney	SMR	Gaseous	Medium	2,990.54

Hydrogen transportation Number of vehicles = 3

Hydrogen form	Origin	Destination	Hydrogen flux (kg H_2/d)
Gaseous	Besançon	Tavaux	246.46
Gaseous	Besançon	Valdahon	397.86
Gaseous	Pontarlier	Saint-Claude	59.36
Gaseous	Pontarlier	Valdahon	120.15
Gaseous	Pontarlier	Villers-le-Lac	436.39
Gaseous	Valentigney	Bavans	705.51
Gaseous	Valentigney	Beaucourt	700.74
Gaseous	Valentigney	Héricourt	537.75

No.16 Set-B1-HC-LD

Standard fueling stations

City	Fueling technology	Hydrogen form	Facility size	Fueling rate (kg H_2/d)
Belfort	Standard	Gaseous	ExtraLarge	1,000.00

Feedstock supply sites

City	Feedstock type	Supply rate (Nm^3/d)
Belfort	NaturalGas	4,610.00

Production plants

City	Production technology	Hydrogen form	Facility size	Production rate (kg H_2/d)
Belfort	SMR	Gaseous	Small	1,000.00

No.17 Set-B1-HC-MD

Standard fueling stations

City	Fueling technology	Hydrogen form	Facility size	Fueling rate (kg H_2/d)
Besançon	Standard	Gaseous	ExtraLarge	1,059.77
Champagnole	Standard	Gaseous	Medium	226.70
Valentigney	Standard	Gaseous	ExtraLarge	1,046.54

Feedstock supply sites

City	Feedstock type	Supply rate (Nm^3/d)
Besançon	NaturalGas	5,930.63
Valentigney	NaturalGas	4,824.55

Production plants

City	Production technology	Hydrogen form	Facility size	Production rate (kg H_2/d)
Besançon	SMR	Gaseous	Small	1,286.47
Valentigney	SMR	Gaseous	Small	1,046.54

Hydrogen transportation Number of vehicles = 1

Hydrogen form	Origin	Destination	Hydrogen flux (kg H_2/d)
Gaseous	Besançon	Champagnole	226.70

No.18 Set-B1-HC-HD

Standard fueling stations

City	Fueling technology	Hydrogen form	Facility size	Fueling rate (kg H_2/d)
Bavans	Standard	Gaseous	ExtraLarge	705.51
Beaucourt	Standard	Gaseous	ExtraLarge	700.74
Besançon	Standard	Gaseous	ExtraLarge	1,059.77
Héricourt	Standard	Gaseous	Large	537.75
Pontarlier	Standard	Gaseous	Large	384.10
Saint-Claude	Standard	Gaseous	Small	59.36
Tavaux	Standard	Gaseous	Medium	246.46
Valdahon	Standard	Gaseous	Large	518.01
Valentigney	Standard	Gaseous	ExtraLarge	1,046.54
Villers-le-Lac	Standard	Gaseous	Large	436.39

Feedstock supply sites

City	Feedstock type	Supply rate (Nm^3/d)
Besançon	NaturalGas	7,855.85
Pontarlier	NaturalGas	4,610.00
Valentigney	NaturalGas	13,786.39

Production plants

City	Production technology	Hydrogen form	Facility size	Production rate (kg H_2/d)
Besançon	SMR	Gaseous	Small	1,704.09
Pontarlier	SMR	Gaseous	Small	1,000.00
Valentigney	SMR	Gaseous	Medium	2,990.54

Hydrogen transportation Number of vehicles = 3

Hydrogen form	Origin	Destination	Hydrogen flux (kg H_2/d)
Gaseous	Besançon	Tavaux	246.46
Gaseous	Besançon	Valdahon	397.86
Gaseous	Pontarlier	Saint-Claude	59.36
Gaseous	Pontarlier	Valdahon	120.15
Gaseous	Pontarlier	Villers-le-Lac	436.39
Gaseous	Valentigney	Bavans	705.51
Gaseous	Valentigney	Beaucourt	700.74
Gaseous	Valentigney	Héricourt	537.75

No.19 Set-B2-LC-LD

Standard fueling stations

City	Fueling technology	Hydrogen form	Facility size	Fueling rate (kg H_2/d)
Héricourt	Standard	Liquid	ExtraLarge	1,000.00

Feedstock supply sites

City	Feedstock type	Supply rate (Nm^3/d)

Héricourt	NaturalGas	4,610.00		
Production plants				
City	Production technology	Hydrogen form	Facility size	Production rate (kg H_2/d)
Héricourt	SMR	Liquid	Small	1,000.00

No.20 Set-B2-LC-MD

Standard fueling stations				
City	Fueling technology	Hydrogen form	Facility size	Fueling rate (kg H_2/d)
Montbéliard	Standard	Liquid	ExtraLarge	1,011.68
Pont-de-Roide-Vermondans	Standard	Liquid	ExtraLarge	970.31
Valdahon	Standard	Liquid	Large	518.01
Feedstock supply sites				
City	Feedstock type	Supply rate (Nm^3/d)		
Pont-de-Roide-Vermondans	NaturalGas	11,525.00		
Production plants				
City	Production technology	Hydrogen form	Facility size	Production rate (kg H_2/d)
Pont-de-Roide-Vermondans	SMR	Liquid	Medium	2,500.00
Hydrogen transportation	Number of vehicles = 1			
Hydrogen form	Origin	Destination	Hydrogen flux (kg H_2/d)	
Liquid	Pont-de-Roide-Vermondans	Montbéliard	1,011.68	
Liquid	Pont-de-Roide-Vermondans	Valdahon	518.01	

No.21 Set-B2-LC-HD

Standard fueling stations				
City	Fueling technology	Hydrogen form	Facility size	Fueling rate (kg H_2/d)
Bavans	Standard	Liquid	ExtraLarge	705.51
Beaucourt	Standard	Liquid	ExtraLarge	700.74
Besançon	Standard	Liquid	ExtraLarge	1,059.77
Héricourt	Standard	Liquid	Large	537.75
Pontarlier	Standard	Liquid	Large	384.10
Saint-Claude	Standard	Liquid	Small	59.36
Tavaux	Standard	Liquid	Medium	246.46
Valdahon	Standard	Liquid	Large	518.01
Valentigney	Standard	Liquid	ExtraLarge	1,046.54
Villers-le-Lac	Standard	Liquid	Large	436.39
Feedstock supply sites				
City	Feedstock type	Supply rate (Nm^3/d)		
Besançon	NaturalGas	4,610.00		
Valentigney	NaturalGas	21,642.24		
Production plants				
City	Production technology	Hydrogen form	Facility size	Production rate (kg H_2/d)
Besançon	SMR	Liquid	Small	1,000.00
Valentigney	SMR	Liquid	Large	4,694.63
Hydrogen transportation	Number of vehicles = 1			
Hydrogen form	Origin	Destination	Hydrogen flux (kg H_2/d)	
Liquid	Valentigney	Bavans	705.51	
Liquid	Valentigney	Beaucourt	700.74	
Liquid	Valentigney	Besançon	59.77	
Liquid	Valentigney	Héricourt	537.75	
Liquid	Valentigney	Pontarlier	384.10	
Liquid	Valentigney	Saint-Claude	59.36	
Liquid	Valentigney	Tavaux	246.46	
Liquid	Valentigney	Valdahon	518.01	
Liquid	Valentigney	Villers-le-Lac	436.39	

No.22 Set-B2-HC-LD

Standard fueling stations				
City	Fueling technology	Hydrogen form	Facility size	Fueling rate (kg H_2/d)
Héricourt	Standard	Liquid	ExtraLarge	1,000.00
Feedstock supply sites				
City	Feedstock type	Supply rate (Nm^3/d)		

Héricourt	NaturalGas	4,610.00		
Production plants				
City	Production technology	Hydrogen form	Facility size	Production rate (kg H_2/d)
Héricourt	SMR	Liquid	Small	1,000.00

No.23 Set-B2-HC-MD

Standard fueling stations				
City	Fueling technology	Hydrogen form	Facility size	Fueling rate (kg H_2/d)
Montbéliard	Standard	Liquid	ExtraLarge	1,011.68
Pont-de-Roide-Vermondans	Standard	Liquid	ExtraLarge	970.31
Valdahon	Standard	Liquid	Large	518.01
Feedstock supply sites				
City	Feedstock type	Supply rate (Nm^3/d)		
Pont-de-Roide-Vermondans	NaturalGas	11,525.00		
Production plants				
City	Production technology	Hydrogen form	Facility size	Production rate (kg H_2/d)
Pont-de-Roide-Vermondans	SMR	Liquid	Medium	2,500.00
Hydrogen transportation	Number of vehicles = 1			
Hydrogen form	Origin	Destination	Hydrogen flux (kg H_2/d)	
Liquid	Pont-de-Roide-Vermondans	Montbéliard	1,011.68	
Liquid	Pont-de-Roide-Vermondans	Valdahon	518.01	

No.24 Set-B2-HC-HD

Standard fueling stations				
City	Fueling technology	Hydrogen form	Facility size	Fueling rate (kg H_2/d)
Bavans	Standard	Liquid	ExtraLarge	705.51
Beaucourt	Standard	Liquid	ExtraLarge	700.74
Besançon	Standard	Liquid	ExtraLarge	1,059.77
Héricourt	Standard	Liquid	Large	537.75
Pontarlier	Standard	Liquid	Large	384.10
Saint-Claude	Standard	Liquid	Small	59.36
Tavaux	Standard	Liquid	Medium	246.46
Valdahon	Standard	Liquid	Large	518.01
Valentigney	Standard	Liquid	ExtraLarge	1,046.54
Villers-le-Lac	Standard	Liquid	Large	436.39
Feedstock supply sites				
City	Feedstock type	Supply rate (Nm^3/d)		
Besançon	NaturalGas	4,610.00		
Valentigney	NaturalGas	21,642.24		
Production plants				
City	Production technology	Hydrogen form	Facility size	Production rate (kg H_2/d)
Besançon	SMR	Liquid	Small	1,000.00
Valentigney	SMR	Liquid	Large	4,694.63
Hydrogen transportation	Number of vehicles = 1			
Hydrogen form	Origin	Destination	Hydrogen flux (kg H_2/d)	
Liquid	Valentigney	Bavans	705.51	
Liquid	Valentigney	Beaucourt	700.74	
Liquid	Valentigney	Besançon	59.77	
Liquid	Valentigney	Héricourt	537.75	
Liquid	Valentigney	Pontarlier	384.10	
Liquid	Valentigney	Saint-Claude	59.36	
Liquid	Valentigney	Tavaux	246.46	
Liquid	Valentigney	Valdahon	518.01	
Liquid	Valentigney	Villers-le-Lac	436.39	

No.25 Set-B3-LC-LD

Standard fueling stations				
City	Fueling technology	Hydrogen form	Facility size	Fueling rate (kg H_2/d)
Valdahon	Standard	Gaseous	ExtraLarge	1,000.00
Feedstock supply sites				
City	Feedstock type	Supply rate (kg/d)		

Valdahon	Biomass	13,880.00		

Production plants

City	Production technology	Hydrogen form	Facility size	Production rate (kg H_2/d)
Valdahon	BG	Gaseous	Small	1,000.00

No.26 Set-B3-LC-MD

Standard fueling stations

City	Fueling technology	Hydrogen form	Facility size	Fueling rate (kg H_2/d)
Besançon	Standard	Gaseous	ExtraLarge	1,059.77
Héricourt	Standard	Gaseous	Large	537.75
Pontarlier	Standard	Gaseous	Large	466.09
Villers-le-Lac	Standard	Gaseous	Large	436.39

Feedstock supply sites

City	Feedstock type	Supply rate (kg/d)
Valdahon	Biomass	34,700.00

Production plants

City	Production technology	Hydrogen form	Facility size	Production rate (kg H_2/d)
Valdahon	BG	Gaseous	Medium	2,500.00

Hydrogen transportation Number of vehicles = 3

Hydrogen form	Origin	Destination	Hydrogen flux (kg H_2/d)
Gaseous	Valdahon	Besançon	1,059.77
Gaseous	Valdahon	Héricourt	537.75
Gaseous	Valdahon	Pontarlier	466.09
Gaseous	Valdahon	Villers-le-Lac	436.39

No.27 Set-B3-LC-HD

Standard fueling stations

City	Fueling technology	Hydrogen form	Facility size	Fueling rate (kg H_2/d)
Bavans	Standard	Gaseous	ExtraLarge	705.51
Beaucourt	Standard	Gaseous	ExtraLarge	700.74
Besançon	Standard	Gaseous	ExtraLarge	1,059.77
Héricourt	Standard	Gaseous	Large	537.75
Pontarlier	Standard	Gaseous	Large	384.10
Saint-Claude	Standard	Gaseous	Small	59.36
Tavaux	Standard	Gaseous	Medium	246.46
Valdahon	Standard	Gaseous	Large	518.01
Valentigney	Standard	Gaseous	ExtraLarge	1,046.54
Villers-le-Lac	Standard	Gaseous	Large	436.39

Feedstock supply sites

City	Feedstock type	Supply rate (kg/d)
Luxeuil-les-Bains	Biomass	13,880.00
Valdahon	Biomass	65,161.46

Production plants

City	Production technology	Hydrogen form	Facility size	Production rate (kg H_2/d)
Luxeuil-les-Bains	BG	Gaseous	Small	1,000.00
Valdahon	BG	Gaseous	Large	4,694.63

Hydrogen transportation Number of vehicles = 7

Hydrogen form	Origin	Destination	Hydrogen flux (kg H_2/d)
Gaseous	Luxeuil-les-Bains	Beaucourt	462.25
Gaseous	Luxeuil-les-Bains	Héricourt	537.75
Gaseous	Valdahon	Bavans	705.51
Gaseous	Valdahon	Beaucourt	238.49
Gaseous	Valdahon	Besançon	1,059.77
Gaseous	Valdahon	Pontarlier	384.10
Gaseous	Valdahon	Saint-Claude	59.36
Gaseous	Valdahon	Tavaux	246.46
Gaseous	Valdahon	Valentigney	1,046.54
Gaseous	Valdahon	Villers-le-Lac	436.39

No.28 Set-B3-HC-LD

Standard fueling stations

City	Fueling technology	Hydrogen form	Facility size	Fueling rate (kg H_2/d)
Valdahon	Standard	Gaseous	ExtraLarge	1,000.00

Feedstock supply sites

City	Feedstock type	Supply rate (kg/d)
Valdahon	Biomass	13,880.00

Production plants

City	Production technology	Hydrogen form	Facility size	Production rate (kg H_2/d)
Valdahon	BG	Gaseous	Small	1,000.00

No.29 Set-B3-HC-MD

Standard fueling stations

City	Fueling technology	Hydrogen form	Facility size	Fueling rate (kg H_2/d)
Besançon	Standard	Gaseous	ExtraLarge	1,059.77
Héricourt	Standard	Gaseous	Large	537.75
Pontarlier	Standard	Gaseous	Large	466.09
Villers-le-Lac	Standard	Gaseous	Large	436.39

Feedstock supply sites

City	Feedstock type	Supply rate (kg/d)
Valdahon	Biomass	34,700.00

Production plants

City	Production technology	Hydrogen form	Facility size	Production rate (kg H_2/d)
Valdahon	BG	Gaseous	Medium	2,500.00

Hydrogen transportation Number of vehicles = 3

Hydrogen form	Origin	Destination	Hydrogen flux (kg H_2/d)
Gaseous	Valdahon	Besançon	1,059.77
Gaseous	Valdahon	Héricourt	537.75
Gaseous	Valdahon	Pontarlier	466.09
Gaseous	Valdahon	Villers-le-Lac	436.39

No.30 Set-B3-HC-HD

Standard fueling stations

City	Fueling technology	Hydrogen form	Facility size	Fueling rate (kg H_2/d)
Bavans	Standard	Gaseous	ExtraLarge	705.51
Beaucourt	Standard	Gaseous	ExtraLarge	700.74
Besançon	Standard	Gaseous	ExtraLarge	1,059.77
Héricourt	Standard	Gaseous	Large	537.75
Pontarlier	Standard	Gaseous	Large	384.10
Saint-Claude	Standard	Gaseous	Small	59.36
Tavaux	Standard	Gaseous	Medium	246.46
Valdahon	Standard	Gaseous	Large	518.01
Valentigney	Standard	Gaseous	ExtraLarge	1,046.54
Villers-le-Lac	Standard	Gaseous	Large	436.39

Feedstock supply sites

City	Feedstock type	Supply rate (kg/d)
Luxeuil-les-Bains	Biomass	13,880.00
Valdahon	Biomass	65,161.46

Production plants

City	Production technology	Hydrogen form	Facility size	Production rate (kg H_2/d)
Luxeuil-les-Bains	BG	Gaseous	Small	1,000.00
Valdahon	BG	Gaseous	Large	4,694.63

Hydrogen transportation Number of vehicles = 7

Hydrogen form	Origin	Destination	Hydrogen flux (kg H_2/d)
Gaseous	Luxeuil-les-Bains	Beaucourt	462.25
Gaseous	Luxeuil-les-Bains	Héricourt	537.75
Gaseous	Valdahon	Bavans	705.51
Gaseous	Valdahon	Beaucourt	238.49
Gaseous	Valdahon	Besançon	1,059.77
Gaseous	Valdahon	Pontarlier	384.10
Gaseous	Valdahon	Saint-Claude	59.36
Gaseous	Valdahon	Tavaux	246.46
Gaseous	Valdahon	Valentigney	1,046.54

Gaseous	Valdahon	Villers-le-Lac	436.39

No.31 Set-C-LC-LD

Onsite fueling stations

City	Fueling technology	Facility size	Fueling rate (kg H_2/d)
Belfort	Onsite-SMR	Large	454.06

No.32 Set-C-LC-MD

Standard fueling stations

City	Fueling technology	Hydrogen form	Facility size	Fueling rate (kg H_2/d)
Besançon	Standard	Gaseous	ExtraLarge	1,059.77
Champagnole	Standard	Gaseous	Medium	226.70
Valentigney	Standard	Gaseous	ExtraLarge	1,046.54

Feedstock supply sites

City	Feedstock type	Supply rate (Nm^3/d)
Besançon	NaturalGas	5,930.63
Valentigney	NaturalGas	4,824.55

Production plants

City	Production technology	Hydrogen form	Facility size	Production rate (kg H_2/d)
Besançon	SMR	Gaseous	Small	1,286.47
Valentigney	SMR	Gaseous	Small	1,046.54

Hydrogen transportation Number of vehicles = 1

Hydrogen form	Origin	Destination	Hydrogen flux (kg H_2/d)
Gaseous	Besançon	Champagnole	226.70

No.33 Set-C-LC-HD

Onsite fueling stations

City	Fueling technology	Facility size	Fueling rate (kg H_2/d)
Champagnole	Onsite-SMR	Medium	226.70

Standard fueling stations

City	Fueling technology	Hydrogen form	Facility size	Fueling rate (kg H_2/d)
Bavans	Standard	Gaseous	ExtraLarge	705.51
Beaucourt	Standard	Gaseous	ExtraLarge	700.74
Besançon	Standard	Gaseous	ExtraLarge	1,059.77
Dole	Standard	Gaseous	Large	370.15
Fougerolles	Standard	Gaseous	Small	92.84
Héricourt	Standard	Gaseous	Large	537.75
Valdahon	Standard	Gaseous	Large	518.01
Valentigney	Standard	Gaseous	ExtraLarge	1,046.54
Villers-le-Lac	Standard	Gaseous	Large	436.39

Feedstock supply sites

City	Feedstock type	Supply rate (Nm^3/d)
Besançon	NaturalGas	9,210.46
Valentigney	NaturalGas	15,995.64

Production plants

City	Production technology	Hydrogen form	Facility size	Production rate (kg H_2/d)
Besançon	SMR	Gaseous	Small	1,997.93
Valentigney	SMR	Gaseous	Medium	3,469.77

Hydrogen transportation Number of vehicles = 4

Hydrogen form	Origin	Destination	Hydrogen flux (kg H_2/d)
Gaseous	Besançon	Dole	370.15
Gaseous	Besançon	Valdahon	518.01
Gaseous	Besançon	Villers-le-Lac	50.00
Gaseous	Valentigney	Bavans	705.51
Gaseous	Valentigney	Beaucourt	700.74
Gaseous	Valentigney	Fougerolles	92.84
Gaseous	Valentigney	Héricourt	537.75
Gaseous	Valentigney	Villers-le-Lac	386.39

No.34 Set-C-HC-LD

Onsite fueling stations

City	Fueling technology	Facility size	Fueling rate (kg H_2/d)
Belfort	Onsite-SMR	Large	454.06

No.35 Set-C-HC-MD

Standard fueling stations

City	Fueling technology	Hydrogen form	Facility size	Fueling rate (kg H_2/d)
Besançon	Standard	Gaseous	ExtraLarge	1,059.77
Champagnole	Standard	Gaseous	Medium	226.70
Valentigney	Standard	Gaseous	ExtraLarge	1,046.54

Feedstock supply sites

City	Feedstock type	Supply rate (Nm^3/d)
Besançon	NaturalGas	5,930.63
Valentigney	NaturalGas	4,824.55

Production plants

City	Production technology	Hydrogen form	Facility size	Production rate (kg H_2/d)
Besançon	SMR	Gaseous	Small	1,286.47
Valentigney	SMR	Gaseous	Small	1,046.54

Hydrogen transportation Number of vehicles = 1

Hydrogen form	Origin	Destination	Hydrogen flux (kg H_2/d)
Gaseous	Besançon	Champagnole	226.70

No.36 Set-C-HC-HD

Standard fueling stations

City	Fueling technology	Hydrogen form	Facility size	Fueling rate (kg H_2/d)
Bavans	Standard	Gaseous	ExtraLarge	705.51
Beaucourt	Standard	Gaseous	ExtraLarge	700.74
Besançon	Standard	Gaseous	ExtraLarge	1,059.77
Héricourt	Standard	Gaseous	Large	537.75
Pontarlier	Standard	Gaseous	Large	384.10
Saint-Claude	Standard	Gaseous	Small	59.36
Tavaux	Standard	Gaseous	Medium	246.46
Valdahon	Standard	Gaseous	Large	518.01
Valentigney	Standard	Gaseous	ExtraLarge	1,046.54
Villers-le-Lac	Standard	Gaseous	Large	436.39

Feedstock supply sites

City	Feedstock type	Supply rate (Nm^3/d)
Besançon	NaturalGas	6,021.72
Pontarlier	NaturalGas	6,444.13
Valentigney	NaturalGas	13,786.39

Production plants

City	Production technology	Hydrogen form	Facility size	Production rate (kg H_2/d)
Besançon	SMR	Gaseous	Small	1,306.23
Pontarlier	SMR	Gaseous	Small	1,397.86
Valentigney	SMR	Gaseous	Medium	2,990.54

Hydrogen transportation Number of vehicles = 3

Hydrogen form	Origin	Destination	Hydrogen flux (kg H_2/d)
Gaseous	Besançon	Tavaux	246.46
Gaseous	Pontarlier	Saint-Claude	59.36
Gaseous	Pontarlier	Valdahon	518.01
Gaseous	Pontarlier	Villers-le-Lac	436.39
Gaseous	Valentigney	Bavans	705.51
Gaseous	Valentigney	Beaucourt	700.74
Gaseous	Valentigney	Héricourt	537.75

No.37 Set-D-LC-LD

Standard fueling stations

City	Fueling technology	Hydrogen form	Facility size	Fueling rate (kg H_2/d)
Valdahon	Standard	Gaseous	ExtraLarge	1,000.00

Feedstock supply sites

City	Feedstock type	Supply rate (kg/d)
Valdahon	Biomass	13,880.00

Production plants

City	Production technology	Hydrogen form	Facility size	Production rate (kg H_2/d)
Valdahon	BG	Gaseous	Small	1,000.00

No.38 Set-D-LC-MD

Standard fueling stations

City	Fueling technology	Hydrogen form	Facility size	Fueling rate (kg H_2/d)
Montbéliard	Standard	Gaseous	ExtraLarge	1,029.24
Pont-de-Roide-Vermondans	Standard	Gaseous	ExtraLarge	952.75
Valdahon	Standard	Gaseous	Large	518.01

Feedstock supply sites

City	Feedstock type	Supply rate (kg/d)
Luxeuil-les-Bains	Biomass	34,700.00

Production plants

City	Production technology	Hydrogen form	Facility size	Production rate (kg H_2/d)
Montbéliard	BG	Gaseous	Medium	2,500.00

Hydrogen transportation Number of vehicles = 2

Hydrogen form	Origin	Destination	Hydrogen flux (kg H_2/d)
Gaseous	Montbéliard	ont-de-Roide-Vermondai	952.75
Gaseous	Montbéliard	Valdahon	518.01

Feedstock transportation Number of vehicles = 1

Feedstock type	Origin	Destination	Feedstock flux (kg/d)
Biomass	Luxeuil-les-Bains	Montbéliard	34,700.00

No.39 Set-D-LC-HD

Standard fueling stations

City	Fueling technology	Hydrogen form	Facility size	Fueling rate (kg H_2/d)
Bavans	Standard	Gaseous	ExtraLarge	705.51
Beaucourt	Standard	Gaseous	ExtraLarge	700.74
Besançon	Standard	Gaseous	ExtraLarge	1,059.77
Héricourt	Standard	Gaseous	Large	537.75
Pontarlier	Standard	Gaseous	Large	384.10
Saint-Claude	Standard	Gaseous	Small	59.36
Tavaux	Standard	Gaseous	Medium	246.46
Valdahon	Standard	Gaseous	Large	518.01
Valentigney	Standard	Gaseous	ExtraLarge	1,046.54
Villers-le-Lac	Standard	Gaseous	Large	436.39

Feedstock supply sites

City	Feedstock type	Supply rate (kg/d)
Luxeuil-les-Bains	Biomass	13,880.00
Valdahon	Biomass	65,161.46

Production plants

City	Production technology	Hydrogen form	Facility size	Production rate (kg H_2/d)
Valdahon	BG	Gaseous	Large	4,694.63
Valentigney	BG	Gaseous	Small	1,000.00

Hydrogen transportation Number of vehicles = 6

Hydrogen form	Origin	Destination	Hydrogen flux (kg H_2/d)
Gaseous	Valdahon	Bavans	705.51
Gaseous	Valdahon	Beaucourt	650.74
Gaseous	Valdahon	Besançon	1,059.77
Gaseous	Valdahon	Héricourt	537.75
Gaseous	Valdahon	Pontarlier	384.10
Gaseous	Valdahon	Saint-Claude	59.36
Gaseous	Valdahon	Tavaux	246.46
Gaseous	Valdahon	Valentigney	96.54
Gaseous	Valdahon	Villers-le-Lac	436.39
Gaseous	Valentigney	Beaucourt	50.00

Feedstock transportation Number of vehicles = 1

Feedstock type	Origin	Destination	Feedstock flux (kg/d)
Biomass	Luxeuil-les-Bains	Valentigney	13,880.00

No.40 Set-D-HC-LD

Standard fueling stations

City	Fueling technology	Hydrogen form	Facility size	Fueling rate (kg H_2/d)
Valdahon	Standard	Gaseous	ExtraLarge	1,000.00

Feedstock supply sites

City	Feedstock type	Supply rate (kg/d)
Valdahon	Biomass	13,880.00

Production plants

City	Production technology	Hydrogen form	Facility size	Production rate (kg H_2/d)
Valdahon	BG	Gaseous	Small	1,000.00

No.41 Set-D-HC-MD

Standard fueling stations

City	Fueling technology	Hydrogen form	Facility size	Fueling rate (kg H_2/d)
Montbéliard	Standard	Gaseous	ExtraLarge	1,029.24
Pont-de-Roide-Vermondans	Standard	Gaseous	ExtraLarge	952.75
Valdahon	Standard	Gaseous	Large	518.01

Feedstock supply sites

City	Feedstock type	Supply rate (kg/d)
Luxeuil-les-Bains	Biomass	34,700.00

Production plants

City	Production technology	Hydrogen form	Facility size	Production rate (kg H_2/d)
Montbéliard	BG	Gaseous	Medium	2,500.00

Hydrogen transportation Number of vehicles = 2

Hydrogen form	Origin	Destination	Hydrogen flux (kg H_2/d)
Gaseous	Montbéliard	ont-de-Roide-Vermondai	952.75
Gaseous	Montbéliard	Valdahon	518.01

Feedstock transportation Number of vehicles = 1

Feedstock type	Origin	Destination	Feedstock flux (kg/d)
Biomass	Luxeuil-les-Bains	Montbéliard	34,700.00

No.42 Set-D-HC-HD

Standard fueling stations

City	Fueling technology	Hydrogen form	Facility size	Fueling rate (kg H_2/d)
Bavans	Standard	Gaseous	ExtraLarge	705.51
Beaucourt	Standard	Gaseous	ExtraLarge	700.74
Besançon	Standard	Gaseous	ExtraLarge	1,059.77
Héricourt	Standard	Gaseous	Large	537.75
Pontarlier	Standard	Gaseous	Large	384.10
Saint-Claude	Standard	Gaseous	Small	59.36
Tavaux	Standard	Gaseous	Medium	246.46
Valdahon	Standard	Gaseous	Large	518.01
Valentigney	Standard	Gaseous	ExtraLarge	1,046.54
Villers-le-Lac	Standard	Gaseous	Large	436.39

Feedstock supply sites

City	Feedstock type	Supply rate (kg/d)
Luxeuil-les-Bains	Biomass	41,508.70
Valdahon	Biomass	37,532.77

Production plants

City	Production technology	Hydrogen form	Facility size	Production rate (kg H_2/d)
Valdahon	BG	Gaseous	Medium	2,704.09
Valentigney	BG	Gaseous	Medium	2,990.54

Hydrogen transportation Number of vehicles = 4

Hydrogen form	Origin	Destination	Hydrogen flux (kg H_2/d)
Gaseous	Valdahon	Besançon	1,059.77
Gaseous	Valdahon	Pontarlier	384.10
Gaseous	Valdahon	Saint-Claude	59.36
Gaseous	Valdahon	Tavaux	246.46
Gaseous	Valdahon	Villers-le-Lac	436.39
Gaseous	Valentigney	Bavans	705.51
Gaseous	Valentigney	Beaucourt	700.74

Gaseous	Valentigney	Héricourt	537.75	
Feedstock transportation	Number of vehicles = 2			
Feedstock type	Origin	Destination	Feedstock flux (kg/d)	
Biomass	Luxeuil-les-Bains	Valentigney	41,508.70	

No.43 Set-E1-LC-LD

Standard fueling stations				
City	Fueling technology	Hydrogen form	Facility size	Fueling rate (kg H_2/d)
Baume-les-Dames	Standard	Gaseous	ExtraLarge	1,000.00
Feedstock supply sites				
City	Feedstock type	Supply rate (Nm^3/d)		
Baume-les-Dames	NaturalGas	4,610.00		
Production plants				
City	Production technology	Hydrogen form	Facility size	Production rate (kg H_2/d)
Baume-les-Dames	SMR	Gaseous	Small	1,000.00

No.44 Set-E1-LC-MD

Standard fueling stations				
City	Fueling technology	Hydrogen form	Facility size	Fueling rate (kg H_2/d)
Besançon	Standard	Gaseous	ExtraLarge	1,059.77
Champagnole	Standard	Gaseous	Medium	226.70
Valentigney	Standard	Gaseous	ExtraLarge	1,046.54
Feedstock supply sites				
City	Feedstock type	Supply rate (Nm^3/d)		
Besançon	NaturalGas	5,930.63		
Valentigney	NaturalGas	4,824.55		
Production plants				
City	Production technology	Hydrogen form	Facility size	Production rate (kg H_2/d)
Besançon	SMR	Gaseous	Small	1,286.47
Valentigney	SMR	Gaseous	Small	1,046.54
Hydrogen transportation	Number of vehicles = 1			
Hydrogen form	Origin	Destination	Hydrogen flux (kg H_2/d)	
Gaseous	Besançon	Champagnole	226.70	

No.45 Set-E1-LC-HD

Standard fueling stations				
City	Fueling technology	Hydrogen form	Facility size	Fueling rate (kg H_2/d)
Bavans	Standard	Gaseous	ExtraLarge	705.51
Beaucourt	Standard	Gaseous	ExtraLarge	700.74
Besançon	Standard	Gaseous	ExtraLarge	1,059.77
Héricourt	Standard	Gaseous	Large	537.75
Pontarlier	Standard	Gaseous	Large	384.10
Saint-Claude	Standard	Gaseous	Small	59.36
Tavaux	Standard	Gaseous	Medium	246.46
Valdahon	Standard	Gaseous	Large	518.01
Valentigney	Standard	Gaseous	ExtraLarge	1,046.54
Villers-le-Lac	Standard	Gaseous	Large	436.39
Feedstock supply sites				
City	Feedstock type	Supply rate (Nm^3/d)		
Besançon	NaturalGas	6,021.72		
Pontarlier	NaturalGas	6,444.13		
Valentigney	NaturalGas	13,786.39		
Production plants				
City	Production technology	Hydrogen form	Facility size	Production rate (kg H_2/d)
Besançon	SMR	Gaseous	Small	1,306.23
Pontarlier	SMR	Gaseous	Small	1,397.86
Valentigney	SMR	Gaseous	Medium	2,990.54
Hydrogen transportation	Number of vehicles = 3			
Hydrogen form	Origin	Destination	Hydrogen flux (kg H_2/d)	
Gaseous	Besançon	Tavaux	246.46	
Gaseous	Pontarlier	Saint-Claude	59.36	

Gaseous	Pontarlier	Valdahon	518.01
Gaseous	Pontarlier	Villers-le-Lac	436.39
Gaseous	Valentigney	Bavans	705.51
Gaseous	Valentigney	Beaucourt	700.74
Gaseous	Valentigney	Héricourt	537.75

No.46 Set-E1-HC-LD

Standard fueling stations

City	Fueling technology	Hydrogen form	Facility size	Fueling rate (kg H_2/d)
Baume-les-Dames	Standard	Gaseous	ExtraLarge	1,000.00

Feedstock supply sites

City	Feedstock type	Supply rate (Nm^3/d)
Baume-les-Dames	NaturalGas	4,610.00

Production plants

City	Production technology	Hydrogen form	Facility size	Production rate (kg H_2/d)
Baume-les-Dames	SMR	Gaseous	Small	1,000.00

No.47 Set-E1-HC-MD

Standard fueling stations

City	Fueling technology	Hydrogen form	Facility size	Fueling rate (kg H_2/d)
Besançon	Standard	Gaseous	ExtraLarge	1,059.77
Champagnole	Standard	Gaseous	Medium	226.70
Valentigney	Standard	Gaseous	ExtraLarge	1,046.54

Feedstock supply sites

City	Feedstock type	Supply rate (Nm^3/d)
Besançon	NaturalGas	5,930.63
Valentigney	NaturalGas	4,824.55

Production plants

City	Production technology	Hydrogen form	Facility size	Production rate (kg H_2/d)
Besançon	SMR	Gaseous	Small	1,286.47
Valentigney	SMR	Gaseous	Small	1,046.54

Hydrogen transportation Number of vehicles = 1

Hydrogen form	Origin	Destination	Hydrogen flux (kg H_2/d)
Gaseous	Besançon	Champagnole	226.70

No.48 Set-E1-HC-HD

Standard fueling stations

City	Fueling technology	Hydrogen form	Facility size	Fueling rate (kg H_2/d)
Bavans	Standard	Gaseous	ExtraLarge	705.51
Beaucourt	Standard	Gaseous	ExtraLarge	700.74
Besançon	Standard	Gaseous	ExtraLarge	1,059.77
Héricourt	Standard	Gaseous	Large	537.75
Pontarlier	Standard	Gaseous	Large	384.10
Saint-Claude	Standard	Gaseous	Small	59.36
Tavaux	Standard	Gaseous	Medium	246.46
Valdahon	Standard	Gaseous	Large	518.01
Valentigney	Standard	Gaseous	ExtraLarge	1,046.54
Villers-le-Lac	Standard	Gaseous	Large	436.39

Feedstock supply sites

City	Feedstock type	Supply rate (Nm^3/d)
Besançon	NaturalGas	6,021.72
Pontarlier	NaturalGas	6,444.13
Valentigney	NaturalGas	13,786.39

Production plants

City	Production technology	Hydrogen form	Facility size	Production rate (kg H_2/d)
Besançon	SMR	Gaseous	Small	1,306.23
Pontarlier	SMR	Gaseous	Small	1,397.86
Valentigney	SMR	Gaseous	Medium	2,990.54

Hydrogen transportation Number of vehicles = 3

Hydrogen form	Origin	Destination	Hydrogen flux (kg H_2/d)
Gaseous	Besançon	Tavaux	246.46

Gaseous	Pontarlier	Saint-Claude	59.36
Gaseous	Pontarlier	Valdahon	518.01
Gaseous	Pontarlier	Villers-le-Lac	436.39
Gaseous	Valentigney	Bavans	705.51
Gaseous	Valentigney	Beaucourt	700.74
Gaseous	Valentigney	Héricourt	537.75

No.49 Set-E2-LC-LD

Standard fueling stations

City	Fueling technology	Hydrogen form	Facility size	Fueling rate (kg H_2/d)
Valdahon	Standard	Gaseous	ExtraLarge	1,000.00

Feedstock supply sites

City	Feedstock type	Supply rate (kg/d)
Valdahon	Biomass	13,880.00

Production plants

City	Production technology	Hydrogen form	Facility size	Production rate (kg H_2/d)
Valdahon	BG	Gaseous	Small	1,000.00

No.50 Set-E2-LC-MD

Standard fueling stations

City	Fueling technology	Hydrogen form	Facility size	Fueling rate (kg H_2/d)
Besançon	Standard	Gaseous	ExtraLarge	1,141.76
Héricourt	Standard	Gaseous	Large	537.75
Pontarlier	Standard	Gaseous	Large	384.10
Villers-le-Lac	Standard	Gaseous	Large	436.39

Feedstock supply sites

City	Feedstock type	Supply rate (kg/d)
Valdahon	Biomass	34,700.00

Production plants

City	Production technology	Hydrogen form	Facility size	Production rate (kg H_2/d)
Valdahon	BG	Gaseous	Medium	2,500.00

Hydrogen transportation Number of vehicles = 3

Hydrogen form	Origin	Destination	Hydrogen flux (kg H_2/d)
Gaseous	Valdahon	Besançon	1,141.76
Gaseous	Valdahon	Héricourt	537.75
Gaseous	Valdahon	Pontarlier	384.10
Gaseous	Valdahon	Villers-le-Lac	436.39

No.51 Set-E2-LC-HD

Standard fueling stations

City	Fueling technology	Hydrogen form	Facility size	Fueling rate (kg H_2/d)
Bavans	Standard	Gaseous	ExtraLarge	705.51
Beaucourt	Standard	Gaseous	ExtraLarge	700.74
Besançon	Standard	Gaseous	ExtraLarge	1,059.77
Héricourt	Standard	Gaseous	Large	537.75
Pontarlier	Standard	Gaseous	Large	384.10
Saint-Claude	Standard	Gaseous	Small	59.36
Tavaux	Standard	Gaseous	Medium	246.46
Valdahon	Standard	Gaseous	Large	518.01
Valentigney	Standard	Gaseous	ExtraLarge	1,046.54
Villers-le-Lac	Standard	Gaseous	Large	436.39

Feedstock supply sites

City	Feedstock type	Supply rate (kg/d)
Luxeuil-les-Bains	Biomass	13,880.00
Valdahon	Biomass	65,161.46

Production plants

City	Production technology	Hydrogen form	Facility size	Production rate (kg H_2/d)
Luxeuil-les-Bains	BG	Gaseous	Small	1,000.00
Valdahon	BG	Gaseous	Large	4,694.63

Hydrogen transportation Number of vehicles = 7

Hydrogen form	Origin	Destination	Hydrogen flux (kg H_2/d)

Gaseous	Luxeuil-les-Bains	Beaucourt	462.25
Gaseous	Luxeuil-les-Bains	Héricourt	537.75
Gaseous	Valdahon	Bavans	705.51
Gaseous	Valdahon	Beaucourt	238.49
Gaseous	Valdahon	Besançon	1,059.77
Gaseous	Valdahon	Pontarlier	384.10
Gaseous	Valdahon	Saint-Claude	59.36
Gaseous	Valdahon	Tavaux	246.46
Gaseous	Valdahon	Valentigney	1,046.54
Gaseous	Valdahon	Villers-le-Lac	436.39

No.52 Set-E2-HC-LD

Standard fueling stations

City	Fueling technology	Hydrogen form	Facility size	Fueling rate (kg H_2/d)
Valdahon	Standard	Gaseous	ExtraLarge	1,000.00

Feedstock supply sites

City	Feedstock type	Supply rate (kg/d)
Valdahon	Biomass	13,880.00

Production plants

City	Production technology	Hydrogen form	Facility size	Production rate (kg H_2/d)
Valdahon	BG	Gaseous	Small	1,000.00

No.53 Set-E2-HC-MD

Standard fueling stations

City	Fueling technology	Hydrogen form	Facility size	Fueling rate (kg H_2/d)
Baume-les-Dames	Standard	Gaseous	Large	597.05
Pontarlier	Standard	Gaseous	Large	384.10
Valdahon	Standard	Gaseous	Large	518.01
Valentigney	Standard	Gaseous	ExtraLarge	1,046.54

Feedstock supply sites

City	Feedstock type	Supply rate (kg/d)
Valdahon	Biomass	35,334.32

Production plants

City	Production technology	Hydrogen form	Facility size	Production rate (kg H_2/d)
Valdahon	BG	Gaseous	Medium	2,545.70

CO2 storage reservoirs

City	Processing rate (kg CO2/d)
Morteau	54,987.12

Hydrogen transportation Number of vehicles = 3

Hydrogen form	Origin	Destination	Hydrogen flux (kg H_2/d)
Gaseous	Valdahon	Baume-les-Dames	597.05
Gaseous	Valdahon	Pontarlier	384.10
Gaseous	Valdahon	Valentigney	1,046.54

CO_2 transportation Length of CO_2 pipeline = 32 km

Origin	Destination	CO_2 flux (kg CO_2/d)
Valdahon	Morteau	54,987.12

No.54 Set-E2-HC-HD

Standard fueling stations

City	Fueling technology	Hydrogen form	Facility size	Fueling rate (kg H_2/d)
Bavans	Standard	Gaseous	ExtraLarge	705.51
Beaucourt	Standard	Gaseous	ExtraLarge	700.74
Besançon	Standard	Gaseous	ExtraLarge	1,059.77
Héricourt	Standard	Gaseous	Large	537.75
Pontarlier	Standard	Gaseous	Large	384.10
Saint-Loup-sur-Semouse	Standard	Gaseous	Small	74.57
Tavaux	Standard	Gaseous	Medium	246.46
Valdahon	Standard	Gaseous	Large	518.01
Valentigney	Standard	Gaseous	ExtraLarge	1,046.54
Villers-le-Lac	Standard	Gaseous	Large	436.39

Feedstock supply sites

City	Feedstock type	Supply rate (kg/d)		
Luxeuil-les-Bains	Biomass	13,880.00		
Valdahon	Biomass	65,372.58		
Production plants				
City	Production technology	Hydrogen form	Facility size	Production rate (kg H_2/d)
Luxeuil-les-Bains	BG	Gaseous	Small	1,000.00
Valdahon	BG	Gaseous	Large	4,709.84
CO2 storage reservoirs				
City	Processing rate (kg CO2/d)			
Morteau	101,732.54			
Hydrogen transportation	Number of vehicles = 7			
Hydrogen form	Origin	Destination	Hydrogen flux (kg H_2/d)	
Gaseous	Luxeuil-les-Bains	Beaucourt	387.68	
Gaseous	Luxeuil-les-Bains	Héricourt	537.75	
Gaseous	Luxeuil-les-Bains	Saint-Loup-sur-Semouse	74.57	
Gaseous	Valdahon	Bavans	705.51	
Gaseous	Valdahon	Beaucourt	313.06	
Gaseous	Valdahon	Besançon	1,059.77	
Gaseous	Valdahon	Pontarlier	384.10	
Gaseous	Valdahon	Tavaux	246.46	
Gaseous	Valdahon	Valentigney	1,046.54	
Gaseous	Valdahon	Villers-le-Lac	436.39	
CO_2 transportation	Length of CO_2 pipeline = 32 km			
Origin	Destination	CO_2 flux (kg CO_2/d)		
Valdahon	Morteau	101,732.54		

No.55 Set-F-LC-LD

Standard fueling stations				
City	Fueling technology	Hydrogen form	Facility size	Fueling rate (kg H_2/d)
Pontarlier	Standard	Gaseous	Large	384.10
Saint-Loup-sur-Semouse	Standard	Gaseous	Small	74.57
Feedstock supply sites				
City	Feedstock type	Supply rate (Nm^3/d)		
Pontarlier	NaturalGas	6,724.47		
Production plants				
City	Production technology	Hydrogen form	Facility size	Production rate (kg H_2/d)
Pontarlier	SMR	Gaseous	Small	1,458.67
Hydrogen transportation	Number of vehicles = 1			
Hydrogen form	Origin	Destination	Hydrogen flux (kg H_2/d)	
Gaseous	Pontarlier	Saint-Claude	500.00	
Gaseous	Pontarlier	Saint-Loup-sur-Semouse	74.57	

No.56 Set-F-LC-MD

Standard fueling stations				
City	Fueling technology	Hydrogen form	Facility size	Fueling rate (kg H_2/d)
Héricourt	Standard	Gaseous	Large	537.75
Pontarlier	Standard	Gaseous	Large	384.10
Valdahon	Standard	Gaseous	Large	518.01
Valentigney	Standard	Gaseous	ExtraLarge	1,046.54
Feedstock supply sites				
City	Feedstock type	Supply rate (Nm^3/d)		
Pontarlier	NaturalGas	8,768.73		
Valentigney	NaturalGas	7,303.58		
Production plants				
City	Production technology	Hydrogen form	Facility size	Production rate (kg H_2/d)
Pontarlier	SMR	Gaseous	Small	1,902.11
Valentigney	SMR	Gaseous	Small	1,584.29
Hydrogen transportation	Number of vehicles = 2			
Hydrogen form	Origin	Destination	Hydrogen flux (kg H_2/d)	
Gaseous	Pontarlier	Saint-Claude	500.00	
Gaseous	Pontarlier	Valdahon	518.01	

Gaseous	Valentigney	Héricourt	537.75	

No.57 Set-F-LC-HD

Standard fueling stations

City	Fueling technology	Hydrogen form	Facility size	Fueling rate (kg H_2/d)
Bavans	Standard	Gaseous	ExtraLarge	705.51
Beaucourt	Standard	Gaseous	ExtraLarge	700.74
Besançon	Standard	Gaseous	ExtraLarge	1,059.77
Héricourt	Standard	Gaseous	Large	537.75
Pontarlier	Standard	Gaseous	Large	384.10
Saint-Claude	Standard	Gaseous	Small	59.36
Tavaux	Standard	Gaseous	Medium	246.46
Valdahon	Standard	Gaseous	Large	518.01
Valentigney	Standard	Gaseous	ExtraLarge	1,046.54
Villers-le-Lac	Standard	Gaseous	Large	436.39

Feedstock supply sites

City	Feedstock type	Supply rate (Nm^3/d)
Besançon	NaturalGas	8,409.75
Pontarlier	NaturalGas	8,666.11
Valentigney	NaturalGas	13,786.39

Production plants

City	Production technology	Hydrogen form	Facility size	Production rate (kg H_2/d)
Besançon	SMR	Gaseous	Small	1,824.24
Pontarlier	SMR	Gaseous	Small	1,879.85
Valentigney	SMR	Gaseous	Medium	2,990.54

Hydrogen transportation Number of vehicles = 4

Hydrogen form	Origin	Destination	Hydrogen flux (kg H_2/d)
Gaseous	Besançon	Tavaux	246.46
Gaseous	Besançon	Valdahon	518.01
Gaseous	Pontarlier	Saint-Claude	559.36
Gaseous	Pontarlier	Villers-le-Lac	436.39
Gaseous	Valentigney	Bavans	705.51
Gaseous	Valentigney	Beaucourt	700.74
Gaseous	Valentigney	Héricourt	537.75

No.58 Set-F-HC-LD

Standard fueling stations

City	Fueling technology	Hydrogen form	Facility size	Fueling rate (kg H_2/d)
Pontarlier	Standard	Gaseous	Large	384.10
Saint-Loup-sur-Semouse	Standard	Gaseous	Small	74.57

Feedstock supply sites

City	Feedstock type	Supply rate (Nm^3/d)
Pontarlier	NaturalGas	6,724.47

Production plants

City	Production technology	Hydrogen form	Facility size	Production rate (kg H_2/d)
Pontarlier	SMR	Gaseous	Small	1,458.67

Hydrogen transportation Number of vehicles = 1

Hydrogen form	Origin	Destination	Hydrogen flux (kg H_2/d)
Gaseous	Pontarlier	Saint-Claude	500.00
Gaseous	Pontarlier	Saint-Loup-sur-Semouse	74.57

No.59 Set-F-HC-MD

Standard fueling stations

City	Fueling technology	Hydrogen form	Facility size	Fueling rate (kg H_2/d)
Lure	Standard	Gaseous	Large	379.13
Pontarlier	Standard	Gaseous	Large	384.10
Saint-Vit	Standard	Gaseous	Large	553.44
Valentigney	Standard	Gaseous	ExtraLarge	1,046.54

Feedstock supply sites

City	Feedstock type	Supply rate (Nm^3/d)
Pontarlier	NaturalGas	8,932.06

Valentigney	NaturalGas	6,572.34		
Production plants				
City	Production technology	Hydrogen form	Facility size	Production rate (kg H_2/d)
Pontarlier	SMR	Gaseous	Small	1,937.54
Valentigney	SMR	Gaseous	Small	1,425.67
Hydrogen transportation	Number of vehicles = 3			
Hydrogen form	Origin	Destination	Hydrogen flux (kg H_2/d)	
Gaseous	Pontarlier	Saint-Claude	500.00	
Gaseous	Pontarlier	Saint-Vit	553.44	
Gaseous	Valentigney	Lure	379.13	

No.60 Set-F-HC-HD

Standard fueling stations				
City	Fueling technology	Hydrogen form	Facility size	Fueling rate (kg H_2/d)
Bavans	Standard	Gaseous	ExtraLarge	705.51
Beaucourt	Standard	Gaseous	ExtraLarge	700.74
Besançon	Standard	Gaseous	ExtraLarge	1,059.77
Héricourt	Standard	Gaseous	Large	537.75
Pontarlier	Standard	Gaseous	Large	384.10
Saint-Claude	Standard	Gaseous	Small	59.36
Tavaux	Standard	Gaseous	Medium	246.46
Valdahon	Standard	Gaseous	Large	518.01
Valentigney	Standard	Gaseous	ExtraLarge	1,046.54
Villers-le-Lac	Standard	Gaseous	Large	436.39
Feedstock supply sites				
City	Feedstock type	Supply rate (Nm^3/d)		
Besançon	NaturalGas	8,409.75		
Pontarlier	NaturalGas	8,666.11		
Valentigney	NaturalGas	13,786.39		
Production plants				
City	Production technology	Hydrogen form	Facility size	Production rate (kg H_2/d)
Besançon	SMR	Gaseous	Small	1,824.24
Pontarlier	SMR	Gaseous	Small	1,879.85
Valentigney	SMR	Gaseous	Medium	2,990.54
Hydrogen transportation	Number of vehicles = 4			
Hydrogen form	Origin	Destination	Hydrogen flux (kg H_2/d)	
Gaseous	Besançon	Tavaux	246.46	
Gaseous	Besançon	Valdahon	518.01	
Gaseous	Pontarlier	Saint-Claude	559.36	
Gaseous	Pontarlier	Villers-le-Lac	436.39	
Gaseous	Valentigney	Bavans	705.51	
Gaseous	Valentigney	Beaucourt	700.74	
Gaseous	Valentigney	Héricourt	537.75	

No.61 Set-G-LC-LD

Standard fueling stations				
City	Fueling technology	Hydrogen form	Facility size	Fueling rate (kg H_2/d)
Pontarlier	Standard	Gaseous	Large	384.10
Saint-Loup-sur-Semouse	Standard	Gaseous	Small	74.57
Feedstock supply sites				
City	Feedstock type	Supply rate (Nm^3/d)		
Pontarlier	NaturalGas	6,724.47		
Production plants				
City	Production technology	Hydrogen form	Facility size	Production rate (kg H_2/d)
Pontarlier	SMR	Gaseous	Small	1,458.67
Hydrogen transportation	Number of vehicles = 1			
Hydrogen form	Origin	Destination	Hydrogen flux (kg H_2/d)	
Gaseous	Pontarlier	Saint-Claude	500.00	
Gaseous	Pontarlier	Saint-Loup-sur-Semouse	74.57	

No.62 Set-G-LC-MD

Standard fueling stations

City	Fueling technology	Hydrogen form	Facility size	Fueling rate (kg H_2/d)
Héricourt	Standard	Gaseous	Large	537.75
Pontarlier	Standard	Gaseous	Large	384.10
Valdahon	Standard	Gaseous	Large	518.01
Valentigney	Standard	Gaseous	ExtraLarge	1,046.54

Feedstock supply sites

City	Feedstock type	Supply rate (Nm^3/d)
Pontarlier	NaturalGas	8,768.73
Valentigney	NaturalGas	7,303.58

Production plants

City	Production technology	Hydrogen form	Facility size	Production rate (kg H_2/d)
Pontarlier	SMR	Gaseous	Small	1,902.11
Valentigney	SMR	Gaseous	Small	1,584.29

Hydrogen transportation Number of vehicles = 2

Hydrogen form	Origin	Destination	Hydrogen flux (kg H_2/d)
Gaseous	Pontarlier	Saint-Claude	500.00
Gaseous	Pontarlier	Valdahon	518.01
Gaseous	Valentigney	Héricourt	537.75

No.63 Set-G-LC-HD

Standard fueling stations

City	Fueling technology	Hydrogen form	Facility size	Fueling rate (kg H_2/d)
Bavans	Standard	Gaseous	ExtraLarge	705.51
Beaucourt	Standard	Gaseous	ExtraLarge	700.74
Besançon	Standard	Gaseous	ExtraLarge	1,059.77
Héricourt	Standard	Gaseous	Large	537.75
Pontarlier	Standard	Gaseous	Large	384.10
Saint-Claude	Standard	Gaseous	Small	59.36
Tavaux	Standard	Gaseous	Medium	246.46
Valdahon	Standard	Gaseous	Large	518.01
Valentigney	Standard	Gaseous	ExtraLarge	1,046.54
Villers-le-Lac	Standard	Gaseous	Large	436.39

Feedstock supply sites

City	Feedstock type	Supply rate (Nm^3/d)
Besançon	NaturalGas	8,409.75
Pontarlier	NaturalGas	8,666.11
Valentigney	NaturalGas	13,786.39

Production plants

City	Production technology	Hydrogen form	Facility size	Production rate (kg H_2/d)
Besançon	SMR	Gaseous	Small	1,824.24
Pontarlier	SMR	Gaseous	Small	1,879.85
Valentigney	SMR	Gaseous	Medium	2,990.54

Hydrogen transportation Number of vehicles = 4

Hydrogen form	Origin	Destination	Hydrogen flux (kg H_2/d)
Gaseous	Besançon	Tavaux	246.46
Gaseous	Besançon	Valdahon	518.01
Gaseous	Pontarlier	Saint-Claude	559.36
Gaseous	Pontarlier	Villers-le-Lac	436.39
Gaseous	Valentigney	Bavans	705.51
Gaseous	Valentigney	Beaucourt	700.74
Gaseous	Valentigney	Héricourt	537.75

No.64 Set-G-HC-LD

Standard fueling stations

City	Fueling technology	Hydrogen form	Facility size	Fueling rate (kg H_2/d)
Pontarlier	Standard	Gaseous	Large	384.10
Saint-Loup-sur-Semouse	Standard	Gaseous	Small	74.57

Feedstock supply sites

City	Feedstock type	Supply rate (Nm^3/d)
Pontarlier	NaturalGas	6,724.47

Production plants

City	Production technology	Hydrogen form	Facility size	Production rate (kg H_2/d)
Pontarlier	SMR	Gaseous	Small	1,458.67

Hydrogen transportation Number of vehicles = 1

Hydrogen form	Origin	Destination	Hydrogen flux (kg H_2/d)
Gaseous	Pontarlier	Saint-Claude	500.00
Gaseous	Pontarlier	Saint-Loup-sur-Semouse	74.57

No.65 Set-G-HC-MD

Standard fueling stations

City	Fueling technology	Hydrogen form	Facility size	Fueling rate (kg H_2/d)
Baume-les-Dames	Standard	Gaseous	Large	600.00
Pontarlier	Standard	Gaseous	Large	600.00
Valentigney	Standard	Gaseous	ExtraLarge	1,200.00
Villers-le-Lac	Standard	Gaseous	Large	600.00

Feedstock supply sites

City	Feedstock type	Supply rate (kg/d)
Valdahon	Biomass	55,520.00

Production plants

City	Production technology	Hydrogen form	Facility size	Production rate (kg H_2/d)
Morteau	BG	Gaseous	Large	4,000.00

CO2 storage reservoirs

City	Processing rate (kg CO2/d)
Morteau	86,400.00

Hydrogen transportation Number of vehicles = 5

Hydrogen form	Origin	Destination	Hydrogen flux (kg H_2/d)
Gaseous	Morteau	Baume-les-Dames	600.00
Gaseous	Morteau	Pontarlier	1,100.00
Gaseous	Morteau	Saint-Claude	500.00
Gaseous	Morteau	Valentigney	1,200.00
Gaseous	Morteau	Villers-le-Lac	600.00

Feedstock transportation Number of vehicles = 2

Feedstock type	Origin	Destination	Feedstock flux (kg/d)
Biomass	Valdahon	Morteau	55,520.00

No.66 Set-G-HC-HD

Standard fueling stations

City	Fueling technology	Hydrogen form	Facility size	Fueling rate (kg H_2/d)
Bavans	Standard	Gaseous	ExtraLarge	705.51
Beaucourt	Standard	Gaseous	ExtraLarge	700.74
Besançon	Standard	Gaseous	ExtraLarge	1,059.77
Héricourt	Standard	Gaseous	Large	537.75
Pontarlier	Standard	Gaseous	Large	384.10
Saint-Claude	Standard	Gaseous	Small	59.36
Tavaux	Standard	Gaseous	Medium	246.46
Valdahon	Standard	Gaseous	Large	518.01
Valentigney	Standard	Gaseous	ExtraLarge	1,046.54
Villers-le-Lac	Standard	Gaseous	Large	436.39

Feedstock supply sites

City	Feedstock type	Supply rate (kg/d)
Luxeuil-les-Bains	Biomass	23,521.46
Valdahon	Biomass	69,400.00

Production plants

City	Production technology	Hydrogen form	Facility size	Production rate (kg H_2/d)
Morteau	BG	Gaseous	Large	5,000.00
Villers-le-Lac	BG	Gaseous	Small	1,694.63

CO2 storage reservoirs

City	Processing rate (kg CO2/d)
Morteau	144,604.01

Hydrogen transportation Number of vehicles = 9

Hydrogen form	Origin	Destination	Hydrogen flux (kg H_2/d)

Gaseous	Morteau	Bavans	98.01
Gaseous	Morteau	Beaucourt	50.00
Gaseous	Morteau	Besançon	1,059.77
Gaseous	Morteau	Héricourt	537.75
Gaseous	Morteau	Pontarlier	884.10
Gaseous	Morteau	Saint-Claude	559.36
Gaseous	Morteau	Tavaux	246.46
Gaseous	Morteau	Valdahon	518.01
Gaseous	Morteau	Valentigney	1,046.54
Gaseous	Villers-le-Lac	Bavans	607.50
Gaseous	Villers-le-Lac	Beaucourt	650.74

Feedstock transportation	Number of vehicles = 3		
Feedstock type	Origin	Destination	Feedstock flux (kg/d)
Biomass	Luxeuil-les-Bains	Villers-le-Lac	23,521.46
Biomass	Valdahon	Morteau	69,400.00

CO_2 transportation	Length of CO_2 pipeline = 7 km	
Origin	Destination	CO_2 flux (kg CO_2/d)
Villers-le-Lac	Morteau	36,604.01

C

Detailed results of case study in Chapter 4

C1. Instance results and performance of the two proposed approaches (FC-G-Ho)

Results_GA_FC-G-Ho-R1/NBS = 50/Max_Pop = 100/Max_iter = 150/Max_M = 12/Time = 225 s							
Solution	Coverage_GA (%)	Cost_GA (€/d)	Coverage_cplex (%)	Cost_cplex (€/d)	Time_cplex (s)	Cplex_sol_statu	Gap (%)
1	13.64	5,546.42	13.64	5,583.82	0.88	optimal	-
2	16.12	7,168.59	16.12	7,081.74	2.70	optimal	1.23
3	24.21	7,278.59	24.21	7,200.61	0.47	optimal	1.08
4	30.89	11,187.80	30.89	9,541.01	4.49	optimal	17.26
5	47.09	11,291.30	47.09	11,289.52	0.52	optimal	0.02
6	58.26	15,286.00	58.26	15,260.21	4.81	optimal	0.17
7	68.57	19,299.70	68.57	17,822.12	7.02	optimal	8.29
8	76.86	23,324.40	76.85	21,345.38	7.25	optimal	9.27
9	81.48	27,340.10	81.48	24,901.93	7,214.98	0.0057	9.79
10	91.30	33,076.00	91.30	31,042.76	27.31	optimal	6.55
11	94.51	44,720.80	94.51	34,902.79	7,213.75	0.0063	28.13
12	96.26	48,839.30	96.26	38,147.49	7,216.16	0.0081	28.03
13	96.99	50,281.50	96.99	38,974.58	7,209.28	0.0107	29.01
14	97.49	50,589.00	97.49	40,366.82	7,202.56	0.0078	25.32
15	97.57	51,771.30	97.57	40,366.82	3,116.53	optimal	28.25
16	99.15	56,311.90	99.15	45,363.31	7,208.81	0.0077	24.14
17	99.87	59,355.50	99.87	49,073.32	7,205.14	0.0070	20.95
18	100.00	63,455.10	100.00	50,637.10	7,211.89	0.0117	25.31
Resultats_ALNS_FC-G-Ho_R1/Nb_iter_max = 150/W1 = 1.3/W2 = 0.9/Time = 2,472 s							
Solution	Coverage_ALNS (%)	Cost_ALNS (€/d)	Coverage_cplex (%)	Cost_cplex (€/d)	Time_cplex (s)	Cplex_sol_statu	Gap (%)
1	24.21	7,199.73	24.21	7,200.61	0.47	optimal	-
2	47.09	11,288.60	47.09	11,289.52	0.52	optimal	-
3	68.57	19,428.30	68.57	17,822.12	7.02	optimal	9.01

(FC-G-He)

Results_GA_FC-G-He-R1/NBS = 50/Max_Pop = 100/Max_iter = 150/Max_M = 12/time = 259 s							
Solution	Coverage_GA (%)	Cost_GA (€/d)	Coverage_cplex (%)	Cost_cplex (€/d)	Time_cplex (s)	Cplex_sol_statu	Gap (%)
1	13.64	5,326.93	13.64	5,364.31	0.31	optimal	-
2	16.12	7,168.59	16.12	7,020.60	2.08	optimal	2.11
3	24.21	7,278.59	24.21	7,200.61	0.75	optimal	1.08
4	27.38	9,303.64	27.38	8,966.22	3.75	optimal	3.76
5	29.95	10,757.70	29.95	9,095.28	1.61	optimal	18.28
6	36.84	11,181.30	36.84	11,052.57	4.72	optimal	1.16
7	47.09	11,291.30	47.09	11,289.52	0.41	optimal	0.02
8	58.26	15,286.00	58.26	15,235.30	3.22	optimal	0.33
9	68.57	19,299.70	68.57	17,602.63	3.53	optimal	9.64
10	76.86	23,324.40	76.85	21,345.38	5.23	optimal	9.27
11	81.48	27,340.10	81.48	24,803.31	152.44	optimal	10.23
12	91.30	33,552.30	91.30	31,042.76	35.69	optimal	8.08
13	93.16	43,085.80	93.16	32,940.84	75.75	optimal	30.80
14	94.90	46,676.10	94.90	36,225.38	7,205.47	0.0068	28.85
15	94.99	46,904.70	94.99	36,225.38	2,221.03	0.0001	29.48
16	95.33	47,260.40	95.33	36,461.98	7,206.92	0.0100	29.62
17	99.33	52,571.70	99.33	46,950.79	7,210.03	0.0092	11.97
18	99.77	54,974.30	99.77	48,921.65	7,205.06	0.0065	12.37
19	100.00	61,306.20	100.00	50,637.10	7,206.14	0.0086	21.07

Resultats_ALNS_FC-G-He_R1/Nb_iter_max = 150/W1 = 1.3/W2 = 0.9/time = 2,145 s							
Solution	Coverage_ALNS (%)	Cost_ALNS (€/d)	Coverage_cplex (%)	Cost_cplex (€/d)	Time_cplex (s)	Cplex_sol_statu	Gap (%)
1	24.21	7,199.73	24.21	7,200.61	0.75	optimal	-
2	47.09	11,288.60	47.09	11,289.52	0.41	optimal	-
3	68.57	19,428.30	68.57	17,602.63	3.53	optimal	10.37

(FC-L-Ho)

Results_GA_FC-L-Ho-R1/NBS = 50/Max_Pop = 100/Max_iter = 150/Max_M = 12/time = 353 s							
Solution	Coverage_GA (%)	Cost_GA (€/d)	Coverage_cplex (%)	Cost_cplex (€/d)	Time_cplex (s)	Cplex_sol_statu	Gap (%)
1	8.77	46,011.80	8.77	45,923.13	0.41	optimal	0.19
2	16.12	47,359.10	16.12	47,391.07	1.17	optimal	-
3	24.21	47,469.10	24.21	47,391.07	0.45	optimal	0.16
4	39.04	50,410.10	39.04	50,448.18	2.31	optimal	-
5	47.09	50,416.10	47.09	50,465.30	0.52	optimal	-
6	58.26	53,386.20	58.26	53,424.28	2.67	optimal	-
7	68.57	56,713.60	68.57	55,062.22	2.09	optimal	3.00
8	69.40	58,207.00	69.40	56,732.08	117.23	optimal	2.60
9	71.65	58,608.00	71.65	56,817.10	5.56	optimal	3.15
10	76.86	59,685.70	76.85	58,339.10	5.00	optimal	2.31
11	81.48	62,634.70	81.48	61,236.45	446.36	optimal	2.28
12	85.44	66,087.00	85.44	62,790.36	342.81	optimal	5.25
13	91.30	67,485.40	91.30	65,849.82	3,388.94	optimal	2.48
14	95.30	76,776.80	95.30	70,311.62	7,202.50	0.0022	9.20
15	95.82	80,855.60	95.82	70,629.20	7,202.58	0.0031	14.48
16	96.66	81,339.30	96.66	72,060.58	7,208.03	0.0023	12.88
17	96.86	81,396.10	96.86	72,152.51	7,207.70	0.0032	12.81
18	97.46	82,747.30	97.46	73,556.55	7,207.94	0.0052	12.49
19	99.32	84,205.70	99.32	78,018.01	7,204.75	0.0030	7.93
20	99.60	86,074.30	99.60	79,483.64	7,203.22	0.0028	8.29
21	100.00	94,260.30	100.00	82,385.25	7,209.84	0.0033	14.41
Resultats_ALNS_FC-L-Ho_R1/Nb_iter_max = 150/W1 = 1.3/W2 = 0.9/time = 1,122 s							
Solution	Coverage_ALNS (%)	Cost_ALNS (€/d)	Coverage_cplex (%)	Cost_cplex (€/d)	Time_cplex (s)	Cplex_sol_statu	Gap (%)
1	47.09	50,464.70	47.09	50,465.30	0.52	optimal	-
2	62.78	55,313.00	62.78	53,535.62	2.70	optimal	3.32
3	68.57	56,728.90	68.57	55,062.22	2.09	optimal	3.03
4	85.09	64,604.30	85.09	62,781.13	352.72	optimal	2.90
5	88.75	65,813.30	88.75	64,313.36	7,203.39	0.0022	2.33
6	89.09	67,627.80	89.09	64,313.36	2,101.45	0.0001	5.15
7	92.41	69,240.00	92.41	67,270.35	7,204.34	0.0015	2.93
8	95.08	72,406.80	95.08	70,311.62	7,202.53	0.0026	2.98
9	95.60	74,150.80	95.60	70,323.16	7,204.22	0.0015	5.44
10	96.31	75,655.90	96.31	72,060.57	7,201.98	0.0030	4.99
11	96.55	75,692.20	96.55	72,060.57	7,205.66	0.0026	5.04
12	98.13	76,915.00	98.13	75,024.80	7,204.14	0.0034	2.52
13	98.65	78,659.00	98.65	76,449.96	7,208.28	0.0026	2.89
14	99.43	81,779.00	99.43	79,403.57	7,206.94	0.0033	2.99
15	99.53	84,937.40	99.53	79,403.57	7,207.89	0.0031	6.97
16	100.00	87,979.70	100.00	82,385.25	7,209.84	0.0033	6.79

(FC-L-He)

Results_GA_FC-L-He-R2/NBS = 50/Max_Pop = 100/Max_iter = 150/Max_M = 12/time = 261 s							
Solution	Coverage_GA (%)	Cost_GA (€/d)	Coverage_cplex (%)	Cost_cplex (€/d)	Time_cplex (s)	Cplex_sol_statu	Gap (%)
1	13.64	45,792.30	13.64	45,829.74	0.99	optimal	-
2	16.12	47,186.60	16.12	47,218.64	2.81	optimal	-
3	24.21	47,296.60	24.21	47,218.64	1.08	optimal	0.17
4	47.09	50,450.70	47.09	50,448.87	1.11	optimal	0.00
5	58.26	53,586.70	58.26	53,424.28	5.86	optimal	0.30
6	58.73	55,847.20	58.73	53,424.28	5.24	optimal	4.54
7	68.57	56,741.70	68.57	55,062.22	3.97	optimal	3.05
8	70.01	59,012.10	70.01	56,574.15	158.95	optimal	4.31
9	76.86	59,969.30	76.85	58,166.67	6.28	optimal	3.10
10	81.48	63,187.90	81.48	61,125.60	1,136.30	optimal	3.37
11	82.27	65,014.30	82.27	61,166.75	7,208.81	0.0023	6.29
12	91.30	67,926.80	91.30	65,849.82	7,207.66	0.0027	3.15
13	93.71	77,250.20	93.71	68,774.49	7,209.59	0.0025	12.32
14	96.53	77,536.90	96.53	71,888.14	7,203.08	0.0037	7.86
15	96.94	80,090.00	96.94	71,980.08	7,202.59	0.0038	11.27
16	96.94	80,224.60	96.94	71,980.08	7,203.95	0.0038	11.45
17	97.42	81,373.40	97.42	73,348.52	7,203.75	0.0021	10.94
18	98.15	84,439.50	98.15	74,904.43	7,202.53	0.0037	12.73
19	98.30	85,178.90	98.30	74,904.43	7,205.59	0.0036	13.72
20	98.58	87,964.70	98.58	75,039.45	7,203.48	0.0040	17.22
21	98.62	89,487.30	98.62	76,339.11	7,201.81	0.0028	17.22
22	100.00	92,340.20	100.00	82,383.64	7,203.14	0.0045	12.09
Resultats_ALNS_FC-L-He_R1/Nb_iter_max = 150/W1 = 1.3/W2 = 0.9/time = 1,577 s							
Solution	Coverage_ALNS (%)	Cost_ALNS (€/d)	Coverage_cplex (%)	Cost_cplex (€/d)	Time_cplex (s)	Cplex_sol_statu	Gap (%)
1	24.21	47,218.10	24.21	47,218.64	1.08	optimal	-
2	27.56	48,730.80	27.56	48,771.53	3.97	optimal	-
3	47.09	50,448.30	47.09	50,448.87	1.11	optimal	-
4	57.40	53,678.50	57.40	53,418.35	8.92	optimal	0.49
5	61.61	55,117.50	61.61	53,519.82	5.02	optimal	2.99
6	68.57	56,618.30	68.57	55,062.22	3.97	optimal	2.83
7	71.91	58,131.10	71.91	56,653.90	2,408.17	optimal	2.61
8	88.75	65,986.40	88.75	64,293.97	7,206.47	0.0035	2.63
9	89.92	67,583.10	89.92	65,745.73	7,203.67	0.0034	2.79
10	93.22	69,116.90	93.22	67,343.11	7,202.97	0.0017	2.63
11	96.94	75,413.10	96.94	71,980.08	7,204.55	0.0038	4.77
12	97.52	78,912.20	97.52	73,384.12	7,202.59	0.0035	7.53
13	98.59	80,424.90	98.59	75,017.73	7,209.86	0.0039	7.21
14	99.17	81,742.60	99.17	77,917.73	7,204.25	0.0037	4.91
15	99.29	83,447.80	99.29	77,926.93	7,211.00	0.0036	7.08
16	99.52	83,582.10	99.52	79,410.52	7,208.72	0.0048	5.25
17	99.77	85,033.90	99.77	80,923.58	7,211.14	0.0045	5.08
18	99.92	86,534.20	99.92	80,906.19	7,203.28	0.0038	6.96
19	100.00	86,545.00	100.00	82,383.64	7,203.14	0.0045	5.05

(BFC-G-Ho)

Results_GA_BFC-G-Ho-R1/NBS = 50/Max_Pop = 100/Max_iter = 150/Max_M = 12/time = 1582 s							
Solution	Coverage_GA (%)	Cost_GA (€/d)	Coverage_cplex (%)	Cost_cplex (€/d)	Time_cplex (s)	Cplex_sol_statu	Gap (%)
1	6.40	6,586.28	6.40	6,457.52	7.27	optimal	1.99
2	9.88	8,173.45	9.88	8,046.99	39.95	optimal	1.57
3	17.49	8,215.45	17.49	8,291.63	4.00	optimal	-
4	29.30	12,217.20	29.30	12,160.27	45.95	optimal	0.47
5	30.77	12,263.20	30.77	12,259.38	27.27	optimal	0.03
6	32.83	16,150.90	32.83	12,356.09	10.22	optimal	30.71
7	41.02	16,297.90	41.02	16,065.11	211.27	optimal	1.45
8	43.21	21,441.20	43.21	16,314.93	7,204.98	0.0121	31.42
9	56.81	24,274.30	56.81	21,995.84	7,212.58	0.0142	10.36
10	63.18	26,714.80	63.18	24,494.95	590.25	optimal	9.06
11	72.93	34,624.20	72.93	30,970.36	7,205.31	0.0086	11.80
12	80.27	38,631.50	80.27	37,291.67	7,200.19	0.0080	3.59
13	83.77	51,317.60	83.77	40,997.68	7,201.63	0.0138	25.17
14	84.91	51,650.10	84.91	42,729.98	7,205.88	0.0253	20.88
15	85.54	52,930.80	85.54	42,808.03	7,204.47	0.0069	23.65
16	90.58	53,618.90	90.58	50,334.84	7,209.50	0.0170	6.52
17	90.95	71,857.90	90.95	51,585.23	7,207.81	0.0272	39.30
18	92.59	73,088.00	92.59	54,231.34	7,208.42	0.0220	34.77
19	95.10	80,235.60	95.10	59,401.68	7,210.86	0.0141	35.07
20	95.99	82,326.60	95.99	61,916.62	7,203.58	0.0170	32.96
21	96.57	85,566.00	96.57	63,737.27	7,201.59	0.0184	34.25
22	96.92	86,544.60	96.92	65,713.26	7,206.16	0.0302	31.70
23	97.02	98,293.80	97.02	65,872.97	7,203.86	0.0260	49.22
24	98.63	101,303.00	98.63	72,805.25	7,210.22	0.0219	39.14
25	99.37	102,940.00	99.37	79,660.28	7,203.92	0.0299	29.22
26	99.63	107,297.00	99.63	80,595.88	7,207.91	0.0141	33.13
27	99.86	110,464.00	99.86	86,368.05	7,202.28	0.0211	27.90
28	100.00	115,602.00	100.00	89,379.96	7,211.38	0.0166	29.34
Resultats_ALNS_BFC-G-Ho_R1/Nb_iter_max = 150/W1 = 1.3/W2 = 0.9/time = 21193 s							
Solution	Coverage_ALNS (%)	Cost_ALNS (€/d)	Coverage_cplex (%)	Cost_cplex (€/d)	Time_cplex (s)	Cplex_sol_statu	Gap (%)
1	3.03	6,278.74	3.03	6,279.48	9.09	optimal	-
2	6.33	8,369.96	6.33	6,457.52	7.13	optimal	29.62
3	17.49	8,290.91	17.49	8,291.63	4.00	optimal	-
4	20.50	10,367.60	20.50	10,368.39	57.84	optimal	-
5	31.29	14,601.70	31.29	12,346.87	14.00	optimal	18.26
6	41.02	16,218.50	41.02	16,065.11	211.27	optimal	0.95
7	42.04	18,569.40	42.04	16,261.59	158.53	optimal	14.19
8	55.72	22,658.30	55.72	21,900.45	7,206.19	0.0387	3.46
9	57.23	24,735.10	57.23	22,072.23	7,209.20	0.0111	12.06
10	60.57	26,685.30	60.57	24,134.81	7,202.05	0.0323	10.57
11	61.30	26,734.00	61.30	24,171.70	435.59	optimal	10.60
12	68.43	30,784.80	68.43	28,242.82	7,209.30	0.0230	9.00

(BFC-G-He)

Results_GA_BFC-G-He-R1/NBS = 50/Max_Pop = 100/Max_iter = 150/Max_M = 12/time = 1,811 s							
Solution	Coverage_GA (%)	Cost_GA (€/d)	Coverage_cplex (%)	Cost_cplex (€/d)	Time_cplex (s)	Cplex_sol_statu	Gap (%)
1	6.40	6,366.79	6.40	6,238.03	25.94	optimal	2.06
2	9.88	8,173.45	9.88	7,982.56	79.55	optimal	2.39
3	17.49	8,215.45	17.49	8,291.63	23.38	optimal	-
4	29.30	12,217.20	29.30	12,138.65	41.66	optimal	0.65
5	30.77	12,263.20	30.77	12,259.38	33.78	optimal	0.03
6	41.02	16,297.90	41.02	15,862.08	360.99	optimal	2.75
7	56.81	24,274.30	56.81	21,995.84	7,207.20	0.0054	10.36
8	63.18	26,495.30	63.18	24,494.95	109.81	optimal	8.17
9	72.93	34,404.80	72.93	30,750.87	871.89	optimal	11.88
10	80.27	38,662.90	80.27	37,291.67	7,203.69	0.0098	3.68
11	90.58	53,625.20	90.58	50,323.64	7,210.02	0.0168	6.56
12	93.70	75,075.40	93.70	56,788.76	7,206.02	0.0259	32.20
13	94.63	85,051.80	94.63	58,506.40	7,213.83	0.0180	45.37
14	98.69	94,160.10	98.69	72,334.67	7,208.86	0.0150	30.17
15	98.88	95,446.30	98.88	74,071.85	7,208.27	0.0174	28.86
16	99.74	111,031.00	99.74	84,187.04	7,212.94	0.0204	31.89
17	99.95	111,918.00	99.95	88,582.23	7,203.52	0.0209	26.34
18	100.00	116,019.00	100.00	89,306.45	7,204.56	0.0155	29.91
Resultats_ALNS_BFC-G-He_R1/Nb_iter_max = 150/W1 = 1.3/W2 = 0.9/time = 19,435 s							
Solution	Coverage_ALNS (%)	Cost_ALNS (€/d)	Coverage_cplex (%)	Cost_cplex (€/d)	Time_cplex (s)	Cplex_sol_statu	Gap (%)
1	3.03	6,278.74	3.03	5,938.05	43.48	optimal	5.74
2	15.75	9,889.59	15.75	8,267.18	25.84	optimal	19.62
3	30.77	12,258.60	30.77	12,259.38	33.78	optimal	-
4	41.02	16,218.50	41.02	15,862.08	360.99	optimal	2.25
5	68.43	30,565.30	68.43	27,975.15	7,207.11	0.0043	9.26

(BFC-L-Ho)

Results_GA_BFC-L-Ho-R1/NBS = 50/Max_Pop = 100/Max_iter = 150/Max_M = 12/time = 1,399 s							
Solution	Coverage_GA (%)	Cost_GA (€/d)	Coverage_cplex (%)	Cost_cplex (€/d)	Time_cplex (s)	Cplex_sol_statu	Gap (%)
1	9.88	61,679.00	9.88	61,611.46	11.17	optimal	0.11
2	17.49	61,721.00	17.49	61,797.18	4.31	optimal	-
3	29.30	64,688.00	29.30	64,750.23	9.92	optimal	-
4	30.77	64,703.00	30.77	64,750.23	3.33	optimal	-
5	41.02	67,710.10	41.02	67,761.23	54.80	optimal	-
6	56.81	73,987.60	56.81	72,605.20	7,204.64	0.0007	1.90
7	63.18	75,593.40	63.18	74,214.50	44.28	optimal	1.86
8	72.93	81,440.50	72.93	78,759.35	85.69	optimal	3.40
9	80.27	84,883.40	80.27	84,586.62	7,204.58	0.0017	0.35
10	90.58	96,638.90	90.58	95,308.69	7,208.06	0.0019	1.40
11	92.86	105,036.00	92.86	99,806.36	7,224.61	0.0080	5.24
12	93.88	116,123.00	93.88	101,381.97	7,226.13	0.0062	14.54
13	96.19	121,277.00	96.19	106,095.19	7,212.17	0.0024	14.31
14	98.10	131,905.00	98.10	112,030.90	7,210.61	0.0028	17.74
15	98.91	140,786.00	98.91	116,310.84	7,224.09	0.0032	21.04
16	98.94	150,513.00	98.94	116,262.04	7,216.64	0.0030	29.46
17	99.61	154,809.00	99.61	122,139.66	7,218.63	0.0034	26.75
18	99.93	160,634.00	99.93	128,101.76	7,228.48	0.0040	25.40
19	100.00	163,447.00	100.00	129,408.59	7,223.31	0.0032	26.30
Resultats_ALNS_BFC-L-Ho_R1/Nb_iter_max = 150/W1 = 1.3/W2 = 0.9/time = 28,764 s							
Solution	Coverage_ALNS (%)	Cost_ALNS (€/d)	Coverage_cplex (%)	Cost_cplex (€/d)	Time_cplex (s)	Cplex_sol_statu	Gap (%)
1	41.02	67,764.70	41.02	67,761.23	54.80	optimal	0.01
2	41.26	69,347.20	41.26	67,804.74	63.84	optimal	2.27
3	42.60	69,508.70	42.60	67,817.91	17.58	optimal	2.49
4	45.93	70,753.30	45.93	67,991.82	5.89	optimal	4.06
5	49.23	70,913.30	49.23	69,421.23	32.94	optimal	2.15
6	63.18	75,720.10	63.18	74,214.50	44.28	optimal	2.03
7	68.43	78,781.10	68.43	77,158.28	7,201.63	0.0012	2.10
8	68.57	80,399.60	68.57	77,158.28	7,202.39	0.0008	4.20
9	70.79	81,888.90	70.79	78,603.49	7,216.00	0.0036	4.18
10	73.34	83,483.90	73.34	80,060.22	7,207.74	0.0027	4.28
11	85.58	91,267.50	85.58	89,311.99	7,204.17	0.0021	2.19
12	90.73	97,671.40	90.73	95,426.30	7,204.77	0.0022	2.35

(BFC-L-He)

Results_GA_BFC-L-He-R1/NBS = 50/Max_Pop = 100/Max_iter = 150/Max_M = 12/time = 1,379 s							
Solution	Coverage_GA (%)	Cost_GA (€/d)	Coverage_cplex (%)	Cost_cplex (€/d)	Time_cplex (s)	Cplex_sol_statu	Gap (%)
1	6.40	60,147.30	6.40	60,018.51	10.30	optimal	0.21
2	9.88	61,506.60	9.88	61,439.03	27.27	optimal	0.11
3	17.49	61,548.60	17.49	61,624.75	11.17	optimal	-
4	29.30	64,691.60	29.30	64,639.38	23.42	optimal	0.08
5	30.77	64,737.60	30.77	64,639.38	13.81	optimal	0.15
6	34.18	67,471.00	34.18	66,219.14	7,209.45	0.0020	1.89
7	41.02	67,913.60	41.02	67,740.53	3,662.33	optimal	0.26
8	44.18	70,495.40	44.18	67,959.27	52.05	optimal	3.73
9	45.83	73,773.50	45.83	67,989.84	38.17	optimal	8.51
10	56.81	74,172.70	56.81	72,449.89	7,221.36	0.0017	2.38
11	63.18	76,044.00	63.18	74,103.65	421.44	optimal	2.62
12	72.93	82,091.60	72.93	78,734.70	2,920.52	optimal	4.26
13	80.27	85,085.20	80.27	84,586.62	7,205.39	0.0023	0.59
14	90.58	97,304.80	90.58	95,308.69	7,209.89	0.0030	2.09
15	94.93	115,615.00	94.93	103,025.54	7,214.83	0.0036	12.22
16	96.86	120,146.00	96.86	107,462.53	7,206.14	0.0030	11.80
17	98.48	130,758.00	98.48	113,541.95	7,272.42	0.0049	15.16
18	98.50	137,566.00	98.50	113,523.30	7,247.52	0.0045	21.18
19	98.86	141,078.00	98.86	116,451.48	7,232.61	0.0074	21.15
20	99.25	145,254.00	99.25	119,195.90	7,240.28	0.0046	21.86
21	99.75	149,544.00	99.75	125,266.89	7,263.52	0.0062	19.38
22	100.00	157,266.00	100.00	129,685.28	7,251.14	0.0055	21.27
Resultats_ALNS_BFC-L-He_R2/Nb_iter_max = 10/W1 = 1.3/W2 = 0.9/time = 7,026 s							
Solution	Coverage_ALNS (%)	Cost_ALNS (€/d)	Coverage_cplex (%)	Cost_cplex (€/d)	Time_cplex (s)	Cplex_sol_statu	Gap (%)
1	41.02	67,834.40	41.02	67,740.53	3,662.33	optimal	0.14
2	48.29	74,466.90	48.29	69,358.34	375.53	optimal	7.37
3	54.32	74,649.70	54.32	71,021.85	689.44	optimal	5.11
4	60.57	76,014.70	60.57	73,970.22	7,207.34	0.0020	2.76
5	61.96	77,758.70	61.96	74,024.24	981.11	optimal	5.04
6	68.43	78,978.90	68.43	77,093.23	7,206.92	0.0032	2.45
7	74.04	83,876.80	74.04	80,119.59	7,205.19	0.0031	4.69
8	82.27	88,675.00	82.27	86,151.81	7,221.02	0.0030	2.93
9	83.98	90,159.00	83.98	87,684.47	7,227.22	0.0034	2.82
10	88.36	94,971.10	88.36	92,247.76	7,204.86	0.0026	2.95
11	89.12	96,715.20	89.12	93,774.84	7,214.92	0.0065	3.14

C2. Configurations of hydrogen supply chain network

FC-G-Ho (Coverage = 16.12%)	
Stations opened:	Poligny, Saint-Vit
Delivery routes:	
Vehicle 1 (Capacity = 1,100 kg)	Tavaux->Dole->Saint-Vit->Besançon->Poligny->Tavaux
FC-G-Ho (Coverage = 47.09%)	
Stations opened:	Besançon, Valentigney
Delivery routes:	
Vehicle 1 (Capacity = 1,100 kg)	Tavaux->Dole->Saint-Vit->Besançon->Baume-les-Dames->Pont-de-Roide-Vermondans->Valentigney->Pont-de-Roide-Vermondans->Baume-les-Dames->Besançon->Saint-Vit->Dole->Tavaux
Vehicle 2 (Capacity = 1,100 kg)	Tavaux->Dole->Saint-Vit->Besançon->Saint-Vit->Dole->Tavaux
FC-G-Ho (Coverage = 91.30%)	
Stations opened:	Bavans, Beaucourt, Besançon, Dole, Héricourt, Luxeuil-les-Bains, Pontarlier, Valdahon, Valentigney, Villers-le-Lac
Delivery routes:	
Vehicle 1 (Capacity = 1,100 kg)	Tavaux->Dole->Saint-Vit->Besançon->Baume-les-Dames->Bavans->Baume-les-Dames->Besançon->Saint-Vit->Dole->Tavaux
Vehicle 2 (Capacity = 1,100 kg)	Tavaux->Dole->Saint-Vit->Besançon->Vesoul->Luxeuil-les-Bains->Lure->Héricourt->Montbéliard->Beaucourt->Hérimoncourt->Pont-de-Roide-Vermondans->Baume-les-Dames->Besançon->Saint-Vit->Dole->Tavaux
Vehicle 3 (Capacity = 1,100 kg)	Tavaux->Dole->Saint-Vit->Besançon->Saint-Vit->Dole->Tavaux
Vehicle 4 (Capacity = 1,100 kg)	Tavaux->Dole->Saint-Vit->Besançon->Baume-les-Dames->Bavans->Héricourt->Bavans->Pont-de-Roide-Vermondans->Maîche->Villers-le-Lac->Morteau->Valdahon->Besançon->Saint-Vit->Dole->Tavaux
Vehicle 5 (Capacity = 1,100 kg)	Tavaux->Dole->Saint-Vit->Besançon->Valdahon->Pontarlier->Champagnole->Poligny->Tavaux
Vehicle 6 (Capacity = 1,100 kg)	Tavaux->Dole->Saint-Vit->Besançon->Saint-Vit->Dole->Tavaux
Vehicle 7 (Capacity = 1,100 kg)	Tavaux->Dole->Saint-Vit->Besançon->Baume-les-Dames->Pont-de-Roide-Vermondans->Valentigney->Pont-de-Roide-Vermondans->Baume-les-Dames->Besançon->Saint-Vit->Dole->Tavaux
FC-G-He (Coverage = 16.12%)	
Stations opened:	Poligny, Saint-Vit
Delivery routes:	
Vehicle 1 (Capacity = 300 kg)	Tavaux->Poligny->Tavaux
Vehicle 2 (Capacity = 600 kg)	Tavaux->Dole->Saint-Vit->Dole->Tavaux
FC-G-He (Coverage = 47.09%)	
Stations opened:	Besançon, Valentigney

Delivery routes:

Vehicle 1 (Capacity = 1,100 kg): Tavaux->Dole->Saint-Vit->Besançon->Baume-les-Dames->Pont-de-Roide-Vermondans->Valentigney->Pont-de-Roide-Vermondans->Baume-les-Dames->Besançon->Saint-Vit->Dole->Tavaux

Vehicle 2 (Capacity = 1,100 kg): Tavaux->Dole->Saint-Vit->Besançon->Saint-Vit->Dole->Tavaux

---

FC-G-He (Coverage = 91.30%)

Stations opened: Bavans, Beaucourt, Besançon, Dole, Héricourt, Luxeuil-les-Bains, Pontarlier, Valdahon, Valentigney, Villers-le-Lac

Delivery routes:

Vehicle 1 (Capacity = 1,100 kg): Tavaux->Dole->Saint-Vit->Besançon->Baume-les-Dames->Bavans->Baume-les-Dames->Besançon->Saint-Vit->Dole->Tavaux

Vehicle 2 (Capacity = 1,100 kg): Tavaux->Dole->Saint-Vit->Besançon->Baume-les-Dames->Pont-de-Roide-Vermondans->Hérimoncourt->Beaucourt->Montbéliard->Héricourt->Lure->->Luxeuil-les-Bains->Vesoul->Besançon->Saint-Vit->Dole->Tavaux

Vehicle 3 (Capacity = 1,100 kg): Tavaux->Dole->Saint-Vit->Besançon->Saint-Vit->Dole->Tavaux

Vehicle 4 (Capacity = 1,100 kg): Tavaux->Dole->Saint-Vit->Besançon->Baume-les-Dames->Bavans->Héricourt->Bavans->Pont-de-Roide-Vermondans->Maîche->Villers-le-Lac->Morteau->Valdahon->Besançon->Saint-Vit->Dole->Tavaux

Vehicle 5 (Capacity = 1,100 kg): Tavaux->Dole->Saint-Vit->Besançon->Valdahon->Pontarlier->Champagnole->Poligny->Tavaux

Vehicle 6 (Capacity = 1,100 kg): Tavaux->Dole->Saint-Vit->Besançon->Saint-Vit->Dole->Tavaux

Vehicle 7 (Capacity = 1,100 kg): Tavaux->Dole->Saint-Vit->Besançon->Baume-les-Dames->Pont-de-Roide-Vermondans->Valentigney->Pont-de-Roide-Vermondans->Baume-les-Dames->Besançon->Saint-Vit->Dole->Tavaux

---

FC-L-Ho (Coverage = 16.12%)

Stations opened: Besançon

Delivery routes:

Vehicle 1 (Capacity = 3,500 kg): Tavaux->Dole->Saint-Vit->Besançon->Saint-Vit->Dole->Tavaux

---

FC-L-Ho (Coverage = 47.09%)

Stations opened: Besançon, Valentigney

Delivery routes:

Vehicle 1 (Capacity = 3,500 kg): Tavaux->Dole->Saint-Vit->Besançon->Baume-les-Dames->Pont-de-Roide-Vermondans->Valentigney->Pont-de-Roide-Vermondans->Baume-les-Dames->Besançon->Saint-Vit->Dole->Tavaux

---

FC-L-Ho (Coverage = 91.30%)

Stations opened: Bavans, Beaucourt, Besançon, Dole, Héricourt, Luxeuil-les-Bains, Pontarlier, Valdahon, Valentigney, Villers-le-Lac

Delivery routes:

Vehicle 1 (Capacity = 3,500 kg)	Tavaux->Dole->Saint-Vit->Besançon->Vesoul->Luxeuil-les-Bains->Lure->Héricourt->Montbéliard->Beaucourt->Valentigney->Bavans->Baume-les-Dames->Besançon->Saint-Vit->Dole->Tavaux
Vehicle 2 (Capacity = 3,500 kg)	Tavaux->Poligny->Champagnole->Pontarlier->Morteau->Villers-le-Lac->Morteau->Valdahon->Besançon->Saint-Vit->Dole->Tavaux

FC-L-He (Coverage = 16.12%)	
Stations opened:	Besançon
Delivery routes:	
Vehicle 1 (Capacity = 1,100 kg)	Tavaux->Dole->Saint-Vit->Besançon->Saint-Vit->Dole->Tavaux

FC-L-He (Coverage = 47.09%)	
Stations opened:	Besançon, Valentigney
Delivery routes:	
Vehicle 1 (Capacity = 1,100 kg)	Tavaux->Dole->Saint-Vit->Besançon->Saint-Vit->Dole->Tavaux
Vehicle 2 (Capacity = 1,100 kg)	Tavaux->Dole->Saint-Vit->Besançon->Baume-les-Dames->Pont-de-Roide-Vermondans->Valentigney->Pont-de-Roide-Vermondans->Baume-les-Dames->Besançon->Saint-Vit->Dole->Tavaux

FC-L-He (Coverage = 91.30%)	
Stations opened:	Bavans, Beaucourt, Besançon, Dole, Héricourt, Luxeuil-les-Bains, Pontarlier, Valdahon, Valentigney, Villers-le-Lac
Delivery routes:	
Vehicle 1 (Capacity = 3,500 kg)	Tavaux->Dole->Saint-Vit->Besançon->Vesoul->Luxeuil-les-Bains->Lure->Héricourt->Montbéliard->Beaucourt->Valentigney->Bavans->Baume-les-Dames->Besançon->Saint-Vit->Dole->Tavaux
Vehicle 2 (Capacity = 3,500 kg)	Tavaux->Dole->Saint-Vit->Besançon->Valdahon->Morteau->Villers-le-Lac->Morteau->Pontarlier->Champagnole->Poligny->Tavaux

BFC-G-Ho (Coverage = 9.88%)	
Stations opened:	Genlis, Is-sur-Tille
Delivery routes:	
Vehicle 1 (Capacity = 1,100 kg)	Tavaux->Genlis->Dijon->Is-sur-Tille->Dijon->Genlis->Tavaux

BFC-G-Ho (Coverage = 56.81%)	
Stations opened:	Héricourt, Poligny, Valdahon, Valentigney, Villers-le-Lac, Genlis, Chalon-sur-Saône, Le Creusot
Delivery routes:	
Vehicle 1 (Capacity = 1,100 kg)	Tavaux->Dole->Saint-Vit->Besançon->Baume-les-Dames->Bavans->Héricourt->Lure->Vesoul->Gray->Genlis->Tavaux
Vehicle 2 (Capacity = 1,100 kg)	Tavaux->Poligny->Champagnole->Pontarlier->Morteau->Villers-le-Lac->Morteau->Valdahon->Besançon->Saint-Vit->Dole->Tavaux

Vehicle 3 (Capacity = 1,100 kg)	Tavaux->Dole->Saint-Vit->Besançon->Baume-les-Dames->Pont-de-Roide-Vermondans->Valentigney->Pont-de-Roide-Vermondans->Baume-les-Dames->Besançon->Saint-Vit->Dole->Tavaux
Vehicle 4 (Capacity = 1,100 kg)	Tavaux->Chalon-sur-Saône->Montchanin->Le Creusot->Montchanin->Chalon-sur-Saône->Tavaux

BFC-G-Ho (Coverage = 90.58%)

Stations opened:	Bavans, Beaucourt, Besançon, Champagnole, Dole, Héricourt, Lons-le-Saunier, Luxeuil-les-Bains, Maîche, Valdahon, Valentigney, Villers-le-Lac, Beaune, Dijon, Chalon-sur-Saône, Gueugnon, Autun, Montchanin
Delivery routes:	
Vehicle 1 (Capacity = 1,100 kg)	Tavaux->Chalon-sur-Saône->Tavaux->Dole->Saint-Vit->Besançon->Valdahon->Besançon->Saint-Vit->Dole->Tavaux
Vehicle 2 (Capacity = 1,100 kg)	Tavaux->Dole->Saint-Vit->Besançon->Poligny->Champagnole->Poligny->Tavaux
Vehicle 3 (Capacity = 1,100 kg)	Tavaux->Dole->Saint-Vit->Besançon->Valdahon->Morteau->Villers-le-Lac->Maîche->Pont-de-Roide-Vermondans->Bavans->Baume-les-Dames->Besançon->Saint-Vit->Dole->Tavaux
Vehicle 4 (Capacity = 1,100 kg)	Tavaux->Dole->Saint-Vit->Besançon->Vesoul->Luxeuil-les-Bains->Lure->Héricourt->Montbéliard->Beaucourt->Hérimoncourt->Pont-de-Roide-Vermondans->Baume-les-Dames->Besançon->Saint-Vit->Dole->Tavaux
Vehicle 5 (Capacity = 1,100 kg)	Tavaux->Genlis->Dijon->Nuits-Saint-Georges->Beaune->Tavaux
Vehicle 6 (Capacity = 1,100 kg)	Tavaux->Dole->Saint-Vit->Besançon->Baume-les-Dames->Pont-de-Roide-Vermondans->Valentigney->Pont-de-Roide-Vermondans->Baume-les-Dames->Besançon->Saint-Vit->Dole->Tavaux
Vehicle 7 (Capacity = 1,100 kg)	Tavaux->Dole->Saint-Vit->Besançon->Baume-les-Dames->Bavans->Héricourt->Bavans->Pont-de-Roide-Vermondans->Maîche->Valdahon->Besançon->Saint-Vit->Dole->Tavaux
Vehicle 8 (Capacity = 1,100 kg)	Tavaux->Chalon-sur-Saône->Chagny->Autun->Gueugnon->Montceau-les-Mines->Montchanin->Chalon-sur-Saône->Tavaux
Vehicle 9 (Capacity = 1,100 kg)	Tavaux->Lons-le-Saunier->Tavaux->Dole->Tavaux

BFC-G-He (Coverage = 9.88%)

Stations opened:	Poligny, Genlis
Delivery routes:	
Vehicle 1 (Capacity = 300 kg)	Tavaux->Poligny->Tavaux
Vehicle 2 (Capacity = 600 kg)	Tavaux->Genlis->Tavaux

BFC-G-He (Coverage = 56.81%)

Stations opened:	Héricourt, Poligny, Valdahon, Valentigney, Villers-le-Lac, Genlis, Chalon-sur-Saône, Le Creusot
Delivery routes:	
Vehicle 1 (Capacity = 1,100 kg)	Tavaux->Dole->Saint-Vit->Besançon->Baume-les-Dames->Pont-de-Roide-Vermondans->Valentigney->Pont-de-Roide-Vermondans->Baume-les-Dames->Besançon->Saint-Vit->Dole->Tavaux

Vehicle 2 (Capacity = 1,100 kg)	Tavaux->Dole->Saint-Vit->Besançon->Baume-les-Dames->Bavans->Héricourt->Lure->Vesoul->Gray->Genlis->Tavaux
Vehicle 3 (Capacity = 1,100 kg)	Tavaux->Chalon-sur-Saône->Montchanin->Le Creusot->Montchanin->Chalon-sur-Saône->Tavaux
Vehicle 4 (Capacity = 1,100 kg)	Tavaux->Poligny->Champagnole->Pontarlier->Morteau->Villers-le-Lac->Morteau->Valdahon->Besançon->Saint-Vit->Dole->Tavaux

BFC-G-He (Coverage = 90.58%)

Stations opened: Bavans, Beaucourt, Besançon, Champagnole, Dole, Héricourt, Lons-le-Saunier, Luxeuil-les-Bains, Maîche, Valdahon, Valentigney, Villers-le-Lac, Beaune, Dijon, Chalon-sur-Saône, Gueugnon, Autun, Montchanin

Delivery routes:

Vehicle 1 (Capacity = 1,100 kg)	Tavaux->Dole->Saint-Vit->Besançon->Valdahon->Pontarlier->Champagnole->Lons-le-Saunier->Louhans->Chalon-sur-Saône->Montchanin->Montceau-les-Mines->Gueugnon->Autun->Chagny->Chalon-sur-Saône->Tavaux
Vehicle 2 (Capacity = 1,100 kg)	Tavaux->Chalon-sur-Saône->Montchanin->Chalon-sur-Saône->Tavaux
Vehicle 3 (Capacity = 1,100 kg)	Tavaux->Dole->Tavaux
Vehicle 4 (Capacity = 1,100 kg)	Tavaux->Dole->Saint-Vit->Besançon->Baume-les-Dames->Bavans->Pont-de-Roide-Vermondans->Maîche->Valdahon->Besançon->Saint-Vit->Dole->Tavaux
Vehicle 5 (Capacity = 1,100 kg)	Tavaux->Beaune->Nuits-Saint-Georges->Dijon->Genlis->Tavaux
Vehicle 6 (Capacity = 1,100 kg)	Tavaux->Dole->Saint-Vit->Besançon->Vesoul->Luxeuil-les-Bains->Lure->Héricourt->Montbéliard->Beaucourt->Hérimoncourt->Pont-de-Roide-Vermondans->Baume-les-Dames->Besançon->Saint-Vit->Dole->Tavaux
Vehicle 7 (Capacity = 1,100 kg)	Tavaux->Dole->Saint-Vit->Besançon->Baume-les-Dames->Pont-de-Roide-Vermondans->Valentigney->Pont-de-Roide-Vermondans->Baume-les-Dames->Besançon->Saint-Vit->Dole->Tavaux
Vehicle 8 (Capacity = 1,100 kg)	Tavaux->Poligny->Champagnole->Poligny->Besançon->Saint-Vit->Dole->Tavaux
Vehicle 9 (Capacity = 1,100 kg)	Tavaux->Dole->Saint-Vit->Besançon->Valdahon->Morteau->Villers-le-Lac->Maîche->Pont-de-Roide-Vermondans->Bavans->Héricourt->Héricourt->Bavans->Baume-les-Dames->Besançon->Saint-Vit->Dole->Tavaux

BFC-L-Ho (Coverage = 9.88%)

Stations opened: Dole

Delivery routes:

Vehicle 1 (Capacity = 3,500 kg)	Tavaux->Dole->Tavaux

BFC-L-Ho (Coverage = 56.81%)

Stations opened: Besançon, Valentigney, Villers-le-Lac, Dijon, Chalon-sur-Saône, Le Creusot

Delivery route:

Vehicle 1 (Capacity = 3,500 kg)	Tavaux->Dole->Saint-Vit->Besançon->Baume-les-Dames->Pont-de-Roide-Vermondans->Valentigney->Pont-de-Roide-Vermondans->Maîche->Villers-le-Lac->Morteau->Valdahon->Besançon->Saint-Vit->Dole->Tavaux
Vehicle 2 (Capacity = 3,500 kg)	Tavaux->Genlis->Dijon->Nuits-Saint-Georges->Beaune->Chagny->Le Creusot->Montchanin->Chalon-sur-Saône->Tavaux

BFC-L-Ho (Coverage = 90.58%)

Stations opened:	Bavans, Beaucourt, Besançon, Champagnole, Dole, Héricourt, Lons-le-Saunier, Luxeuil-les-Bains, Maîche, Valdahon, Valentigney, Villers-le-Lac, Beaune, Dijon, Chalon-sur-Saône, Gueugnon, Autun, Montchanin
Delivery routes:	
Vehicle 1 (Capacity = 3,500 kg)	Tavaux->Chalon-sur-Saône->Montchanin->Montceau-les-Mines->Gueugnon->Autun->Chagny->Beaune->Nuits-Saint-Georges->Dijon->Genlis->Tavaux
Vehicle 2 (Capacity = 3,500 kg)	Tavaux->Dole->Saint-Vit->Besançon->Valdahon->Maîche->Villers-le-Lac->Morteau->Pontarlier->Champagnole->Lons-le-Saunier->Tavaux
Vehicle 3 (Capacity = 3,500 kg)	Tavaux->Dole->Saint-Vit->Besançon->Vesoul->Luxeuil-les-Bains->Lure->Héricourt->Montbéliard->Beaucourt->Valentigney->Bavans->Baume-les-Dames->Besançon->Saint-Vit->Dole->Tavaux

BFC-L-He (Coverage = 9.88%)

Stations opened:	Dole
Delivery routes:	
Vehicle 1 (Capacity = 1,100 kg)	Tavaux->Dole->Tavaux

BFC-L-He (Coverage = 56.81%)

Stations opened:	Besançon, Héricourt, Valentigney, Villers-le-Lac, Dijon, Le Creusot
Delivery routes:	
Vehicle 1 (Capacity = 1,100 kg)	Tavaux->Chalon-sur-Saône->Montchanin->Le Creusot->Chagny->Beaune->Nuits-Saint-Georges->Dijon->Genlis->Tavaux
Vehicle 2 (Capacity = 3,500 kg)	Tavaux->Dole->Saint-Vit->Besançon->Baume-les-Dames->Bavans->Héricourt->Montbéliard->Valentigney->Pont-de-Roide-Vermondans->Maîche->Villers-le-Lac->Morteau->Valdahon->Besançon->Saint-Vit->Dole->Tavaux

BFC-L-He (Coverage = 90.58%)

Stations opened:	Bavans, Beaucourt, Besançon, Champagnole, Dole, Héricourt, Lons-le-Saunier, Luxeuil-les-Bains, Maîche, Valdahon, Valentigney, Villers-le-Lac, Beaune, Dijon, Chalon-sur-Saône, Gueugnon, Autun, Montchanin
Delivery routes:	
Vehicle 1 (Capacity = 3,500 kg)	Tavaux->Dole->Saint-Vit->Besançon->Valdahon->Maîche->Villers-le-Lac->Morteau->Pontarlier->Champagnole->Lons-le-Saunier->Tavaux
Vehicle 2 (Capacity = 3,500 kg)	Tavaux->Dole->Saint-Vit->Besançon->Vesoul->Luxeuil-les-Bains->Lure->Héricourt->Montbéliard->Beaucourt->Valentigney->Bavans->Baume-les-Dames->Besançon->Saint-Vit->Dole->Tavaux

Vehicle 3 (Capacity = 3,500 kg)	Tavaux->Genlis->Dijon->Nuits-Saint-Georges->Beaune->Chagny->Autun->Gueugnon->Montceau-les-Mines->Montchanin->Chalon-sur-Saône->Tavaux

SPIM
école doctorale **sciences pour l'ingénieur et microtechniques**

Title: Hydrogen supply chain design

Keywords: Hydrogen, Supply chain, Design and Optimization, Integrated model, Routing planning

Abstract:

This thesis contributes to the deployment of the hydrogen infrastructures by proposing new strategies based on optimization approaches. A state of the art on the design of the hydrogen supply chain has been previously carried out, and allows to identify in the literature two research perspectives. The first one concerns the coverage of the entire supply chain, on the one hand upstream at the level of the location of raw material suppliers and the supply of production centres (transport aspect), and on the other hand downstream at the level of the location of distribution points (refueling stations) and their supply (transport). To integrate these components, a new planning model is developed. It merges the classical models, more precisely an HSCND (Hydrogen Supply Chain Network Design) model at the central level, i.e. at the level of production and storage, and an HSRP (Hydrogen Refueling Station Planning) model at the end of the chain, which considers distribution. This new model also integrates the consideration of supply sources. It is expressed as a mixed number integer linear program, with the objective of minimizing the least cost of hydrogen (LCOH). Its interest is validated by a case study representing Franche-Comté in France. The second research area explored is the integration of the strategic and tactical decision-making levels. The aim is to simultaneously optimize the location of refueling stations and the routes to supply these stations, by considering as actuated the decisions previously taken from the supply sources to the hydrogen production centers. The objective is to maximize the refueling demand flow captured, while minimizing the total daily cost. Two metaheuristic algorithms are developed to solve this problem, one based on an adaptive large neighbourhood search, the other on a genetic algorithm. The proposed model and algorithms are applied to the Bourgogne-Franche-Comté region in France.

Titre : Conception de la chaîne logistique de l'hydrogène

Mots-clés : Hydrogène, Chaîne logistique, Conception et Optimisation, Modèle intégré, Planification de tournées

Résumé :

Cette thèse contribue au déploiement de l'infrastructure liée à l'énergie renouvelable qu'est l'hydrogène, en proposant de nouvelles stratégies basées sur des approches d'optimisation. Un état de l'art sur la conception de la chaîne logistique de l'hydrogène est préalablement réalisé, et permet d'identifier dans la littérature deux perspectives de recherche. La première concerne la couverture de la chaîne logistique globale, qui n'est pas assurée, d'une part en amont au niveau de la localisation des fournisseurs de matières premières et de l'approvisionnement des centres de production (aspect transport), d'autre part en aval au niveau de la localisation des points de distribution (stations-service) et de leur approvisionnement (transport). Pour intégrer ces composantes, un nouveau modèle de planification est élaboré. Il fusionne les modèles classiques, plus précisément un modèle de HSCND (Hydrogen Supply Chain Network Design) au niveau central, c'est-à-dire au niveau de la production et du stockage, et un modèle de HSRP (Hydrogen Refueling Station Planning) en bout de chaîne, qui considère la distribution. Ce nouveau modèle intègre également la prise en compte des sources d'approvisionnement. Il est exprimé sous forme d'un programme linéaire en nombres entiers mixtes, avec pour objectif la minimisation du coût de l'hydrogène à la pompe (LCOH). Son intérêt est validé par une étude de cas représentant la Franche-Comté en France. La seconde voie explorée est l'intégration des niveaux de décision stratégique et tactique. Il s'agit d'optimiser simultanément la localisation des stations-service et des tournées de ravitaillement de ces stations, en considérant comme actées les décisions prises précédemment depuis les sources d'approvisionnement jusqu'aux centres de production en hydrogène. L'objectif est de maximiser la capture du flux de demande, tout en minimisant le coût quotidien total. Deux algorithmes approchés sont développés pour résoudre ce problème, l'un basé sur une recherche adaptative de grand voisinage, l'autre sur un algorithme génétique. Le modèle et les algorithmes proposés sont appliqués à la région Bourgogne Franche-Comté en France.

UBFC UNIVERSITÉ BOURGOGNE FRANCHE-COMTÉ
Université Bourgogne Franche-Comté
32, avenue de l'Observatoire
25000 Besançon, France